Vitamin E encapsulation within pharmaceutical drug carriers prepared using membrane contactors

Abdallah Laouini

N° d'ordre 300 Année 2013

DIPLOME DE DOCTORAT
(Arrêté du 7 août 2006)

Délivré par:

L'UNIVERSITE CLAUDE BERNARD LYON 1

ECOLE DOCTORALE DE CHIMIE

THESE DE L'UNIVERSITE DE LYON

Soutenue publiquement:
Le Mardi 03 Décembre 2013

Par:
M. *Abdallah LAOUINI*

Encapsulation de la Vitamine E dans des Vecteurs Pharmaceutiques Inhalables Préparés par des Contacteurs à Membrane

Directeur de thèse:
Dr *Catherine CHARCOSSET* (Directeur de recherche CNRS – LAGEP Lyon)

JURY:

Dr *Marie-Pierre BELLEVILLE*	Institut Européen des Membranes, Montpellier	(Rapporteur)
Dr *Mohamed SKIBA*	Faculté de pharmacie, Université de Rouen	(Rapporteur)
Pr *Hatem FESSI*	Faculté de pharmacie, Université Lyon 1	(Examinateur)
Pr *Souad SFAR*	Faculté de pharmacie, Université de Monastir	(Examinateur)
Dr *Goran VLADISAVLJEVIC*	Université de Loughborough	(Examinateur)
Dr *Véronique ANDRIEU*	Faculté de Pharmacie, Université d'Aix-Marseille	(Examinateur)

UNIVERSITE CLAUDE BERNARD - LYON 1

Président de l'Université	**M. François-Noël GILLY**
Vice-président du Conseil d'Administration	M. le Professeur Hamda BEN HADID
Vice-président du Conseil des Etudes et de la Vie Universitaire	M. le Professeur Philippe LALLE
Vice-président du Conseil Scientifique	M. le Professeur Germain GILLET
Directeur Général des Services	M. Alain HELLEU

COMPOSANTES SANTE

Faculté de Médecine Lyon Est – Claude Bernard	Directeur : M. le Professeur J. ETIENNE
Faculté de Médecine et de Maïeutique Lyon Sud – Charles Mérieux	Directeur : Mme la Professeure C. BURILLON
Faculté d'Odontologie	Directeur : M. le Professeur D. BOURGEOIS
Institut des Sciences Pharmaceutiques et Biologiques	Directeur : Mme la Professeure C. VINCIGUERRA
Institut des Sciences et Techniques de la Réadaptation	Directeur : M. le Professeur Y. MATILLON
Département de formation et Centre de Recherche en Biologie Humaine	Directeur : M. le Professeur P. FARGE

COMPOSANTES ET DEPARTEMENTS DE SCIENCES ET TECHNOLOGIE

Faculté des Sciences et Technologies	Directeur : M. le Professeur F. DE MARCHI
Département Biologie	Directeur : M. le Professeur F. FLEURY
Département Chimie Biochimie	Directeur : Mme le Professeur H. PARROT
Département GEP	Directeur : M. N. SIAUVE
Département Informatique	Directeur : M. le Professeur S. AKKOUCHE
Département Mathématiques	Directeur : M. le Professeur A. GOLDMAN
Département Mécanique	Directeur : M. le Professeur H. BEN HADID
Département Physique	Directeur : Mme S. FLECK
Département Sciences de la Terre	Directeur : Mme la Professeure I. DANIEL
UFR Sciences et Techniques des Activités Physiques et Sportives	Directeur : M. C. COLLIGNON
Observatoire des Sciences de l'Univers de Lyon	Directeur : M. B. GUIDERDONI
Polytech Lyon	Directeur : M. P. FOURNIER
Ecole Supérieure de Chimie Physique Electronique	Directeur : M. G. PIGNAULT
Institut Universitaire de Technologie de Lyon 1	Directeur : M. C. VITON
Institut Universitaire de Formation des Maîtres	Directeur : M. A. MOUGNIOTTE
Institut de Science Financière et d'Assurances	Administrateur provisoire : M. N. LEBOISNE

Remerciements

Pr Hatem Fessi

Tout d'abord, Je tiens à vous remercier d'avoir accepter de m'accueillir dans votre unité de recherche : le Laboratoire d'Automatique et de Génie des Procédés (LAGEP). Vous m'avez guidé et patiemment aidé tout le long de ce travail. Je suis très touché par votre sympathie et votre modestie. Veuillez accepter ma vive gratitude pour tous les conseils que vous m'avez prodigués.

Dr Catherine Charcosset

Je vous remercie vivement pour l'honneur que vous m'avez fait en me confiant ce sujet de thèse et pour l'aide précieuse que vous m'avez apportée tout au long de la réalisation de ce travail. Vous avez su me donner une grande liberté d'initiative tout en restant toujours présente pour discuter des difficultés que j'ai pu rencontrer.

Vos très hautes qualités humaines, votre modestie, et votre très grande compétence suscitent mon respect et mon admiration. Faire partie de vos disciples est à la fois un grand honneur et une immense fierté. Veuillez trouver ici l'expression de ma profonde reconnaissance pour votre contribution si précieuse et votre dévouement si immense.

Dr Marie-Pierre Belleville
Dr Mohamed Skiba

Je suis très sensible à l'honneur que vous me faites en acceptant de participer à ce jury de thèse et d'en être les rapporteurs. Je vous remercie pour l'intérêt que vous porterez à mon travail. En attendant vos conseils et suggestions constructives qui me permettront certes d'améliorer la qualité de mon manuscrit, veuillez accepter mes plus sincères remerciements.

Dr Goran Vladisavljevic
Dr Karin Shroen

My sincere thanks go to you for offering me internship opportunities in your groups and leading me working on diverse exciting projects.

I would like to express my sincere gratitude for your continuous support, your enthusiasm and your immense knowledge.

Dr Véronique Andrieu

Vous m'avez bien accueilli et aider à réaliser mes expériences au sein de votre laboratoire dans les meilleures conditions. Je vous remercie pour votre soutien, vos encouragements et votre disponibilité.

Pr Souad Sfar

Je suis très sensible de l'honneur que vous me faites en acceptant de siéger à notre Jury et juger ce travail. Je salue en vous vos compétences professionnelles, vos qualités humaines ainsi que votre esprit critique. Puisse ce travail vous satisfaire et témoigner de mon profond respect et ma grande estime.

A tout le personnel du Laboratoire d'Automatique et de Génie des Procédés (Lyon, France), du « Departement of Chemical Engineering » (Loughborough, Royaume-Uni) et du « Food Process Engineering Laboratory » (Wageningen, Pays-Bas), en particulier ***Dr Chiraz Jaafar-Maalej****,* ***Dr Marijana Dragosovac, Dr Laurent Vecellio*** *et* ***Mr Sami Sahin*** *: En signe de reconnaissance pour votre aide précieuse et votre soutien perpétuel lors de la réalisation de ce travail.*

Dédicaces

Nulle dédicace ne saurait exprimer mes profonds sentiments envers tous ceux pour qui je porte de l'affection, du respect, de l'amour et de la reconnaissance.

C'est à travers ces mots simples que je dédie ce travail:

A ceux qui n'ont jamais porté d'aussi suprême espérance que celle de ma réussite.
A ceux qui m'ont toujours comblé de leur amour et entouré de leur affection.
A ceux qui m'ont aidé à dépasser et à défier les difficultés que j'ai pu rencontrer.
A ceux que j'aime le plus au monde.

A mon père

A celui qui a guidé mes pas…
Grâce à toi le besoin n'a jamais croisé mon chemin.
Je te dois tout et je ferais de mon mieux pour rester celui dont tu as toujours été fier sans jamais te décevoir.
Nulle dédicace ne saurait exprimer ma gratitude et ma reconnaissance pour tes prodigieux conseils et ta grande patience.
Ce travail paraît bien dérisoire pour traduire une reconnaissance infinie à un père aussi merveilleux que toi.
Que Dieu te préserve et t'alloue bonne santé et longue vie.

A ma mère

A toi la plus douce, la plus tendre et la plus adorable des mamans,
Tu m'as généreusement comblé d'affection et de bienveillance.
Tu as toujours fait de ton mieux pour m'assurer bonheur et confort.
Pour ton amour profond, ton soutien infaillible et tes sacrifices innombrables, je dédie ce modeste travail en témoignage de mon éternelle reconnaissance et de mon très grand attachement.
Que le tout puissant te garde le plus longtemps parmi nous, te procure santé, bonheur et sérénité et te protège de tout mal.

A mes sœurs, mon frère, ma belle-sœur, mon beau-frère, et mes neveux

Votre amour et votre soutien ne m'ont jamais fait défaut.
Qu'il me soit permis de vous exprimer toute mon adoration et mon indéfectible attachement.
Que Dieu vous accorde une vie pleine de bonheur et de santé.

A tous mes amis et amies

Adnene, Akrem, Audrey, Chiraz, Jeremy, Jerome, Julien, Karim, Mariem, Nathalie, Nicolas, Sarah et Wafa.

A tous ceux dont l'oubli du nom n'est pas celui du cœur.

Sommaire

Sommaire

Introduction

Introduction

De nos jours, il est évident que la recherche et le développement de nouvelles molécules thérapeutiques ne suffisent pas à assurer les progrès des traitements médicamenteux. Une stratégie prometteuse consiste à associer le principe actif à un vecteur. Ainsi, après son administration le devenir du médicament dans l'organisme ne dépendra plus des propriétés de la molécule active mais sera soumis à celles du vecteur choisi.

La vectorisation a plusieurs objectifs, elle permet de :
- Protéger le principe actif après son administration en lui permettant de mieux s'opposer aux mécanismes biologiques de dégradation.
- Moduler les propriétés physico-chimiques de la molécule d'intérêt; l'exemple le plus connu est celui de l'amélioration de la solubilité des molécules ayant une hydrophobie trop élevée.
- Moduler les propriétés pharmacologiques de la substance active afin d'optimiser son efficacité thérapeutiques et surtout réduire ses effets indésirables.
- Contrôler la distribution du principe actif dans l'organisme permettant ainsi son ciblage vers les sites d'action.

Un bon vecteur doit répondre à un certain nombre de critères : il doit être stable, biocompatible, efficace et non toxique. Par ailleurs, il doit être adapté au principe actif c.-à-d. capable de le stocker en quantité suffisante et de le relarguer par la suite de la manière désirée. De même la production industrielle du vecteur ne doit pas poser de problèmes.

Aujourd'hui, le développement des nanotechnologies a permis de concrétiser l'idée de vectorisation des principes actifs qui est devenue un axe de recherche suscitant un véritable engouement dans le domaine pharmaceutique. S'appuyant sur de nouveaux concepts physico-chimiques et sur de nouveaux matériaux, la recherche a ainsi pu imaginer des systèmes submicroniques d'administration des médicaments. Les exemples des « drug-carriers » utilisés en pharmacie sont multiples; on peut citer les liposomes, les nano-capsules, les nano-sphères, les micelles, les nano-émulsions, etc.

La production de ces nano-systèmes pour la vectorisation des principes actifs constitue un véritable défi. En effet, un procédé de fabrication doit être reproductible et permettre une production à large échelle avec un coût minimum. Cependant la grande majorité des techniques de préparation reportées permettent seulement une production à l'échelle du laboratoire. Par ailleurs, ces procédés consomment dans la plupart des cas beaucoup d'énergie et se basent sur des méthodes empiriques qui manquent de reproductibilité.

Au cours de ce travail, nous proposerons une alternative aux procédés classiques pour la préparation des vecteurs pharmaceutiques en se basant sur l'utilisation des membranes.

Une membrane est une barrière semi-perméable qui sous l'effet d'une force de transfert va permettre ou interdire le passage de certains composants entre les deux milieux qu'elle sépare. Les membranes ont été utilisées initialement pour la séparation et la filtration des particules; aujourd'hui elles sont exploitées en tant que « contacteurs ». C'est alors la capacité de ces barrières matérielles à générer une interface entre deux phases, qui est exploitée. Les contacteurs membranaires ont trouvé des applications dans le secteur de l'agro-alimentaire, de la chimie, de l'industrie du textile, du papier, de la métallurgie, de la micro-électronique, etc. Actuellement, dans le secteur pharmaceutique, une application des contacteurs membranaires porte sur le traitement de l'eau en vue de l'élimination du CO_2 dissous.

Technologie mature et sur le marché depuis plus de trente ans, les contacteurs membranaires sont considérés comme des technologies dominantes aux États-Unis, en Chine et au Japon. Les investissements industriels dans ce domaine sont importants et croissent rapidement. En France, selon le rapport d'une étude prospective technologique menée par le ministère de l'économie, de la finance et de l'industrie « Technologies clés 2015 », les applications des procédés membranaires ne sont pas tout à fait exploitées. Ainsi, l'association des technologies membranaires à la production des nano-produits serait un atout considérable pour l'intensification des procédés industriels.

L'utilisation des membranes présente plusieurs points forts dont :

- La possibilité de préparer des particules de faible taille en une seule étape avec un apport d'énergie inférieur à celui des méthodes conventionnelles. L'utilisation réduite de l'énergie garantit d'une part le respect de l'environnement et permet d'autre part un coût d'exploitation modéré.
- Le travail dans des systèmes fermés permet d'éviter les contaminations extérieures; ceci représente un avantage certain en industrie pharmaceutique.
- L'usage de la modélisation permet d'établir des relations entre propriétés structurales des membranes, conditions opératoires, avec l'efficacité du procédé permettant ainsi son optimisation.
- Le développement de la simulation permet de prévoir la performance des membranes ce qui assurerait un développement rapide des procédés membranaires.
- La possibilité de développer des procédés continus et automatisables.
- Un fort potentiel d'innovation (fonctionnalisation des membranes, usage des procédés hybrides…) répondant aux contraintes de développement durable.

L'objectif de ce travail est donc d'appliquer cette technologie propre et innovante pour la préparation de différents vecteurs permettant l'encapsulation des principes actifs en pharmacie. Dans cette étude, le choix du principe actif à encapsuler s'est porté sur lα -tocophérol qui est une forme de la vitamine E présente en grande quantités dans les huiles végétales.

A température ambiante, la vitamine E se présente sous forme d'une huile visqueuse de coloration jaune pâle. Elle est peu sensible à la chaleur mais très sensible à l'oxydation d'ou son rôle physiologique d'antioxydant contre les dérivés réactifs de l'oxygène appelés radicaux libres. Les radicaux libres sont des molécules contenant un nombre impair d'électrons, ils sont produits suite aux oxydations cellulaires induites par l'oxygène. La présence de ces radicaux libres entraîne une agression des cellules que l'on appelle le stress oxydatif. Ce phénomène physiologique, est impliqué dans le vieillissement de l'Homme. Le stress oxydatif devient une situation pathologique dès que le système de protection antioxydant est submergé par une production accrue de radicaux libres.

Parmi les pathologies liées au stress oxydatif, on trouve les maladies broncho-pulmonaires liées à la consommation du tabac. En effet le tabac contient des molécules oxydantes qui accentuent la production des radicaux libres. Lorsque les défenses naturelles, constituées par des antioxydants, s'avèrent insuffisantes, les radicaux libres toxiques vont s'attaquer aux cellules entraînant une perte de l'élasticité des poumons (fibrose pulmonaire) responsable entre autre de bronchites chroniques et parfois de cancers pulmonaires. Ces conséquences du stress oxydatif au niveau pulmonaire soulèvent donc l'importance du maintien d'un équilibre adéquat entre antioxydants et oxydants. Les antioxydants (dont la vitamine E), capables de neutraliser les radicaux libres, peuvent alors être utilisés pour prévenir ce genre de toxicité pulmonaire. Toutefois l'administration par voie systémique (orale, intraveineuse…) n'a pas permis d'atteindre un niveau adéquat de vitamine E au niveau de son site d'action broncho-alvéolaire. D'où l'idée de développer des nano-systèmes inhalables qui permettront l'encapsulation de la vitamine E puis sa délivrance au niveau pulmonaire.

Pour une action locale, la voie d'administration respiratoire offre l'avantage de cibler la zone à traiter; la délivrance du principe actif *in situ* procure alors une meilleure efficacité à dose plus faible et provoque par la même occasion moins d'effets secondaires comparativement aux autres voies d'administration. De plus, le médicament directement délivré vers sa cible permet d'avoir un début d'action rapide puisque il n'a pas besoin d'être ni absorbé ni transporté pour agir. Le devenir d'un médicament inhalé et par conséquent son efficacité thérapeutique dépend avant tout de la taille des particules de l'aérosol. Pour atteindre l'arbre trachéo-bronchique d'un adulte, les particules doivent idéalement présenter une taille inférieure à 5 µm. Il est donc nécessaire de pouvoir caractériser un aérosol en

terme de taille de particules pour prédire son site de dépôt, et de vérifier ainsi l'adéquation entre la zone à traiter et le site de dépôt.

Cette thèse comporte six chapitres :

- Le premier chapitre présente des notions de base sur les contacteurs à membrane et sur les systèmes colloïdaux.
- les quatre chapitres qui suivent présentent le développement de vecteurs encapsulant la vitamine E en utilisant des méthodes basées sur des contacteurs à membranes (respectivement liposomes, nano-émulsion, micelles et particules lipidiques solides).
- Le dernier chapitre présente les résultats de caractérisation des aérosols générés et la prédiction du niveau de dépôt pulmonaire.

Contacteurs à membrane et systèmes colloïdaux

Contacteurs à membrane et systèmes colloïdaux

Dans le cadre de cette thèse, la vitamine E a été encapsulée dans des vecteurs colloïdaux en utilisant des procédés basés sur des contacteurs à membrane. Quelques notions bibliographiques concernant les contacteurs à membranes et les systèmes colloïdaux sont présentées brièvement ci-dessous.

1. Les contacteurs à membrane

1.1 Définition

Une membrane est un matériau poreux qui sépare deux milieux permettant ainsi un échange contrôlé de matière. Les procédés membranaires les plus utilisés sont les procédés de filtration, développés depuis les années 1960. Ils permettent de séparer et de concentrer des molécules, des espèces ioniques en solution, des particules ou des microorganismes en suspension dans un liquide. Parallèlement à leur utilisation dans les procédés bien établis d'ultrafiltration et de microfiltration, les membranes font l'objet de nouvelles applications dans les industries pharmaceutiques et biotechnologiques, comme les bioréacteurs membranaires, les membranes chromatographiques, et les contacteurs à membrane **[1]**. Cet intérêt croissant est dû au fait que les systèmes à membrane présentent l'avantage d'être sélectifs, d'offrir une surface importante par unité de volume et la possibilité de contrôler le contact et/ou le mélange entre deux phases **[2].**

Le terme de contacteur membranaire désigne un procédé où une première phase est introduite sous pression à travers les pores d'une membrane microporeuse, dans une deuxième phase. Les pores de la membrane jouent le rôle de capillaires parallèles pour l'introduction sous pression de la phase dispersée dans la phase continue **[3]**. La **figure 1** montre un schéma représentatif d'un contacteur à membrane.

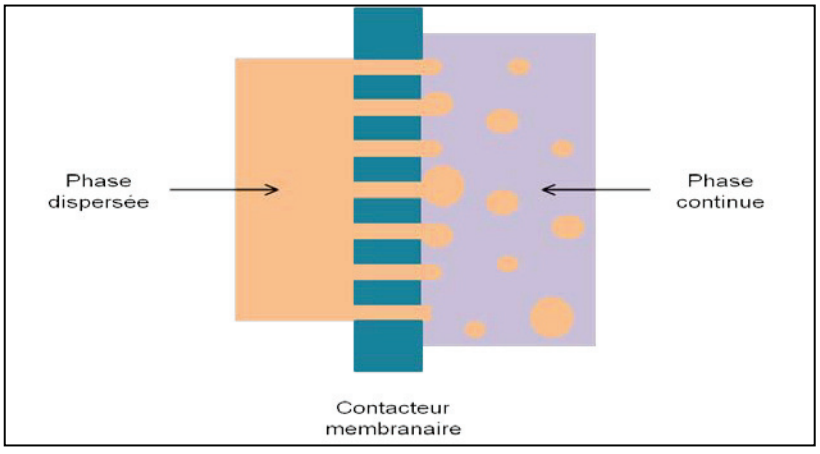

Figure 1. Schéma représentatif du principe d'un contacteur membranaire

1.2 Différentes configurations expérimentales

Dans le cas de l'émulsification directe, le passage de la phase dispersée à travers les pores de la membrane entraîne la formation de fines gouttelettes à l'interface membrane/phase continue. Afin d'assurer un détachement uniforme de ces gouttelettes, une force de cisaillement est généralement requise. Cette force peut être générée par la circulation tangentielle de la phase continue **[1]**, comme le montre la **figure 2. a**. Le débit de circulation de la phase continue doit être suffisant afin de garantir un détachement régulier des gouttelettes formées, mais pas très élevé pour ne pas altérer la structure des particules déjà préparées.

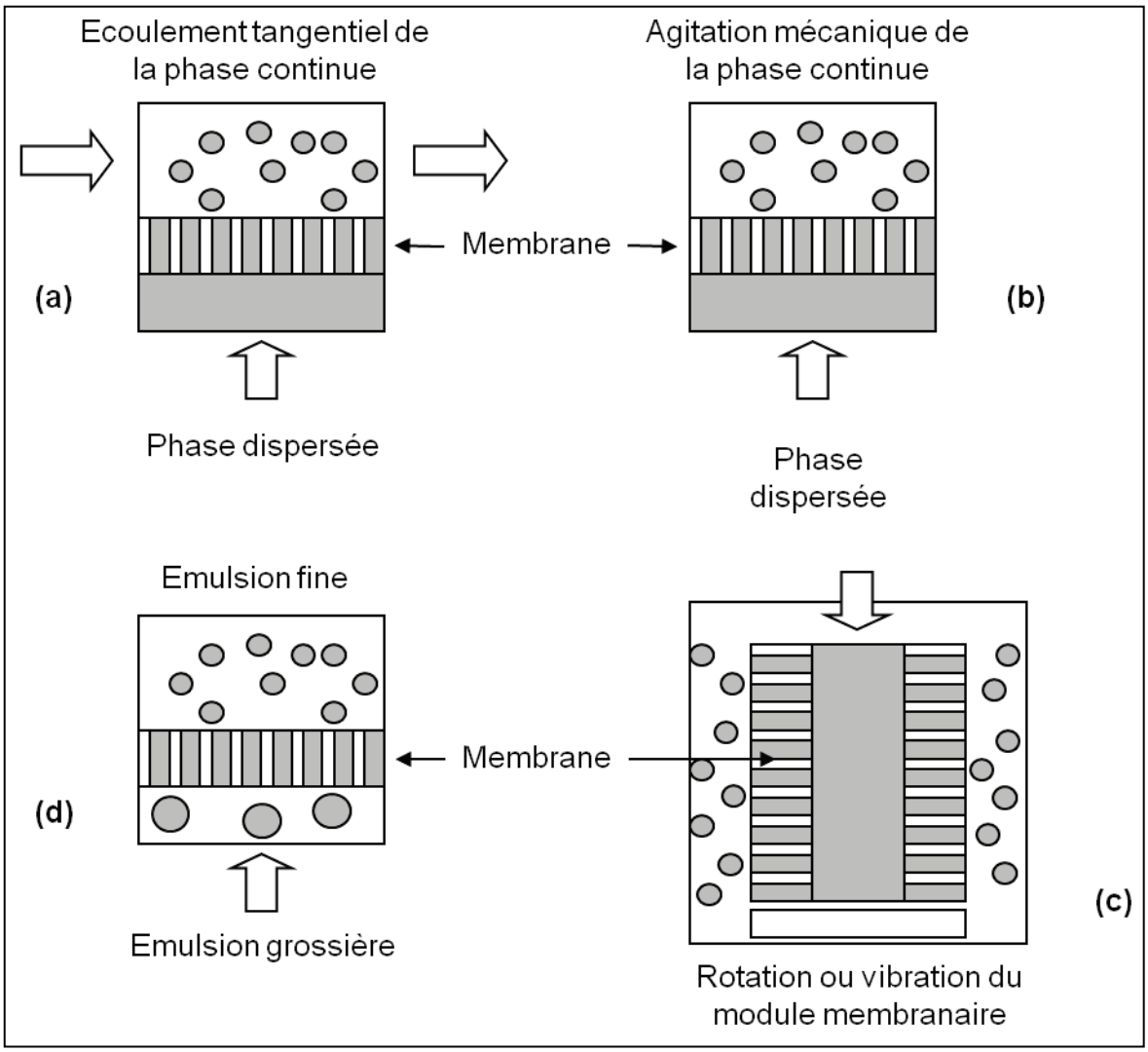

Figure 2. Représentation schématique des différentes configurations expérimentales des modules membranaires. **(a)**, **(b)** et **(c)** : émulsification directe, **(d)** « premix emulsification ». Dans le cas de l'émulsification directe, la force de cisaillement assurant le détachement des gouttelettes peut être obtenue par : **(a)** circulation tangentielle de la phase continue, **(b)** agitation mécanique de la phase continue, ou **(c)** mouvement de la membrane au sein d'une phase continue stationnaire.

Le détachement des gouttelettes à la surface membranaire peut avoir lieu sans flux tangentiel mais par agitation mécanique de la phase continue, comme dans le cas d'une cellule d'agitation **[4]** (**Figure 2. b**). Le principal inconvénient de cette configuration est que la force de cisaillement générée à la surface membranaire, par l'agitation mécanique, varie dans l'espace. Ceci peut se répercuter sur l'uniformité de taille des particules obtenues. Toutefois certaines études, ayant utilisé des cellules d'agitation, ont décrit la préparation d'émulsions dont la distribution de taille était étroite **[5]**. Par ailleurs, la cellule d'agitation ne permet pas de préparer de grands volumes, mais elle s'avère être un outil intéressant pour étudier l'influence des différents paramètres opératoires sur le procédé de fabrication afin de l'optimiser. Un passage à une échelle de production plus importante peut être alors envisagé grâce à d'autres configurations de contacteurs membranaires.

D'autres configurations impliquent l'utilisation de modules membranaires dotés de mouvement de rotation ou de vibration au sein d'une phase continue stationnaire (**Figure 2. c**). Ce type de configuration présente un grand intérêt car il permet d'éviter la recirculation tangentielle de la préparation et est donc adapté à la fabrication de particules ayant une structure fragile pouvant être altérée suite aux passages multiples à travers la pompe et les différents conduits **[6, 7]**.

Contrairement à l'émulsification directe, où la phase discontinue est directement dispersée dans la phase continue, la « premix emulsification » met en jeu une émulsion grossière qui passe à travers les pores d'une membrane microporeuse entraînant ainsi une réduction de la taille des globules lipidiques (**Figure 2. d**). Ce procédé peut être appliqué à la préparation d'émulsions simples ou multiples. Pour une membrane de taille de pores donnée, les études ont montré que les émulsions préparées par le procédé de « premix emulsification » présentent une taille inférieure à celles préparées par émulsification directe. Le procédé de « premix emulsification » peut être amélioré en effectuant des passages répétitifs de l'émulsion à travers la membrane **[8, 9]**.

1.3 Différents modules membranaires

Divers modules membranaires sont disponibles sur le marché; les plus communément utilisés sont les membranes SPG « Shirasu Porous Glass » (Ise Chemical Co, Japon). Ces membranes sont préparées à partir d'un type de verre extrait du magma d'un volcan Japonais « Shirasu ». Elles sont caractérisées par la présence de micropores interconnectés avec une distribution de taille étroite. Ces membranes sont disponibles avec des tailles de pores allant de 0.05 jusqu'à 30 µm et elles se présentent sous forme tubulaire avec des porosités élevées de 50 à 60 % **[10, 11]**.

Récemment, les membranes microsieves ont connu une utilisation croissante (Aquamarijn Micro Filtration BV, Pays-Bas et Micropores Technologies, Royaume-

Uni). Ces membranes sont caractérisées par une surface plane et lisse et une faible résistance membranaire. Leur avantage majeur est la grande uniformité de la taille des pores et la régularité des distances inter-pores **[12]**.

Par ailleurs, des modules fibres creuses ont été utilisés pour la préparation de particules colloïdales **[13]**. Les fibres creuses sont de fines membranes tubulaires qui sont assemblées parallèlement dans un module. Ces fibres poreuses ont un diamètre interne compris entre 0.2 et 1 mm, et une longueur de 10 à 100 cm. Le nombre de fibres dans un module varie de quelques fibres à plusieurs milliers. La composition chimique des fibres est très variée (polypropylène, polyamide, etc), offrant une large gamme de compatibilité chimique. Les modules fibres creuses sont disponibles sous de nombreuses configurations (taille des pores, longueurs des fibres, nombre de fibres par modules) permettant de s'adapter à de nombreuses applications dans l'industrie.

D'autres types de membranes peuvent être utilisés pour les procédés d'émulsification membranaire. On peut citer : les membranes en céramique, les membranes en poytetrafluoroethylene (PTFE), les membranes en polycarbonate, etc.

1.4 Applications

L'émulsification membranaire a été introduite au Japon en 1988 par *Nakashima et al.* **[14]** lors des rencontres annuelles des ingénieurs chimistes Japonais. Depuis, cette technique suscite un engouement croissant comme alternative aux méthodes classiques d'émulsification. En effet, elle nécessite un apport modéré d'énergie (10^4 à 10^6 J/m^3) comparé aux méthodes conventionnelles (10^6 à 10^8 J/m^3).

De nombreuses applications ont été décrites dans la littérature. Quelques exemples sont donnés ci-dessous concernant l'encapsulation de principes actifs. L'émulsification membranaire avec une membrane SPG a été utilisée pour la préparation d'une émulsion de chlorure de méthylène dans de l'eau déminéralisée en utilisant un mélange de Tween 20 et Tween 80 comme tensioactifs et de l'alcool polyvinylique (PVA) comme stabilisateur. La méthode a permis d'encapsuler le flurbiprofène dans des gouttelettes de taille avoisinant les 100 nm **[15]**.

L'utilisation d'un contacteur à membrane a permis de préparer une double émulsion eau/huile/eau pour le traitement, par chimiothérapie, du cancer de foie par injection artérielle **[16].** La solution aqueuse contenant le principe actif (épirubicine ou carboplatine) est émulsionnée avec la phase huileuse (huile de graine de pavot iodé ou lipidol) avec un sonicateur pour obtenir une émulsion submicronique de type eau/huile. Cette émulsion est ensuite utilisée comme phase dispersée dans un procédé d'émulsification membranaire où la phase continue est composée d'une solution glucosée, permettant d'obtenir une double émulsion.

Des microsphères de taille uniforme ont également été préparées pour contrôler la libération de divers principes actifs tels que l'anthracycline **[17]**, l'astaxanthine caroténoide **[18]** et l'insuline **[19]**.

La méthode de contacteur membranaire a permis également la préparation de nanoparticules lipidiques solides encapsulant la vitamine E **[20]**, de nanocapsules de spironolactone **[21]** et récemment de liposomes encapsulant divers principes actifs (indométacine, dipropionate de béclométhasone et spironolactone) **[13, 22]**.

2. Les systèmes colloïdaux

Un système colloïdal est un système constitué par une fine dispersion d'une phase dans une autre; la phase dispersée présente une taille allant de quelques nanomètres à quelques micromètres. Les suspensions colloïdales font l'objet de la science des colloïdes et des interfaces, science initiée en 1861 par le chimiste Ecossais Thomas Graham. Les systèmes vectoriels d'encapsulation des principes actifs sont considérés, de part leurs tailles, comme des systèmes colloïdaux. Dans ce qui suit, on présentera brièvement les vecteurs colloïdaux qui ont été développés au cours de cette thèse.

2.1 Les liposomes

Les liposomes ont été fabriqués pour la première fois en 1965 par Bangham et ses collègues alors qu'ils faisaient des recherches sur la membrane cellulaire, au Centre de Recherche Agricole de l'Institut de Physiologie Animale à Babrham en Angleterre. Les liposomes sont des particules sphériques constituées d'un espace aqueux interne entouré d'une ou de plusieurs bicouche(s) de phospholipide(s) (**Figure 3**). La taille du liposome va dépendre de la technique utilisée pour le fabriquer, mais généralement leur diamètre varie entre quelques dizaines de nanomètres et quelques dizaines de microns **[23]**.

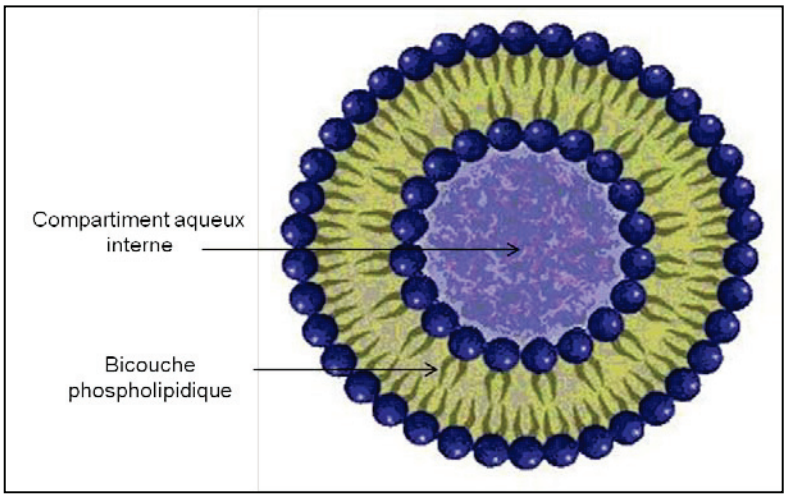

Figure 3. Structure d'un liposome

Historiquement, la première méthode utilisée pour la préparation des liposomes est la méthode de *Bangham*. Elle consiste à évaporer une solution organique de phospholipides (généralement dans du chloroforme) jusqu'à la formation d'un film phospholipidique sec sur les parois d'un récipient. La dispersion du film lipidique dans un milieu aqueux accompagnée d'une agitation régulière permet d'obtenir des liposomes **[24]**. La méthode d'évaporation en phase inverse consiste à disperser le film phospholipidique dans un solvant organique non miscible à l'eau afin de former une émulsion. L'évaporation sous vide du solvant organique conduit à la formation de micelles inverses (constituées par une monocouche lipidique entourant un espace aqueux). La réduction de la pression permet l'évaporation totale du solvant organique et entraîne un rapprochement des monocouches lipidiques pour former des liposomes **[25]**. La méthode d'injection de solvant consiste à injecter une solution organique contenant les phospholipides dans une solution aqueuse, qui entraîne une formation instantanée de liposomes. Cette méthode présente l'avantage d'être simple, rapide et conduire à la formation de vésicules de faible taille et de distribution de taille assez étroite **[26]**. Ainsi, plusieurs auteurs ont cherché à modifier cette méthode en vue de l'améliorer. Par exemple, *Wagner et al.* **[27]** ont utilisé, pour l'injection de la phase organique, un module permettant la circulation de la phase aqueuse selon un flux tangentiel. Ceci a permis de réaliser des préparations à plus large échelle. *Jaafar-Maalej et al.* **[22]** ont effectué l'injection de la phase organique dans la phase aqueuse à travers les pores d'une membrane. Ceci a permis une meilleure maîtrise du procédé de fabrication et a conduit à des résultats reproductibles.

Les liposomes peuvent être utilisés comme vecteurs pour la délivrance des médicaments. Différentes formes pharmaceutiques à base de liposomes ont été mises au point tel que les suspensions, les aérosols ou les formes semi-solides comme les gels et les crèmes. L'administration de ces formes se fait soit par voie intraveineuse soit par voie topique. Les liposomes peuvent être utilisés comme vecteurs de thérapie génique en encapsulant des gènes ou des plasmides. Ils peuvent aussi être employés pour exposer des protéines virales à leur surface, dans ce cas on les appelle des virosomes et sont donc utilisés comme vaccins. A coté de ces utilisations en pharmacie, les liposomes sont également utilisés en cosmétologie et dans l'industrie agro-alimentaire.

2.2 Les micelles

Les micelles sont des vésicules sphériques formées par des molécules amphiphiles lorsqu'elles sont présentes dans le milieu à une concentration supérieure à leur concentration micellaire critique (CMC). La formation des micelles résulte de l'auto-assemblage des chaînes hydrophobes à l'intérieur de la vésicule et l'exposition des têtes hydrophiles à l'extérieur (**Figure 4**). Ce comportement résulte des interactions attractives et répulsives au niveau des têtes polaires et des chaînes hydrophobes.

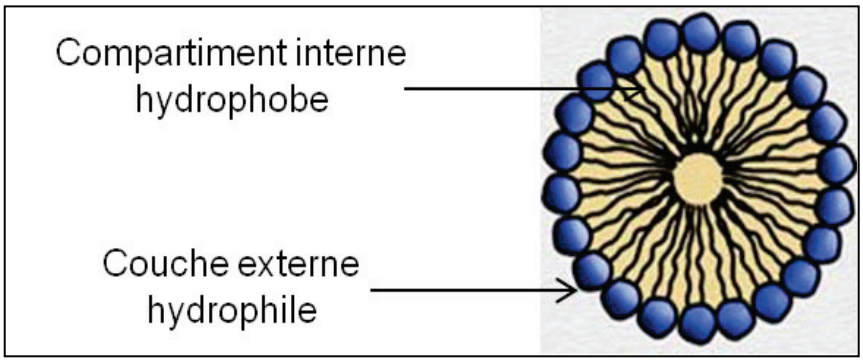

Figure 3. Structure d'une micelle

Les copolymères de synthèse ayant un caractère amphiphile permettent de préparer des micelles polymériques. Ce type de micelles est largement étudié car il présente une meilleure stabilité comparée aux micelles obtenues avec des molécules de tensioactifs et permet une grande capacité d'encapsulation des principes actifs hydrophobes **[28]**.

Les méthodes de préparation des micelles dépendent de la solubilité du copolymère. Lorsque le copolymère est soluble dans l'eau, les micelles peuvent être obtenues par dissolution directe du polymère dans la phase aqueuse **[29]**. Une autre technique consiste à dissoudre le polymère dans un solvant organique volatile qui sera évaporé par la suite; l'hydratation du film polymérique entraîne alors la formation de micelles. Généralement, ces deux méthodes conduisent à la formation de particules avec une distribution de taille polydisperse parfois bimodale **[30]**. Lorsque le copolymère est insoluble dans l'eau, trois méthodes de préparation de micelles ont été décrites : la méthode de dialyse, la méthode d'émulsification et la méthode d'évaporation du co-solvant. Dans la méthode de dialyse, le polymère est d'abord dissout dans un solvant organique miscible à l'eau; après le solvant organique est remplacé par de l'eau en utilisant la technique de dialyse **[31]**. Cette technique est longue et peut durer des jours. La méthode d'émulsification consiste à dissoudre le polymère dans un solvant organique non miscible à l'eau. La phase organique est ensuite émulsifiée avec la phase aqueuse; l'évaporation du solvant entraîne la formation de micelles. La méthode d'évaporation du co-solvant est identique à la méthode précédente mais le solvant organique utilisé est miscible à l'eau **[32]**.

Toutes les méthodes précédemment reportées pour la formation des micelles polymériques sont difficiles à transposer de l'échelle du laboratoire à l'échelle de production industrielle. Ces méthodes manquent aussi de reproductibilité et ne permettent pas une bonne maîtrise de la taille des particules **[33]**. L'émulsification membranaire, jusqu'à présent pas utilisée pour la formation des micelles, pourrait donc constituer une bonne alternative aux méthodes de préparation conventionnelles en permettant une production maîtrisée et à large échelle.

2.3 Les nano-émulsions

Les émulsions sont des mélanges de deux liquides non miscibles; la phase discontinue est dispersée dans la phase continue. La nature des phases interne et externe permet de définir deux types d'émulsion : huile/eau et eau/huile. Les nano-émulsions (structure présentée dans la **Figure 4**) sont une classe d'émulsions dont le diamètre des globules lipidiques dispersées dans la phase aqueuse est compris dans une gamme nanométrique. Il n'y a cependant pas de consensus dans la littérature concernant cette gamme qui peut varier fortement. Nous retiendrons ici la définition de *Solans et al.* **[34]**, soit un diamètre compris entre 20 et 200 nm.

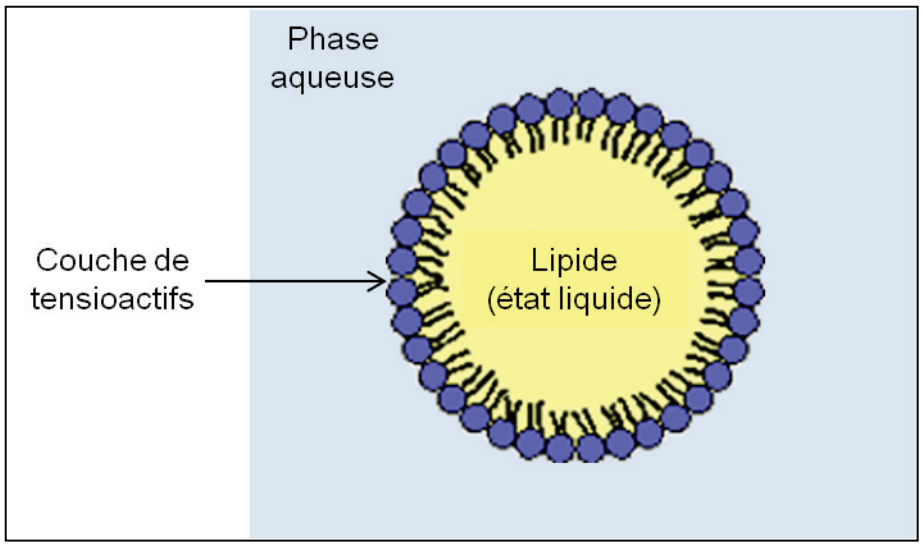

Figure 4. Structure d'une nano-émulsion

De nombreuses propriétés découlent de la faible taille des gouttelettes constituant les nano-émulsions : une grande stabilité, une relative transparence et la possibilité de stérilisation par filtration. Tous ces avantages font que les nano-émulsions sont de plus en plus étudiées pour la vectorisation des principes actifs en pharmacie.

Les premières méthodes décrites pour la préparation des émulsions utilisent des dispositifs du type rotor/stator ou des homogénéisateurs à pression élevée. Ces méthodes permettent grâce à un apport élevé d'énergie de réduire la taille des globules lipidiques dans le mélange huile/eau **[35, 36]**. Toutefois, il a été établit que ces techniques ne permettent pas de contrôler efficacement le procédé d'émulsification car les émulsions ainsi obtenues présentent des distributions de taille très large **[37]**. Les recherches se sont donc tournées vers d'autres techniques moins énergivores et qui pourraient permettre de mieux contrôler le procédé d'émulsification. La méthode d'émulsification par inversion de phase consiste à ajouter de la phase interne à une émulsion dans des conditions spécifiques (ajout très lent, assorti d'une longue agitation de faible intensité) jusqu'à ce que la phase continue devienne la phase dispersée.

L'inversion de phase peut aussi être provoquée par une modification de la température sous agitation de façon à affecter le HLB du système **[38]**. L'intérêt principal de cette méthode est qu'elle permet de préparer des émulsions de petite taille avec un faible apport d'énergie. Toutefois, cette méthode nécessite l'utilisation d'un mélange de tensioactifs en grande quantité ce qui fait qu'elle ne peut pas s'adapter facilement à une production industrielle.

L'émulsification membranaire présente une alternative intéressante, puisqu'elle nécessite un apport modéré d'énergie et permet un meilleur contrôle des propriétés des émulsions obtenues. Bien que de nombreux travaux ont étudié la préparation des émulsions en utilisant des membranes, à notre connaissance une seule étude a décrit la fabrication de nano-émulsions par le procédé d'émulsification membranaire **[15]**.

2.4 Les particules lipidiques solides

Les particules lipidiques solides ont une structure similaire à celle des émulsions, toutefois la phase lipidique dispersée est à l'état solide à température ambiante (voir **Figure 5**). Ces particules lipidiques sont stabilisées par l'ajout d'un tensioactif. Quand elles sont utilisées comme vecteurs de principe actif, ce dernier est dissout ou dispersé dans la phase lipidique.

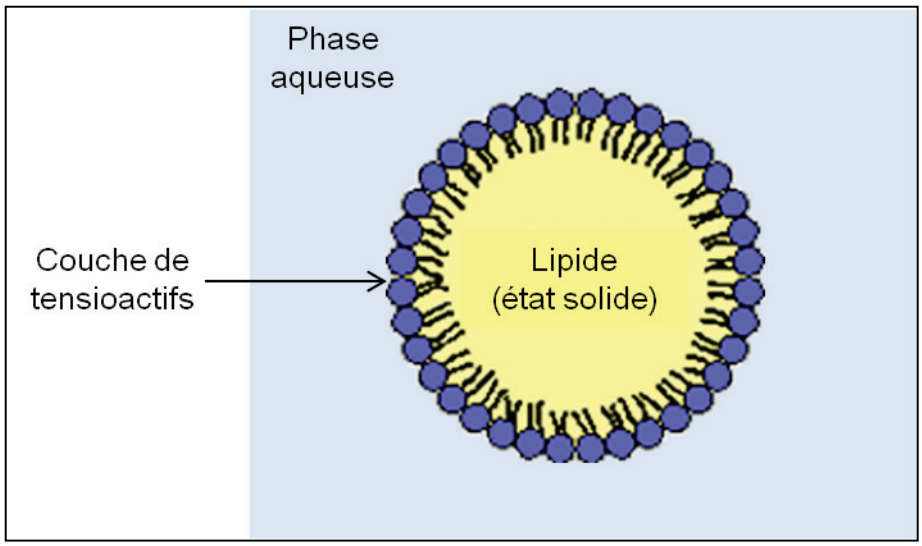

Figure 5. Structure d'une particule lipidique solide.

Ces formes colloïdales présentent de nombreux avantages : (i) selon le mode de fabrication choisi il est possible d'éviter l'utilisation de solvants organiques, (ii) les coûts des matières premières sont peu élevés et la production à l'échelle industrielle est facile, et (iii) la stabilité physico-chimique est meilleure comparée aux émulsions classiques **[39]**.

Les méthodes de préparation des particules lipidiques solides sont nombreuses, dans ce qui suit nous décrirons celles qui sont couramment utilisées. Dans la méthode par évaporation du solvant, le lipide est dissous dans la phase organique qui est ensuite émulsifiée dans la phase aqueuse contenant le tensioactif. La formation des particules lipidiques est obtenue par évaporation du solvant organique. Cette technique offre l'avantage d'éviter une étape de chauffage et est recommandée pour les principes actifs thermosensibles mais nécessite l'utilisation de solvants organiques avec le risque de retrouver des résidus de solvants dans le produit fini **[40]**. Afin d'éviter l'utilisation de solvants organiques, une autre technique consiste à faire fondre le lipide et l'émulsifier à chaud avec une solution aqueuse contenant le tensioactif. Cette technique est fréquemment utilisée car elle est simple et offre de bons rendements d'encapsulation des molécules lipophiles **[41]**. La méthode d'homogénéisation sous haute pression à froid consiste à dissoudre le principe actif dans les lipides fondus, à laisser solidifier l'ensemble puis à le porphyriser dans un mortier. Les particules obtenues sont dispersées dans une phase aqueuse contenant un tensioactif. La taille des particules de la suspension obtenue sera réduite par un ou plusieurs passages sous pression à travers l'homogénéisateur **[42]**.

L'émulsification membranaire a été également appliquée à la préparation de particules lipidiques solides **[20]**. Dans ce cas, les deux phases sont chauffées séparément à une température supérieure à la température de fusion du lipide. Une pression est appliquée à la phase lipidique afin de passer à travers les pores d'une membrane dans la phase aqueuse. Il y a alors formation de gouttelettes lipidiques à la sortie des pores membranaires sous un flux de phase aqueuse, générant une émulsion H/E, qui après refroidissement donnera lieu à une suspension de particules lipidiques solides. Cette technique présente l'avantage de se faire en une seule étape et de fournir des particules monodisperses, toutefois le colmatage des membranes résultant du passage de la phase lipidique peut limiter son utilisation.

Les particules lipidiques solides peuvent être administrées par voie orale, intramusculaire, sous-cutanée, topique, etc **[43]**. La voie d'administration pulmonaire n'a été, jusqu'à présent, que très peu étudiée.

3. Utilisation des contacteurs à membrane pour la préparation des formes colloïdales

Après ce bref état des lieux, il apparaît que les formes colloïdales d'encapsulation des principes actifs représentent par excellence les formes médicamenteuses d'avenir. Afin de garantir un développement rapide de ces formes, qui permettraient de les mettre rapidement sur le marché, il existe un besoin réel de développer des procédés de fabrication fiables, simples, faciles et permettant, de façon reproductible, la préparation de vecteurs présentant des caractéristiques appropriées. Les procédés à

base de contacteurs à membrane semblent répondre aux exigences requises d'un procédé pharmaceutique et peuvent donc convenir à la préparation des systèmes d'encapsulation des molécules actives. L'application des technologies membranaires à la production des nano-vecteurs serait un atout considérable pour le développement et l'intensification des procédés industriels de fabrication. Une grande partie de cette thèse sera consacrée au développement des formes colloïdales (liposomes, micelles, nano-émulsion, particules lipidiques solides) par des méthodes basées sur des contacteurs membranaires.

Références

[1] Vladisavljević G. T., Williams R. A., Recent developments in manufacturing emulsions and particulate products using membranes, Advanced Colloid and Interface Science 113 (2005) 1–20.

[2] Charcosset C. Membrane processes in biotechnology: an overview. Biotechnology Advances 24 (2006) 482–492.

[3] Drioli E., Curcio E., Di Profio G. State of the art and recent progresses in membrane contactors. Chemical Engineering Research and Design 83 A3 (2005) 223–233.

[4] Stillwell M. T., Holdich R. G., Kosvintsev S. R., Gasparini G., Cumming I. W. Stirred cell membrane emulsification and factors influencing dispersion drop size and uniformity. Industrial and Engineering Chemistry Research 46 (2007) 965–972.

[5] Kosvintsev S. R., Gasparini G., Holdich R. G., Cumming I. W., Stillwell M. T. Liquid-liquid membrane dispersion in a stirred cell with and without controlled shear. Industrial and Engineering Chemistry Research 44 (2005) 9323–9330.

[6] Aryanti N., Hou R., Williams R. A., Performance of a rotating membrane emulsifier for production of coarse droplets, Journal of Membrane Science 326 (2009) 9–18.

[7] Aryanti N., Williams R. A., Hou R., Vladisavljevic G. T. Performance of rotating membrane emulsification for o/w production. Desalination 200 (2006) 572–574.

[8] Vladisavljević G. T., Shimizu M., Nakashima T. Preparation of monodisperse multiple emulsions at high production rates by multi-stage premix membrane emulsification. Journal of Membrane Science 244 (2004) 97–106.

[9] Nazir A., Schroën K., Boom R. Premix emulsification: A review. Journal of Membrane Science 362 (2010) 1–11.

[10] Vladisavljević G. T., Shimizu M., Nakashima T. Permeability of hydrophilic and hydrophobic Shirasu-porous-glass (SPG) membranes to pure liquids and its microstructure. Journal of Membrane Science 250 (2005) 69–77.

[11] Vladisavljević G. T., Kobayashi I., Nakajima M., Williams R. A., Shimizu M., Nakashima T. Shirasu porous glass membrane emulsification: Characterization of membrane structure by high-resolution X-ray microtomography and microscopic observation of droplet formation in real time. Journal of Membrane Science 302 (2007) 243–253.

[12] Geerken M. J., Lammertink R. G. H., Wessling M. Tailoring surface properties for controlling droplet formation at microsieve membranes. Colloids and Surface A 292 (2007) 224–235.

[13] Laouini A., Jaafar-Maalej C., Sfar S., Charcosset C., Fessi H. Liposome preparation using a hollow fiber membrane contactor–Application to spironolactone encapsulation. International Journal of Pharmaceutics 415 (2011) 53-61.

[14] Nakashima T., Shimizu M., Kukizaki M. Particle control of emulsion by membrane emulsification and its application. Advanced Drug Delivery Reviews 45 (2000) 47–56.

[15] Oh D. H., Balakrishnan P., Ohc Y. K., Kim D. D., Yong C. S., Choi H. G. Effect of process parameters on nanoemulsion droplet size and distribution in SPG membrane emulsification. International Journal of Pharmaceutics 404 (2011) 191–197.

[16] Higashi S. et Setoguchi T. Hepatical arterial injection chemotherapy for hepatocellular carcinoma with epirubicin aqueous solution as numerous vesicles in iodinated poppyseed oil microdroplets: clinical application of water in oil in water emulsion prepared using a membrane emulsification technique. Advanced Drug Delivery Reviews 45 (2000) 57–64.

[17] Costa M. et Cardoso M. Effect of uniform sized polymeric microspheres prepared by membrane emulsification technique on controlled release anthracycline anti-cancer drugs. Desalination 200 (2006) 498–500.

[18] Ribeiro H., Rico L., Badolato G., Schubert H. Production of O/W emulsions containing astaxanthin by repeated premix membrane emulsification. Journal of Food Science E 70 (2005) 117–123.

[19] Liu R., Huang S., Wan Y., Ma G., Su Z. Preparation of insulin-loaded PLA/PLGA microcapsules by a novel membrane emulsification method and its release in vitro. Colloids and Surfaces B 51 (2006) 30–38.

[20] Charcosset C., El Harati A., Fessi H. Preparation of solid lipid nanoparticles using a membrane contactor. Journal of Controlled Release 108 (2005) 112–120.

[21] Limayem-Blouza I., Charcosset C., Sfar S., Fessi H. Preparation and characterization of spironolactone-loaded nanocapsules for paediatric use. International Journal of Pharmaceutics 325 (2006) 124–131.

[22] Jaafar-Maalej C., Charcosset C., Fessi H. A new method of liposome preparation using a membrane contactor. Journal of Liposome Research 3 (2011) 313-320.

[23] Edwards K. A. et Baeumner A. J. Analysis of liposomes. Talanta 68 (2006) 1432-1441.

[24] Bangham A. D., Standish M. M., Watkins J.C. Diffusion of univalent ions across the lamellae of swollen phospholipids. Journal of Molecular Biology 13 (1965) 238–252.

[25] Szoka F. et Papahadjopoulos D. Procedure of preparation of liposomes with large internal aqueous space and high capture by reverse-phase evaporation. Biochemistry 75 (1978) 4194–4198.

[26] Batzri S. et Korn E. D. Single bilayer liposomes prepared without sonication. Biochimica and Biophysica Acta 298 (1973) 1015–1019.

[27] Wagner A., Vorauer-Uhl K., Kreismayr G., Katinger H. Enhanced protein loading into liposomes by the multiple crossflow injection technique. Journal of Liposome Research 12 (2002) 271-283.

[28] Jones M. C. et Leroux J. C. Polymeric micelles – A new generation of colloidal drug carriers. European Journal of Pharmaceutics and Biopharmaceutics 48 (1999) 101-111.

[29] Yang L., Wu X., Liu F., Duan Y., Li S. Novel biodegradable polylactide/poly(ethylene glycol) micelles prepared by direct dissolution method for controlled delivery of anticancer drugs. Pharmaceutical Research 26 (2009) 2332−2342.

[30] Zeng, F., Liu, J., Allen C. Synthesis and Characterization of Biodegradable Poly(ethylene glycol)-block-poly(5-benzyloxy-trimethylene carbonate) Copolymers for Drug Delivery. Biomacromolecules 5 (2004) 1810−1817.

[31] Yokoyama M., Opanasopit P., Okano T., Kawano K., Maitani Y. Polymer design and incorporation methods for polymeric micelle carrier system containing water-insoluble anti-cancer agent camptothecin. Journal of Drug Targeting 12 (2004) 373−384.

[32] Tyrrell Z. L., Shen Y., Rados M. Fabrication of micellar nanoparticles for drug delivery through the self-assembly of block copolymers Progress in Polymer Science 35 (2010) 1128−1143.

[33] Aliabadi H. M. et Lavasanifar A. Polymeric micelles for drug delivery. Expert Opinion in Drug Delivery 3 (2006) 139−162.

[34] Solans C., Izquiedro P., Nolla J., Azemar N., Garcia-Celma M. J. Nano-emulsions. Current opinion in Colloid and Interface Science 10 (2005) 102-110.

[35] Urban K., Wagner G., Schaffner D., Roglin D., Ulrich J. Rotor–stator and disc systems for emulsification processes. Chemical Engineering Technology 29 (2006) 24–31.

[36] Schutz S., Wagner G., Urban K., Ulrich J. High-pressure homogenization as a process for emulsion formation. Chemial Engineering Technology 27 (2004) 361–368.

[37] Floury J., Desrumaux A., Legrand J. Effect of ultra-high-pressure homogenization on structure and on rheological properties of soy protein-stabilized emulsions. Journal of Food Science 67 (2002) 3388–3395.

[38] Izquiedro P., Esquena J., Tadros T. F., Dederen C., Feng J., Garcia M. J. et al. Formation and stability of nano-emulsions prepared using the phase inversion temperature method. Langmuir 18 (2002) 26–30.

[39] Mehnert W. et Mader K. Solid lipid nanoparticles : Production, characterization and applications. Advanced Drug Delivery Reviews 47 (2001) 165-196.

[40] Reithmeier H., Herrmann J., Gopferich A. Development and characterization of lipid microparticles as a drug carrier for somatostatin. International Journal of Pharmaceutics 218 (2001) 133-143.

[41] Bodmeier R., Wang J., Bhagwatwar H. Process and formulation variables in the preparation of wax microparticles by a melt dispersion technique. I: Oil-in-water technique for water-insoluble drugs. Journal of Microencapsulation 9 (1992) 89-98.

[42] Demirel M., Yazan Y., Muller R. H., Kilic F., Bozan B. Formulation and in vitro-in vivo evaluation of piribedil solid lipid micro- and nanoparticles. Journal of Microencapsulation 18 (2001) 359-371.

[43] Esposito E., Cortesi R., Nastruzzi C. Production of lipospheres for bioactive compound delivery. In: Lipospheres in drug targets and delivery: Approaches, methods and applications, Nastruzzi C. Ed (2005) 23-40.

Encapsulation de la Vitamine E dans des Liposomes en Utilisant des Membranes Microsieves

Encapsulation de la vitamine E dans des liposomes en utilisant des membranes microsieves

Les liposomes sont des vésicules constituées d'un volume interne aqueux entouré d'une ou de plusieurs bicouches lipidiques concentriques. Ils sont de plus en plus développés dans la recherche pharmaceutique comme vecteurs de médicaments car ils permettent d'encapsuler des principes actifs de solubilité différente.

Depuis la découverte des liposomes par Bangham dans les années 1960, plusieurs techniques de préparation ont été rapportées dans la littérature. On peut citer : la méthode de réhydratation du film lipidique, la méthode d'évaporation en phase inverse, la méthode par sonication et la méthode d'injection de solvant. L'utilisation des contacteurs à membrane pour la préparation des liposomes constitue une amélioration de la méthode d'injection de solvant puisqu'elle permet un meilleur contrôle de la diffusion de la phase organique au sein de la phase aqueuse.

Au cours de ce travail, principalement réalisé à l'Université de Loughborough (Grande Bretagne), des membranes microsieves ont été utilisé pour la première fois pour la préparation de suspensions de liposomes. Ces membranes ont la particularité de présenter une parfaite uniformité de la taille des pores et de la distance inter-pores; propriété qui pourrait permettre une meilleure maîtrise des caractéristiques des liposomes en particulier la distribution de taille.

Il en sort principalement de ce travail que la taille des liposomes peut être parfaitement ajustée par la variation des différents paramètres expérimentaux : concentration en phospholipides, vitesse d'agitation de la phase aqueuse, caractéristiques de la membrane utilisée, etc. Le procédé optimisé présente une bonne reproductibilité et s'apprête facilement à une production à large échelle. Les liposomes préparés présentent une bonne stabilité

Ce chapitre sera présenté sous forme de quatre articles :

- Le premier article est une revue bibliographique publiée en 2012 dans le « Journal of Colloid Science and Biotechnology ». Cette revue présente les différentes méthodes de préparation et les diverses techniques de caractérisation des liposomes. Elle présente aussi les différentes applications des liposomes principalement en pharmacie.

- Le deuxième article, publié en 2013 dans « RSC Advances » (un journal de la « Royal Society of Chemistry ») décrit les différentes étapes de développement d'un procédé de préparation des liposomes en utilisant des membranes microsieves.

Le procédé de fabrication ainsi optimisé est appliqué à l'encapsulation de la vitamine E.

- Le troisième article, publié en 2013 dans « Colloids and Surface B », détaille le « scale-up » du procédé de préparation des liposomes de l'échelle du laboratoire à une échelle plus large; différentes techniques sont comparées.

- Le quatrième article, soumis pour publication dans « Colloids and Surface A », présente les résultats de préparation de liposomes en utilisant un système micro-fluidique. Des enregistrements vidéo, ayant permis l'observation de la formation des vésicules lipidiques suite au contact entre les phases aqueuse et organique, sont comparés à des simulations réalisées à l'aide d'un logiciel mathématique.

Preparation, Characterization and Applications of Liposomes: State of the Art

Abdallah Laouini[1], Chiraz Jaafar-Maalej[1], Imen Limayem-Blouza[2], Souad Sfar-Gandoura[2], Catherine Charcosset[1], Hatem Fessi[1]

[1] : Université Claude Bernard Lyon 1, Laboratoire d'Automatique et de Génie des Procédés (LAGEP), UMR-CNRS 5007, CPE Lyon, Bât 308G, 43 Boulevard du 11 Novembre 1918, F-69622 Villeurbanne Cedex, France.

[2] : Université de Monastir, Laboratoire de Pharmacie Galénique, Faculté de Pharmacie, Rue Avicenne, 5000 Monastir, Tunisie

Journal of Colloid Science and Biotechnology, 1, 147-168, 2012

Abstract

Liposomes, spherical-shaped nanovesicles, were discovered in the 60ies by Bangham. Since that, they were extensively studied as potential drug carrier. Due to their composition variability and structural properties, liposomes are extremely versatile leading to a large number of applications including pharmaceutical, cosmetics and food industrial fields. This bibliographic paper offers a general review on the background and development of liposomes with a focus on preparation methods including classic (thin film hydration, reverse-phase evaporation, ethanol injection…) and novel scalable techniques. Furthermore, liposome characterization techniques including mean size, zeta potential, lamellarity, encapsulation efficiency, in vitro drug release, vesicles stability and lipid analysis synthesized from different published works are reported. The current deepening and widening of liposome interest in many scientific disciplines and their application in pharmaceutics, cosmetics and food industries as promising novel breakthroughs and products were also handled. Finally, an opinion on the usefulness of liposomes in various applications ranging from unsubstantiated optimism to undeserved pessimism is given. The obtained information allows establishing criteria for selecting liposomes as a drug carrier according to its advantages and limitations.

Key words: Liposomes - Preparation Methods - Characterization – Phospholipids - Therapeutic Application – Cosmetic - Food.

Contents

1. Introduction

Liposomes, defined as microscopic spherical-shaped vesicles, consist of an internal aqueous compartment entrapped by one or multiple concentric lipidic bilayers. Liposomes membrane is composed of natural and/or synthetic lipids which are relatively biocompatible, biodegradable and non-immunogenic material. Because of their unique bilayer-structure properties, liposomes are used as carriers for both lipophilic and water-soluble molecules. Hydrophilic substances are encapsulated in the interior aqueous compartments. Lipophilic drugs are mainly entrapped within lipid bilayers.

As asserted by different authors, liposomes have attractive biological properties, including the biocompatibility and biodegradability. They show promise as active vectors due to their capacity to enhance the encapsulant performance by increasing drug solubility, and stability; delivering encapsulated drugs to specific target sites, and providing sustained drug release **[1]**. Their sub-cellular size allows relatively higher intracellular uptake than other particulate systems; improving *in vivo* drug bioavailability. Other advantages of liposomes include high encapsulation efficiency inspite of drug solubility, low toxicity due to phospholipids content, drug protection against degradation factors like pH and light and the reduction of tissue irritation.

Liposomes have been extensively studied as drug carriers in the pharmaceutical and medical fields **[1, 2]**.Research has expanded considerably over the last 30 years, increasing applications area from drug and gene delivery to diagnostics, cosmetics, long-lasting immune-contraception to food and chemical industry **[3]**. The superiority of liposomes as drug carriers has been widely recognized. Ten liposomal and lipid-based formulations have been approved by regulatory authorities and many liposomal drugs are in preclinical development or in clinical trials **[4]**.

Several reviews about liposomes as drug delivery systems **[5]** and specific application via oral **[6, 7]**, topical **[8]**, pulmonary **[9, 10]**, and ophthalmic **[11]** route have been published. Clearly, within the frame of a single review paper it is impossible to address all the pertinent issues, this bibliographic paper attempt to review liposomes current technology with respect to numerous multidisciplinary applications. As a contribution for updating the state of knowledge, a focuses on liposomes preparation method and recent characterization techniques including mean size, zeta-potential, lamellarity, encapsulating efficiency, in vitro active release, stability and lipid analysis have been described as well as the most significant achievements and applications.

2. Liposomes

2.1 Definition

Liposomes were first produced in England in the 60's, by Bangham who was studying phospholipids and blood clotting **[12]**. According to legend, he was experimenting with new laboratory equipment, and he made a noted observation about phospholipids forming closed multilamellar vesicle spontaneously in aqueous solution which took two years to be proved. The phospholipid reorganisation in aqueous solution is mainly driven by the hydrophobic effect which organizes amphiphilic molecules (phospholipids) so as to minimize entropically unfavorable interactions between hydrophobic acyl-chains and surrounding aqueous medium **[13, 14]**.This effect is further settled by various intermolecular forces such as electrostatic interactions, hydrogen bonding, as well as Vanderwaals and dispersion forces **[15]**.

Liposomes were defined as an artificial microscopic vesicle consisting of a central aqueous compartment surrounded by one or more concentric phospholipid layers (lamellas) **(Fig. 1)**. Furthermore, hydrophilic (in the aqueous cavity), hydrophobic (within lipidic membrane) and amphiphilic substances are able to be incorporated within these vesicles developing large potential applications. Numerous researchers have worked with these structures since Bangham's discovery, making of liposomes the most popular nanocarrier systems **[16]**.

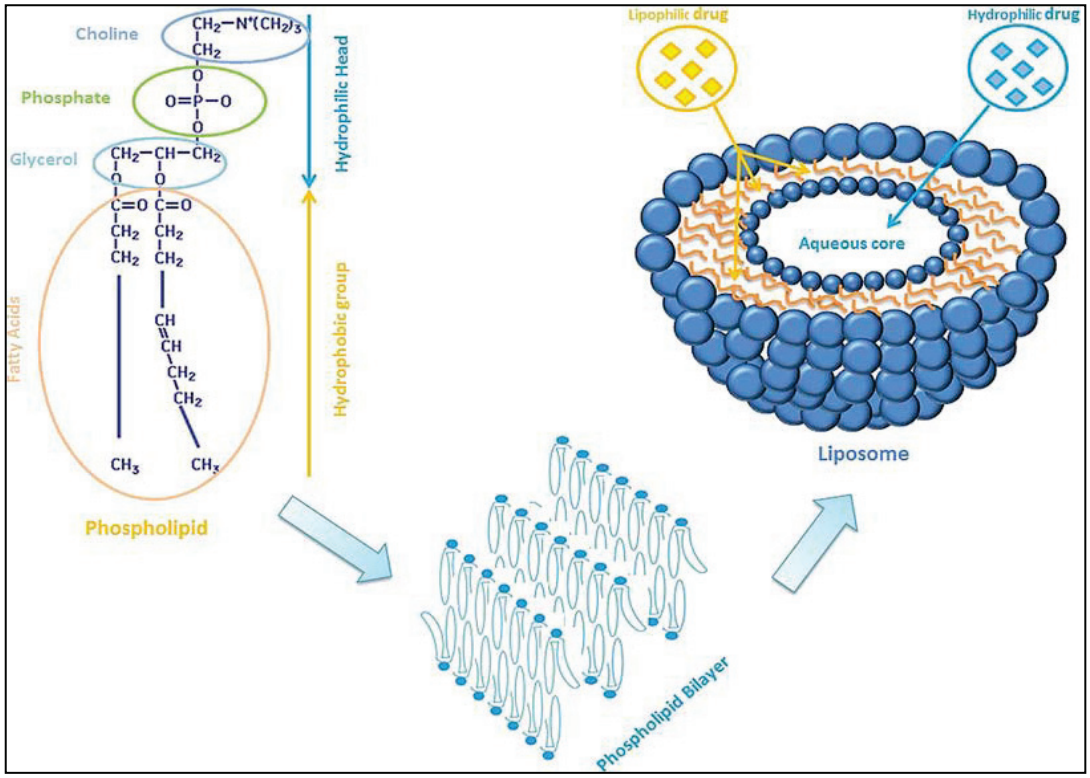

Fig. 1. Schematic drawing of liposomes structure and lipophilic or hydrophilic drug entrapment models.

2.2 Classification

Liposomes can be classified in terms of composition and mechanism of intracellular delivery into five types **[17]**: (i) conventional liposomes; (ii) pH-sensitive liposomes; (iii) cationic liposomes; (iv) immunoliposomes and (v) long-circulating liposomes.

Otherwise, vesicle size is a critical parameter in determining circulation half-life of liposomes, and both size and number of bilayers influence the extent of drug encapsulation within liposomes. Thus, liposomes were typically classified on the basis of their size and number of bilayers into **(Fig. 2)**: (i) Small unilamellar vesicles (SUV): 20 – 100 nm; (ii) Large unilamellar vesicles (LUV): > 100 nm; (iii) Giant unilamellar vesicles (GUV): > 1000 nm; (iv) Oligolamellar vesicle (OLV): 100 – 500 nm and (v) Multilamellar vesicles (MLV): > 500 nm **[18]**. New developed types of liposome, designated as double liposome (DL) **[19]** and multivesicular vesicles (MVV) **[20]**, were recently reported. These liposomes, which could be prepared by novel preparative technique, are thought to improve drug protection against several enzymes **[21]**.

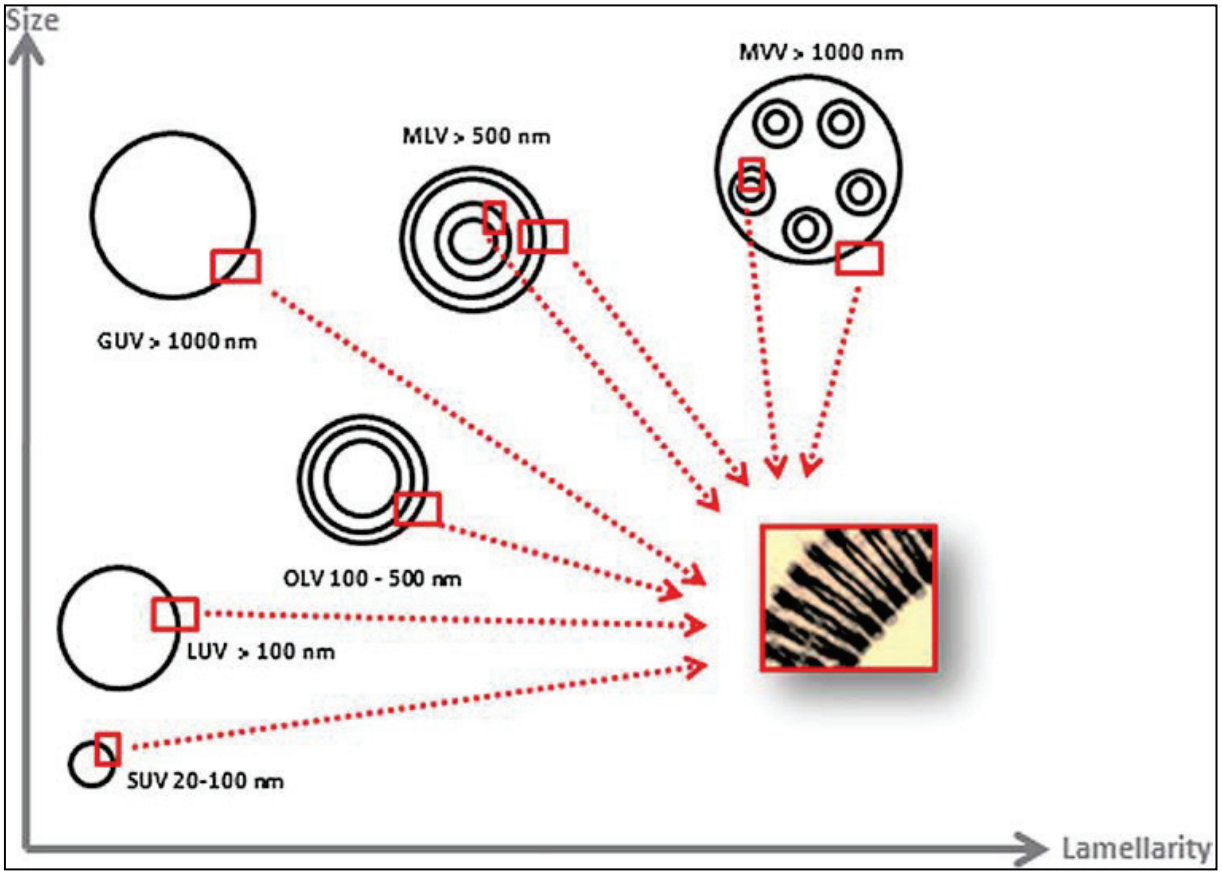

Fig. 2. Liposomes classification based on size and lamellarity.

3. Liposomes preparation procedures

3.1 General ingredients

Generally, liposome composition includes natural and/or synthetic phospholipids (Phosphatidylethanolamine, Phosphatidylglycerol, Phosphatidylcholline, Phosphatidylserine, Phosphatidylinositol) Phosphatidylcholine (also known as lecithin) and phosphatidylethanolamine constitute the two major structural components of most biological membranes. Liposome bilayers may also contain other constituents such as cholesterol, hydrophilic polymer conjugated lipids and water. Cholesterol has been largely used to improve the bilayer characteristics of the liposomes. It improves the membrane fluidity, bilayer stability and reduces the permeability of water soluble molecules through the membrane **[22]**. A clear advantage of liposomes is the fact that the lipid membrane is made from physiological lipids which decreases the danger of acute and chronic toxicity.

3.2 Preparation methods

3.2.1 Classical techniques

There are four classical methods of liposome manufacture. The difference between the various methods is the way in which lipids are drying down from organic solvents and then redispersed in aqueous media **[23]**. These steps are performed individually or are mostly combined.

Hydration of a thin lipid film: Bangham method. This is the original method which was initially used for liposomes production **[24]**. A mixture of phospholipid and cholesterol were dispersed in organic solvent. Then, the organic solvent was removed by means of evaporation (using a rotary evaporator at reduced pressure). Finally, the dry lipidic film deposited on the flask wall was hydrated by adding an aqueous buffer solution under agitation at temperature above the lipid transition temperature. This method is widespread and easy to handle, however, dispersed-phospholipids in aqueous buffer yields a population of multilamellar liposomes (MLVs) heterogeneous both in size and shape (1 – 5 μm diameter). Thus, liposome size reduction techniques, such as sonication for SUVs formation or extrusion through polycarbonate filters forming LUVs **[25, 26]** were useful to produce smaller and more uniformly sized population of vesicles.

Reverse-phase evaporation (REV) technique. A lipidic film is prepared by evaporating organic solvent under reduced pressure. The system is purged with nitrogen and the lipids are re-dissolved in a second organic phase which is usually constituted by diethyl ether and/or isopropyl ether. Large unilamellar and oligolamellar vesicles are formed when an aqueous buffer is introduced into this mixture. The organic solvent is subsequently removed and the system is maintained

under continuous nitrogen. These vesicles have aqueous volume to lipid ratios that are 30 times higher than sonicated preparations and 4 times higher than multilamellar vesicles. Most importantly, a substantial fraction of the aqueous phase (up to 62% at low salt concentrations) is entrapped within the vesicles, encapsulating even large macromolecular assemblies with high efficiency **[27]**.

Solvent (ether or ethanol) injection technique. The solvent injection methods involve the dissolution of the lipid into an organic phase (ethanol or ether), followed by the injection of the lipid solution into aqueous media, forming liposomes **[28]**. The ethanol injection method was first described in 1973 **[29]**. The main relevance of the ethanol injection method resides in the observation that a narrow distribution of small liposomes (under 100 nm) can be obtained by simply injecting an ethanolic lipid solution in water, in one step, without extrusion or sonication **[30]**. The ether injection method differs from the ethanol injection method since the ether is immiscible with the aqueous phase, which is also heated so that the solvent is removed from the liposomal product. The method involves injection of ether-lipid solutions into warmed aqueous phases above the boiling point of the ether. The ether vaporizes upon contacting the aqueous phase, and the dispersed lipid forms primarily unilamellar liposomes **[31]**. An advantage of the ether injection method compared to the ethanol injection method is the removal of the solvent from the product, enabling the process to be run for extended periods forming a concentrated liposomal product with high entrapment efficiencies.

Detergent Dialysis. Liposomes, in the size range of 40–180 nm, are formed when lipids are solubilized with detergent, yielding defined mixed micelles **[32]**. As the detergent is subsequently removed by controlled dialysis, phospholipids form homogeneous unilamellar vesicles with usefully large encapsulated volume.

Other methods have been already used for liposomes preparation such as: calcium induced fusion **[33]**, nanoprecipitation **[34]**, and emulsion techniques **[35, 36]**.

The described classical techniques require large amounts of organic solvent, which are harmful both to the environment and to human health, requiring complete removal of residual organic solvent. Furthermore, conventional methods consist of many steps for size homogenization and consume a large amount of energy which is unsuitable for the mass production of liposomes.

3.2.2 New large-scale techniques

Since industrial scale production of liposomes has become reality, the range of liposome preparation methods has been extended by a number of techniques such as heating method, spray drying, freeze drying, super critical reverse phase evaporation

(SCRPE), and several modified ethanol injection techniques which are increasingly attractive.

Heating method. A new method for fast production of liposomes without the use of any hazardous chemical or process has been described **[23]**. This method involves the hydration of liposome components in an aqueous medium followed by the heating of these components, in the presence of glycerol (3% v/v), up to 120 °C. Glycerol is a water-soluble and physiologically acceptable chemical with the ability to increase the stability of lipid vesicles and does not need to be removed from the final liposomal product. Temperature and mechanical stirring provide adequate energy for the formation of stable liposomes. *Reza Mozafari et al.* confirmed by TLC that no degradation of the used lipids occurred at the above mentioned temperatures **[37]**. The particle size can be controlled by the phospholipid nature and charge, the speed of the stirring and the shape of the reaction vessel. Otherwise, employment of heat abolishes the need to carry out any further sterilisation procedure reducing the time and cost of liposome production.

Spray-Drying. Since spray-drying is a very simple and industrially applicable method, the direct spray-drying of a mixture of lipid and drug was applied in the preparation of liposomes **[38]**. The spray-drying process is considered to be a fast single-step procedure applied in the nanoparticles formulation. Hence, liposomes were prepared by suspending lecithin and mannitol in chloroform. The mixture was sonicated for 8 min (bath sonicator) and subjected to spray-drying on a Buchi 190 M Mini Spray Dryer. The spray-drying conditions were as follows: inlet and outlet temperatures were 120 °C and 80°C, respectively; airflow rate was 700 NI/hr; and the flow rate was 1000 ml/hr. The dried product was hydrated with different volumes of phosphate buffered saline (PBS; pH 7.4) by stirring for 45 min **[38]**. The main factor influencing the liposomal size was the volume of aqueous medium used for hydration of the spray-dried product **[38]**. However, mannitol plays an important role in increasing the surface area of the lipid mixture, enabling successful hydration of the spray-dried product.

Freeze Drying. This new method was described for the preparation of sterile and pyrogen-free submicron narrow sized liposomes **[39, 40]**. It is based on the formation of a homogenous dispersion of lipids in water-soluble carrier materials. Liposome-forming lipids and water-soluble carrier materials such as sucrose were dissolved in tert-butyl alcohol/water cosolvent systems in appropriate ratios to form a clear isotropic monophase solution. Then the monophase solution was sterilized by filtration and filled into freeze-drying vials. In recent study, a laboratory freeze drier was used and freeze-drying process was as follows: freezing at − 40 °C for 8 h; primary drying at − 40 °C for 48 h and secondary drying at 25 °C for 10 h **[39]**. The chamber pressure was maintained at 20 Pascal during the drying process. On addition of water, the

lyophilized product spontaneously forms homogenous liposome preparation. After investigation of the various parameters associated with this method it is found that the lipid/carrier ratio is the key factor affecting the size and the polydispersity of the liposome preparation **[39]**. Therefore, TBA/water cosolvent system was used for economy concerns.

Super critical reverse phase evaporation (SCRPE). The SCRPE is a one-step new method that has been developed for liposomes preparation using supercritical carbon dioxide **[41]**. This method allowed aqueous dispersions of liposomes to be obtained through emulsion formation by introducing a given amount of water into a homogeneous mixture of supercritical carbon dioxide/LR-dipalmitoylphosphatidylcholine/ethanol under sufficient stirring and subsequent pressure reduction. Transmission electron microscopy observations revealed that vesicles are large unilamellar with diameters of 0.1 – 1.2 μm **[41]**. The trapping efficiency of these liposomes indicated more than 5 times higher values for the water-soluble solute compared to multilamellar vesicles prepared by the Bangham method. The trapping efficiency for an oil-soluble substance, the cholesterol, was about 63%. Results showed that the SCRPE is an excellent technique that permits one-step preparation of large unilamellar liposomes exhibiting a high trapping efficiency for both water-soluble and oil-soluble compounds **[42, 43]**.

Modified Ethanol Injection Method. Novel approaches based on the principle of the ethanol injection technique such as the microfluidic channel method **[44 – 46]**, the crossflow-injection technique **[47 – 50]**, and the membrane contactor method **[51]** were recently reported for liposome production.

The Crossflow Injection Technique. The concept of continuous crossflow injection is a promising approach as a novel scalable liposome preparation technique for pharmaceutical application. *Wagner et al.* used a cross flow injection module made of two tubes welded together forming a cross **[47 – 50]**. At the connecting point, the modules were adapted with an injection hole. The influencing parameters such as the lipid concentration, the injection hole diameter, the injection pressure, the buffer flow rate, and system performance were investigated **[47]**. A minimum of buffer flow rate is required to affect batch homogeneity and strongly influencing parameters are lipid concentration in combination with increasing injection pressures. After exceeding the upper pressure limit of the linear range, where injection velocities remain constant, the vesicle batches are narrowly distributed, also when injecting higher lipid concentrations. Reproducibility and scalability data show similar results with respect to vesicle size and size distribution and demonstrate the stability and robustness of the novel continuous liposome preparation technique **[49]**.

Table1. Preparation methods and applications through published papers

Preparation method	Active substance	Vesicle composition	Solvent / adjuvants	Size	Zeta potential (mV)	Encapsulation efficiency (%)	Study details	References
Hydration lipid film	Ibuprofen	- Egg Phosphatidylcholine - Distearoyl Phosphatidylcholine - Dilignoceroyl phosphatidylcholine - Stearylamine - Dicetylphosphate - Cholesterol	- Solvent mixture of chloroform and methanol - Distilled water	4.2 – 6 µm	-52 – 54	17 – 61	- Effect of the cholesterol content, lipid alkyl chain length, and charged lipids on liposomes characteristics	**[52]**
Reverse phase evaporation	Acetazolamide	- Egg phosphatidylcholine - Cholesterol - Stearylamine - Dicetyl phosphate	- Solvent mixture of chloroform and methanol - Ether	5.8 – 7.5 µm		10 – 45	- Effect of cholesterol contents and charged lipids on liposomes characteristics. - Photomicroscopic analysis. - Differential scanning calorimetry measurements. - Stability study. - *In-vivo* studies (male rabbits).	**[53]**

Preparation method	Active substance	Vesicle composition	Solvent / adjuvants	Size	Zeta potential (mV)	Encapsulation efficiency (%)	Study details	References
Ethanol injection	Salidroside	- Egg yolk phosphatidylcholine - Cholesterol	- Absolute ethanol	50 – 100 nm	0 – -18	20 – 40	- Effect of salidroside loading amount on encapsulation efficiency. - Effect of cholesterol on encapsulation efficiency and particle size. - Turbidity measurements. - *In-vitro* release study.	**[54]**
Detergent dialysis		- Egg phosphatidylcholine - Egg phosphatidylglycerol	- 2 detergents: sodium cholate and octyl-d-glucopyranoside - Custom made dialysis cell (7.1 cm^2 exchange area)	60 – 160 nm	-7 – -51		- Dynamic light scattering and zeta potential measurements. - Cryo-transmission electron microscopy. - Comparison of size and size distribution data obtained from both methods	**[55]**

Preparation method	Active substance	Vesicle composition	Solvent / adjuvants	Size	Zeta potential (mV)	Encapsulation efficiency (%)	Study details	References
Emulsion (double emulsification process)	Bovin serum albumin (BSA)	- Egg phosphatidylcholine - Triolein - Cholesterol	- Chloroform and ether - 4% glucose aqueous solution	10 – 30 µm		43 – 71	- Factors impacting encapsulation efficiency of multivesicular liposomes. - Analysis of BSA in liposomes-in-alginate (LIA) - *In-vitro* protein release from (LIA) - Check the improvement in entrapment efficiency and release behavior	**[56]**
Heating method	Plasmid DNA from E. Coli	- Dipalmitoyl-phosphatidylcholine - Dicetylphosphate - Cholesterol	- Sterile phosphate buffered saline glycerol	160 – 2250 nm			- Evaluation of transfection efficiency and cytotoxicity using Chinese hamster ovary K1 cells	**[57]**
Spray drying	Metronidazole / Verapamil hydrochlride	- Lecithin	- Mannitol - Chloroform	268 – 395 nm		24 – 47	- Serum stability study	**[38]**

Preparation method	Active substance	Vesicle composition	Solvent / adjuvants	Size	Zeta potential (mV)	Encapsulation efficiency (%)	Study details	References
Freeze drying	Ketoprofen / Ciprofloxacin lactate / Propanolol hydrochloride	- Soybean phosphatidylcholine - Soybean phosphatidylserine	- Sucrose - Tert-butyl alcohol - water	110 – 410 nm			- Size measurments - entrapment studies - Electron microscopy - Thermal analysis - X-ray diffraction	**[39]**
	Calcein	- Soybean phosphatidylcholine - Hydrogenated soybean phosphatidylserine - Cholesterol	- Sucrose - Tert-butyl alcohol - water	100 nm			- Size measurment - Entrapment efficiency - Thermal analysis - Cryomicroscopy - Mass loss analysis - Residual solvent content	**[40]**
Supercritical reverse phase evaporation	Glucose	- Dipalmitoyl-phosphatidylcholine		< 2000 nm	0 – 30	15 – 20	- Trapping efficiency - Dynamic light scattering - Zeta potential - Freeze-fracture transmission electron microscopy	**[42, 43]**

Preparation method	Active substance	Vesicle composition	Solvent / adjuvants	Size	Zeta potential (mV)	Encapsulation efficiency (%)	Study details	References
Microfluidic channel		- Egg phosphatidylcholine - Hydrogenated Soy phosphatidylcholine - Cholesterol	- Ethanol - tert-butanol	50 – 160 nm				**[46]**
		- Dimyristoyl-phosphatidylcholine - Cholesterol - Dihexadecyl-phosphate	- Isopropyl alcohol	25 – 50 nm				**[44]**
Cross flow injection		- Dipalmitoyl-phosphatidylcholine - Cholesterol - Stearylamine	- Ethanol	100 – 200 nm				**[48]**
	Recombinant human superoxide dismutase from E. Coli	- Dipalmitoyl-phosphatidylcholine - Cholesterol - Stearylamine	- Ethanol	200 – 300 nm		25 – 27		**[47]**
Membrane contactor	Indomethacin / Beclomethasone diproprionate	- Lipoid E 80 - Cholesterol	- Ethanol - Tert-butanol	100 – 180 nm	-35 – -6	63 - 98	- Size measurement - Zeta potential - Entrapment efficiency - Thermal analysis - Electron transmission microscopy	**[51]**

Microfluidization. By using a microfluidic hydrodynamic focusing (MHF) platform, *Jahn et al.* generated liposomes by injecting the lipid phase and the water phase into a microchannel **[45]**. Microfluidic flow is generally laminar due to the small channel dimensions and relatively low flow rates. Well-defined mixing is then obtained by interfacial diffusion when multiple flow streams are injected in a microchannel. The size of the liposomes was mainly controlled by changing the flow rate **[44]**.

Membrane Contactor. Recently, *Jaafar-Maalej et al.* applied the ethanol injection technique while using a membrane contactor for large scale liposomes production. In this method, a lipid phase (ethanol, phospholipid and cholesterol) was pressed through the membrane with a specified pore size. Nitrogen gas at pressure below 5 bar was sufficient for passing the organic phase through the membrane. At the same time, the aqueous phase flew tangentially to the membrane surface and swept away the formed liposomes within the membrane device. The new process advantages are the design simplicity, the control of the liposome size by tuning the process parameters and the scaling-up abilities **[51]**. As a result, these techniques lead from the conventional batch process to potential large scale continuous procedures.

4. *In-vitro* liposomes characterization

In order to assess the liposome quality and to obtain quantitative measures that allow comparison between different batches of liposomes, various parameters should be monitored. For liposomes applications in analytical and bioanalytical fields, the main characteristics include the average mean diameter and polydispersity index; encapsulation efficiency; the ratio of phospholipids to drug concentration and lamellarity determination. Other commonly monitored parameters include surface charge through zeta potential measurement, phase transitions through differential scanning calorimetry and quantification of residual solvents through gas chromatography. A detailed description of today's most commonly methods and novel techniques of liposome characterization is presented in this report.

4.1 Lamellarity determination

Lipid bilayers number of liposomes influences the encapsulation efficiency and the drugs release kinetics. Furthermore, when liposomes are taken up or processed in the cell, the intracellular fate is affected by the lamellarity. The liposomes lamellarity made from different lipids or preparation procedures varies widely. That is why, the analysis of liposomes lamellarity is an important parameter to be considered.

Liposome lamellarity is often accomplished by methods that are based on the visible or fluorescence signal change of lipids marker upon reagents addition. This approach is reviewed in more detail, since it is a relatively simple procedure that can be easily carried out in a standard lab. Several lipids can be used and results rely on the

comparison of the total signal to the signal achieved from the reaction between the lipids marker and the specified reagents **[58]**.

For example the UV absorbance of 2,4,6-trinitrobenzensulfonic acid (TNBS) at 420 nm increases in the mixture as a result of complex formation with primary amines. This property has been used for the detection of aminolipids at 420 nm. As the lipid bilayers are slightly permeable to the TNBS reagent, an overestimate of the external surface can be expected. To correct the reagent leakage through the bilayer, three incubation times were used. The obtained external surface area at each incubation time was plotted against incubation time and the graph was extrapolated to time zero. Under certain conditions, the bilayer permeability of TNBS is minimized such as the only aminolipids on the exterior bilayer contribute to the signal. Lysis of liposomes by a detergent such as Triton X-100 allows TNBS to interact with interior aminolipids and yields the total signal. TNBS has remained the commonly used method for the estimation of the degree of lamallarity. However, this method has disadvantages which make it impotent in most cases; the TNBS assay requires large amount of material (milligrams) which makes the multiple sample application difficult and affect assay precision when the amount is limited **[59, 60]**.

In another method, the addition of periodate to phosphatidylglycerol results in the diol oxidation and releasing of formaldehyde. The released formaldehyde reacted with chromotropic acid to yield a product which was subsequently detected at 570 nm. This method has been used for the determination of external reactive groups on liposomes **[58]**.

Otherwise, the quenching of N-(7-nitrobenz-2-oxa-1,3-diazol-4-yl) (NBD) fluorescence is obtained by sodium dithionite. NBD-labeled lipids are highly fluorescent at low concentration (<1 mol%) in membranes, but undergo self-quenching at increased concentrations. In this approach, the initial NBD labelled lipids fluorescence is from all lipids in the sample. Under appropriate conditions, the addition of sodium dithionite quenches the fluorescence of only the NBD labelled existing on the outer bilayer. Fluorescence was monitored on spectrofluorometer with excitation and emission wavelengths of 450 nm and 530 nm respectively. The percentage of external lipid is found by dividing the change in fluorescence upon dithionite addition by the total fluorescence **[61 – 63]**.

These methods appear to close a gap in the methodology to determine external surface structure of vesicles. However, these methods assume that the lipid of interest is distributed evenly over all lipid layers, and the reagents used to elicit the signal change are impermeable to the membrane over the time course of the measurements **[64]**.

Other numerous methods for the lamellarity determination such as magnetic resonance were mainly used to study the outside-inside distribution of phospholipids within bilayer and the characterization of model membrane structures. A straightforward application of nuclear magnetic resonance in the quality control of liposomes is the determination of size and lamellarity. Dispersions of MLVs give rise to very broad powder 31P-NMR spectra due to the restricted anisotropic motion whereas SUVs are characterized using a narrow line spectra. It is well known that the paramagnetic ion Mn2+ interacts with the negatively charged phospholipids phosphate causing perturbations of the nuclear spin relaxation times which broaden the 31P-NMR resonance and reduces the quantifiable signal. Presuming that the shift reagent (Mn2+) only interacts with the phospholipids located in the outermost monolayer, the degree of lamellarity can be calculated by the ratio of 31P-NMR signal before and after Mn2+ addition. Used for a long time in the field of liposome research, this technique has been found to be quite sensitive to experimental conditions which can have distinct effect on the analysis. For example, Mn2+ is able to penetrate the liposomal bilayer especially when used at high concentrations. At low pH or in the presence of complexing agents (such as HEPES or TRIS buffer at certain concentration), no penetration of Mn2+ occurs. Therefore, under well-defined conditions, the analysis of liposomes by 31P-NMR is the presence of shift reagent in an elegant and accurate method giving useful information about the outer to inner phospholipids ratio amount **[65,66]**.

Other techniques for lamellarity determination include small angle X-ray scattering (SAXS). For this purpose, liposome dispersions put into glass capillaries and curves were recorded with a camera equipped with a one-dimensional position sensitive detector. Blank scattering curves were obtained from the same capillaries filled with the liposome suspension solvent. Data were evaluated using the Indirect Fourier Transformation which provides the electron distance distribution p(r) (the probability to find two electrons with distance r in the measured sample). SAXS is considered as a good method evaluating vesicles lamellarity with high accuracy **[67, 68]**.

To confirm the lamellarity results by an imaging method, freeze fracture technique with subsequent transmission electron microscopy was used. For this purpose, carbon film grids were used for specimen preparation. A drop of the sample was put on the untreated coated grid. Most of the liquid was removed with blotting paper leaving a thin film stretched over the holes. The specimens were instantly shock-frozen in melting nitrogen or by plunging them into liquid ethane or propane in a temperature controlled freezing unit. After freezing, the specimens were inserted into a cryo-transfer holder and transferred to a cryo-electron microscope. To determine the mean lamellarity, micrographs of three different areas of the specimen were investigated **[66, 69, 70]**.

Whatever is the technique, the lamellarity determination is essential to define liposome structure as it is a very important prerequisite for liposomes success in therapy.

4.2 Size analysis

The average size and size distribution of liposomes are important parameters especially when the liposomes are intended for therapeutic use by inhalation or parenteral route. Several techniques are available for assessing submicrometer liposome size and size distribution which include microscopy techniques, size-exclusion chromatography (SEC), field-flow fractionation and static or dynamic light scattering.

Several variations on electron microscopy (EM) such as transmission EM using negative staining, freeze fracture TEM, and cryo EM, provide valuable information on liposome preparations since they yield a view of morphology and can resolve particles of varying size. However, sample preparation is complicated as it requires removal of liposomes from their native environment. These techniques can also generate artefacts, induce shrinkage and shape distortion, and are time consuming to obtain a representative size distribution of the population, thus are not amenable to being routine measurements. Some of these problems may be overcome yielding reproducible and accurate results by giving careful attention to sample preparation. A recently developed microscopic technique known as atomic force microscopy (AFM) has been utilized to study liposome morphology, size and stability. AFM, scanning probe microscopes with dimensional resolution approaching 0.1 nm, provides unique possibility for visualizing small liposomes in natural environment even without sample manipulation. The result is with a high resolution three-dimensional profile of the vesicle surface under study. The technique permits liposomes visualization without alteration of their native form; given that the requisite surface immobilization does not adversely affect the sample and that the force of the probe itself does not have deleterious effects on the vesicles. AFM analysis is rapid, powerful and relatively non invasive technique. It can provide information on morphology, size, as well as on the possible aggregation processes of liposomes during their storage. Imaging in aqueous medium allows the liposomes observation under physiological condition. Using AFM technology, experimental data indicate that liposomes in water dispersion maintained their integrity only few minutes after deposition on mica support, after which they collapsed. For this reason, the liposomes images have to be obtained within 10 min after deposition. Therefore, special attention has to be given to the experimental conditions and especially the analytical times, AFM technique can replace the wide variety of microscopic techniques measuring liposomal size **[71 – 74]**.

HPLC using SEC can be used to separate and quantify liposome populations according to a time-based resolution of hydrodynamic size. The porous packing material used in

this technique excludes larges species from the internal pore volume leading to their shorter retention on the column. This mechanism leads to separation based on large particles elution before smaller particles. Conventional SEC is frequently used for liposomes separation from unencapsulated materials as a final purification step, but the use of HPLC-SEC for analysis offers increased resolution of liposome populations and reduced sample size and enhances reproducibility. One recommended commercially available column is the ethylene glycol-metacrylate gel which has a separation range from 20 to 500 nm, this 'hydroxylated poly-ether-based' gel shows a larger exclusion limit than other gels. An osmotically balanced mobile phase flowing at relatively low pressures (1–1.5 megapascal) helps to prevent damages, swelling or shrinkage of liposomes. HPLC-SEC can offer a powerful technique for not only size distribution determination, but also stability in terms of aggregation and vesicle permeability. Three methods have been described in literature: dynamic light-scattering analysis of SEC fractions; re-chromatography of SEC fractions on a calibrated column with turbidity measurements; and SEC with on-line turbidity and refractive index detection. The re-chromatography method was judged to be the most reliable, although the sensitivity suffered from the dilution in the two chromatographic steps. Disadvantages of HPLC for liposomes size determination mainly stem from recovery issues. These include unwanted adsorption of lipids on the column packing and destruction of liposomes containing lipids with higher affinity to the column material than the composite lipids. Both lipids necessitate a preliminary step of presaturation of the LC column with lipids prior to analysis. In addition, the lipid bilayer rigidity, which is a function of the lipid composition, plays a role in the liposomes retention and recovery. The bilayer rigidity dictates whether liposomes of large diameter can be deformed and thereby pass through relatively narrow pores or liposomes of small diameter which may be excluded from relatively large pores, dependent on pore's shape and orientation. The net effect is therefore difficult to predict. Thus, while hydrodynamic size and subsequent molecular weight information can be obtained through this technique, the accuracy of this determination is based on the use of well-matched (both by shape and chemical composition) set of standards. Lastly, while suitable packing materials are available for small to moderately sized liposomes resolution, it is not the case for large liposomes (>800 nm) **[75 – 77]**.

Field-flow fractionation (FFF) is a technique which overcomes some of the limitations of HPLC in liposomes analysis. It includes electrical, thermal, sedimentation and flow FFF techniques that rely on a field application which is perpendicular to the direction of flow. FFF uses a channel wall which consists of a semipermeable membrane chosen with a MWCO suitable for the liposomes under study. This membrane allows only the carrier fluid to pass. In flow FFF, there are two liquids flows acting on the sample components. The channel flow that runs through the channel and the crossflow that flowing perpendicular to the channel passes through the inlet frit into this channel and

exits through the membrane and outlet frit. A common procedure for sample injection is called 'stop-flow relaxation', in which a small volume sample is injected into the channel flow. After a short delay period that allows the sample to move into the channel from the injector, the channel flow is stopped for a time, allowing only the crossflow to act on the sample. The laminar flow profile slow down the movement of particles located closer to the channel walls, while the perpendicular flow propels all particles toward the membrane wall. Diffusion due to Brownian motion of particles in a size-based manner reduces the accumulation of smaller particles against the membrane wall. Retention times in this technique are proportional to the hydrodynamic diameter of the particles since smaller particles reach an equilibrium position further from the channel walls. Whereas in HPLC-SEC, large liposomes elute first, in normal mode FFF, small liposomes elute first due to their higher diffusion coefficient. The carrier liquid used in FFF needs to be chosen carefully so that there is no appreciable swelling of the membrane, as this can lead to non-uniform flows in the channel. Aqueous solutions are usually used as carrier liquids, although non-aqueous solvents have also been used. Many detectors have been used in FFF, but the most common is a UV/VIS spectrophotometer. Photodiode arrays have been used to obtain the entire spectra of eluting samples instead of monitoring a single wavelength. The FFF mechanism for liposomes analysis differs in that FFF flow separates vesicles on a hydrodynamic size basis, whereas sedimentation FFF separates them on a weight basis. Flow FFF enables rapid, convenient and non invasive measurement of vesicle size distribution without prior calibration using size standards. Other advantage of the FFF technique is the wide range of particle sizes that can be separated (1 nm – 100 μm) with high resolution. The only limit of this technique is the complexity and expense of instrumentation **[78 – 81]**.

Dynamic light scattering (DLS), otherwise known as photon correlation spectroscopy (PCS), is extensively used in liposome size distribution analysis. DLS measures the time-dependant fluctuations of light scattered from particles experiencing Brownian motion, which results from collisions between suspended particles and solvent molecules. When a particle is suspended in a solution and illuminated by light, it scatters light given that its index of refraction differs from that of suspending solvent. In other words, its polarizability differs from that of the solvent. This means that the arriving electric field is oscillating and is able to displace the cloud of electrons and thereby cause atoms to oscillate. The strengths of the technique include the ability to make measurements in native environments; its sensitivity to small quantities of high molecular weight aggregate; ease of commercially available operating instrument; minimal sample volume, concentration and preparation requirements. It also covers a large size range of species spanning the low nanometer to low micrometer range. However, the technique does not yield particle shape information; it can yield a bias

towards reporting larger diameters when small quantities of high molecular weight or aggregates or impurities are present in the sample **[82 – 84]**.

Measurement of particle size distribution could also be achieved using density gradient stabilized sedimentation whereby particles that are lower in density than the fluid in which they are suspended can be accurately analysed **[85, 86]**. Centrifugal sedimentation of particles suspended in a fluid is a well-known method of measuring the size distribution of particles in the range of 0.015 – 30 μm in diameter. The sedimentation velocity of any particle could be calculated if the particle density, fluid density, fluid viscosity and centrifugal acceleration are known. If the conditions of sedimentation are stable, the particles begin sedimentation as a very thin layer at the surface of the fluid. A light beam or an X-ray beam passes through the centrifuge at some distance below the surface of the fluid and measures the concentration of particle as they settle. The time required for particles to reach the detecting beam depends upon the speed and geometry of the centrifuge, the difference in density between the particles and the fluid and the diameter of the particles. The particles sediment at velocities, depending upon their size until reaching the detector beam which is positioned at a known distance below the fluid's surface **[86]**. Sedimentation velocity increases as the square of the particle diameter, so that particles which differ in size by only few percent settle at significantly different rates. The time needed to reach the detector is used to calculate the size of the particles. This method for size analysis has a high resolution compared to the other analysis method, it has also a high sensitivity which enables him to detect small additional peaks and pick up small changes. Moreover, high accuracy is assured since all analyses are run against a known calibration standard; the calibration can be either external (standard injected before the sample) or internal (standard mixed with the sample) **[85]**.

Several other techniques, considered to be less conventional, have been applied for liposome size distribution analysis but are not discussed in this paper, such as NMR, flow cytometry, capillary zone electrophoresis, etc.

4.3 Zeta potential

Three of the fundamental states of matter are solids, liquids and gases. If one of these states is finely dispersed in another then we have a 'colloidal system'. Most colloidal dispersions in aqueous media carry an electric charge. There are many origins of this surface charge depending upon the nature of the particle and its surrounding medium. The more important mechanisms are: ionization of surface groups (dissociation of acidic groups on the surface of a particle giving a negatively charged surface, conversely a basic surface will take on a positive charge) and adsorption of charged species (surfactant ions may be specifically adsorbed on the particle surface leading in

the case of cationic surfactants to a positively charged surface and in the case of anionic surfactants to a negatively one).

The zeta potential of a particle is the overall charge that a particle acquires in a particular medium. It is a physical property which is exhibited by any particle in suspension. It has long been recognized that the zeta potential is a very good index of the interaction magnitude between colloidal particles. Measurements of zeta potential are commonly used to predict the stability of colloidal systems. If all the particles in suspension have a large negative or positive zeta potential then they will tend to repel each other and there will be no tendency to aggregation. However, if the particles have low zeta potential values then there will be no force to prevent the particles flocculating.

To measure the zeta potential, a laser is used to provide a light source illuminating particles within the samples. The incident laser beam passes through the centre of the sample cell and the scattered light at an angle of about 13 ° is detected. When an electric field is applied to the cell, any particles moving through the measurement volume will lead to fluctuation of the detected light with a frequency proportional to the particle speed. This information is passed to a digital signal processor, then to a computer and hence potential zeta is calculated. Particles suspension with zeta potentials > +30 mV or < −30 mV are normally considered stable **[87, 88]**.

4.4 Encapsulation efficiency

The liposome preparations are a mixture of encapsulated and un-encapsulated drug fractions. The first step for the determination of the encapsulation efficiency is the separation between the encapsulated drug (within the carrier) and the free drug. Several separation techniques have been reported in the literature. The mini-column centrifugation is a method based on the difference of size between the drug loaded liposomes and the free drug. Indeed, undiluted liposome suspension is applied dropwise to the top of sephadex gel column and the column is spun at 2000 rpm for 3 min to expel the void volume containing the liposomes into the centrifuge tube. Then 250 µl of water was added and centrifugation was repeated. The non entrapped drug remained bound to the gel, while vesicles traversed the gel and were collected from the first and second stage of centrifugation **[89]**.

The separation between the free drug and the encapsulated drug could also be achieved by the use of a dialysis membrane with an appropriate cut-off. The liposme sample is dialysed against a buffer solution for 2 hours **[84]**.

The ultracentrifugation technique was reported as a simple and fast method for the separation of drug-loaded liposomes from their medium. The sample is centrifuged at 50000 rpm for 50 min at +4 °C **[90]**. Centrifugation at 3000 rpm for 30 minutes can

also be used. But prior to the centrifugation, liposomes should be aggregated in order to enable their sedimentation by adding an equal volume of protamine solution (10 mg/ml) to the sample **[91, 92]**.

Once drug-loaded liposomes are separated from their medium, the lipidic bilayer is disrupted with methanol or Triton X-100 and the released material is then quantified. Techniques used for this quantification depend on the nature of the encapsulant and include spectrophotometry, fluorescence spectroscopy, enzyme-based methods and electrochemical techniques.

Other methods such as HPLC or FFF can also be applied for the determination of the encapsulation efficiency. In this case, the encapsulation percent can be expressed as the ratio of the un-encapsulated peak area to that of a reference standard at the same initial concentration. This method can be applied if the liposomes do not undergo any purification (SEC, dialysis…) following preparation. Either technique are applied to separate liposome encapsulating materials from un-encapsulated drug and hence can also be used to monitor the storage stability in terms of leakage or the effect of various disruptive conditions on the retention of encapsulants. In some cases, size distribution and encapsulation efficiency determinations could be combined in one assay by using FFF coupled to a concentration detector suitable for the encapsulant.

The terminology varies widely with respect to the ability of various liposome formulations to encapsulate the target molecules. Many papers express results in term of 'percent encapsulation', 'incorporation efficiency', 'trapping efficiency' or 'encapsulation efficiency (EE)' which is typically defined as the total amount of encapsulant found in the liposome solution versus the total initial input of encapsulant solution. This value depends not only on the ability of the liposomes to capture the encapsulant molecules (dependent on lipid/buffer composition, liposome lamellarity, preparation procedure…) but also on the initial molar amount of encapsulant **[93]**.

Other authors define the encapsulation efficiency, or encapsulation capacity, as the molar amount of marker per mole of lipid which is obtained by dividing the concentration of encapsulant by the concentration of lipid. A similar definition is suggested expressing EE on a weight (mg) encapsulant per mM of lipid basis **[22]**. Another commonly used parameter is the captured volume, defined as µL of entrapped volume/µmol of lipid. This number ranges from 0.5 µL/nmol for SUV and MLV to 30 µl/nmol for LUV. Unlike the 'percent encapsulation' parameter cited previously, these representations require knowledge of the phospholipids concentration **[94, 95]**.

4.5 Lipid analysis

Several chemistry techniques are commonly used for the determination of phospholipid content. Most of these techniques include the use of molybdate-

containing reagents yielding a blue-colored product. One such method is the *Bartlett* assay which relies on the digestion of organic materials in liposome samples by 160 °C sulfuric acid, oxidation to inorganic phosphates by hydrogen peroxide, phosphomolybdate formation upon interaction with ammonium molybdate, followed by reduction through interaction with 1,2,6-aminonaphtolsulfonic acid at 100 °C. A blue product is formed which can then be analysed at 830 nm for the quantitative assessment of the phospholipids in the preparation **[96]**.

In the ascorbic acid method, ammonium molybdate reacts with orthophosphates formed from acid digestion to yield phosphomolybdic acid. This compound is then reduced with ascorbic acid to yield a blue-colored solution, analysed at 820 nm **[96]**.

Phospholipids can also be analyzed through complex formation with ammonium ferrothiocyante, extraction into chloroform, and absorbance measurement at 488 nm **[96]**.

A convenient and sensitive fluorescence assay for phospholipid vesicles has also been reported by *London et al.* **[97]**: when phospholipid vesicles are added to an aqueous solution of 1,6-diphenyl-1,3,5-hexatriene (DPH) a fluorescence enhancement of several hundred-fold is observed which can be used for a phospholipid concentration determination. The fluorescence is a function of the type of phospholipid, salt concentration, and time of incubation.

Enzymatic assays for phosphatidylcholine and cholesterol analysis are commercially available and widely used. The former method used phospholipase D to hydrolyze phospholipids and release free choline. The free choline is then oxidized to form betaine aldehyde, betaine and hydrogen peroxide, by choline oxydase. The generated hydrogen peroxide causes oxidative coupling of phenol and 4-aminoantipyrine mediated by peroxidase to yield quinoneimine dye which is quantified at 505 nm **[98]**.

The latter method relies on hydrolysis of cholesterol esters with cholesterol ester hydrolase, followed by oxidation of the cholesterol by cholesterol oxidase and subsequent production of hydrogen peroxide. This product also oxidatively couples 4-aminoantipyrine to phenol in the presence of peroxidase to yield a blue coloured quinoneimine dye which shows strong absorption at 505 nm **[98, 99]**.

Chromatographic techniques such as HPLC, GC and thin layer chromatography (TLC) can be used to separate and quantify the lipids composing lipid bilayers **[100]**. Chromatographic approaches are advantageous since they can separate and quantify each lipid in the mixture. TLC methods for phospholipid analysis often rely on lipid separation using a mixture of chloroform, methanol and water. Detection is frequently accomplished using molybdenum blue in sulfuric acid and ninhydrin stains for the detection of phosphate and primary amino groups, respectively. For HPLC analysis,

detection of lipids in the UV range is limited to 200–210 nm due to their lack of chromophores. GC analysis of lipids typically requires a derivatization step to ensure sufficient volatility of the components, either through trimethyl silylation or methyl esterification prior to detection by flame ionization or mass spectroscopy. In many cases, pre-treatment of liposomes to disrupt the lipid bilayers is completed prior to chromatographic analysis including dilution of the liposome suspension with alcohols such as 2-propanol, ethanol or methanol. The procedure choice is dependent on the mobile phase and the degree of lipid solubility.

4.6 *In-vitro* drug release

In vitro drug release can be performed using the dialysis tube diffusion technique. The dialysis bag membrane should be selected following screening of various membrane, no drug adsorption may occur and the membrane should be freely permeable to the active ingredient (the cut off molecular weight shouldn't be a limiting step in the diffusion process). Some milliliters aliquot of liposome suspension is placed in the dialysis bag, hermetically tied and dropped in the receptor compartment containing the dissolution medium. The entire system is kept at 37 °C under continuous magnetic stirring and the receptor medium is closed to avoid evaporation of the dissolution medium. The kinetic experiments are carried out respecting the sink conditions in the receptor compartment. Samples of the dialysate are taken at various time intervals and assayed for the drug by HPLC, spectrophotometer or any other convenient method. The sample volume is replaced with fresh dissolution medium so as the volume of the receptor compartment remains constant. Every kinetic experiment is performed in triplicate and the average values are taken to establish the release profile of the drug from the liposome suspension **[101, 102]**.

4.7 Liposomes stability

The liposomes stability is a major consideration for liposome production and administration steps: from process to storage and delivery.

A stable pharmaceutical dosage form maintains its physical integrity and does not adversely influence the chemical integrity of the active ingredient during its life. Researchers are attempting to deliver low and high molecular weight drugs in a variety of polymer matrices and liposome suspensions. The successful introduction of dosage forms depends upon a well-defined stability study. In designing a stability study, physical, chemical and microbial parameters must be considered and evaluated. This wisdom is also required for the liposome dosage form. A stability study must include a section for product characterization and another section concerning the product stability during storage.

All liposome preparations are heterogeneous in size, the average size distribution of liposomes changes upon their storage. Liposomes tend to fuse and grow into bigger vesicles, which is a thermodynamically more favourable state. Fusion and breakage of liposomes on storage also poses a critical problem leading to drug leakage from the vesicles. Therefore, visual appearance and size distribution are important parameters to evaluate physical stability.

In the other hand, the major ingredient in the liposome formulations is the lipid. The liposomes lipids are derived from natural and/or synthetic phospholipid sources containing unsaturated fatty acids which are known to undergo oxidative reactions. These reactions products can cause permeability changes within liposome bilayer. In addition, interactions of drug with the phospholipid also alter the chemical stability; hence the stability profile of a drug molecule may entirely be different from its liposome preparation stability profile. Thus, it is essential to develop stability protocols evaluating the chemical integrity of the drug over a period of time.

Finally, majority of therapeutic liposome formulations are parenteral products and therefore must be sterilized to remove the microbial contamination from the product. Thus, it is important to control microbial stability of liposomal preparations **[103, 104]**.

5. Liposomes application

5.1 Pharmaceutical applications

The use of liposomes as systemic and topical drug delivery systems has attracted increasing attention. Liposomes can be formulated in liquid (suspension), solid (dry powder) or semi-solid (gel, cream) forms. *In vivo*, they can be administered topically or via parenteral route.

5.1.1 Systemic liposomal drugs

After systemic (usually intravenous) administration, liposomes are typically recognized as foreign particles and consequently endocytosed by the mononuclear phagocytic system cells (MPS), mostly fixed Kuppfer cells, in the liver and spleen. Liposomes can serve as an excellent drug-delivery vehicle to these cells. Thus, sterically stabilized liposome, which are not avidly taken up by MPS cells, have different biodistributions properties and have shown enhanced accumulation in sites of trauma, such as tumours, infections and inflammation. This accumulation is simply due to their prolonged circulation and small size; enabling them to extravasate **[105]**.

Based on the liposome properties introduced above, several techniques of drug delivery can be envisaged:

- Liposomes can be applied to protect the entrapped drug against enzymatic degradation whilst in circulation. The lipids used in their formulation are not susceptible to enzymatic degradation; the entrapped drug is thus protected while the lipid vesicles circulate within the extracellular fluid. As an example, β-lactamase sensitive antibiotics such as the penicillins and cephalosporins have been encapsulated in order to be protected against the β-lactamase enzyme. *Rowland et al.* reported that liposomes offer protection in the gastrointestinal tract environment of encapsulated drug and facilitate the gastrointestinal transport of a variety of compounds **[106]**. As clearly evidenced by *Dapergolas*, liposomes are candidates to be explored for oral delivery of peptides (insulin) and proteins (vaccines), which are orally degradable **[107]**.

- Liposomes can be used for drug targeting. It has been proved that restricting the distribution of the drug to the specific target site should allow efficacy increase at low dose with attendant decrease of toxicity. Indeed, pumping a drug through the whole body is not only wasteful but, more fundamentally, increase undesirable side effects. Hence, the benefits of drug targeting include reducing drug waste, and it is possible to deliver a drug to a tissue or cell region not normally accessible to the free or untargeted drug **[108]**. Liposomes have been widely applied in drug targeting especially in cancer treatment. Effective chemotherapy is severely limited by the toxic side effects of the drugs. Liposome encapsulation can alter the spatial and temporal distribution of the encapsulated drug molecules in the body, which may significantly reduce unwanted toxic side effects and increase the efficacy of the treatment. The first step, therefore, is to determine the antigens that are produced by the tumour cells. Then to target the drug via specific receptor ligands, which may be specific antibodies for antigens produced by tumour cells **[109]**. Two liposomal formulations have been approved by the US food and drug administration (FDA) and are commercially available in the USA, Europe and Japan for the treatment of Kaposi's sarcoma. Doxil® is a formulation of doxorubicin precipitated in sterically stabilized liposomes (on the market since 1995) and DaunoXome® is daunorubicin encapsulated in small liposomes (on the market since 1990). Doxil® has been shown to have a 4.5-times-lower medium-pathology score for doxorubicin induced cardiotoxicity than the free drug. In squamous cell lung carcinoma, the same drug is capable of reducing tumor burden to a significant extent **[110]**.

- In order to enhance solubilisation, the amphotericin B, which is the drug of choice in the treatment of systemic fungal infections, has been widely studied for liposome encapsulation. Owing to its aqueous insolubility, amphotericin B is typically formulated into detergent micelles. But, micelles are unstable upon systemic administration, and several neuro- and nephrotoxicity limit the dose that can be administered.

Table 2. Liposomes application in the pharmaceutical field

Intention of the encapsulation	Molecule	Therapeutic class	Study conclusions	Reference
Protection against enzymatic degradation	Insulin	Hypoglycaemic agent	1.3 units of insulin entrapped in dipalmitoyl phosphatidylcholine / cholesterol liposomes administered to normal rats decreased blood glucose level in 4 h to about 77% of those before treatment. Higher doses (4.2 and 8.4 units) extended this effect over 24 h. 1.0 units of insulin entrapped in the same liposomes had an even more pronounced effect in diabetic rats: levels of blood-glucose were reduced to 57% of pre-treatment values after 4 h.	**[107]**
			Liposome-entrapped insulin significantly reduced glucose and raised insulin in 54% of rats and 67% of the rabbits. Among the rats that responded, blood glucose fell from a basal of 318±21 mg/dl to a nadir of 186±22 mg/dl at 2 h. while insulin rose from 30±7 μU/ml to a peak of 399±75 μU/ml at 1 h.	**[126]**
	Factor-VIII	Coagulation factor	Factor-VIII loaded liposomes were given orally to a patient with severe haemophilia A. Plasma concentration of factor-VIII rose to therapeutically effective levels. Factor-VIII activity did not rise when the free drug is orally administered.	**[127]**
	Cysteamine	Treatment of acute radiation syndrom "ARS"	Oral administration of liposome-entrapped cysteamine induces an increase in the concentration of exogenous sulphur compounds in plasma, liver and spleen. This fact can be related to a protection of cysteamine in the digestive tract.	**[128]**
	Penicillins cephalosporins	Antibiotics	The entrapped drugs are protected against β-lactamase enzyme while they are in circulation in the extracellular fluid.	**[109]**

Intention of the encapsulation	Molecule	Therapeutic class	Study conclusions	Reference
Drug targeting	Cyclosporine	Immunosuppressive	The in vivo pharmacokinetics and renal toxicity of a liposomal formulation and the commercially available cyclosporine are compared. The apparent volume of distribution was significantly greater in liposomal formulation compared to the commercially form (13.82±2.9 vs 7.67±3.01 L/Kg), most likely due to the significantly prolonged biologic half-life (47.91±13.15 vs 30.95±8.89 h). Kidney function was assessed via the calculation of the glomerular filtration rate "GFR", no dose-limiting nephrotoxicity was found with the liposomal formulation, suggesting a potential alternative to the toxic commercial formulation.	**[129]**
			A change in the pharmacokinetic parameters of cyclosporine due to liposomal encapsulation was observed. A peak concentration was reached in 50 min in case of liposomes compared with 225 min in case of commercially available formulation. The rate of absorption was significantly faster following the liposome administration. Generally, there was less inter-individual variation in pharmacokinetics parameters when cyclosporine was orally administered in the liposomal formulation. Thus, an oral liposomal formulation can be developed to offer the advantages of low variability and fast onset of action.	**[130]**
	Doxorubicin	Antineoplastic	Doxorubicin has been shown to have a 4.5-times-lower medium-pathology score for doxorubicin-induced cardiotoxicity than the free drug. In squamous cell lung carcinoma, the same drug is capable of reducing tumor burden to a significant extent.	**[110]**

Intention of the encapsulation	Molecule	Therapeutic class	Study conclusions	Reference
Drug targeting	Amikacin	Antibiotic	The clearance of liposomal amikacin was over 100-fold lower than the conventional amikacin clearance. Half-life in plasma was longer than that reported for other amikacin formulations. The levels in plasma remained > 180 mg/ml for 6 days after the administration of the last dose and the free amikacin concentration in plasma never exceeded 17.4 6 1 mg/ml. The low volume of distribution (45 ml/kg) indicates that the amikacin in plasma largely remained sequestered in long circulating liposomes. Less than half the amikacin was recovered in the urine, suggesting that the level of renal exposure to filtered free amikacin was reduced, possibly as a result of intracellular uptake or the metabolism of liposomal amikacin. Thus, by sequestering this antibiotic in liposomes with long circulation times, this formulation not only maintained antibiotic levels in the body for over 1 week after treatment, but also, significantly alters the disposition of amikacin within the body and therefore decreases the potentially toxic level of renal tubular exposure.	**[131]**
Enhancement of drug solubilisation	Amphotericin B	Treatment of fungal systemic infections	Owing to its aqueous insolubility, amphotericin B is typically formulated into detergent micelles. However, micelles are unstable upon systemic administration, and several neuro- and nephrotoxicity limit the dose that can be administered. If the drug is formulated into liposomes, it is delivered much more efficiently to macrophages and, additionally, toxicity can be significantly reduced.	**[111]**
Enhancement of drug uptake	Desferrioxamine	Chelating agent	Liposomal desferrioxamine given intravenously to iron-overloaded ^{59}Fe labeled mice doubled the ^{59}Fe excretion for a given dose of the drug.	**[134]**

Intention of the encapsulation	Molecule	Therapeutic class	Study conclusions	Reference
Enhancement of drug uptake	Vitamin K_1	Prevention or treatment of hemorrhage	The effect of liposomal associated-vitamin K_1, administrated orally, was investigated using rabbits with warfarin-induced hypoprothrombinaemia, and evaluated in comparison with other dosage forms of the vitamin. The coagulation recovery time of the liposomal preparation was much faster than that of the other preparations: This time was 6.2 h for the oral liposomal preparation, 13.6 h for solubilised vitamin and 19.6 h for stabilized emulsion.	**[133]**
	Polyvinylpyrrolidone	Blood plasma substitute	At an equal concentration of 125I-labelled polyvinylpyrrolidone, the rate of uptake of the liposome-entrapped macromolecule by the tissue was over 4-times that of the free macromolecule.	**[132]**
Vaccination	Inactivated hepatitis A virus	Prevention of hepatitis A	Purified hepatitis-A-virion capsule, viral phospholipids and envelope glycoprotein from influenza virus are mixed with phosphatidylcholine and phosphatidylethanolamine in the presence of excess of detergent. Liposomes containing antigen and some viral lipids and proteins are formed. The liposomes potentiate the immune response to the vaccine antigen.	**[113]**

However in a stable colloid particle, such as liposomes, encapsulated drug is delivered much more efficiently to macrophages and, additionally, toxicity can be significantly reduced **[111]**. Following this rationale, a lipid-based amphotericin B formulation is actually commercially available in the Europe and US market (respectively since 1990 and 1997): AmBisome® including amphotericin B into small liposomes.

- Otherwise, liposomes can also be used to enhance the drug intracellular uptake. The lipid formulation promotes the cellular penetration of the encapsulated drug especially antibiotics, reducing the effective dose and incidence of toxicity.

- According to the studies performed by *Sullivan et al.*, liposomes may be useful as immunotherapeutic agents: the use of antigen-presenting liposomes may be a promising approach in the therapy of infectious diseases like HIV infection or Herpes simplex virus genital infection **[112]**. A liposomal vaccine against hepatitis A has been successfully launched by the Swiss Serum Institute in 1994. Purified hepatitis-A-virion capsule, viral phospholipids and envelope glycoprotein from influenza virus are mixed with phosphatidylcholine and phosphatidylethanolamine in the presence of excess detergent forming liposomes leading to potentiate the immune response. The same company is developing vaccines for influenza, hepatitis B, diphtheria and tetanus **[113]**.

- Cationic liposomes have been shown to complex (negatively charged) DNA, and such complexes were able to transfect cells *in vitro*, resulting in the expression of the protein encoded in the DNA plasmid in the target cells, and making liposomes useful in direct gene transfer. Obviously for gene therapy (the treatment of diseases on the molecular level by switching genes on or off), it was discovered that cationic lipid-based DNA complexes can transfect certain cells *in vivo* upon localized or systemic administration **[13]**.

Today, enthusiasm for the systemic use of liposomal drugs is not as widespread as it was. While the long list of diseases considered candidate for systemic application of liposomal drugs has been reduced to just a few indications, the topical application of liposomal preparations has recently attracted more interest.

5.1.2 Topical liposomal drugs

Skin treatment applications of liposomes are based on the similarity between the lipid vesicles bilayer structure and natural membranes which includes the ability of lipid vesicles, with specific lipid composition, to alter cell membrane fluidity and to fuse with them. In the dermatological field, liposomes were initially used because of their moisturizing and restoring action **[114]**.

In *Schmid*'s work, stratum corneum liposomes have been used in the treatment of atopic dry skin in order to restore the barrier function and to vehicle an active substance at the same time **[115]**. The composition and properties of liposomes play an important role in their interaction and possible penetration within the epidermis. In addition, liposomes provide valuable raw material for the regeneration of skin by replenishing lipid molecules and moisture. Lipids are well hydrated and, even in the absence of active ingredients, humidify the skin. Often this is enough to improve skin elasticity and barrier function, which are the main causes of skin aging.

Later, the liposomes ability of enclosing many different biological materials and delivering them to the epidermal cells or even deeper cell layers was investigated. This offered new perspectives and leads to the conclusion that liposomes may be useful vehicles for topical drug delivery for varying skin diseases treatment.

Typically, conventional dosage forms, such as solution, creams, and ointments, deliver drugs in a concentration dependant manner across the stratum corneum. However, multilamellar liposomes can deliver drugs within 30 minutes to the stratum corneum, epidermidis, and dermis in significantly higher concentrations than conventional preparations.

Among the great variety of candidates for liposome encapsulation, there are mainly three groups of drugs to be considered: corticoids, retinoids and local anaesthetics.

Mezei et al. was the first to report increased corticosteroid concentrations in epidermis and corium combined with a reduced percutaneous absorption in an animal model **[116]**. This is particularly important as far as adverse effects from extensive corticosteroid therapy are reduced. These findings were the same with human skin; Lasch investigated the effect of liposomally entrapped cortisol on human skin *ex vivo*; he revealed improved cortisol concentration profiles which is of real importance because cortisol is known to have no adverse effects in long-term therapy but to be often insufficient in the therapy of acute dermatoses **[117]**. For this reason, higher drug concentrations will mean an improved therapeutic effect. In a clinical trial, Korting investigated the effect of betamethasone dipropionate in a liposomal preparation and in a commercial conventional preparation in patient suffering from atopic eczema **[118]**. In this double-blind, randomized, paired trial the liposomal preparation, containing markedly less active substance was slightly superior in patients with atopic eczema reducing parameters of inflammation compared to the conventional preparation.

The retinoids is the second important group of drug which seems to be a promising candidate for liposomal encapsulation. One main field for the topical administration of retinoids is uncomplicated acne vulgaris. Commercial tretinoin gels shows local irritant effects and flare-up reactions at the beginning of the treatment. These

characteristics, often compromising patient compliance, can be overcome by the liposomal formulation of tretinoin. *Masini et al.* reported a reduced irritancy in animal experiments after treatment with liposomal tretinoin, which may be explained by gradual drug release from the liposomal preparation **[119]**. *Schafer-Korting et al.* performed a double blind study to evaluate the efficacy and tolerability of liposomal tretinoin in patients with uncomplicated acne vulgaris **[120]**. The results clearly showed that the less concentrated liposomal drug commands equal efficacy and less skin irritation compared to its commercial conventional counterparts. This equal efficacy might be attributed to an improved bioavailability combined with a slower drug release. In conclusion, the liposomally encapsulated tretinoin seems to be superior to the conventional dosage form.

During the last few years, many attempts have been made to provide adequate local anaesthesia of the skin. For this, prolonged application time and high anaesthetic concentration are required. Studies performed by *Gesztes et al.* indicated that tetracaine encapsulated liposomes provide better local anaesthesia (low drug concentration and long anaesthesia duration) than a conventional anaesthetic cream. Similar results were obtained using other local anaesthetics such as lidocaine which is commercialized in the US market since 1998 (ELA-Max®) **[121]**.

Furthermore, it has been commonly believed that high concentrations of ethanol are detrimental to liposomal formulations. Therefore, when liposomes are prepared from ethanolic solutions of phospholipids much care is taken to remove the remaining traces of alcohol. Data presented by *Touitou et al.* indicated that the presence of ethanol with a relatively high concentration in systems of lipid vesicles, termed ethosomes, was reported to influence the stratum corneum penetration and permeation of drugs **[122]**. Encapsulation experiments showed that ethosomes are able to entrap both hydrophilic and lipophilic drugs. These entrapment results were supported by *in vitro* studies on the delivery of drugs in and through the skin. Again, the ethosomal system was shown to be far superior to the control systems, both in terms of the drug concentration in the skin and the flux of the drug through the skin. Patches containing testosterone in an ethosomal system were compared *in vivo* in rabbits with the commercial patch Testoderm®. The results showed significantly higher testosterone blood levels from the ethosomal system. *Horwitz et al.* tested clinically the ethosomal carrier for dermal delivery of the antiviral drug, acyclovir in a double-blind randomized study with Zovirax® **[123]**. Results indicated that ethosomes performed significantly better than the commercial drug form. For example, the average time to crusting of lesions was shorter for the ethosomal system. The permeation enhancement from ethosomes suggests a synergetic mechanism between ethanol, lipid vesicles and skin. Indeed, in comparison to liposomes, ethosomes are less rigid.

Table 3. Liposome-based products on the market

Molecule	Treated disease	Product	Company	Status
Doxorubicin	Kaposi's sarcoma and AIDS-related cancers, ovarian cancer and multiple myeloma	DOXIL	Ben Venue Laboratories for Johnson and Johnson, USA	On the market since 1995 (USA) and 1996 (Europe)
		CAELYX	Shering-Plough, Europe	
		MYOCET	Enzon Pharmaceuticals for Cephalon, Europe and for Sopherion Therapeutics, USA and Canada	
Amphotericin B	Systemic fungal infections	AMBISOME	First Next star Pharmaceuticals which was acquired by Gilead Sciences in 1999. Thus, the drug is marketed by Gilead in Europe and licensed to Astellas Pharma (formerly Fujisawa Pharmaceuticals) for marketing in the USA, and Sumitomo Pharmaceuticals in Japan.	On the market since 1990 (Europe) and 1997 (USA)
		FUNGISOME	Lifecare Innovations, India	
		AMPHOTEC	Intermune, USA	
		ABELCET	Enzon Pharmaceuticals, USA	
		AMPHOLIP	Bharat Serum and Vaccines, India	
		AMPHOCIL	Samaritan Pharmaceuticals, USA	
		ABLC	The liposome company, USA	
Daunorubicin	Specific types of leukemia (acute myeloid leukemia and acute lymphatic leukemia)	DAUNOXOME	First, NeXstar Pharmaceuticals. Then the drug was sold to Diatos in 2006	On the market since 1996 (USA and Europe)

Molecule	Treated disease	Product	Company	Status
Inactivated hepatitis A virus	Hepatitis A	EPAXAL	Crucell Company who merged with the Swiss Serum and Vaccine Institute in 2006	On the Swiss market since 1994 and now in more than 40 country.
Lidocaine	Anaesthesia for skin itching, burning or pain.	LMX4 LMX5	Ferndale Laboratories, USA	On the US market since 1998

Thus, the effects of ethanol which were considered to be harmful to classic liposomal formulations may provide the vesicles with soft flexible characteristics which allow them to penetrate more easily into deeper layers of skin. In another hand ethanol may disturbs the organization of the stratum corneum lipid bilayer and enhances its lipid fluidity.

Liposomes based on a natural marine lipid extract containing a highly polyunsaturated fatty acid ratio were recently introduced as Marinosomes® by *Moussaoui et al.* for the prevention and treatment of skin diseases **[124]**. *Cansell et al.* have reported that Marinosomes® contributed to reduce inflammation induced by croton oil by regulating PGE2 and IL-8 production in keratinocyte cultures **[125]**.

5.2 Cosmetic applications

The properties of liposomes can be utilized also in the delivery of ingredients in cosmetics. Liposomes offer advantages because lipids are well hydrated and can reduce the dryness of the skin which is a primary cause for ageing. Also, liposomes can supply replenish lipids and importantly linolenic acid to the skin. The first liposomal cosmetic product to appear on the market was the anti-ageing cream "Capture" launched by Christian Dior in 1986 **[135]**. Liposomes have been also used in the treatment of hair loss; minoxidil, a vasodilator, is in the active ingredient in products like "Regaine" that claim to prevent or slow hair loss **[136]**. The skin care preparations with empty or moisture loaded liposome reduce the transdermal water loss and are suitable for the treatment of dry skin. They also enhance the supply of lipids and water to the stratum corneum **[137]**. Various liposome formulations were compared *in vivo* for cosmetics application **[114]**; liposome formulations prepared from egg phospholipids exhibited a 1.5-fold increase in skin water content, whereas liposome formulations prepared from soya phospholipids showed no advantage compared to the references. Skin water content was measured daily and the results showed that skin humidity was increased significantly for the formulation containing 20% egg phospholipids during 6 days.

Since 1987, several cosmetic products have been commercially available; they range from simple liposome pastes which are used as a replacement for creams, gels and ointments to formulations containing various extracts, moisturizers, antibiotics, etc. Unrinsable sunscreens, long lasting perfumes, hair conditioners, aftershaves, lipsticks, make-up and similar products are also gaining large fractions of the market **[138]**. Some of the liposomal cosmetic formulations currently available in the market are shown in **Table 4**.

Table 4. Some liposomal cosmetic formulations currently on the market

Product	Manufacturer	Key ingredients
Capture	Christian Dior	Liposomes in gel
Effet du soleil	L'Oréal	Tanning agents in liposomes
Future Perfect Skin Gel	Estée Lauder	Vitamin E, A, Cerebroside, Ceramide
Aquasome LA	Nikko Chemical Co	Liposomes with humectant
Eye Perfector	Avon	Soothing cream with eye irritation
Flawless Finish	Elisabeth Arden	Liquid make-up

5.3 Food applications

The majority of microencapsulation techniques currently used in the food industry are based on biopolymer matrices composed of sugars, starches, gums, proteins, synthetics, dextrin and alginates. Nevertheless, liposomes have recently begun to gain in importance in food products **[139, 140]**. Indeed, the ability of liposomes to solubilise compounds with demanding solubility properties, sequester compounds from potentially harmful medium, and release incorporated molecules in a sustained and predictable way can be used in food processing industry. Based on studies on liposomes for pharmaceutical and medical uses, food scientists have begun to utilize liposomes for controlled delivery of functional components such as proteins, enzymes, vitamins, antioxidants, and flavours. The applications are for example dairy products preparation, stabilization of food components against degradation, and delivery and enhanced efficiency of antimicrobial peptides.

The sustained release system concept can be used in various fermentation processes in which the encapsulated enzymes can greatly shorten fermentation times and improve the quality of the product. A classical example is cheese-making; after preliminary studies in which liposome systems were optimized the cheese ripening times were shorten by 30 to 50%. This means a substantial economic profit knowing that ripening times of some cheeses, such as Cheddar, are about one year during which they require well controlled conditions **[141]**.

In addition to improved fermentation, liposomes were tried in the preservation of cheeses. Addition of nitrates to cheese milk to suppress the growth of spore-forming bacteria is questioned due to health concerns and natural alternatives are under study. Lysozyme is effective but quickly inactivated due to binding to casein. Liposome encapsulation can both preserve potency and increase effectiveness because liposomes become localized in the water spaces between the casein matrix and fat globules of curd and cheese **[142]**. These applications of enhancing natural preservatives, including antioxidants such as vitamin E and C, will undoubtedly become very

important due to recent dietary trends which tend to reduce the addition of artificial preservatives and increase portion of unsaturated fats in the diet.

In other areas of the agro-food industry, biocides encapsulated into liposomes have shown superior action due to prolonged presence of fungicides, herbicides, or pesticides at reduced damage to other life forms. Liposome surface can be made sticky so that they remain on the leafs for longer times and they do not wash into the ground **[143]**.

6. Conclusion

Since they have been discovered in the 60's by Bangham, liposomes have drawn attention of researchers. Nowadays, they always remain a topical issue; new preparation methods have been developed as well as new characterization techniques.

In the pharmaceutical field, liposomes have long been of great interest by offering a promising way for both systemic and locally acting drugs used for therapeutic applications in humans and animals. As a result of the great potential of liposomes in the area of drug delivery, several companies have been actively engaged in expansion and evaluation of liposome products. Most of them concern anticancer and antifungal drugs that, administered in their free form, are toxic or exhibit serious side-effects and their encapsulation into liposomal vesicles significantly diminishes these unwanted properties. However, there are few commercially available pharmaceutical products based on drug-in-liposome formulations. Liposome based formulation have not entered the market in great numbers because of some problems limiting their development.

Even that batch to batch reproducibility, low drug entrapment, particle size control, and short circulation half-life of vesicles seem to have been resolved, some other problems are still limiting the widespread use of liposomes, among them the stability issues, sterilization method and production of large batch sizes.

Some of the stability problems may be overcome by lyophilisation. The final product is freeze-dried liposome mixed with a suitable cryoprotectant that are particularly stable and have to be reconstituted immediately prior to administration.

Another challenge is the identification of a suitable method for sterilization of liposome formulations as phospholipids are thermolabile and sensitive substance to procedures involving the use of heat, radiation and/or chemical sterilizing agents. The alternative technique of liposome sterilization is filtration through sterile membranes (0.22 _m). However, this method is limited by liposome size and is not suitable for large vesicles (>0_22 _m).

Finally, the major challenge for liposome is the large scale production method. Pharmaceutically acceptable procedures are those that can be easily scaled to larger batch sizes and economically feasible. However, unlike the classical pharmaceutical dosage forms (tablets, capsules, suppository…) which are produced in large batch sizes, liposome based drugs even those already in the market are produced in small size batches and thus are costly for the manufacturers. Scale-up process to larger size batches is often a monumental task for the process development scientists. However the accumulation of many novel experiences studying the practical aspects of liposomes, added to new developments in basic research, will bring the field of liposome biotechnology to the place it deserves in the future. An encouraging sign is the increasing number of clinical trials involving liposomes.

References

[1] T. Lian and R. J. Ho, *J. Pharm. Sci.* 90, 667 (2001).

[2] R. Banerjee, *J. Biomater. Appl.* 16, 14 (2001).

[3] B. Keller, *Trends Food Sci. Technol.* 12, 25 (2001).

[4] N. Maurer, D. B. Fenske, and P. R. Cullis, *Expert Opin. Biol. Ther.* 1, 923 (2001).

[5] A. Samad, Y. Sultana, and M. Aqil, *Curr. Drug Deliv.* 4, 297 (2007).

[6] J. A. Rogers and K. E. Anderson, *Crit. Rev. Ther. Drug Carrier Syst.* 15, 421 (1998).

[7] S. M. Michalek, N. K. Childers, J. Katz, F. R. Denys, A. K. Berry, J. H. Eldridge, J. R. McGhee, and R. Curtiss, *Curr. Top Microbiol. Immunol.* 146, 51 (1989).

[8] K. Egbaria and N. Weiner, *Adv. Drug Deliv. Rev.* 5, 287 (1990).

[9] I. Kellaway and S. Farr, *Adv. Drug Deliv. Rev.* 5, 149 (1990).

[10] H. Schreier, R. Gonzalez-Rothib, and A. Stecenkoc, *J. Control Rel.* 24, 209 (1993).

[11] S. Ebrahim, G. Peyman, and P. Lee, *Surv. ophthalmol.* 50, 167 (2005).

[12] A. D. Bangham, J. C. Glover, S. Hollingshead, and B. A. Pethica, *Biochem. J.* 84, 513 (1962).

[13] D. D. Lasic, *Trends Biotechnol.* 16, 307 (1998).

[14] D. Lasic and D. Papadjopoulos, *Science* 267, 1275 (1995).

[15] J. Israelachvili, S. Marcelja, and R. Horn, *Rev. Biophys.* 13, 121 (1980).

[16] A. D. Bangham, M. M. Standish, and G. Weissmann, *J. Mol. Biol.* 13, 253 (1965).

[17] A. Sharma and U. Sharma, *Int. J. Pharm.* 154, 123 (1997).

[18] F. Bordi C. Cametti, and S. Sennato, Advances in Planar Lipid Bilayers and Liposomes edited by Academic Press (2006), pp 281–320.

[19] Y. Ebato, Y. Kato, H. Onishi, T. Nagai, and Y. Machida, *Drug Develop. Res.* 58, 253 (2003).

[20] G. J. Grant, Y. Barenholz, E. M. Bolotin, M. Bansinath, H. Turndorf, B. Piskoun, and E. M. Davidson, *Anesthesiology* 101, 133 (2004).

[21] K. Katayama, Y. Kato, H. Onishi, T. Nagai, and Y. Machida, *Drug Dev. Ind. Pharm.* 29, 725 (2003).

[22] S. Vemuri and C. T. Rhodes, *Pharm. Acta Helv.* 70, 95 (1995).

[23] M. R. Mozafari, *Cell Mol. Biol. Lett.* 10, 711 (2005).

[24] A. Bangham, J. De Gier, and G. Greville, *Chem. Phys. Lipids* 1, 225 (1967).

[25] F. Olson, C. A. Hunt, F. C. Szoka, W. J. Vail, and D. Papahadjopoulos, *Biochim. Biophys. Acta* 557, 9 (1979).

[26] B. Mui, L. Chow, and M. J. Hope, *Methods Enzymol.* 367, 3 (2003).

[27] F. J. Szoka and D. Papahadjopoulos, *Proc. Natl. Acad. Sci. USA* 75, 4194 (1978).

[28] J. Szebeni, J. H. Breuer, J. G. Szelenyi, G. Bathori, G. Lelkes, and S, R. Hollan, *Biochim. Biophys. Acta* 798, 60 (1984).

[29] S. Batzri and E. D. Korn, *Biochim. Biophys. Acta* 298, 1015 (1973).

[30] P. Stano, S. Bufali, C. Pisano, F. Bucci, M. Barbarino, M. Santaniello, P. Carminati, and P. L. Luisi, *J. Liposome Res.* 14, 87 (2004).

[31] D. W. Deamer, *Ann. NY Acad. Sci.* 308, 250 (1978).

[32] O. Zumbuehl and H. G. Weder, *Biochim. Biophys. Acta* 640, 252 (1981).

[33] D. Papahadjopoulos, S. Nir, and N. Düzgünes, *J. Bioenerg. Biomembr.* 22, 157 (1990).

[34] E. Cauchetier, H. Fessi, Y. Boulard, M. Deniau, A. Astier, and M. Paul, *Drug Dev. Res.* 47, 155 (1999).

[35] T. Nii and F. Ishii, *Int. J. Pharm.* 298, 198 (2005).

[36] H. Cheung Shum, D. Lee, I. Yoon, T. Kodger, and D. Weitz, *Langmuir* 24, 7651 (2008).

[37] M. R. Mozafari and A. Omri, *J. Pharm. Sci.* 96, 1955 (2007).

[38] N. Skalko-Basnet, Z. Pavelic, and M. Becirevic-Lacan, *Drug Dev. Ind. Pharm.* 26, 1279 (2000).

[39] C. Li and Y. Deng, *J. Pharm. Sci.* 93, 1403 (2004).

[40] J. Cui, C. Li, Y. Deng, Y. Wang, and W. Wang, *Int. J. Pharm.* 312, 131 (2006).

[41] K. Otake, T. Imura, H. Sakai, and M. Abe, *Langmuir* 17, 3898 (2001).

[42] K. Otake, T. Shimomura, T. Goto, T. Imura, T. Furuya, S. Yoda, Y. Takebayashi, H. Sakai, and M. Abe, *Langmuir* 22, 2543 (2006).

[43] T. Imura, K. Otake, S. Hashimoto, T. Gotoh, M. Yuasa, S. Yokoyama, et al., *Colloid Surface B* 27, 133 (2002).

[44] A. Jahn, W. N. Vreeland, D. L. DeVoe, L. E. Locascio, and M. Gaitan, *Langmuir* 23, 6289 (2007).

[45] A. Jahn, W. N. Vreeland, M. Gaitan, and L. E. Locascio, *J. Am. Chem. Soc.* 126, 2674 (2004).

[46] P. Pradhan, J. Guan, D. Lu, P. G. Wang, L. J. Lee, and R. J. Lee, *Anticancer Res.* 28, 943 (2008).

[47] A. Wagner, K. Vorauer-Uhl, and H. Katinger, *Eur. J. Pharm. Biopharm.* 54, 213 (2002c).

[48] A. Wagner, K. Vorauer-Uhl, G. Kreismayr, and H. Katinger, *J. Liposome Res.* 12, 271 (2002b).

[49] A. Wagner, K. Vorauer-Uhl, G. Kreismayr, and H. Katinger, *J. Liposome Res.* 12, 259 (2002a).

[50] A. Wagner, M. Platzgummer, G. Kreismayr, H. Quendler, G. Stiegler, B. Ferko, G. Vecera, K. Vorauer-Uhl, and H. Katinger, *J. Liposome Res.* 16, 311 (2006).

[51] C. Jaafar-Maalej, C. Charcosset, and H. Fessi, *J. Lip. Res.* 21, 1 (2011).

[52] A. R. Mohammed, N. Weston, A. G. A. Coombes, M. Fitzgerald, and Y. Perrie, *Int. J. Pharm.* 285, 23 (2004).

[53] R. M. Hathout, S. Mansour, N. D. Mortada, and A. S. Guinedi, *AAPS. Pharm. Sci. Technol.* 8, 1 (2007).

[54] M. Fan, S. Xu, S. Xia, and X. Zhang, *J. Agric. Food Chem.* 55, 167 (2007).

[55] M. Holzer, S. Barnert, J. Momm, and R. Schubert, *J. Chromatogr. A.* 1216, 5838 (2009).

[56] C. Dai, B. Wang, H. Zhao, B. Li, and J. Wang, *Colloids Surf. B Biointer.* 47, 205 (2006).

[57] S. Moazam Mortazavia, M. Reza Mohammadabadib, K. Khosravi-Daranic, and M. Reza Mozafari, *J. Biotechnol.* 129, 604 (2007).

[58] K. A. Edwards and A. J. Baeumner, *Talanta* 68, 1432 (2006).

[59] T. Morçol, A. Subramanian, and W. Velander, *J. Immunol. Methods* 203, 45 (1997).

[60] E. Brekkan, L. Lu, and P. Lundahl, *J. Chromatogr. A.* 711, 33 (1995).

[61] S. Mukherjee, H. Raghuraman, S. Dasgupta, and A. Chattopadhyay, *Chem. Phys. Lipids.* 127, 91 (2004).

[62] K. Matsuzaki, O. Murase, K. Sugishita, S. Yoneyama, K. Akada, M. Ueha, A. Nakamura, and S. Kobayashi, *Biochim. Biophys. Acta* 1467, 219 (2000).

[63] A. Chattopadhyay, *Chem. Phys. Lipids.* 53, 1 (1990).

[64] H. J. Gruber and H. Schindler, *Biochim. Biophys. Acta* 1189, 212 (1994).

[65] L. D. Mayer, M. J. Hope, and P. R. Cullis, *Biochim. Biophys. Acta* 858, 161 (1986).

[66] M. Fröhlich, V. Brecht, and R. Peschka-Süss, *Chem. Phys. Lipids* 109, 103 (2001).

[67] M. Müller, S. Mackeben, and C. C. Müller-Goymann, *Int. J. Pharm.* 274, 139 (2004).

[68] H. Jousma, H. Talsma Spies, F. Joosten JGH, and Junginger, HE, Crommelin, DJA, *Int. J. Pharm.* 35, 263 (1987).

[69] M. Hope, M. Bally, L. Mayer, A. Janoff, and P. Cullis, *Chem. Phys. Lipids.* 40, 89 (1986).

[70] H. Hauser, *Biochim. Biophys. Acta* 772, 37 (1984).

[71] A. F. Palmer, P. Wingert, and J. Nickels, *Biophys. J.* 85, 1233 (2003).

[72] J. Jass, T. Tjärnhage, and G. Puu, *Methods Enzymol.* 367, 199 (2003).

[73] P. M. Frederik, and D. H. W. Hubert, *Methods Enzymol.* 391, 431 (2005).

[74] B. Ruozi, G. Tosi, F. Forni, M. Fresta, and M. A. Vandelli, *Eur. J. Pharm. Sci.* 25, 81 (2005).

[75] P. Lundahl, C. M. Zeng, C. Lagerquist Hägglund, I. Gottschalk, and E. Greijer, *J. Chromatogr. B Biomed. Sci. Appl.* 722, 103 (1999).

[76] S. Lessieur, C. Gabrielle-Madelmont, M. Paternostre, and M. Ollivon, *Chem. Phys. Lipids.* 64, 57 (1993).

[77] S. Lessieur, C. Gabrielle-Madelmont, M. Paternostre, and M. Ollivon, *Anal. Biochem.* 192, 334 (1991).

[78] M. H. Moon, I. Park, and Y. Kim, *J. Chromatogr. A.* 813, 91 (1998).

[79] B. A. Korgel, J. H. Van Zanten, and H. G. Monbouquette, *Biophys. J.* 74, 3264 (1998).

[80] L. Gimbert, K. Andrew, P. Haygarth, and P. Worsfold, *Trends Anal. Chem.* 22, 615 (2003).

[81] F. Yang, K. Caldwell, and J. Giddings, *J. Colloid Interf. Sci.* 92, 81 (1983).

[82] T. Provder, *Prog. Org. Coat.* 32, 143 (1997).

[83] S. Kölchens, V. Ramaswami, J. Birgenheier, L. Nett, and D. F. O'Brien, *Chem. Phys. Lipids.* 65, 1 (1993).

[84] N. Berger, A. Sachse, J. Bender, R. Schubert, and M. Brandl, *Int. J. Pharm.* 223, 55 (2001).

[85] P. Schuck, *Biophys. J.* 78, 1096 (2000).

[86] S. Fitzpatrick, US patent 5786898 (1998).

[87] J. Lyklema and G. Fleer, *Colloid Surface* 25, 357 (1987).

[88] R. Hunter and H. Midmore, *J. Colloid Interf. Sci.* 237, 147 (2001).

[89] M. N. Padamwar and V. B. Pokharkar, *Int. J. Pharm.* 320, 37 (2006).

[90] A. Laouini, C. Jaafar-Maalej, S. Sfar, C. Charcosset, and H. Fessi, *Int. J. Pharm.* 415, 53 (2011).

[91] W. Sun, N. Zhang, A. Li, W. Zou, and W. Xu, *Int. J. Pharm.* 353, 243 (2008).

[92] X. Wang, L. Cai, X. Zhang, L. Deng, H. Zheng, C. Deng, J. Wen, X. Zhao, Y. Wei, and L. Chen, *Int. J. Pharm.* 410, 169 (2011).

[93] D. R. Arifin and A. F. Palmer, *Biotechnol. Prog.* 19, 1798 (2003).

[94] G. Ramaldes, J. Deverre, J. Grognet, F. Puisieux, and E. Fattal, *Int. J. Pharm.* 143, 1 (1996).

[95] W. Perkins, S. Minchey, and P. Ahl, *Chem. Phys. Lipids.* 64, 197 (1993).

[96] J. C. Stewart, *Anal. Biochem.* 104, 10 (1980).

[97] E. London and G. W. Feligenson, *Anal. Biochem.* 88, 203 (1978).

[98] M. Takayama, S. Itoh, T. Nagasaki, and I. Tanimizu, *Clin. Chim. Acta* 79, 93 (1977).

[99] H. Kobayashi, M. Yoshida, and K. Miyashita, *Chem. Phys. Lipids* 126, 111 (2003).

[100] R. Singh, M. Ajagbe, S. Bhamidipati, Z. Ahmad, and I. Ahmad, *J. Chromatogr. A* 1073, 347 (2005).

[101] L. H. Reddy, K. Vivek, N. Bakshi, and R. S. R. Murthy, *Pharm. Dev. Technol.* 11, 167 (2006).

[102] N. Ammoury, H. Fessi, J. P. Devissaguet, F. Puisieux, and S. Benita, *J. Pharm. Sci.* 79, 763 (1990).

[103] J. Plessis, C. Ramachandran, N. Weiner, and D. Müller, *Int. J. Pharm.* 127, 273 (1996).

[104] E. Casals, A. M. Galán, G. Escolar, M. Gallardo, and J. Estelrich, *Chem. Phys. Lipids* 125, 139 (2003).

[105] R. K. Jain, *Adv. Drug Deliv. Rev.* 46, 149 (2001).

[106] R. N. Rowland and J. F. Woodley, *Biochim. Biophys. Acta* 620, 400 (1980).

[107] G. Dapergolas and G. Gregoriadis, *Lancet* 2, 824 (1976).

[108] R. M. Fielding, *Clin. Pharmacokinet* 21, 155 (1991).

[109] M. Uhumwangho and R. Okor, *J. Med. Biomed. Res.* 4, 9 (2005).

[110] D. D. Lasic, *Nature* 380, 561 (1996).

[111] J. Adler-moore and R. Proffit, *J. lip. Res.* 3, 429 (1993).

[112] S. M. Sullivan, R. K. Gieseler, S. Lenzner, J. Ruppert, T. G. Gabrysiak, J. H. Peters, G. Cox, L. Richer, W. J. Martin, and M. J. Scolaro, *Antisense Res. Dev.* 2, 187 (1992).

[113] R. Glück, R. Mischler, B. Finkel, J. U. Que, B. Scarpa, and S. J. J. Cryz, *Lancet* 344, 160 (1994).

[114] G. Betz, A. Aeppli, N. Menshutina, and H. Leuenberger, *Int. J. Pharm.* 296, 44 (2005).

[115] M. Schmid and H. Korting, *Adv. Drug Deliv. Rev.* 6, 335 (199).

[116] M. Mezei and V. Gulasekharam, *Life Sci.* 26, 1473 (1980).

[117] J. Lasch and W. Wohlrab, *Biomed. Biochim. Acta* 45, 1295 (1986).

[118] H. C. Korting, H. Zienicke, M. Schäfer-Korting, and O. Braun-Falco, *Eur. J. Clin. Pharmacol.* 39, 349 (1990).

[119] V. Masini, F. Bonte, A. Meybeck, and J. Wepierre, *J. Pharm. Sci.* 82, 17 (1993).

[120] M. Schäfer-Korting, H. C. Korting, and E. Ponce-Pöschl, *Clin. Investig* 72, 1086 (1994).

[121] A. Gesztes and M. Mezei, *Anesth. Analg.* 67, 1079 (1988).

[122] E. Touitou, N. Dayan, L. Bergelson, B. Godin, and M. Eliaz, *J. Control Release* 65, 403 (2000).

[123] E. Horwitz, S. Pisanty, R. Czerninski, M. Helser, E. Eliav, and E. Touitou, *Oral Surg. Oral Med. Oral Pathol. Oral Radiol. Endod.* 87, 700 (1999).

[124] N. Moussaoui, M. Cansell, and A. Denizot, *Int. J. Pharm.* 242, 361 (2002).

[125] M. S. Cansell, N. Moussaoui, and M. Mancini, *Int. J. Pharm.* 343, 277 (2007).

[126] J. F. Arrieta-Molero, K. Aleck, M. K. Sinha, C. M. Brownscheidle, L. J. Shapiro, and M. A. Sperling, *Horm. Res.* 16, 249 (1982).

[127] H. C. Hemker, W. T. Hermens, A. D. Muller, and R. F. Zwaal, *Lancet* 1, 70 (1980).

[128] D. Jaskierowicz, F. Genissel, V. Roman, F. Berleur, and M. Fatome, *Int. J. Radiat. Biol. Relat. Stud. Phys. Chem. Med.* 47, 615 (1985).

[129] K. Vadiei, R. Perez-Soler, G. Lopez-Berestein, and D. Luke, *Int. J. Pharm.* 57, 125 (1989).

[130] M. Al-Meshal, S. Khidr, M. Bayomi, and A. Al-Angary, *Int. J. Pharm.* 168, 163 (1998).

[131] R. M. Fielding, L. Moon-McDermott, R. O. Lewis, and M. J. Horner, *Antimicrob. Agents Chemother.* 43, 503 (1999).

[132] R. N. Rowland and J. F. Woodley, *Biochim. Biophys. Acta* 673, 217 (1981).

[133] M. Nagata, T. Yotsuyanagi, M. Nonomura, and K. Ikeda, *J. Pharm. Pharmacol.* 36, 527 (1984).

[134] S. P. Young, E. Baker, and E. R. Huehns, *Br. J. Haematol.* 41, 357 (1979).

[135] C. C. Miiller-Goymann, *European Journal of Pharmaceutics and Biopharmaceutics* 58, 343 (2004).

[136] H. Lautenschläger, Liposomes Handbook of Cosmetic Science and Technology, Taylor and Francis Group, CRC Press, Boca Raton (2006), pp. 155–163.

[137] V. B. Patravale and S. D. Mandawgade, *International Journal of Cosmetic Science* 30, 19 (2008).

[138] A. Sharma, S. Kumar, and M. N. Mahadevan, *IJRAPR* 2, 54 (2012).

[139] T. M. Taylor, P. M. Davidson, B. D. Bruce, and J. Weiss, *Crit. Rev. Food Sci. Nutr.* 45, 587 (2005).

[140] M. R. Mozafari, C. Johnson, S. Hatziantoniou, and C. Demetzos, *J. Liposome Res.* 18, 309 (2008).

[141] B. A. Law and J. S. King, *J. Diary Res.* 52, 183 (1991).

[142] C. Kirby, *Delivery Systems for Enzymes. Chem. Br.* 26, 847 (1990).

[143] A. Tahibi, J. D. Sakurai, R. Mathur, and D. F. H. Wallach, *Proc. Symp. Contr. Rel. Bioact. Mat.* 18, 231 (1991).

Preparation of Liposomes: A Novel Application of Microengineered Membranes - Investigation of the Process Parameters and Application to the Encapsulation of Vitamin E

Abdallah Laouini[1, 2], Catherine Charcosset[2], Hatem Fessi[2], Richard G. Holdich[1], Goran T. Vladisavljevic[1]

[1]: Loughborough University, Department of Chemical Engineering, Loughborough, Leicestershire, LE11 3TU, United Kingdom.

[2] : Université Claude Bernard Lyon 1, Laboratoire d'Automatique et de Génie des Procédés (LAGEP), UMR-CNRS 5007, CPE Lyon, Bât 308G, 43 Boulevard du 11 Novembre 1918, F-69622 Villeurbanne Cedex, France.

Royal Society of Chemistry (RSC) Advances, 3, 4985-4994, 2013

Impact factor: 2.562 (partial)

Abstract

Liposomes with a mean size of 59 – 308 nm suitable for pulmonary drug delivery were prepared by the ethanol injection method using nickel microengineered flat disc membranes with a uniform pore size of 5 – 40 mm and a pore spacing of 80 or 200 mm. An ethanolic phase containing 20 – 50 mg/ml phospholipid (1-palmitoyl-2-oleoyl-sn-glycero-3-phosphocholine (POPC) or Lipoid1 E80), 5 – 12.5 mg/ml stabilizer (cholesterol, stearic acid or cocoa butter), and 0 or 5 mg/ml vitamin E was injected through the membrane into an agitated aqueous phase at a controlled flux of 142 – 355 l/m^2/h and a shear stress on the membrane surface of 0.80 – 16 Pa. The mean particle size obtained under optimal conditions was 84 and 59 nm for Lipoid E80 and POPC liposomes, respectively. The particle size of the prepared liposomes increased with an increase in the pore size of the membrane and decreased with an increase in the pore spacing. Lipoid E80 liposomes stabilized by cholesterol or stearic acid maintained their initial size within 3 months. A high entrapment efficiency of 99.87% was achieved when Lipoid E80 liposomes were loaded with vitamin E. Transmission electron microscopy images revealed spherical multi-lamellar structure of vesicles. The reproducibility of the developed fabrication method was high.

Key words: Liposomes – Vitamin E - Encapsulation – Microsieve membrane – Membrane emulsification.

Contents

1. Introduction

Over the last decades, advances in pharmaceutical science and technology have facilitated the availability of an extensive range of novel drug carriers including nanoparticles, nanocapsules, nanospheres and liposomes. Liposomes are known as self-assembled vesicles with a phospholipid bilayer structure, which contains an aqueous cavity **[1]**. Because of their structure, liposomes can entrap hydrophilic agents in their internal aqueous compartment and lipophilic ones within the lipid membrane **[2]**. Owing to their biocompatibility, biodegradability and low toxicity, liposomes have attracted much attention in a wide variety of fields including contrast agents, cosmetics, and drug delivery systems **[3]**.

Rational liposome design can be done by selecting an appropriate formulation and production method. For pharmaceutical and clinical use, several criteria must be fulfilled in terms of size and size distribution which are of critical importance for in vivo applications of a liposomal formulation. In particular, the size of liposomes affects drug loading, biodistribution, targeting, acoustic response, therapeutic efficacy and rate of clearance from the body. In addition, the method used for liposome preparation must be reproducible and process conditions must allow production at reasonable costs and economic scale-up **[4]**.

Since the pioneering discovery of *Bangham* several decades ago **[1]**, the development of liposomes preparation methods has been astonishing. Indeed, numerous preparation techniques have been reported in the literature. Thin film hydration, reversed phase evaporation, detergent dialysis and solvent injection are the most commonly applied methods for liposome formulation. More details can be found in a recent review on liposomes **[5]**.

The conventional ethanol injection technique first described by *Batzari and Korn* **[6]** offers many advantages, such as simplicity, the absence of potentially harmful chemicals and complicated physical treatments, the possibility of production of small-sized liposomes with minimal technical requirements and the possibility of scale up. Several novel approaches based on the ethanol injection technique are reported such as the microfluidic channel method **[7]** and the cross flow injection technique **[8]** whereby substantial progress was achieved, leading from conventional batch process to potential large scale continuous procedure.

Microporous membranes are increasingly used for the preparation of emulsions and micro/nano particles, such as lipid nanoparticles **[9]**, nanocapsules **[10]**, gel microbeads **[11]**, microcapsules **[12]** and liposomes **[13]**. Recently, a new microengineered nickel membrane has become available, consisting of an array of regulary spaced, rectilinear pores. Microengineered membranes are analogous to an array of parallel microfluidic channels through which one fluid phase can be

introduced into another fluid at an overall much higher flow rate than is possible in microfluidic devices.

The membrane contactor method of liposome preparation used in this study was based for the first time on microengineered membranes. These membranes, which have a perfect hexagonal array of uniform pores, allow a much more uniform and controllable injection of lipid-containing organic phase into an aqueous phase. Therefore, the use of microengineered membranes enables a better control over diffusive mixing at the liquid/membrane interface where the lipids selfassemble into vesicles. This may provide fine control of liposome size distribution and make easier the extrapolation of the results for an industrial large scale production.

This new method of liposome preparation was applied to the encapsulation of α-tocopherol (one isomer of vitamin E), which prevents oxidative damage and lipid peroxidation in central and peripheral nervous systems **[14]**. Because of its promising therapeutic potential and safety, α-tocopherol has been tested to prevent cigarette smoke toxicity as several pulmonary disorders are mainly caused by oxidative stress phenomena **[15]**. However, oral or intravenous administration failed to restore the broncho-alveolar level of vitamin E **[16]**. Recently, attention has been drawn to the pulmonary delivery of nanoencapsulated drugs, showing high intracellular uptake and improved stability and solubility of active substances; in particular liposome formulations have been used for the solubilization of poorly water-soluble drugs. Vitamin E-loaded liposomes with appropriate size distribution and high loading capacity could be an effective drug carrier to target the lungs after its pulmonary administration via aerosol.

The aims of the present study were: (i) to develop and optimize a novel liposome preparation method using microengineered membranes: the experiments have been done to investigate the effects of process parameters (aqueous to organic phase volume ratio, organic phase flow rate, agitation speed), phospholipid type and concentration, stabilizer type, and membrane microstructure on the characteristics of the vesicles; (ii) to apply the optimized process to the encapsulation of vitamin E; (ii) to study the process reproducibility and the stability of liposomal suspensions.

2. Material and methods

2.1 Materials

2.1.1 Reagents

The phospholipids used were POPC (1-palmitoyl-2-oleoyl-sn-glycero-3-phosphocholine) and Lipoid1 E80, purchased from Lipoı¨d GmbH (Ludwigshafen, Germany). Lipoid E80 is obtained from egg yolk lecithin and contains 82% of phosphatidyl-choline and 9% of phosphatidyl-ethanolamine. Vitamin E, cholesterol and phosphotungstic acid were supplied by Sigma-Aldrich Chemicals (Saint Quentin

Fallavier, France). All reagents were acquired with their analysis certificate. Ethanol 95% was supplied by Fisher Scientific (United Kingdom) and was of analytical grade and used without further purification. Ultra-pure water was obtained from a Millipore Synergy system (Ultrapure Water System, Millipore).

2.1.2 Microengineered membranes and stirred cell

The liposomes suspension was prepared using a stirred cell with a flat disc membrane fitted under the paddle blade stirrer, as shown in **Fig. 1(a)**.

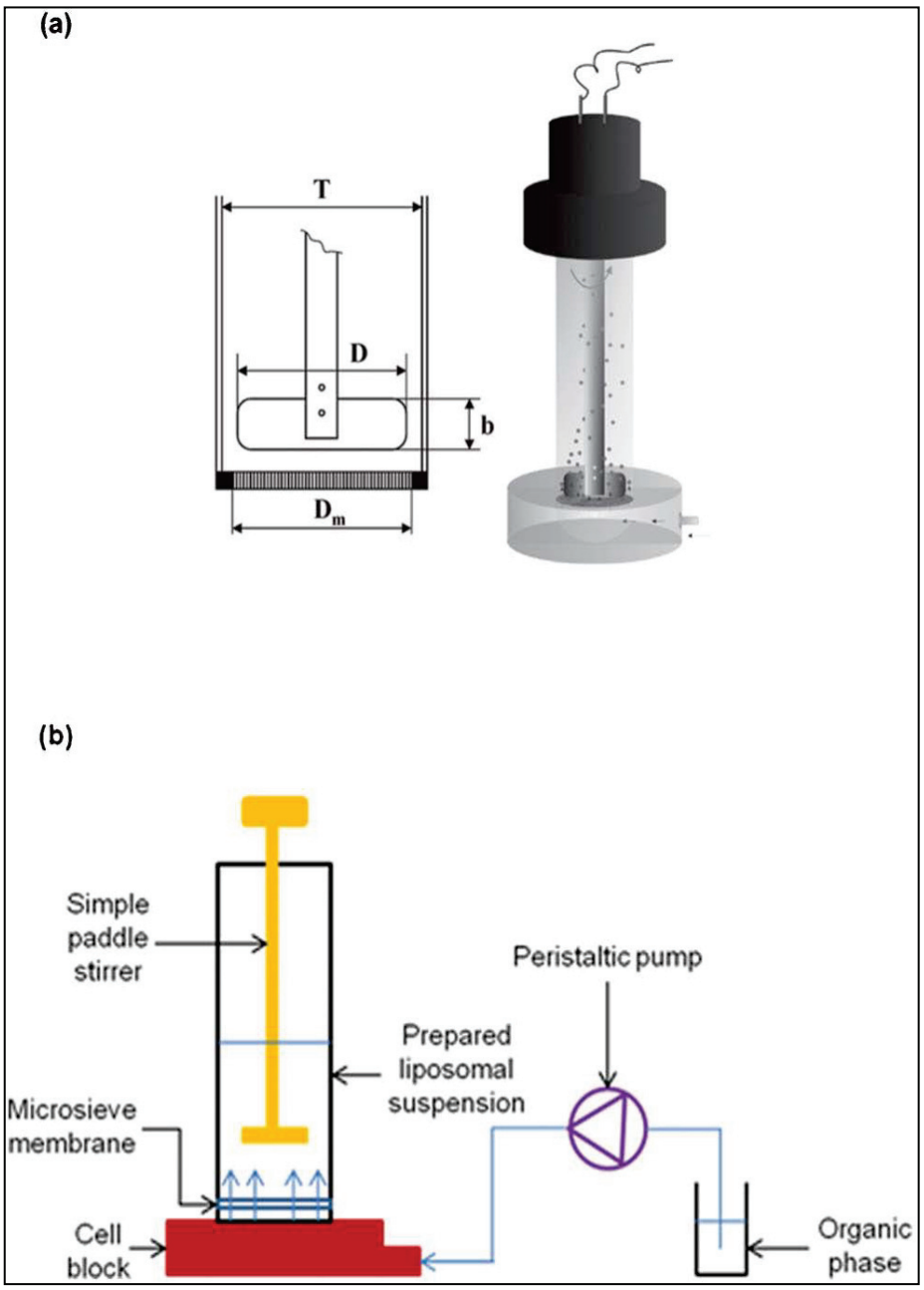

Fig. 1 (a) Schematic illustration of the stirred cell with a simple paddle stirrer above a flat disc membrane (b = 12 mm, D = 32 mm, Dm = 33 mm, nb = 2 and T = 40 mm). **(b)** Schematic diagram of the experimental set-up.

Both stirred cell and membranes were supplied by Micropore Technologies Ltd. (Hatton, Derbyshire, United Kingdom). The agitator was driven by a 24 V DC motor (INSTEK model PR 3060) and the paddle rotation speed could be controlled in the range from 200 to 1300 rpm by the applied voltage. The membranes used were nickel microengineered membranes containing uniform cylindrical pores with a diameter of 5, 10, 20 or 40 μm, arranged at a uniform spacing of 80 or 200 μm. The membranes were fabricated by the UVLIGA process, which involves galvanic deposition of nickel onto the template formed by photolithography **[17]**. A perfect hexagonal array of pores with a pore at the centre of each hexagonal cell can be seen in the supplementary material (**Fig. S1**).

The porosity of a membrane with the hexagonal pore array is given by:

$$\varepsilon = \pi/(2\sqrt{3})(\mathrm{dp/L})^2 \quad (1)$$

where dp is the pore diameter and L is the interpore distance. The porosities of the membranes used in this study, were calculated from eqn (1) and expressed as percentages, and are given in the supplementary material (**Table S1**).

2.2 Protocol for preparation of liposomes

A schematic diagram of the experimental set-up is shown in **Fig. 1(b)**. The required amounts of phospholipid (20 or 50 mg/ml Lipoid E80 or POPC) and stabilizer (cholesterol, stearic acid or cocoa butter, 25% w/w based on phospholipid dry matter) were dissolved in ethanol. The organic phase was injected through the membrane using a peristaltic pump (Watson Marlow 101U, Cornwall, UK) at a constant flow rate of 2 – 5 ml/min corresponding to the dispersed phase flux of 142 – 355 l/m^2/h. The stirring speed ranged from 200 to 1300 rpm, which generated a shear stress on the membrane surface between 0.80 to 15.5 Pa. The cell was filled with 20 – 60 ml of ultrapure water and the experiment was run until a predetermined organic to aqueous phase ratio was achieved. Spontaneous formation of liposomes started as soon as the organic phase was brought in contact with the aqueous phase. The liposomal suspension was kept under stirring for 15 min and finally the suspension was collected and the ethanol was removed by evaporation under reduced pressure (Buchi, Flawil, Switzerland).

After each experiment, the membrane was sonicated in ethanol for 1 h, followed by soaking in a siloxane-based wetting agent for 30 min (in order to increase the hydrophilicity of the membrane surface). Drug-loaded liposomes were prepared as described above, with the only difference being that 5 mg/ml vitamin E was dissolved in the ethanolic phase containing a mixture of phospholipid and stabilizer.

2.3 Characterization of liposomes

In order to assess the quality of liposomes and to allow comparison between different batches, various analyses were performed: particle size distribution, zeta potential, encapsulation efficiency, and microscopic observation.

2.3.1 Size analysis

In this study, two different techniques for particle size characterization were used: dynamic light scattering (DLS) otherwise known as photon correlation spectroscopy (PCS) and differential centrifugal sedimentation (DCS). A Malvern Zetasizer Nano-series (Zetamaster 3000 HSA, Malvern, UK) was used for DLS measurements. Each sample was diluted 100-fold with ultra-pure water before measurement and was then analyzed in triplicate at 25 °C. The average particle size was expressed as the Z-average and polydispersity was expressed as the polydispersity index, PDI. A CPS disc centrifuge, model DC 24000 (CPS instruments, Florida, USA), was used for DCS measurements. A light beam near the outside edge of the rotating disc passes through the centrifuge at some distance below the surface of the fluid and measures the concentration of particles as they settle. The time required for particles to reach the detecting beam depends upon the speed and geometry of the centrifuge, the difference in density between the particles and the fluid, and the diameter of the particles. Thus, when operating conditions are stable, sedimentation velocity increases with the particle diameter, so that the time needed to reach the detector beam is used to calculate the size of the particles **[18, 19]**. In this study, a sucrose gradient (from 18% to 26%) was built and the sample was diluted in a sucrose solution (30%) before being injected. Prior to the analysis, the instrument was calibrated using an aqueous dispersion of polybutadiene particles of a known size distribution (mean size of the calibration standard = 402 nm). The mean particle size was expressed as the number average mean diameter, d_{av} and the polydispersity was expressed as the coefficient of variation, $CV = (\sigma/d_{av}) \times 100$, where σ is the standard deviation of particle diameters in a suspension. A smaller CV or PDI value indicates a narrower size distribution **[20, 21]**. All values of the mean particle size and PDI or CV are expressed as the mean ± standard deviation (S.D.).

2.3.2 Zeta potential determination

The zeta potential was measured using a Malvern Zetasizer Nano-series (Zetamaster 3000 HSA, Malvern, UK) and used to predict the colloidal stability of the liposome suspension. The measurements were repeated at least three times after sample dilution in water. The zeta potential was calculated from the electrophoretic mobility using the Helmholtz-Smoluchowski equation **[22]**.

2.3.3 Encapsulation efficiency

Liposome preparations are a mixture of encapsulated and non-encapsulated drug fractions. Methods to determine the fraction of encapsulated material within liposomes typically rely on destruction of the lipid bilayer and subsequent quantification of the released material. In the present study, the drug encapsulation efficiency was determined using the protamine aggregation method, as described by *Wang et al.* **[23]** and *Sun et al.* **[24]**. Briefly, the total amount of vitamin E (TA) was determined after disrupting and dissolving vitamin E-loaded liposomes in ethanol using an ultrasound bath for 10 min. The amount of encapsulated vitamin E was determined after non-disruptive aggregation of liposomes with an equal volume of protamine solution (10 mg/ml) and a normal saline solution. The mixture was centrifuged (Heraeus, Thermo scientific, Philadelphia, USA) at 15 000 rpm for 50 min at +4 °C to remove the supernatant from the liposome–protamine aggregates. The resulting liposomal pellet was dissolved in ethanol and assayed for encapsulated vitamin E amount (EA). The vitamin E encapsulation efficiency (EE) was calculated as follows:

$$EE = EA/TA \times 100 \quad (2)$$

The encapsulation efficiency was determined in triplicate.

The concentration of vitamin E was measured using an HPLC system (Agilent System series 1100, Agilent Technologies, California, USA). The HPLC equipment consisted of a pump, an auto-sampler and a UV/VIS detector. The column used was a LiChrospher RP C18 column (5 mm, 15 cm × 0.46 cm) (Supelco, Bellefonte, USA). The separation was carried out using a mixture of methanol and water (96 : 4 v/v) as the mobile phase at a flow rate of 1.6 ml/min. The eluent was monitored at 292 nm and peaks were recorded using the chromatography data system software provided by Agilent. Before the chromatographic data were collected, the column was equilibrated for 30 min with a minimum of 30 column volumes. At the end of the assay, the column was washed using water–acetonitrile mixture (50 : 50 v/v) for 60 min. This HPLC analytical method was validated (data not shown).

2.3.4 Microscopic observation

The morphology of the liposomes was observed by Transmission Electron Microscopy (TEM) using a CM 120 microscope (Philips, Eindhoven, Netherlands) operating at an accelerating voltage of 80 kV. The sample was prepared as described in our previous study **[25]**. A drop of the liposome dispersion was placed on a copper grid. A thin film of the liposome dispersion was obtained by removing excess solution using a filter paper. Negative staining using a 2% phosphotungstic acid solution (w/w) was performed directly on the deposit during 1 min. Finally, the excess of phosphotungstic

solution was removed with a filter paper after which the stained samples were transferred to the TEM for imaging.

2.4 Reproducibility test

Once all the process parameters were assessed, the experiment under optimal conditions was repeated two times. The technique reproducibility was evaluated in terms of mean particle size and size distribution.

2.5 Stability study

Stability assessment is a major consideration for liposomes production. Since liposome preparations are heterogeneous in size, the average size distribution changes upon storage. Liposomes tend to fuse and grow into bigger vesicles, which are thermodynamically more stable. Hence, time variation of the size distribution is a good indicator of the long-term stability of liposomes. Moreover, breakage of liposomes during production and storage presents a significant problem leading to drug leakage from the vesicles. Therefore, encapsulation efficiency is also an important indication of the stability of liposomes **[5]**.

The liposomal samples were stored under conditions required by the 2008 guidelines of the ICH (International Conference on Harmonization of Technical Requirements for Registration of Pharmaceutical for Human Use): 5 ± 3 °C for normal stability study. The storage period was about 3 months for drug-free liposomes and 2 months for drug-loaded liposomes. The stability was assessed by comparing the initial mean size, zeta potential and encapsulation efficiency with those achieved after the storage period.

3. Results and discussion

3.1 Mechanism of liposomes formation

In our study, an ethanolic solution of vesicle-forming lipids was injected through the membrane into an agitated aqueous phase, leading to the formation of numerous micro-streams of the organic phase within a boundary layer of the aqueous phase. Due to inter-diffusion of the two miscible phases, phospholipids in the ethanol–water mixture reached a solubility limit and self-assembled into vesicles **[13]**. The exact mechanism of liposomes formation is not yet well understood. A model of vesicle formation was proposed by *Lasic* **[26]**; this model suggests that during the injection process, the phospholipids which are completely soluble in the organic phase, precipitate at the water–ethanol phase boundary due to change in their solubility. The phospholipid bilayers peel off the precipitated phase and form bilayered phospholipid fragments (BPFs) in the aqueous phase. The thermodynamic instability at the edges of the BPF causes bending and when the BPF closes upon itself, a vesicle is formed. The BPF was suggested to be an intermediate structure in all the vesicle formation processes.

3.2 Optimization of phospholipid concentration

As can be seen from **Table 1**, as the phospholipid concentration in the organic phase was increased from 20 to 50 mg/ml, the mean vesicle size increased from 187 to 227 nm and the PDI increased from 22 to 29%. Probably, at the higher phospholipid concentration in the organic phase, more phospholipid molecules are incorporated into each vesicle and larger vesicles are formed.

Our results are in agreement with those reported elsewhere. *Laouini et al.* **[27]** observed that the mean size of liposomes, prepared using a hollow fiber membrane contactor, increased from 114 to 228 nm when the phospholipid concentration in the organic phase increased from 20 to 80 mg/ml. In addition, *Jaafar-Maalej et al.* **[13]** prepared liposomes using Shirasu Porous Glass (SPG) membranes and observed that the average size was around 50 and 95 nm at the phospholipid concentration in the organic phase of 20 and 60 mg/ml, respectively. Similar trends with larger vesicles at higher phospholipid contents in the organic phase were reported in other liposome preparation techniques such as the modified ethanol injection method **[28]** and the microfluidic method **[29]**.

Therefore, 20 mg/ml was selected as the optimum phospholipid concentration in the ethanolic phase in the subsequent parts of the study, since it gave vesicles with a smaller mean size.

3.3 Optimization of the aqueous to organic phase ratio

In order to investigate the effect of aqueous phase volume, liposomes were prepared using approximately 13 ml of the organic phase and respectively 20, 40 and 60 ml of water; corresponding to an aqueous to organic phase volume ratio of 1.5, 3 and 4.5. As can be seen in **Table 1**, the mean size of the liposomes decreased as the aqueous phase volume increased. Indeed, at the higher aqueous to organic phase volume ratio, phospholipids from the organic phase become more diluted after mixing with the aqueous phase, which may result in the formation of smaller vesicles. Moreover, formation of a more diluted liposomal suspension may help to prevent the fusion of small liposomes to larger vesicles, which can occur immediately after their formation.

Similar results were obtained using a hollow fiber membrane module **[27]**; increasing the aqueous to organic phase volume ratio from 0.4 to 2 led to a decrease in the mean size of the liposomes from 189 to 114 nm. When the organic phase was injected through a 0.9 mm SPG membrane into the aqueous phase with a volume of 400 and 500 ml, the mean particle size of the liposomes was 203 and 61 nm, respectively **[13]**.

Table 1. Influence of formulation factors and process parameters (phospholipid concentration, aqueous to organic phase volume ratio, agitation speed, transmembrane flux, stabilizer type and phospholipid type) on liposomes characteristics (mean size and PDI). The method used for size characterization was the DLS

Phospholipid concentration (mg/ml)	Aqueous to organic phase volume ratio	Agitation speed (rpm)	Transmembrane flux ($l/m^2/h$)	Stabiliser nature	Phospholipid nature	Mean size* (nm)	PDI* (%)
20	3	600	355	Cholesterol	Lipoid E80	187 ± 3	22 ± 1
50	3	600	355	Cholesterol	Lipoid E80	227 ± 3	29 ± 1
20	1.5	600	355	Cholesterol	Lipoid E80	308 ± 2	21 ± 1
20	4.5	600	355	Cholesterol	Lipoid E80	121 ± 1	22 ± 1
20	4.5	200	355	Cholesterol	Lipoid E80	219 ± 3	8 ± 1
20	4.5	1300	355	Cholesterol	Lipoid E80	92 ± 1	41 ± 1
20	4.5	600	142	Cholesterol	Lipoid E80	84 ± 2	24 ± 1
20	4.5	600	142	Stearic acid	Lipoid E80	154 ± 4	37 ± 1
20	4.5	600	142	Cocoa butter	Lipoid E80	135 ± 2	24 ± 1
20	4.5	600	142	cholesterol	POPC	59 ± 2	30 ± 2

*: Each value represents the mean ± S.D. (n=3)

Our data suggests that the optimum aqueous to organic phase volume ratio is 4.5 since it produced liposomes with the smallest mean size. Thus, in the following experiments, the aqueous phase volume was set at 60 ml and the organic phase volume was set at approximately 13 ml.

3.4 Optimization of the agitation speed

Table 1 also illustrates the effect of the stirrer speed on the particle size distribution of the prepared liposomes. When the stirrer speed was increased by a factor of 6.5 (from 200 to 1300 rpm), the mean size decreased by 58% (from 219 to 92 nm). The decrease in the particle size was the most pronounced in the range from 200 to 600 rpm. In addition, an increase in the agitator speed from 200 to 1300 rpm led to a broader size distribution (the PDI was 8, 22 and 41% for the agitation speed of 200, 600 and 1300 rpm, respectively). A decrease in the particle size with an increase in the stirrer speed was due to an increase in the inter-diffusion rate of the two phases. The faster diffusion rates generally lead to smaller vesicles because the local phospholipid concentration during vesicle formation is lower due to a more uniform distribution of phospholipids over the ethanol–water mixture. A similar trend was reported by *Dragosavac et al.* **[30]** in membrane emulsification using the same stirred cell device and it was attributed to the higher drag force acting on droplets on the membrane surface. The droplet size was significantly reduced when the stirrer speed increased up to 600 rpm, but this effect was less pronounced at the higher stirrer speeds; the average droplet size was almost constant at stirrer speeds above 1100 rpm. Our results are also in agreement with other membrane emulsification studies using the stirred cell device **[31, 32]**. In this study, 600 rpm was selected as the optimum agitation speed taking into consideration both the size of liposomes and their uniformity.

3.5 Optimization of the organic phase flow rate

As the flow rate of the organic phase decreased, so did the liposome size. **Table 1** shows that the liposome size was 121 and 84 nm at flow rates of 5 and 2 ml/min, respectively. These two flow rates are equivalent to the transmembrane flux of 142 and 355 $l/m^2/h$, respectively. Increase in the flow rate of the organic phase leads to an increase in the rate of transfer of phospholipids (PL) to the membrane surface, given by the product: CoQo, where Co is the PL concentration in the organic phase and Qo is the organic phase flow rate. Our results indicate that the size of the liposomes increases with an increase in the rate of transfer of PL to the membrane surface or a decrease in the rate of transfer of PL away from the membrane surface. Therefore, the largest vesicles are formed at the conditions corresponding to the maximum concentration of PL at the membrane–aqueous phase interface. Similar trends were observed in liposome preparation using the SPG membrane and the hollow fiber membrane. *Laouini et al.* **[27]** observed a decrease of the liposome size from 129 to

114 nm when the organic phase pressure was reduced from 3.8 to 1.8 bar. *Jaafar-Maalej et al.* **[13]** found that a peak in the particle size distribution of liposomes was shifted from around 45 to 80 nm as the organic phase pressure increased from 3 to 5 bar. *Sheibat-Othman et al.* **[33]** have produced pH-sensitive particles by injecting organic phase into aqueous phase in a membrane contactor and obtained larger particles at higher organic phase flow rates. In this study, based on the obtained results 2 ml/min was considered as the optimum organic phase flow rate, since it produced smaller sized liposomes at an acceptable production rate.

3.6 Choice of the stabilizer

The liposomal preparation method developed in this study is intended to be aerosolized in order to target the smokers' lungs. Therefore, it would be meaningful if cholesterol used as a stabilizer could be replaced by another lipid, since cholesterol is usually associated with atherosclerosis and cardio-vascular diseases **[34]**. In the present study, we have investigated the use of stearic acid and cocoa butter as alternative stabilizers to cholesterol.

Stearic acid has already been tested in liposomal formulations **[35, 36]**; however only the encapsulation efficiency was assessed and no investigation on long-term stability was carried out. Cocoa butter has never been used in a liposome preparation; it was chosen since it is a widely used excipient in pharmaceuticals and exhibits a better biocompatibility and lower in vivo toxicity than semi-synthetic lipids. Cocoa butter contains 41% stearic acid of its typical fatty acid content, it is solid at room temperature and melts between 32 and 38 °C. As shown in Table 1, under the same experimental conditions (the phospholipid concentration of 20 mg/ml, the aqueous to organic phase ratio of 4.5, the agitator speed of 600 rpm, and the transmembrane flux of 142 l/m^2/h), the initial vesicle size was 84, 154, and 135 nm for liposomes stabilized by cholesterol, stearic acid and cocoa butter, respectively.

However, only liposomes prepared using cholesterol or stearic acid maintained their initial mean size after 3 months (**Fig. 2**). Liposomes prepared using cocoa butter doubled in size during the storage period (from 135 nm at day 0 to 324 nm at day 90). Therefore, it can be concluded that stable liposomes can be obtained using cholesterol or stearic acid. Although stearic acid was an efficient long-term stabilizer of liposomes, under the same experimental conditions significantly smaller and more uniform vesicles can be produced using cholesterol (the PDI increased from 24 to 37% and the mean size from 84 to 154 mm when cholesterol was replaced by stearic acid in the liposomal formulation). Cocoa butter was not suitable for long-term stabilisation, although the initial vesicle uniformity was comparable to that achieved with cholesterol.

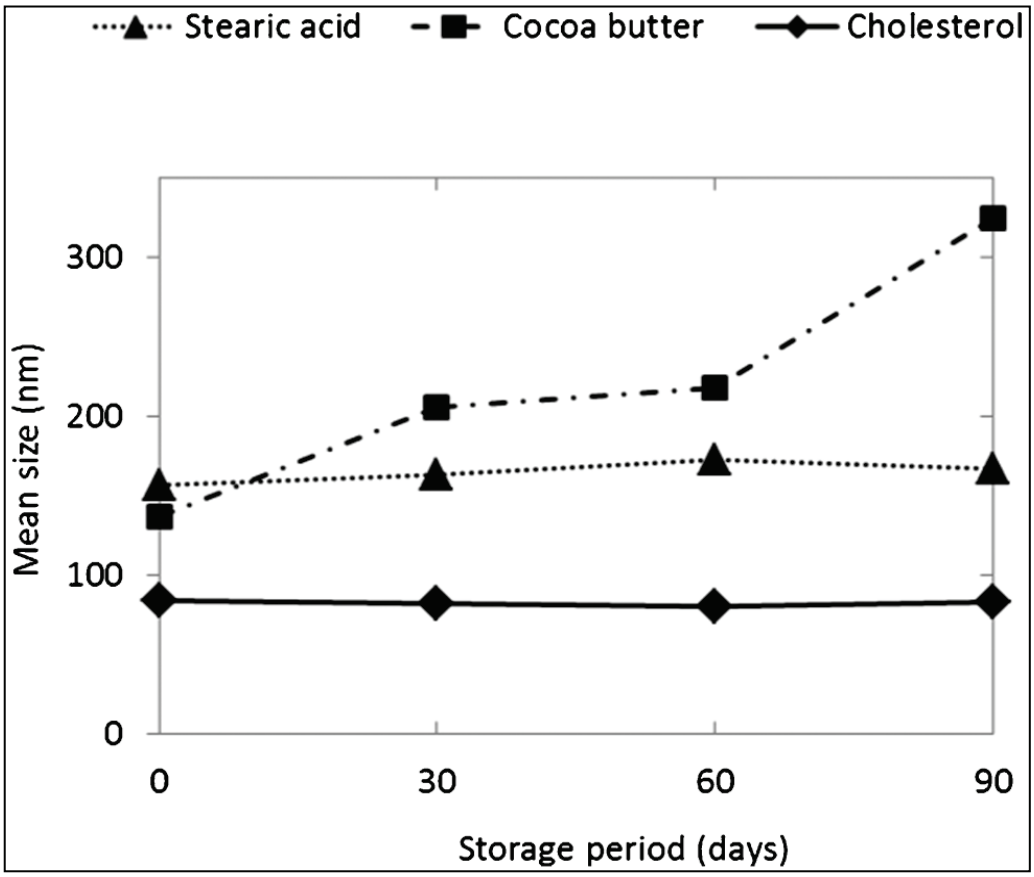

Fig. 2 Stability data for Lipoid E80 liposomes prepared using various lipids (cholesterol, stearic acid or cocoa butter) as stabilizers. The experimental conditions are specified in **Table 1**. The size characterization was performed using DLS.

3.7 Choice of the phospholipid

Two phospholipids were tested in this study: Lipoid E 80 and POPC. **Table 1** shows that under optimal conditions both phospholipids enable the formation of liposomes with a mean size below 85 nm and acceptable size distribution. Therefore our optimized process can be used to prepare liposomes containing any of these two phospholipids.

3.8 Reproducibility of the optimized process

Based on the previous findings, the formulation composed of 60 ml of water and 13 ml of ethanolic phase containing 20 mg/ml of phospholipid (Lipoid E 80 or POPC) and 5 mg/ml of cholesterol was taken to produce an optimal liposome suspension using a microengineered membrane with a mean pore size of 20 µm and a pore spacing 80 µm. The organic phase flow rate was 2 ml/min, which is equivalent to the transmembrane flux of 142 l/m^2/h, and the agitation speed was 600 rpm. The experiment conducted under these optimum conditions was repeated twice with both Lipoid E80 and POPC in order to test the reproducibility of the technique. The

resulting data, presented in **Fig. 3**, revealed very good reproducibility, in terms of mean size and PDI, between different liposome batches produced using the same type of phospholipid.

The other results (not shown here) obtained in repeated experiments performed under identical conditions confirm good reproducibility of the preparation process.

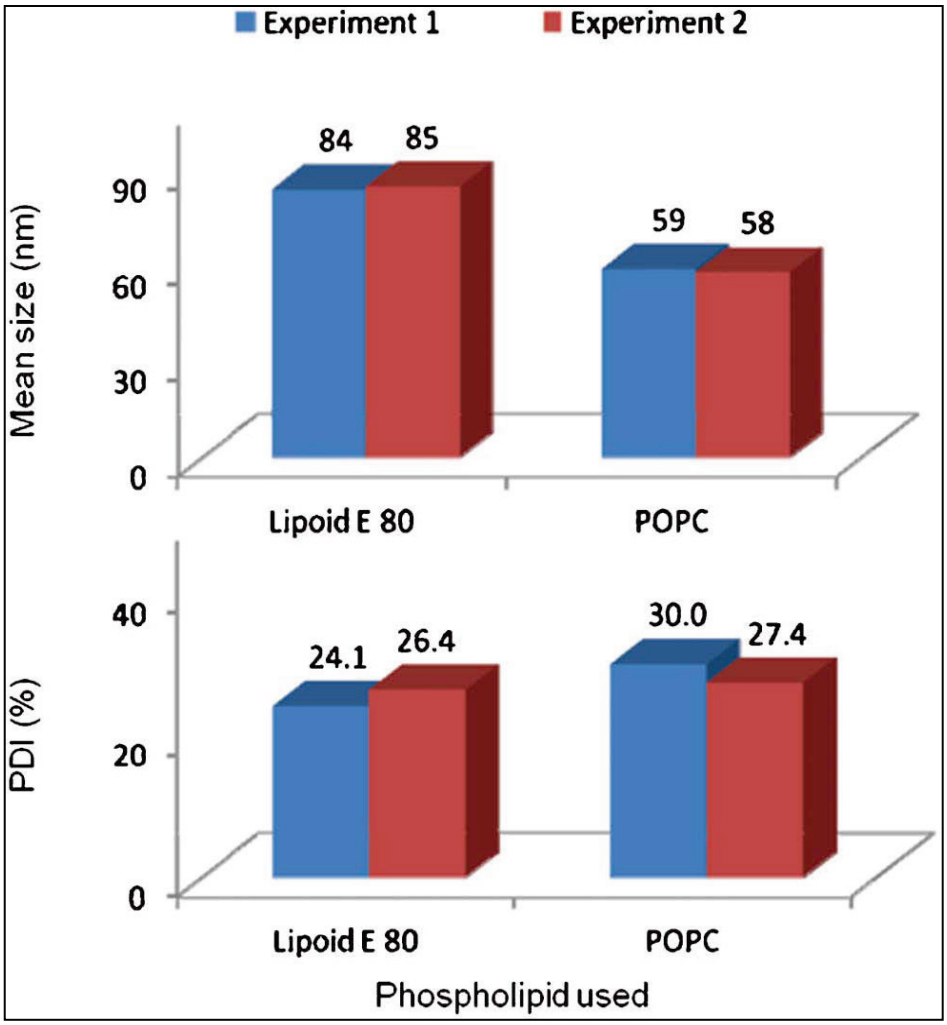

Fig. 3 Reproducibility data for liposome suspensions prepared under optimal conditions. The size characterization was performed using DLS.

3.9 Comparison of different particle size characterization methods

The DLS instrument does not require calibration and sample preparation prior to each measurement. Due to its simplicity and speed, the DLS method was used for size characterization of liposomes during the optimization step. The DCS method requires a density gradient to be built up with 9 different sucrose concentrations (from 18% to 26%) and the sample should be diluted in 30% sucrose solution prior to each measurement. In addition, calibration of the instrument is required using a sample of known particle size. Thus, DCS was only used once the process was optimized to

corroborate the values for particle size by checking for multiple modes in the size distribution. The four reproducibility test batches (two using the lipoid E 80 and two using the POPC) were characterized using DCS and the results were compared with those obtained with the DLS instrument in **Table 2**.

Table 2. Size characterization of liposome suspension containing two different PL types, prepared under optimal conditions, using two different characterization methods

PL		DLS	DCS
Lipoid E80	Mean size* (nm)	84 ± 1	110 ± 3
	PDI or CV* (%)	25 ± 2	37 ± 2
POPC	Mean size* (nm)	58 ± 1	88 ± 1
	PDI or CV* (%)	28 ± 2	34 ± 1

*: Each value represents the mean of the 2 batches of reproducibility ± S.D. (n=3)

As can be seen, the results obtained using the same sample differ significantly depending on the characterization method used. The larger mean particle sizes and broader particle size distributions were obtained using DCS, which can be explained by the fact that in DCS, the sedimentation velocity increases as the square of the particle diameter, so particles that differ in size by only a few percent settle at appreciably different rates. This means that the DCS method can achieve a higher resolution of particle size compared to the DLS method. The DCS method also has a higher sensitivity which enables the detection of small additional peaks and picks up small changes in the size distribution. In addition, all measurements using DCS were run against a known calibration standard which assures a high accuracy of the size analysis. Given that the CPS instrument was more accurate and more sensitive, the DCS method was used for particle size measurements in the subsequent parts of this study.

3.10 The effect of ethanol removal

During the preparation process, the ethanolic phase was injected through the membrane pores into the aqueous phase. The obtained liposomes were in the nanometric range, although the pore diameter ranged between 5 and 40 µm. In order to investigate the effect of solvent evaporation on the vesicle size, the particle size distribution of liposomes was measured before and after rotary evaporation and the results are presented in the supplementary material (Table S2).

As can be seen in **Table S2**, no significant difference in the mean particle size and size distribution was observed in the liposomal suspension before and after solvent removal, which means that the vesicle formation process was mainly controlled and driven by the rate of inter-diffusion of the two phases. Vesicles were formed once the organic phase was brought into contact with the aqueous phase, irrespective of the

ethanol removal rate. Therefore, the critical concentration of phospolipid in the ethanol–water mixture was reached without solvent evaporation, simply by dilution of the organic phase with water present in the cell. Because ethanol evaporation did not affect the liposome size and size distribution, it was not necessary to optimize experimental conditions in the rotary evaporator such as evaporation temperature, pressure, rotation speed of the flask, etc.

3.11 The effect of membrane cleaning and wetting procedure

The membrane was immersed in a siloxane-based wetting agent for 30 min before each experiment in order to improve the hydrophilicity of the membrane surface. The reason for this treatment was to prevent the organic phase from being spread over the membrane surface and to ensure that tiny jets of the organic phase emerging from the membrane pores penetrate thoroughly into the aqueous phase. **Table S3** (supplementary material) summarises the results of two experiments performed under identical conditions with a brand new membrane used without any surface treatment and the one re-used after cleaning and treatment with the wetting agent.

No difference in the mean size of the liposomes and CV was observed between the two membranes, which means that the membrane properties were completely restored after cleaning and that the treatment with a wetting agent, critically important in membrane emulsification, is not needed in liposome production.

3.12 The effect of membrane microstructure

In order to investigate the effect of the membrane characteristics on the liposomes mean size, experiments were conducted using 6 different membranes with nominal pore sizes 5, 10, 20 and 40 μm. The membranes with pore sizes of 5 and 10 μm had a pore spacing of 200 μm, whereas the membranes with 20 and 40 μm were supplied with two different pore spacings (80 and 200 μm). As shown in **Fig. 4(a)**, as the interpore spacing increased, the particle mean size decreased. This may be explained by the fact that when the distance between the membrane pores increased, the newly formed vesicles are less likely to aggregate. The liposome size is determined by a balance between the nucleation and growth rates. The larger the pore spacing, the smaller the number of organic phase micro-streams (potential nuclei) formed in the aqueous phase and the higher the amount of phospholipid delivered through each pore; hence, a smaller number of larger vesicles will be formed. It can also be noticed from **Fig. 4(a)** that the influence of the pore spacing is more pronounced for larger pore sizes.

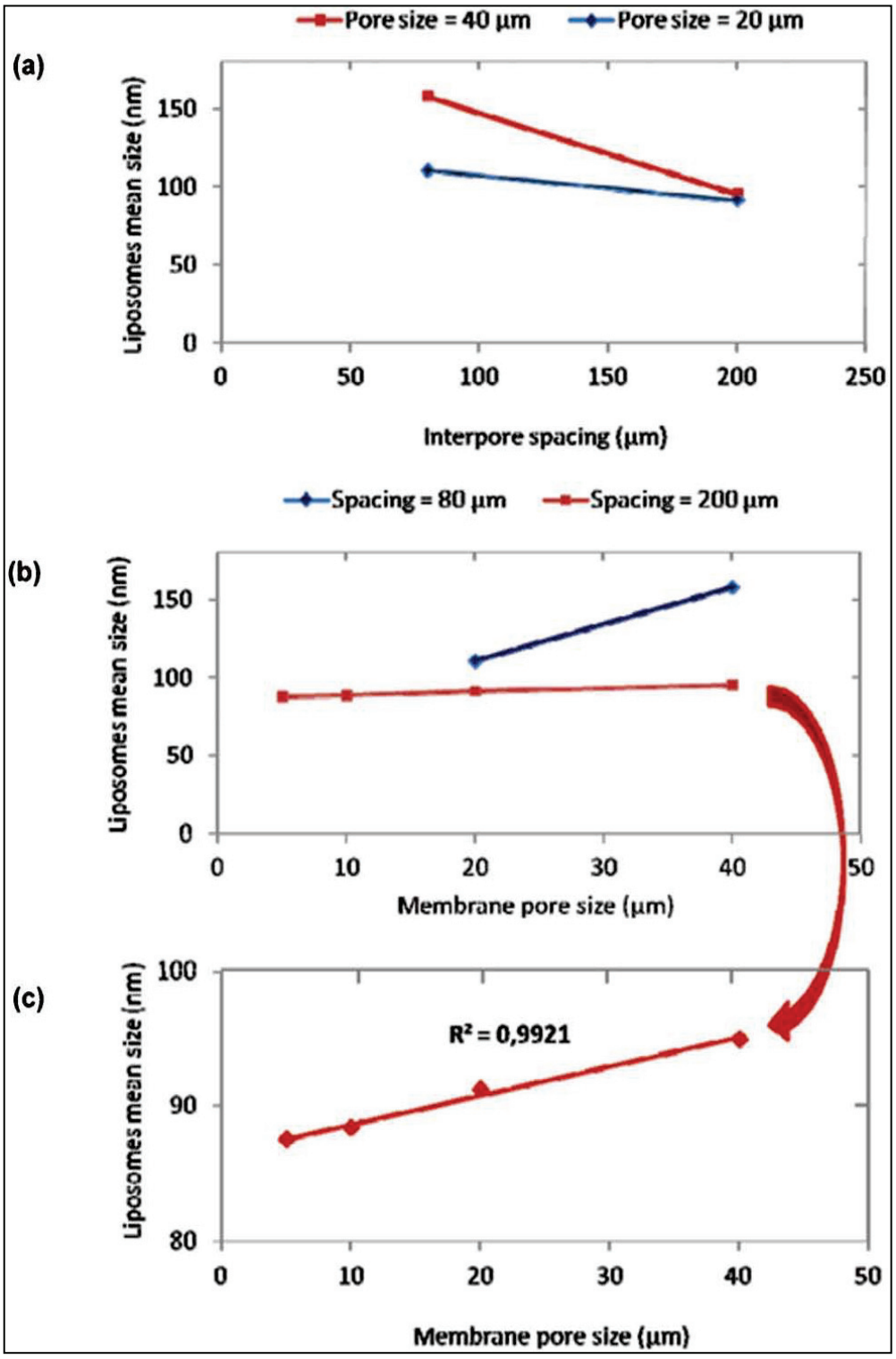

Fig. 4 Influence of the nominal pore size and pore spacing of the membrane on the liposome mean size. The experimental parameters: phospholipid: 20 mg/ml lipoid E80, stabilizer: 5 mg/ml cholesterol, aqueous to organic phase volume ratio: 4.5, agitation speed: 600 rpm, and organic phase flow rate: 2 ml/min. The size characterization was performed using DCS.

Fig. 4(b) summarizes the effect of the membrane pore size on the size of the liposomes produced. Our results are in agreement with those reported for membrane emulsification in the same stirred cell. *Dragosavac et al.* **[30]** used the same type of microengineered membranes to produce oil-in-water emulsions and found that the size of oil drops increased by a factor of 1.8 when the pore size was changed from 19 to 40 μm. Many other studies on membrane emulsification indicate that the particle size increases linearly with an increase in the pore size **[37, 38]**. Our data fitted well with a linear model with a gradient of 0.22 nm/μm and $R_2 = 0.992$ **(Fig. 4c)**. Thus, our study confirmed that the liposome size depends on the membrane structure (pore size, spacing); this underlines the feasibility of controlling the liposome size by using microengineered membranes with different pore sizes and interopore distances.

3.13 Loading of vitamin E into liposomes

Table 3 shows the effect of entrapment of vitamin E on the liposome size and size distribution.

Table 3. Effect of vitamin E loading on the characteristics of liposomal suspension. The experimental parameters: phospholipid: 20 mg/ml Lipoid E80, stabilizer: 5 mg/ml cholesterol, vitamin E: 5 mg/ml, aqueous to organic phase volume ratio: 4.5, stirring speed: 600 rpm, organic phase flow rate: 2 ml/min, pore size: 10 μm, pore spacing: 200 μm. The size characterization was performed using DCS.

Liposome suspension	Mean size* (nm)	CV* (%)	Zeta potential* (mV)	EE* (%)
Drug-free	88 ± 2	32 ± 1	28.0 ± 0.9	
Drug-loaded	96 ± 3	44 ± 2	28.5 ± 0.8	99.8 ± 1.1

*: Each value represents the mean ± S.D. (n=3)

The addition of the drug increased the vesicle mean size from 88 to 96 nm and the CV from 32 to 44%. The increase in the vesicle size could be explained by the entrapment of the drug within the phospholipidic bilayers.

The negative values of the zeta-potential were obtained (around 228 mV), which could be attributed to the presence of negatively charged phospholipids in bilayers. The zeta potential measurements give information on the surface properties of the colloidal system and could therefore be useful to determine the type of the association between the active substance and the colloidal system (for example whether the drug is encapsulated in the lipid matrix or simply adsorbed on the surface) **[39]**. **Table 3** indicates that the presence of the drug did not affect the negative surface charge. This result suggests that all vitamin E was encapsulated within the lipid bilayers without any adsorption to the vesicles surface. The greater the zeta potential the more likely the suspension to be stable, because the charged particles repel each other and this overcomes their natural tendency to aggregate **[40,41]**. It is currently believed that an

absolute value of zeta potential above 15 is required for a good electrostatic stabilization **[42]**. Thus, our zeta-potential values were sufficient to prevent liposomes aggregation and predict a good stability of the liposomal suspensions.

The high encapsulation efficiency of vitamin E within liposomes (99.87 ± 1.14%) was probably due to the high lipophilicity of the drug. This result was in agreement with those reported in the literature. *Marsanasco et al.* **[35]** reported that the percent of vitamin E encapsulated within liposomes prepared by the method of *Bangham* was equal to 98.13 ± 0.02%.

The prepared liposomal suspension is intended to be aerosolized for specific delivery of vitamin E to the alveoli level. Several previous studies have shown that the aerosolization of colloidal systems would enhance their aggregation which is dependent on the nebulizer design. No specific correlation was found between the initial size and the size of the nebulized droplets **[43, 44]**. For instance, the mass median diameters of aerosols generated upon nebulization were 2 to 14.4 folds larger than primary geometric particle diameters **[45]**. Therefore, the aerosolization of our vitamin E-loaded liposomes would generate particles less than 1.5 µm which is suitable for reaching the alveolar space since many studies reported that for specific delivery to the alveoli a size of less than 5 µm was required **[46]**.

3.14 TEM observation

The micrographs of drug-free liposomes (prepared using Lipoid E80 and POPC) and drug-loaded liposomes taken by TEM are given in **Fig. 5**.

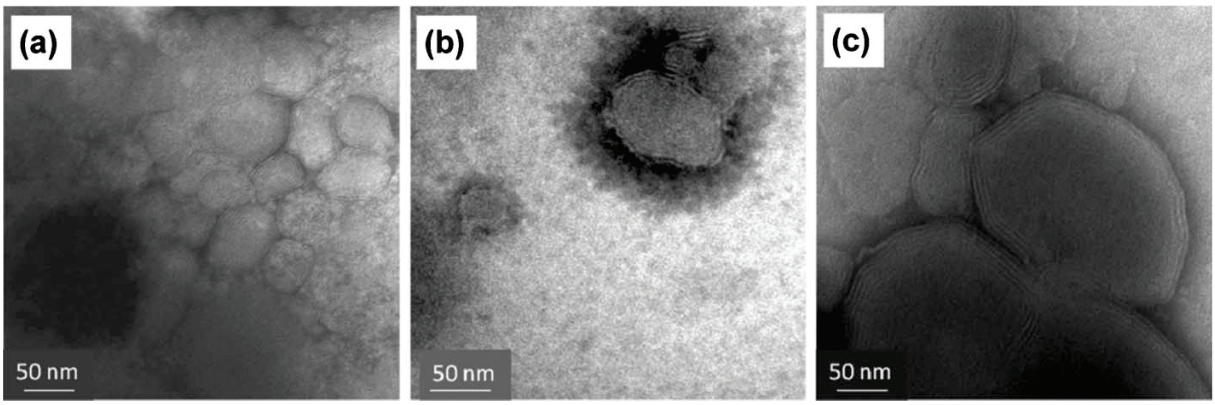

Fig. 5 TEM images of drug-free liposomes prepared using Lipoid E80 (a) or POPC (b) and drug-loaded liposomes (c).

As can be seen, liposomes were of spherical shape with multilayered membrane structure. Their size estimated from TEM pictures was in the range of 50 – 150 nm which is coherent with values obtained using DLS and DCS.

3.15 Stability study

The variations of the zeta potential, the vesicle mean size and CV were followed over a storage time of 3 months for drug-free liposomes and 2 months for drug-loaded liposomes at 5 ± 3 °C. The stability data are shown in **Fig. 6** and **Table 4**.

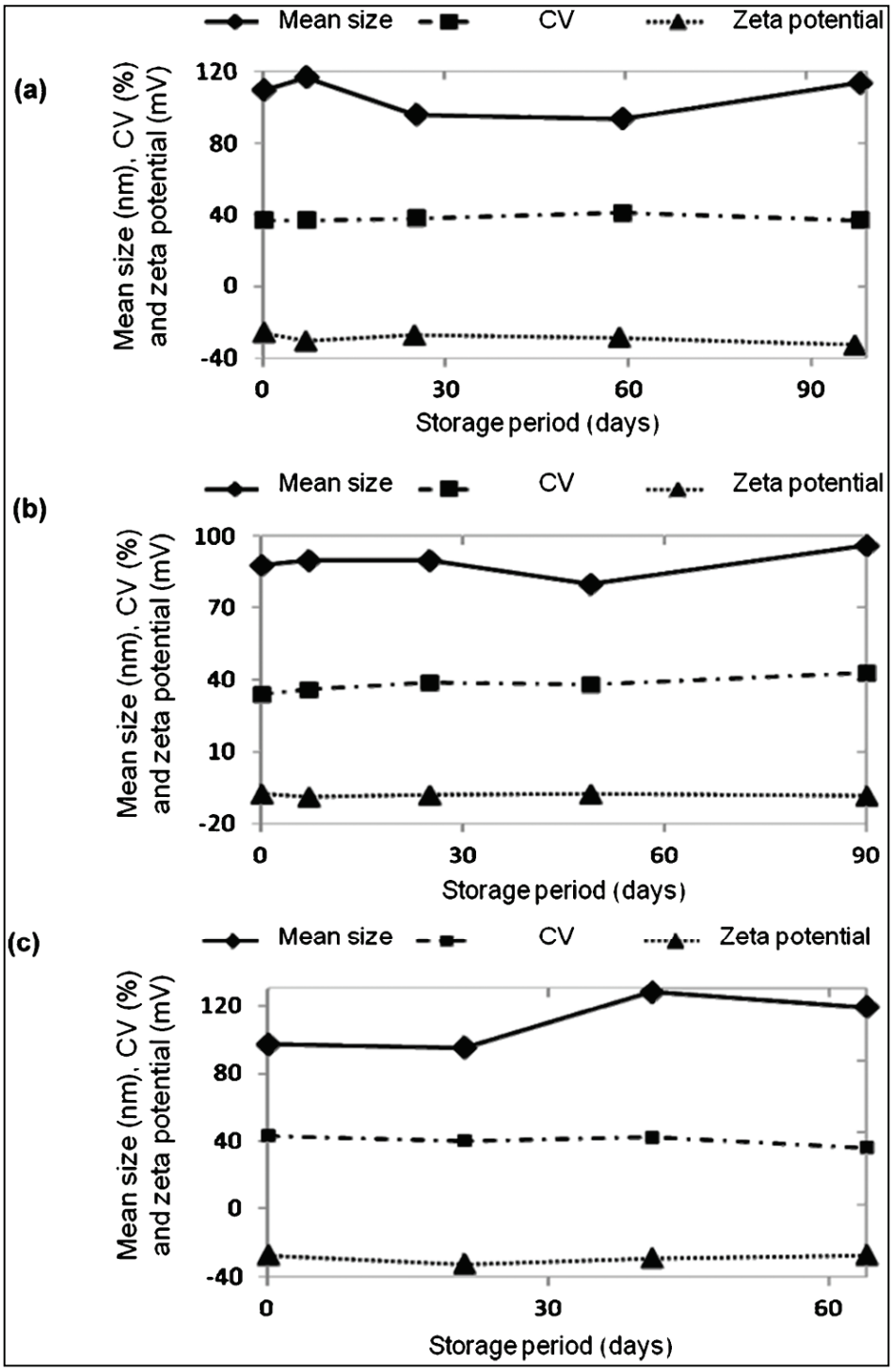

Fig. 6 Stability data of drug-free liposomes prepared using Lipoid E80 **(a)** and POPC **(b)** (results presented are the average of reproducibility batches) and drug-loaded liposomes **(c)**. The size characterization was carried out by DCS.

Table 4. Encapsulation efficiency stability of vitamin E loaded liposome suspension stored at 5 ± 3 °C. Experimental conditions of liposome suspension preparation: phospholipid: 20 mg/ml Lipoid E80, stabilizer: 5 mg/ml cholesterol, 5 mg/ml vitamin E, aqueous to organic phase volume ratio: 4.5, agitation speed: 600 rpm, organic phase flow rate: 2 ml/min, pore size: 10 μm, pore spacing: 200 μm. The size characterization was performed using DCS.

After preparation	After 1 month	After 2 months
99.87 ± 1.14	99.76 ± 1.03	98.81 ± 1.20

*: Each value represents the mean ± S.D. (n=3)

According to *Heurtault et al.*, **[42]** the size determination is a good indicator of stability since in most cases the particle size increased before macroscopic changes appeared. Our stability data show that the average size remained nearly unchanged during the storage period. In addition, the zeta potential was maintained at its initial value and no aggregation or sedimentation was observed during storage. Also, there were no significant changes in the vesicle size distribution during the same period (data not included). These results demonstrate a good stability of the liposome suspensions and thus indicate an adequate formulation of the preparation and optimum selection of process conditions.

4. Conclusion

In this study, we present a novel application of microengineered membranes: the preparation of size-controlled liposomes. The purpose of the research was to study the effect of the formulation factors and the process parameters on the final characteristics of lipid vesicles. The liposome formation was based on a diffusion-driven process in which the dissolved phospholipids (Lipoid E 80 or POPC) self-assemble into liposomes as ethanol quickly diffuses and dilutes into an agitated aqueous stream at the microsieve/aqueous phase interface. The size and size distribution of the liposomes was precisely controlled through adjustment of the phospholipid concentration and flow rate of the organic phase, pore size and spacing of the microengineered membrane used for injection of the organic phase, the degree of agitation in the cell and the mixing ratio of the two phases. This indicates that with a careful choice of formulation factors and process parameters, liposomes could be obtained with a defined size distribution. The rate of evaporation of ethanol did not have any appreciable effect, indicating that the process was controlled by the rate of interdiffusion of the two miscible liquids.

The reproducibility of the optimized process was good, and after each experiment the membrane surface could be easily cleaned and fully regained its hydrophilicity. The prepared samples remained stable for 3 months.

We have shown that a simple low-volume stirred cell is a useful apparatus for the quick testing of different experimental conditions. For continuous and larger-scale production, other experimental set-ups should be employed, such as crossflow and oscillation membrane systems and it will be the subject of our future investigation.

Supplementary material

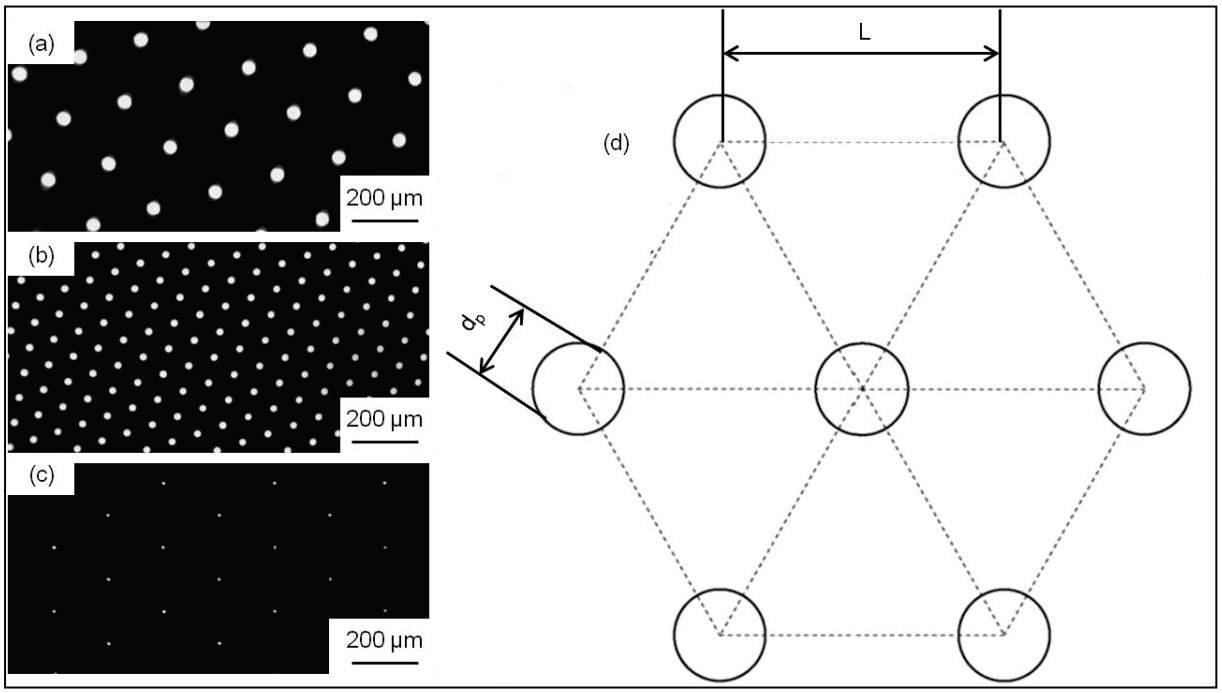

Fig. S1 Microscopic images of some membranes used in this study: **(a)** dp = 40 µm, L = 200 µm, **(b)** dp = 20 µm, L = 80 µm, and **(c)** dp = 10 µm, L = 200 µm. **(d)** Schematic view of the pore arrangement showing a regular hexagonal array of cylindrical pores with uniform pore spacing.

Table S1. Pore diameters, pore spacing and porosities of the membranes used in this study

Pore diameter (µm)	Pore spacing (µm)	Membrane porosity (%)
5	200	0.06
10	200	0.2
20	200	0.9
40	200	3.6
20	80	5.7
40	80	22.7

Table S2. Effect of ethanol evaporation on the liposome size characteristics. The experimental parameters: phospholipid: 20 mg/ml POPC, stabilizer: 5 mg/ml cholesterol, aqueous to organic phase volume ratio: 4.5, agitation speed: 600 rpm, organic phase flow rate: 2 ml/min, membrane pore size: 20 μm, pore spacing: 80 μm. The size characterization was performed using DCS.

	Before ethanol evaporation	After ethanol evaporation
Mean size* (nm)	84 ± 3	89 ± 2
CV* (%)	33 ± 2	34 ± 1

*: Each value represents the mean ± S.D. (n=3)

Table S3. The effect of membrane cleaning and treatment with a wetting agent on the liposome size and size distribution. The experimental parameters: phospholipid: 20 mg/ml Lipoid E80, stabilizer: 5 mg/ml cholesterol, aqueous to organic phase volume ratio: 4.5, agitation speed: 600 rpm, organic phase flow rate: 2 ml/min, pore size: 20 μm, pore spacing: 200 μm. The size characterization was performed using DCS.

	Brand new membrane (without wetting agent treatment)	Used membrane (after cleaning and wetting)
Mean size* (nm)	91 ± 3	91 ± 2
CV* (%)	36 ± 1	35 ± 1

*: Each value represents the mean ± S.D. (n=3)

Nomenclature

b	Blade height (m)
CV	Coefficient of variation
PDI	Polydispersity index
d_p	Pore diameter (m)
D	Stirrer diameter (m)
D_m	Effective membrane diameter (m)
L	Pore spacing (interpore distance) (m)
n_b	Number of blades
T	Internal diameter of tank (m)
ε	Membrane porosity

References

[1] A. D. Bangham and N. Y. Ann, Ann. N. Y. Acad. Sci., 1978, 308, 2–7.

[2] V. T. Torchilin, Nat. Rev. Drug Discovery, 2005, 4, 145–160.

[3] T. Lian and R. J. Y. Ho, J. Pharm. Sci., 2001, 90, 667–680.

[4] A. Wagner, M. Platzgummer and G. Kreismayr, J. Liposome Res., 2006, 16, 311–319.

[5] A. Laouini, C. Jaafar-Maalej, I. Limayem-Blouza, S. Sfar-Gandoura, C. Charcosset and H. Fessi, J Colloid Sci. Biotechnol., 2012, 1, 147–168.

[6] S. Batzri and E. D. Korn, Biochim. Biophys. Acta, Biomembr., 1973, 298, 1015–1019.

[7] A. Jahn, W. N. Vreeland, M. Gaitan and L. E. Locascio, J. Am. Chem. Soc., 2004, 126, 2674–2675.

[8] A. Wagner, K. Vorauer-Uhl and H. Katinger, J. Liposome Res., 2002, 12, 259–270.

[9] C. Charcosset, A. El Harati and H. Fessi, J. Controlled Release, 2005, 108, 112–120.

[10] C. Charcosset and H. Fessi, Drug Dev. Ind. Pharm., 2005, 31, 987–992.

[11] Q. Z. Zhou, L. Y. Wang, G. H. Ma and Z. G. Su, J. Colloid Interface Sci., 2007, 311, 118–127.

[12] N. A. Wagdare, A. T. M. Marcelis, R. M. Boom and C. J. M. Van Rijn, J. Colloid Interface Sci., 2011, 355, 453–457.

[13] C. Jaafar-Maalej, C. Charcosset and H. Fessi, J. Liposome Res., 2011, 21, 213–220.

[14] A. M. Terrasa, M. H. Guajardo, C. A. Marra and G. Zapata, Vet. J., 2009, 182, 463–468.

[15] M. Scherrer-Crosbie, M. Paul,M.Meignan, E. Dahan, G. Lagrue and G. Atlan, et al., J. Appl. Physiol., 1996, 81, 1071–1077.

[16] Y. Kato, K. Watanabe, M. Nakakura, T. Hosokawa, E. Hayakawa and K. Ito, Chem. Pharm. Bull., 1993, 41, 599–604.

[17] G. T. Vladisavljevic´, I. Kobayashi and M. Nakajima, Microfluid. Nanofluid., 2012, 13, 151–178.

[18] S. T.Fitzpatrick, US patent number 5,786,898, 28 July 1998.

[19] P. Schucks, Biophys. J., 2002, 82, 1096–1111.

[20] C. Cheng, L. Chu and R. Xie, J. Colloid Interface Sci., 2006, 300, 375–382.

[21] A. Nazir, K. Schroen and M. Boom, J. Membr. Sci., 2010, 362, 1–11.

[22] R. Hunter and H. Z. Midmore, J. Colloid Interface Sci., 2001, 237, 147–149.

[23] X. H. Wang, L. L. Cai, X. Y. Zhang, L. Y. Deng, H. Zheng and C. Y. Deng, et al., Int. J. Pharm., 2011, 410, 169–174.

[24] W. Sun, N. Zhang, A. Li, W. Zou and W. Xu, Int. J. Pharm., 2008, 353, 243–250.

[25] A. Laouini, C. Jaafar-Maalej, S. Sfar-Gandoura, C. Charcosset and H. Fessi, Prog. Colloid Polym. Sci., 2012, 139, 23–28.

[26] D. D. Lasic, Biochem J., 1988, 256, 1–11.

[27] A. Laouini, C. Jaafar-Maalej, S. Sfar-Gandoura, C. Charcosset and H. Fessi, Int. J. Pharm., 2011, 415, 53–61.

[28] J. M. H. Kremer, M. W. Vander Esker, C. Pathmamanoharan and P. H. Wiessema, Biochemistry, 1977, 16, 3932–3935.

[29] P. Pradhan, J. Guan, D. Lu, P. G. Wang, L. G. Lee and R. Lee, J. Anticancer Res., 2008, 28, 943–948.

[30] M. M. Dragosavac, M. N. Sovilj, S. R. Kosvintsev, R. G. Holdich and G. T. Vladisavljevic´, J. Membr. Sci., 2008, 322, 178–188.

[31] M. T. Stillwell, R. G. Holdich, S. R. Kosvintsev, G. Gasparini and I. W. Cumming, Ind. Eng. Chem. Res., 2007, 46, 965–972.

[32] S. R. Kosvintsev, G. Gasparini, R. G. Holdich, I. W. Cumming and M. T. Stillwell, Ind. Eng. Chem. Res., 2005, 44, 9323–9330.

[33] N. Sheibat-Othman, T. Brune, C. Charcosset and H. Fessi, Colloids Surf., A, 2008, 315, 13–22.

[34] J.C. LaRosa, D. Hunninghake, D. Bush,M.H.Criqui, G. S. Getz and A. M. Gotto Jr., et al., Circulation, 1990, 81, 1721–1733.

[35] M. Marsanasco, A. L. Ma´rquez, J. R. Wagner, S. V. Alonso and N. S. Chiaramoni, Food Res. Int., 2011, 44, 3039–3046.

[36] Y. F. Hsieh, T. L. Chen, Y. T. Wang, J. H. Chang and H. Chang, J. Food Sci., 2002, 67, 2808–2813.

[37] G. T. Vladisavljevic´ and H. Schubert, J. Membr. Sci., 2003, 225, 15–23.

[38] R. A. Williams, S. J. Peng, D. A. Wheeler, N. C. Morley, D. Taylor and M. Whalley, et al., Chem. Eng. Res. Des., 1998, 76, 902–910.

[39] G. Barratt, Cell. Mol. Life Sci., 2003, 60, 21–37.

[40] C. E. Mora-Huertas, H. Fessi and A. Elaissari, Int. J. Pharm., 2010, 385, 113–142.

[41] A.Wiacek and E. Chibowski, Colloids Surf., A, 1999, 159, 253–261.

[42] B. Heurtault, P. Saulnier, B. Pech, J. E. Proust and J. P. Benoit, Biomaterials, 2003, 24, 4283–4300.

[43] L. A. Dailey, T. Schmel, T. Gessler, M. Wittmar, F. Grimminger and W. Seeger, et al., J. Controlled Release, 2003, 86, 131–144.

[44] O. N. M. McCallion, K. M. G. Taylor, M. Thomas and A. J. Taylor, Int. J. Pharm., 1996, 133, 203–214.

[45] C. Bosquillon, P. G. Rouxhet, F. Ahimou, D. Simon, C. Culot and V. Preat, et al., J. Controlled Release, 2004, 99, 357–367.

[46] H. Schreir, R. J. Gonzalez-Rothi and A. A. Stecenko, J. Controlled Release, 1993, 24, 209–223.

Acknowledgments

Abdallah Laouini held a CMIRA Explora 2011 fellowship from ‘‘Région Rhône-Alpes’’.

The authors wish to thank Dr *Marijana Dragosavac* for fruitful discussions and useful advice.

Preparation of Liposomes: A Novel Application of Microengineered Membranes - From Laboratory Scale to Large Scale

Abdallah Laouini[1, 2], Catherine Charcosset[2], Hatem Fessi[2], Richard G. Holdich[1], Goran T. Vladisavljevic[1]

[1]: Loughborough University, Department of Chemical Engineering, Loughborough, Leicestershire, LE11 3TU, United Kingdom.

[2] : Université Claude Bernard Lyon 1, Laboratoire d'Automatique et de Génie des Procédés (LAGEP), UMR-CNRS 5007, CPE Lyon, Bât 308G, 43 Boulevard du 11 Novembre 1918, F-69622 Villeurbanne Cedex, France.

Colloids and Surface B: Biointerfaces, 112, 272-278, 2013

Impact factor: 3.554

Abstract

A novel ethanol injection method using microengineered nickel membrane was employed to produce POPC (1-palmitoyl-2-oleoyl-sn-glycero-3-phosphocholine) and Lipoid E80 liposomes at different production scales. A stirred cell device was used to produce 73 ml of the liposomal suspension and the product volume was then increased by a factor of 8 at the same transmembrane flux (140 l/m^2/h), volume ratio of the aqueous to organic phase (4.5) and peak shear stress on the membrane surface (2.7 Pa). Two different strategies for shear control on the membrane surface have been used in the scaled-up versions of the process: a cross flow recirculation of the aqueous phase across the membrane surface and low frequency oscillation of the membrane surface (~40 Hz) in a direction normal to the flow of the injected organic phase. Using the same membrane with a pore size of 5 μm and pore spacing of 200 μm in all devices, the size of the POPC liposomes produced in all three membrane systems was highly consistent (80-86 nm) and the coefficient of variation ranged between 26 and 36 %. The smallest and most uniform liposomal nanoparticles were produced in a novel oscillating membrane system. The mean vesicle size increased with increasing the pore size of the membrane and the injection time. An increase in the vesicle size over time was caused by deposition of newly formed phospholipid fragments onto the surface of the vesicles already formed in the suspension and this increase was most pronounced for the cross flow system, due to long recirculation time. The final vesicle size in all membrane systems was suitable for their use as drug carriers in pharmaceutical formulations.

Key words: Liposomes – Ethanol injection method - Process scale-up – Stirred cell – Cross flow – Oscillating membrane

Contents

1. Introduction

Liposomes are versatile drug carrier systems that can be tailor-made to accommodate a large variety of drugs for a wide range of therapies. Both lipophilic and hydrophilic drugs can be incorporated in liposomes, within the phospholipid bilayer and in the aqueous core, respectively **[1]**. The behaviour of liposomes *in vivo* and *in vitro* can be controlled by selecting the proper characteristics such as vesicle size, number of bilayers, bilayer fluidity, charge and hydrophilicity of the external surface, and the type of targeting molecules attached to the bilayer surface **[2]**. The applications of lipid vesicles are determined by their properties, which depend on molecular and physicochemical parameters as well as on the method of liposome preparation **[3]**. Therefore, a well-characterized methodology for liposome manufacture with validated operating procedures is the main requirement for producing liposomal populations with acceptable reproducibility and appropriate for the intended use.

Liposomal preparations can be manufactured using a wide variety of methods such as thin film hydration, reversed-phase evaporation, detergent dialysis, and solvent injection **[4]**. The major challenge in liposome production is still large scale production. Indeed, most of the described preparation techniques are not suitable for scaling up from the laboratory level to the industrial production, due to their complexity and a low reproducibility and predictability of the preparations obtained. A lack of predictability of product quality may be attributed to empirical methods traditionally employed for the design of lipid-based delivery systems **[5]**. Thus, there is a strong need to improve traditional manufacturing techniques, leaving behind those poorly characterizable methods, based on small batch sizes.

The ethanol injection method can be used for liposome production at large scale. In this process, an ethanolic solution of the lipid mixture is dispersed into an aqueous solution through fast injection. From the manufacturing point of view, this technique does fulfil the need for a rapid, simple, easily scalable and safe preparation technique. Also, this method does not promote degradation or oxidative alterations either in the lipid mixture or in active agents to be encapsulated **[6]**.

Membrane dispersion, which is considered as an improvement of the ethanol injection technique, is a new method of producing liposomes of predetermined size. It involves mixing of two miscible liquids (the organic and aqueous phase) by injecting the organic phase through a microporous membrane into the aqueous phase. It is similar to membrane emulsification **[7, 8]**, which involves the injection of one liquid (the dispersed phase) into another immiscible liquid (the continuous phase) through a microporous membrane **[9, 10]**. Micro-engineered membranes, which have a perfect hexagonal array of uniform pores, allow a much more uniform and controllable injection of lipid-containing organic phase into an aqueous phase. Thus, their use

enables a better control over diffusive mixing at the liquid/membrane interface where the lipids self-assemble into vesicles. This may provide fine control of liposome size distribution and make easier the extrapolation of the results for an industrial large scale production. The shear stress at the membrane surface can be controlled by **[11]**: (i) stirring the continuous phase using a paddle stirrer (**Figure 1a**); (ii) cross flow of the continuous phase along the membrane surface (**Figure 1b**); (iii) vibrating (oscillating) the membrane in the continuous phase (**Figure 1c**).

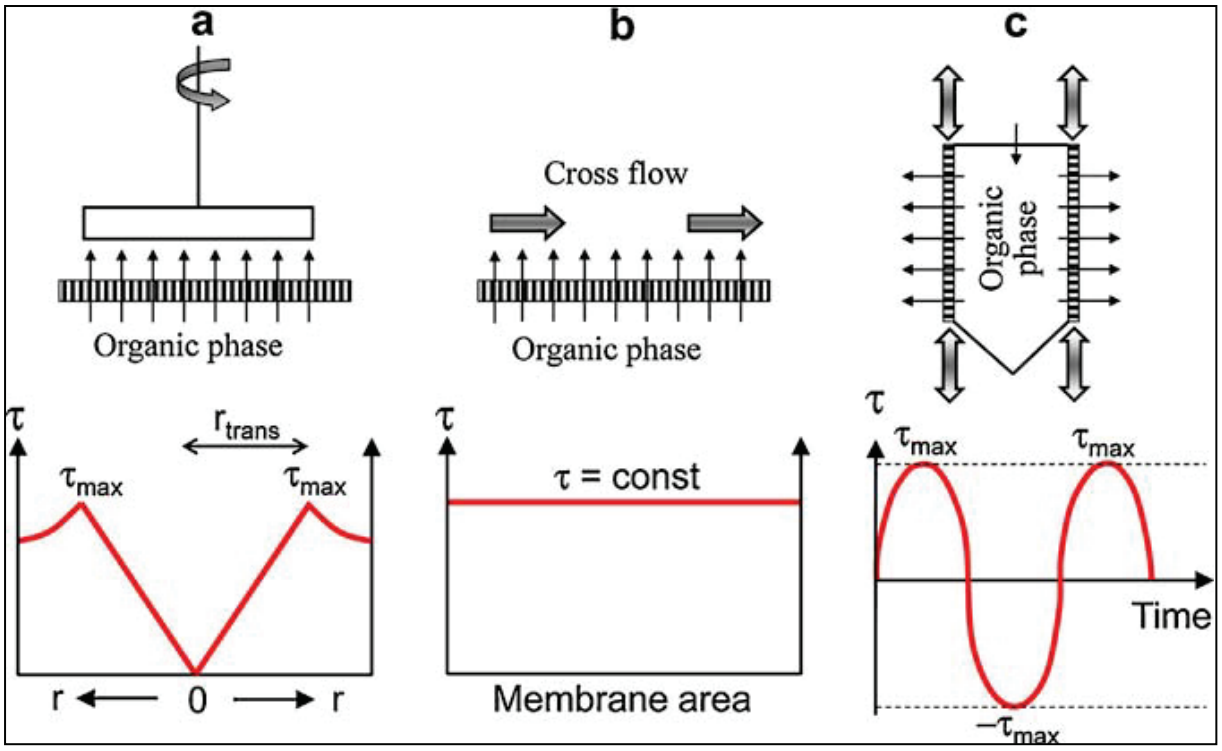

Fig. 1. Generation of shear stress in membrane microfluidic processes and its spatial or temporal distribution over the membrane surface: **(a)** paddle stirrer; **(b)** continuous phase cross flow; **(c)** oscillating membrane. All three methods of shear generation were used in this work to enhance the mixing rate of the two phases.

Recent studies **[10, 12]** were focused on the fabrication of liposomes using Shirasu Porous Glass (SPG) membrane. It was found that the vesicle size decreased with a decrease in the transmembrane flux and phospholipid concentration in the organic phase and with an increase in the aqueous to organic phase ratio and the shear stress on the membrane surface. Despite all the information provided in the literature regarding the effect of different operating and process conditions on vesicle characteristics **[13-15]**, there is a lack of information regarding scale-up of liposomes production.

The aim of this study was to evaluate the scale-up of liposome production by a factor of 8 and beyond using novel ethanol injection method with microengineered membrane. For a small-scale production, a laboratory stirred cell was used, composed of a rotating stirrer above a flat disc membrane. For large scale production, two

different methods were used: (i) recirculation of the continuous phase in cross flow along the membrane surface, and (ii) oscillation of the membrane surface in a direction normal to the flow of the injected phase.

2. Materials and methods

2.1 Reagents

Phospholipids used in this study were POPC (1-palmitoyl-2-oleoyl-sn-glycero-3-phosphocholine) and Lipoid® E80 (obtained from egg yolk lecithin and containing 82% of phosphatidyl-choline and 9% of phosphatidyl-ethanolamine), both purchased from Lipoïd GmbH (Ludwigshafen, Germany). Cholesterol and phosphotungstic acid were supplied by Sigma-Aldrich Chemicals (Saint Quentin Fallavier, France). 95 % analytical-grade ethanol was supplied by Fisher Scientific (United Kingdom) and used as such, without further purification. Ultra-pure water was obtained from a Millipore Synergy® system (Ultrapure Water System, Millipore).

2.2 Membranes

The membranes used were nickel microengineered membranes containing uniform cylindrical pores arranged in a hexagonal array with a diameter of 5 or 20 µm and pore spacing of 200 µm. The membranes were fabricated by the UV-LIGA process, which involves galvanic deposition of nickel onto a template formed by photolithography **[16]**. All membranes were supplied by Micropore Technologies Ltd. (Hatton, Derbyshire, United Kingdom).

2.3 Experimental equipment

Schematic illustration of the equipment used is presented in **Figure 2**.

2.3.1 Stirred cell device

A Dispersion Cell was supplied by Micropore Technologies Ltd. (Hatton, Derbyshire, UK). This device uses a 24 V DC motor (INSTEK model PR 3060) to drive a paddle-blade stirrer at an adjustable speed controlled by the applied voltage. An effective diameter of the membrane fitted at the bottom of the cell was 3.3 cm and a membrane area was 8.55 cm^2. The organic phase was injected through the membrane using a peristaltic pump (Watson Marlow 101U, Cornwall, UK).

2.3.2 Cross flow system

Cross flow module (Micropore Technologies Ltd) was composed of 4 separate disk membranes, each with a diameter of 7 mm, so the total membrane surface area was 1.54 cm^2. The cross flow channel was 20 mm wide and 1 mm high. A syringe pump (Havard Appartus 11 Plus) was used to inject the organic phase through the

membranes and a peristaltic pump (Watson Matlow 603s, Cornwall, UK) was used to recycle the aqueous phase between the module and an aqueous phase tank.

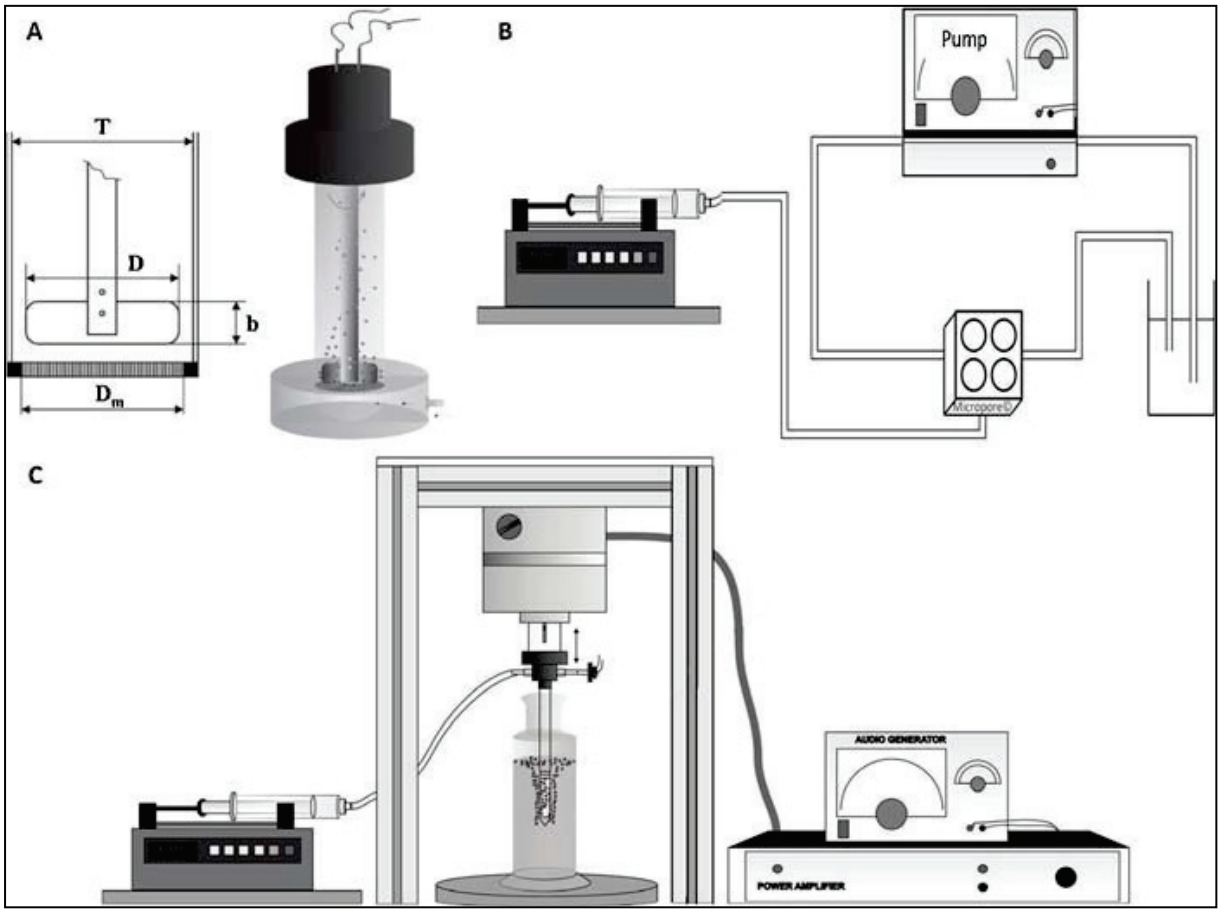

Fig. 2. Schematic illustration of the different equipments used in this study: **(A)** Stirred cell with a simple paddle stirrer above a flat disc membrane (b = 12 mm, D = 32 mm, Dm = 33 mm, n_b = 2 and T = 40 mm); **(B)** Cross flow system; **(C)** Oscillating membrane system.

2.3.3 Oscillating membrane system

This system was also supplied by Micropore Technologies Ltd. The membrane was composed of 2 foils rolled in the form of a ring with a diameter of 30 mm and a length of 20 mm. The membrane had an area of 34.1 cm^2 and was attached to the injection manifold to which an accelerometer was fixed. The accelerometer (PCB Piezotronics model M352C65) was connected to a National Instruments Analogue to Digital Converter (N1 Edaq-9172) which was interfaced to a LabView executable program running on a computer. The information provided by the program from the accelerometer was the frequency and the amplitude of the oscillations, the amplitude being determined by the direction of the travel and the frequency was deduced from the acceleration measurement. The oscillation signal was provided by an audio generator (Rapid Electronics), which fed a power amplifier driving the electro-

mechanical oscillator on which the inlet manifold was mounted. The injection manifold had internal drillings to allow the passage of the organic phase by a syringe pump (Harvard Apparatus 11 Plus).

2.4 Experimental procedure and shear stress calculation

The organic phase was composed of 20 mg/ml of phospholipids and 5 mg/ml of cholesterol (used as a stabilizer) dissolved in ethanol.

2.4.1 Stirred cell device

The cell was filled with 60 ml of ultrapure water and 13 ml of the organic phase was injected through the membrane at 2 ml/min to achieve a final volume ratio of the aqueous to organic phase of 4.5. The organic phase flux, J, was given by:

$$J = Q_o / A \tag{1}$$

where Q_o is the volume flow rate of the organic phase and A is the membrane area. The organic phase flux was 140 l/m^2/h, calculated from Eq. (1), and the stirrer speed was 600 rpm. Previous studies in Dispersion Cell **[17, 18]** have shown that a shear stress is not uniformly distributed over the membrane surface, but varies with the radial distance r, according to the equations **[19]**:

For $r < r_{trans}$ $$\tau = 0.825\eta_{aq}\omega r\frac{1}{\delta} \tag{2}$$

For $r > r_{trans}$ $$\tau = 0.825\eta_{aq}\omega r_{trans}\left(r_{trans}/r\right)^{0.6}\frac{1}{\delta} \tag{3}$$

where r_{trans} is the transitional radius, i.e. the radial distance from the center of the membrane at which the shear stress is greatest:

$$r_{trans} = 1.23\frac{D}{2}\left(0.57 + 0.35\frac{D}{T}\right)\left(\frac{b}{T}\right)^{0.036} n_b^{\,0.116}\,\mathrm{Re}/(1000 + 1.43\,\mathrm{Re}) \tag{4}$$

where D is the stirrer diameter, T is the internal diameter of the stirred cell, b is the blade height, and n_b is the number of blades (**Figure 2a**). The Reynolds number, Re, is given by:

$$\mathrm{Re} = \omega\rho_{aq}D^2/(2\pi\eta_{aq}) \tag{5}$$

where ρ_{aq} and η_{aq} are the density and viscosity of the aqueous phase, respectively, and ω is the angular velocity of the stirrer. The boundary layer thickness, δ, is given by the Landau-Lifshitz equation **[17]**:

$$\delta = \sqrt{\eta_{aq} / (\rho_{aq} \omega)} \tag{6}$$

Since the shear stress at the membrane surface is not constant, it can be argued that the appropriate value that should be used in comparative investigations is either the average or maximum shear. Because the shear stress at r = r_{trans} is the highest, the pressure above the membrane surface at r = r_{trans} has a minimum value, leading to the maximum transmembrane pressure and thus the maximum flux through the membrane. Since the membrane is most productive near the transitional radius, the shear stress at r = r_{trans} (maximum shear stress) will be used as a representative τ value in stirred cell experiments. Using Equation (2) or (3) and (6):

$$\tau_{\max} = \frac{0.825 \eta_{aq} \omega r_{trans}}{\sqrt{\eta_{aq} / (\rho_{aq} \omega)}} \tag{7}$$

In this study, the maximum shear stress was 4.7 Pa and the transitional radius was 1.1 cm. A scale-up of stirred cell membrane systems is complicated, because the shear stress on the membrane surface is a complex function of the system geometry and the shear is non-uniformly distributed over the membrane surface (**Figure 1a**).

2.4.2 Cross flow system

480 ml of the aqueous phase was pumped through the cross-flow channel and overall 107 ml of the organic phase was injected through the membrane at 36 ml/min (140 l/m^2/h) to achieve an aqueous to organic phase volume ratio in the final preparation of 4.5. The shear stress on the membrane surface generated by cross flow in rectangular channel geometry is given by:

$$\tau = 3 Q_{aq} \eta_{aq} / (2 h^2 W) \tag{8}$$

where Q_{aq} is the aqueous phase flow rate, and h and W are the height and width of the channel, respectively. In order to keep the same shear stress on the membrane surface as in the stirred cell device (4.7 Pa), Q_{aq} was set to 3.7 l/min.

2.4.3 Oscillating membrane system

A ring membrane was immersed into a beaker containing 480 ml of the aqueous phase. The aqueous phase was then sucked into the membrane and injection manifold using a syringe in order to ensure that no air bubbles were trapped within the organic phase. When air was completely removed, the injection tube was attached to the syringe pump. Then, overall 107 ml of the organic phase was injected through the membrane at 8 ml/min (140 l/m^2/h) to achieve a final aqueous to organic phase volume ratio of 4.5. Oscillations did not start until the organic phase emerged on the membrane surface in order to prevent pre-mixing within the membrane. In a stirred cell or cross

flow system, the shear stress does not vary over time at any location on the membrane surface. For oscillating membrane system, the shear stress on the membrane surface is a sinusoidal function of time (**Figure 1c**) and the maximum shear is given by:

$$\tau_{\max} = (2\pi)^{3/2}(\mu_{aq}\rho_{aq})^{1/2} af^{3/2} \quad (9)$$

where a and f is the amplitude and frequency of the membrane oscillations. Eq. (9) suggests that the same τ_{max} value can be achieved using many different sets of frequency and amplitude values. In membrane emulsification, the mean droplet size was found to be a function of the maximum shear stress only and not the frequency or amplitude used to achieve it **[20]**. In this study, the frequency and amplitude were adjusted to 40 Hz and 1.2 mm, respectively, to obtain the maximum shear stress on the membrane surface which is consistent with the cross flow and stirred system (4.7 Pa). Equation (9) implies that the oscillating membrane system is easy to scale up, because the surface shear does not depend on the membrane geometry or the geometry of the vessel, or channel, in which the membrane was fitted. A summary of the experimental conditions used in different systems is presented in Table 1.

Table 1. Experimental conditions used in different preparation methods. The aqueous to organic phase volume ratio, transmembrane flux and shear stress on the membrane surface were held constant for all methods to conduct experiments under comparable conditions.

Preparation method	Stirred cell system	Cross flow system	Oscillating membrane system
Aqueous phase volume (ml)	60	480	480
Organic phase volume (ml)	13	107	107
Final aqueous to organic phase volume ratio (-)	**4.5**	**4.5**	**4.5**
Organic phase flow rate (ml/min)	2	0.36	8
Membrane area (cm^2)	8.55	1.54	34.1
Transmembrane flux ($l/m^2/h$)	**140**	**140**	**140**
Agitation speed (rpm)	600	N.A	N.A
Aqueous phase flow rate (l/min)	N.A	3.7	N.A
Maximum shear stress on membrane surface (Pa)	**4.7**	**4.7**	**4.7**

In all systems, formation of vesicles occurred as soon as the organic phase was brought into contact with the aqueous phase. The liposomal suspension was collected and remaining ethanol was removed by evaporation under reduced pressure (Buchi, Flawil, Switzerland). After each experiment, the membrane was washed by sonication

in ethanol for 1 hour, followed by soaking in a siloxane-based wetting agent for 30 min in order to increase the hydrophilicity of the surface.

2.5 Liposomes characterization

2.5.1 Size analysis

The particle size distribution was measured by differential centrifugal sedimentation using a CPS disc centrifuge, model DC 24000 (CPS instruments, Florida, USA). A light beam near the outside edge of the rotating disc passed through the centrifuge at some distance below the surface of the liquid phase and measured the concentration of particles as they settled. The time required for particles to reach the detecting beam depends upon the speed and geometry of the centrifuge, the difference in density between the particles and the surrounding liquid, and the size of the particles. Thus, when operating conditions were stable, sedimentation velocity increased with the particle diameter, so that the time needed to reach the detector beam was used to calculate the size of the particles **[21, 22]**. A sucrose gradient (from 18% to 26%) was built and the sample was diluted in a sucrose solution (30%) before being injected. Prior to the analysis, the instrument was calibrated using an aqueous suspension of polybutadiene particles of a known size distribution and a mean size of 402 nm. The mean particle size of liposomes was expressed as the number-average mean diameter, d_{av} and the polydispersity was expressed as the coefficient of variation, $CV = (\sigma/d_{av}) \times 100$, where σ is the standard deviation of particle diameters in a suspension. The smaller CV values indicate the narrower size distribution **[23, 24]**. All d_{av} and CV values will be expressed as the mean ± standard deviation (S.D.).

2.5.2 Microscopic observation

The morphology of the liposomes was observed by transmission electron microscopy (TEM) using a CM 120 microscope (Philips, Eindhoven, Netherlands) operating at an accelerating voltage of 80 KV. A drop of the liposome dispersion was placed on a holey copper grid. A thin film of the liposome dispersion was obtained by removing excess solution using a filter paper. Negative staining with 2% (w/w) phosphotungstic acid was directly performed on the deposit for 1 min. The excess of phosphotungstic solution was removed with a filter paper after which the stained samples were transferred to the TEM for imaging.

3. Results and discussion

3.1 Effect of the phospholipid type

The characteristics of Lipoid E80 and POPC vesicles obtained in stirred cell and cross-flow systems using membranes with two different pore sizes are compared in **Table 2**. The POPC liposomes prepared using the pore size of 5 μm were smaller and more

uniform than Lipoid E80 liposomes prepared using the same pore size and the difference was more significant for cross-flow system, due to longer fabrication times. It should be noted that both Lipoid E 80 and POPC allow the formation of liposomes with an acceptable size for their use as drug carriers in pharmaceutical formulations. Therefore, both phospholipids can be used for large scale production of liposomes in a cross-flow membrane system.

Table2. Influence of phospholipid type and membrane pore size on the mean vesicle size and CV in stirred cell and cross flow systems. The experimental conditions are specified in **Table 1**.

Preparation method	Phospholipid used	Membrane pore size (μm)	Liposomes mean size* (nm)	CV* (%)
Stirred cell system	Lipoid E80	5	87 ± 3	32 ± 1
		20	91 ± 3	34 ± 1
	POPC	5	81 ± 3	29 ± 1
Cross flow system	Lipoid E80	5	105 ± 3	46 ± 1
		20	204 ± 2	45 ± 2
	POPC	5	86 ± 2	36 ± 2

* Each value represents the mean ± S.D. (n=3).

3.2 Effect of the membrane pore size

The effect of membrane pore size on the mean size of vesicles prepared in stirred cell and cross flow systems can be seen in **Table 2**. Clearly, the mean liposome size increased with increasing the pore size, and the effect was more pronounced for the cross-flow system, due to longer fabrication time. In the cross flow system, new phospholipid molecules supplied through the membrane by the organic phase were partly deposited on the existing liposomal particles that recirculate through the module, and partly form new phospholipid fragments in the aqueous phase. As a result, the liposomal particles formed in the cross flow system are larger than those formed in the stirred cell, where a secondary particle growth is less pronounced due to shorter injection time. The effect of the pore size on the vesicle size can also be seen in **Figure 3**. This figure shows that the mean vesicle size was between 50 and 100 μm when 5 μm membrane was used and 150 to 200 μm when the membrane with a 20 μm pore size was used. In membrane emulsification, the particle size was found to increase linearly with the pore size **[19, 25, 26]**. The results show that it is feasible to tune the size of liposomal particles by using microengineered membranes with different nominal pore sizes, but the effect is limited to a relatively narrow range of mean vesicle sizes.

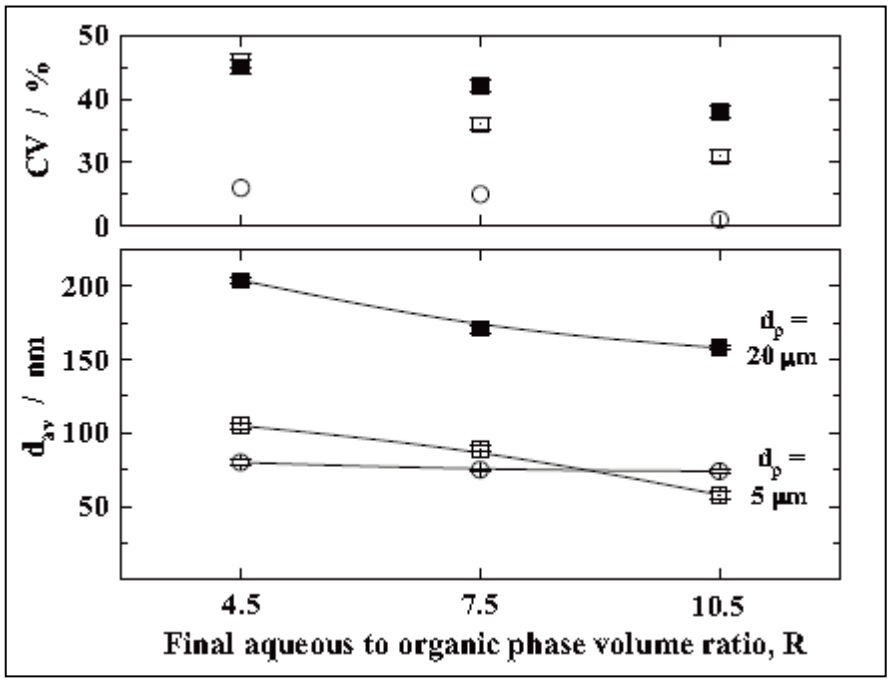

Fig. 3. The variation of the mean vesicle size, d_{av} and its coefficient of variation, CV with the final aqueous to organic phase volume ratio: (□) lipoid E 80, cross flow, dp = 5 µm; (○) POPC, oscillating system, dp = 5 µm; (■) lipoid E 80, cross flow, dp = 20 µm. τ_{max} = 4.7 Pa, J = 142 l/m^2/h. The each data point represents the mean ± S.D. (n = 3).

3.3 Variation of vesicle size with time during scale-up

The samples of liposomal nanosuspension prepared in both the cross flow and oscillating system were taken at predetermined time intervals to investigate the variation of the vesicle size with time. The aqueous to organic phase ratio, R, during the fabrication process was inversely proportional to the process time, t:

$$R = V_{aq} / V_o = V_{aq} / (Q_o t) \tag{10}$$

where V_{aq} is the initial volume of the aqueous phase in the system and Q_o is the flow rate of the organic phase through the membrane, which was kept constant. Thus, higher R values in the samples correspond to shorter processing times. As shown in **Figure 3**, the mean size and CV of vesicles in the liposomal suspension increased with time. It can be explained by assuming that the supersaturation in the aqueous phase was relieved by a combination of nucleation (formation of phospholipid fragments) and particle growth (precipitation of phospholipid fragments onto the surface of the vesicles already present in the suspension). Initially, formation of phospholipid fragments dominates over precipitation but subsequently, precipitation of material onto the existing vesicles becomes increasingly more important, leading to a gradual increase in the mean vesicle size. A polydispersity of vesicles in the suspension

increased as a result of coexistence of small vesicles formed directly from phospholipid fragments and larger vesicles formed by precipitation onto the smaller vesicles. The large vesicles can also be produced at the higher phospholipid concentration in the organic phase, as suggested elsewhere **[9, 10, 27, 28]**.

As shown in **Figure 3**, in the cross flow system, the mean vesicle size increased over time by 80% (from 58 to 108 nm), whereas in the oscillating system the size variation over time was only by 8% (from 74 to 80 nm). The model of vesicles formation proposed by Lasic **[29]** suggests that following their injection, phospholipids precipitate at the water/ethanol boundary and form bilayered phospholipid fragments. The energy needed to curve a flat bilayer fragment into a closed sphere was provided here through agitation of the aqueous phase, cross flow or membrane vibrations. When cross flow system was used, the recirculation of the formed vesicles in a closed loop facilitated their contact with the newly formed small vesicles and phospholipid fragments, which might result in the formation of bigger vesicles. A contact of phospholipid fragments with existing vesicles was pronounced by a narrow cross flow channel with a height of 1 mm and a long recirculation time.

The results in **Figure 3** indicate that the vesicle size can be precisely controlled by monitoring the processing time, thereby controlling the amount of organic phase injected through the membrane. This finding is highly relevant since it can enable continuous production of liposomes with different mean particle sizes using a single pore size. It is important to note that both cross flow and oscillating membrane systems are scalable and the fabrication process developed in a small device can be carried out under the same shear conditions in a cross flow or oscillating system with a much larger membrane area. On the other hand, a stirred system is not scalable due to large spatial variations of the shear stress over the membrane surface (**Fig. 1a**) and a significant effect of the system geometry on the shear stress.

3.4 Comparison of different fabrication methods

Once optimized at small scale (V_{aq} = 60 ml) in stirred cell, the fabrication of POPC liposomes was scaled up by a factor of 8 (V_{aq} = 480 ml) at constant R, J, and τ_{max}. The larger vesicle size and broader particle size distribution was obtained in the cross flow system, compared to that in the stirred cell (**Table 3**). The scale-up was done by maintaining constant V_{aq}/V_o and J values and thus, the fabrication time, t, should be proportional to V_{aq}/A. In the cross-flow system, the membrane area A was 5.6 times smaller than that in the stirred cell and thus, for an eightfold increase in the aqueous phase volume, the process time in the cross-flow device should be 48 times longer than that in the stirred cell (**Table 3**). The recirculation of the liposomal suspension over a time period of 297 min led to an increase in the mean vesicle size since the newly formed bilayered fragments settle upon the already formed vesicles. This can

explain why the mean vesicle size was increased from 81 to 86 nm when the cross flow system was used, instead of the stirred cell.

Table 3. Comparison of different methods of liposome preparation. The phospholipid: POPC, final aqueous to organic phase volume ratio: 4.5, membrane pore size: 5 μm. The other experimental conditions are specified in Table 1.

Preparation method	Stirred cell	Cross flow	Oscillating system
Mean vesicle size* (nm)	81 ± 3	86 ± 2	80 ± 2
CV* (%)	29 ± 1	36 ± 2	26 ± 1
Suspension volume (ml)	73	587	587
Process time (min)	6.5	297	13
Process capacity (ml/min)	11	2	45

* Each value represents the mean ± S.D. (n=3).

The membrane oscillation was used as an alternative to cross flow in order to avoid the requirement for recirculation of the organic phase along the membrane surface. The shear stress on the membrane surface is a sinusoidal function of time (**Fig. 1c**), but at 40 Hz, there were 80 peak shear events per second (one peak shear event every 12.5 ms). The organic phase was split into more than 90 thousand streams within the membrane, before being mixed with an aqueous phase on the other side of the membrane. The average flow velocity of the organic phase in the pores was 7 cm/s and the distance travelled by each stream between two peak shear events was less than 0.9 mm. The mean vesicle size in the oscillating system was the same as that in the stirred cell and the CV improved from 29% to 26% (**Table 3**). *Holdich et al.* **[20]** attributed the better uniformity of the particles produced by the oscillating system to the fact that in such a system the shear stress is only applied at the membrane surface (where it is needed), while it is very low in the bulk of the aqueous phase. In addition, shear conditions on the membrane surface can be more finely adjusted by varying two parameters, the frequency and the amplitude of membrane oscillations. In the stirred cell, the shear can only be controlled by varying the stirrer speed. *Zhu and Barrow* **[30]** reported that the use of a vibrating membrane had a significant effect in reducing the size of the droplets generated in membrane emulsification.

The process capacity, defined as the volume of the liposomal suspension produced per unit time, was the maximum for the oscillating system (**Table 3**). The scale-up was done at constant flux and V_{aq}/V_o and thus, the process capacity was proportional to A/V_{aq} and inversely proportional to the process time. The fabrication time in the oscillating system was about 23 times shorter than that in the cross-flow system resulting in the higher capacity of the oscillating system by a factor of 23.

Table 4 summarises potential advantages and disadvantages of the various membrane systems used for liposomes preparation.

Table 4. Comparison of different membrane systems used in this work for fabrication of liposomes.

Preparation method	Potential advantages	Potential disadvantages
Stirred cell system	- Laboratory test system, easy to use in order to study the effect of different experimental conditions on the preparation characteristics. - High injection rates of the dispersed phase through the membrane. - Suitable for low volumes of aqueous phase.	- Suitable only for small scale production (the batch volume was limited to 120 ml). - Suitable only for batch-wise operation. - A non-uniform shear stress at the surface of the membrane.
Cross flow system	- Constant shear stress at the membrane surface. - Modules widely available and easy to use. - Suitable for large scale production and continuous or semi-continuous operation.	- Particles structure can be damaged during recirculation in pipes and pumps. - Not suitable for low volumes of aqueous phase (At least 400 ml needed for the circulation in pipes and pumps).
Oscillating membrane system	- Uniform spatial distribution of shear stress on the membrane surface. - Suitable for fragile and structured particles. - Suitable for low volumes of aqueous phase. - Suitable for large scale and continuous operation.	- Complicated and more expensive design. - Higher power consumption. - Non-uniform temporal distribution of shear stress on the membrane surface.

An advantage of cross-flow and oscillating system is that the volume of the aqueous phase is decoupled from the membrane area. In a stirred cell, the aqueous phase volume is limited by the membrane area, because D/H should be within certain limits to achieve a satisfactory mixing rate. Another advantage of cross-flow and oscillating membrane systems over batch stirred cells is that cross-flow and oscillating systems can be operated continuously or semi-continuously and a total membrane area in these systems can easily be increased by adding additional membrane elements and assemblies.

3.5 TEM observation

Liposomes prepared with different techniques were observed by Transmission Electron Microscopy (TEM) and TEM micrographs are given in **Figure 4**.

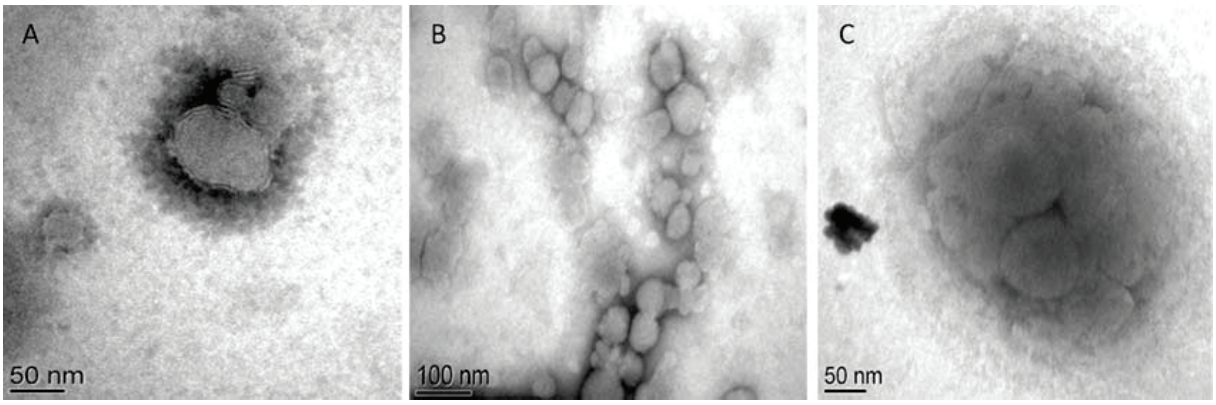

Fig. 4. Transmission electron microscopy of liposomes prepared with **(A)** stirred cell device **(B)** cross flow system and **(C)** oscillating membrane system.

As could be seen, liposomes were spherical with multilayered membrane structure specific to multilamellar vesicles. Their size estimated from TEM pictures ranged from 60 to 120 nm which is coherent with the values obtained using the CPS instrument.

4. Conclusion

Multilamellar phospholipid vesicles were produced by injection of ethanolic phase through a microengineered membrane into aqueous phase using different membrane devices and batch sizes. The process developed in a stirred cell device was scaled-up by a factor of 8 by maintaining the same transmembrane flux, peak shear stress on the membrane surface and aqueous to organic phase phase ratio. In the cross flow system, the vesicle size increased over time due to continual recirculation of the liposomal suspension. The oscillating membrane system, which avoids recirculation of the liposomes was fully capable of maintaining the size and polydispersity of the liposomal nanoparticles during scale-up. This technique can easily be further scaled up by providing a larger membrane area in the oscillating membrane assembly. By an

appropriate manipulation of hydrodynamic conditions during the process scaling up, it is possible to obtain small liposomes with a narrow size distribution. These results show great potential of microengineered membranes with constant pore spacing to be used for design, rationalization and intensification of industrial production of liposomes.

Nomenclature

A	Membrane surface area (m^2)
a	Amplitude of membrane oscillations (m)
b	Blade height (m)
D	Stirrer diameter (m)
D_m	Effective membrane diameter (m)
d_p	Pore diameter (m)
f	Frequency of membrane oscillations (Hz)
H	Height of liquid layer in stirred cell (m)
h	Height of cross flow channel (m)
J	Transmembrane flux ($l\ m^{-2}\ h^{-1}$)
n_b	Number of blades (-)
n_p	Number of pores (-)
Q	Flow rate (ml/min)
R	Aqueous to organic phase volume ratio (-)
Re	Rotational Reynolds number (-)
r	Radial distance from membrane center (m)
r_{trans}	Transitional radius, i.e. a value of r at $\tau = \tau_{max}$ (m)
S	Pore spacing (interpore distance) (m)
T	Internal diameter of stirred tank (m)
t	Time (s)
W	Width of cross flow channel (m)
δ	Boundary layer thickness (m)
ε	Membrane porosity (-)

η	Viscosity (Pa s)
ρ	Density (kg m^{-3})
τ	Shear stress on membrane surface (Pa)
τ_{max}	Peak shear stress on membrane surface (Pa)
ω	Angular velocity (rad s^{-1})

References

[1] V.P. Torchilin, Nat. Rev. Drug Discov. 4 (2005) 145–160.

[2] D. Liu, A. Mori, L. Huang, Biochim. Biophys. Acta 1104 (1992) 95–101.

[3] P. Stano, S. Bufali, A. Domazou, P.L. Luisi, J. Liposome Res. 15 (2005) 29–47.

[4] A. Laouini, C. Jaafar-Maalej, I. Limayem-Blouza, S. Gandoura-Sfar, C. Charcosset, H. Fessi, J. Colloid Sci. Biotechnol. 1 (2012) 147.

[5] M. Chen, Adv. Drug Deliv. Rev. 60 (2008) 768–777.

[6] L.A. Meure, N.R. Foster, F. Dehghani, AAPS Pharm. Sci. Tech. 9 (2008) 798–809.

[7] S.M. Joscelyne, G. Trägårdh, J. Membr. Sci. 169 (2000) 107–117.

[8] C. Charcosset, I. Limayem, H. Fessi, J. Chem. Technol. Biotechnol. 79 (2004) 209–218.

[9] S.M. Joscelyne, G. Trägårdh, J. Membr. Sci. 169 (2000) 107–117.

[10] A. Laouini, C. Jaafar-Maalej, S. Sfar-Gandoura, C. Charcosset, H. Fessi, Int. J. Pharm. 415 (2011) 53–61.

[11] G.T. Vladisavljevi´ c, R.A. Williams, J. Colloid Interface Sci. 299 (2006) 396–402.

[12] A. Laouini, C. Jaafar-Maalej, S. Sfar-Gandoura, C. Charcosset, H. Fessi, Progr. Colloid Polym. Sci. 139 (2012) 23–28.

[13] T.T. Pham, C. Jaafar-Maalej, C. Charcosset, H. Fessi, Colloids Surf B. 94 (2012) 15–21.

[14] O.R. Justo, A.M. Moraes, Chem. Eng. Res. Des. 89 (2011) 785–792.

[15] A. Wagner, V. Karola, K. Gunther, K. Hermann, J. Liposome Res. 12 (2002) 259–270.

[16] G.T. Vladisavljevi´ c, I. Kobayashi, M. Nakajima, Microfluid. Nanofluid. 13 (2012) 151–178.

[17] S.R. Kosvintsev, G. Gasparini, R.G. Holdich, I.W. Cumming, M.T. Stillwell, Ind. Eng. Chem. Res. 44 (2005) 9323–9330.

[18] M.T. Stillwell, R.G. Holdich, S.R. Kosvintsev, G. Gasparini, I.W. Cumming, Ind. Eng. Chem. Res. 46 (2007) 965–972.

[19] M.M. Dragosavac, M.N. Sovilj, S.R. Kosvintsev, R.G. Holdich, G.T. Vladisavljevic, J. Membr. Sci. 322 (2008) 178–188.

[20] R.G. Holdich, M.M. Dragosavac, G.T. Vladisavljevi´ c, S.R. Kosintsev, Ind. Eng. Chem. Res. 49 (2010) 3810–3817.

[21] Fitzpatrick, S. T.; US patent number 5,786,898. 28 July 1998.

[22] P. Schucks, Biophys. J. 82 (2000) 1096–1111.

[23] C. Cheng, L. Chu, R. Xie, J. Colloid Interface Sci. 300 (2006) 375–382.

[24] A. Nazir, K. Schroen, M. Boom, J. Membr. Sci. 362 (2010) 1–11.

[25] Vladisavljevic, G.T. Schubert, H, J. Membr. Sci. 225 (2003) 15–23.

[26] R.A. Williams, S.J. Peng, D.A. Wheeler, N.C. Morley, D. Taylor, M. Whalley, et al., Chem. Eng. Res. Des. 76 A8 (1998) 902–910.

[27] P. Pradhan, J. Guan, D. Lu, P.G. Wang, L.G. Lee, R. Lee, J. Anticancer Res. 28 (2008) 943–948.

[28] J.M.H. Kremer, M.W. Vander Esker, C. Pathmamanoharan, P.H. Wiessema, Biochemistry 16 (1977) 3932–3935.

[29] D.D. Lasic, Biochem. J. 256 (1988) 1–11.

[30] J. Zhu, D. Barrow, J. Membr. Sci. 261 (2005) 136–144.

Acknowledgments

Abdallah Laouini held a CMIRA Explora 2011 fellowship from ‘‘Région Rhône-Alpes’’. The additional funding came from The Engineering and Physical Sciences Research Council of the United Kingdom (reference number: EP/HO29923/1).

The authors wish to thank Dr *Marijana Dragosavac* for fruitful discussions and useful advices.

Production of Liposomes Using Microengineered Membrane and Co-Flow Microfluidic Device

Goran T. Vladisavljevic[1], Abdallah Laouini[1, 2], Catherine Charcosset[2], Hatem Fessi[2], Hemaka Bandulasena[1], Richard G. Holdich[1]

[1]: Loughborough University, Department of Chemical Engineering, Loughborough, Leicestershire, LE11 3TU, United Kingdom.

[2] : Université Claude Bernard Lyon 1, Laboratoire d'Automatique et de Génie des Procédés (LAGEP), UMR-CNRS 5007, CPE Lyon, Bât 308G, 43 Boulevard du 11 Novembre 1918, F-69622 Villeurbanne Cedex, France.

Submitted to Colloids and Surface A: Physicochemical and Engineering Aspects

Abstract

Two novel modifications of the ethanol injection method have been applied to produce Lipoid E80 and POPC (1-palmitoyl-2-oleoyl-sn-glycero-3-phosphocholine) liposomes: (i) injection of organic lipid solution through a microengineered nickel membrane whose surface was kept under controlled shear conditions and (ii) injection of organic phase through a tapered-end glass capillary into co-flowing aqueous stream using coaxial assemblies of glass capillaries. The organic phase was composed of 20 mg/ml of phospholipids and 5 mg/ml of cholesterol dissolved in ethanol and the aqueous phase was ultra-pure water. Self-assembly of phospholipid molecules into multiple concentric bilayers via phospolipid bilayered fragments was initiated by interpenetration of the two miscible solvents after organic phase injection. The mean vesicle size in the membrane method was 80 ± 3 nm and consistent across all of the devices (stirred cell, cross-flow module and oscillating membrane system), indicating that local or temporal variations of the shear stress on the membrane surface had a negligible effect on the vesicle size, on the condition that a maximum shear stress was kept constant. The mean vesicle size in co-flow microfludic device decreased from 131 to 73 nm when the orifice diameter in the injection capillary was reduced from 209 to 42 μm at the aqueous and organic phase flow rate of 25 and 5.55 ml/h, respectively. The vesicle size was significantly affected by the mixing efficiency, which was controlled by the orifice size and phase flow rates. The smallest vesicle size was obtained under conditions that promote the highest mixing rate.

Key words: Liposomes - Laminar co-flow - Micromixing - CFD simulation - Microfluidic mixer - Membrane dispersion

Contents

1. Introduction

Liposomes are spherical core-shell structures with a diameter ranging from 20 nm to several micrometres, composed of concentric bilayers resulting from the self-assembly of phospholipids in an aqueous solution **[1]**. The polar head groups of phospholipids are located at the surface of the bilayer membranes, whereas the fatty acid chains form the hydrophobic core of the membranes. Liposomes can be multi-, oligo- or unilamellar, containing many, a few, or one bilayer shell(s), respectively. Because of the ability of liposomes to encapsulate both hydrophobic and hydrophilic actives, selectively transport molecules across the bilayer(s), and attach site-specific ligands and stabilizing polymers to their surface, liposomes hold great potential as carriers and/or delivery vehicles for pharmaceuticals **[2]**, enzymes **[3]**, genes **[4]**, and gases **[5]**, and as micro/nano-reactors for biomedical applications **[6]**. Conventional liposome formation techniques such as lipid film hydration and solvent dispersion methods (e.g. ethanol or ether injection) rely on the mechanical dispersion of dried lipids or rapid dilution of organic lipid solutions in an aqueous environment under non-uniform mechanical shear. In the traditional ethanol injection method **[7]**, a lipid solution of ethanol is rapidly injected through a syringe into a stirred aqueous phase. Because of the existence of a single injection point, mixing occurs as a result of both bulk motion in the aqueous phase (macromixing) and molecular or eddy diffusion (micromixing) (**Fig. 1a**). Due to irregular shear-stress profile in the vessel and variable mixing length scales, this method typically leads to the formation of polydisperse population of vesicles. Monodispersed liposomes can be produced by utilising W/O or W/O/W emulsions as templates to generate the vesicles **[8, 9]**. However, emulsion templating methods are complicated and used primarily for production of giant liposomes with a vesicle diameter above 1 μm. Uniform liposomes with a mean diameter ranging from 50 to 150 nm were produced using microfluidic flow focusing in microchannels fabricated on a silicon wafer by photolithography and Deep Reactive Ion Etching (DRIE) **[10]**. However, DRIE is an expensive process and the flow rate of the product stream in the device was very low, in the range of 25-100 μl/min. There is a strong need for the cheaper and simpler microfluidic techniques for controlled formation of liposomes that can be used at larger production scales.

In this work, two novel microfluidic strategies of liposome formation were used: (i) injection of ethanolic lipid solution through a microporous membrane whose surface was kept under controlled shear-stress conditions; (ii) injection of ethanolic phase through a tapered-end capillary into co-flowing aqueous phase using coaxial assembly of glass capillaries. Glass capillary devices have been used for making emulsions **[11]**, microparticles **[12]**, and giant vesicles **[9]** with a controllable size. However, so far, these devices have not yet been used for production of nanosized vesicles.

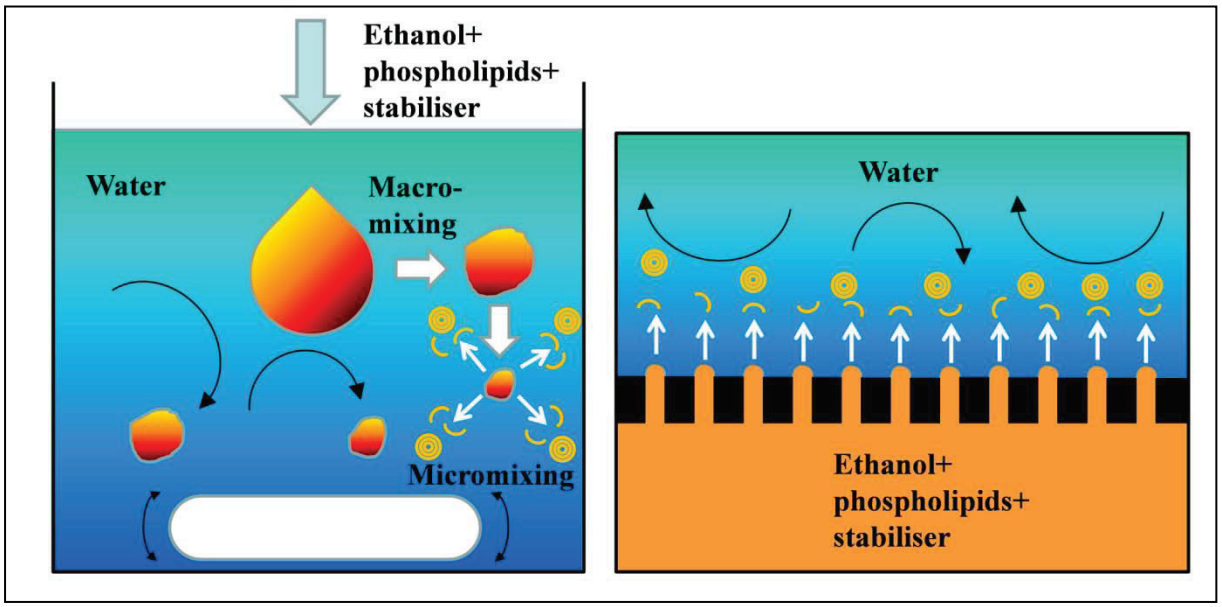

Figure 1. Liposome production by the ethanol injection method: **(a)** direct dissolution (macromixing + micromixing); **(b)** membrane injection (direct micromixing).

In the membrane micromixing process, mixing occurs only at the microscale level, because the membrane provides numerous micro-injection points to finely disperse organic phase into the aqueous phase without intermediate macromixing stage (**Fig. 1b**). Membrane emulsification also involves injection of organic phase into aqueous phase **[13, 14]**, but in membrane micromixing the organic and aqueous phase are completely miscible and the process does not result in formation of emulsion droplets. Liposomes were previously prepared using polymeric hollow fibre and Shirasu Porous Glass (SPG) membranes in cross-flow configuration **[15, 16]**. However, both membrane types have a sponge-like structure with irregularly shaped, interconnected pores **[17]**. In this work, we have used microengineered membranes consisting of evenly spaced, unconnected pores of uniform size and regular cylindrical shape.

2. Materials and methods

2.1 Reagents

Phospholipids used in this work were POPC (1-palmitoyl-2-oleoyl-sn-glycero-3-phosphocholine) and Lipoid E80 (egg yolk lecithin which contains 82% of phosphatidyl-choline and 9% of phosphatidyl-ethanolamine), both purchased from Lipoïd GmbH (Ludwigshafen, Germany). Cholesterol supplied from Sigma-Aldrich Chemicals (Saint Quentin Fallavier, France) was used as a stabiliser of phospholipid bilayers. 95 % analytical-grade ethanol supplied by Fisher Scientific (United Kingdom) was used as a volatile organic solvent to dissolve lipids prior to injection. Ultra-pure water was obtained from a Millipore Synergy® system (Ultrapure Water System, Millipore) and used as a dilution medium for organic lipid solutions.

2.2 Membrane dispersion devices

The membranes used were nickel membranes with a pore size of 5 µm and pore spacing of 200 µm, fabricated using UV-LIGA (Ultraviolet Lithography, Electroplating, and Molding) technology **[18]**, supplied by Micropore Technologies Ltd. (Hatton, Derbyshire, UK). Three different membrane rigs were used, as shown in **Fig. 2**. In the stirred cell (**Fig. 2a**), the aqueous phase was agitated by a paddle-blade stirrer attached above the membrane and the organic phase was injected through the membrane using a peristaltic pump (Watson Marlow 101U, Cornwall, UK). The effective diameter of the membrane was 3.3 cm and a corresponding membrane area was 8.55 cm^2. The cross flow module (**Fig. 2b**) contained a flat membrane with 4 separate active regions, each with a diameter of 7 mm, providing the total membrane area of 1.54 cm^2. A shear stress was provided by recirculating the aqueous phase above the membrane surface through a cross-flow channel, 20 mm wide and 1 mm high. The organic phase was injected through the membrane using a syringe pump (Havard Appartus 11 Plus), while a peristaltic pump (Watson Matlow 603S) was used to recycle the aqueous phase between the module and an aqueous phase tank. The oscillating membrane rig (**Fig. 2c**) was composed of a ring membrane with a diameter of 30 mm, a height of 20 mm, and an effective area of 34.1 cm^2. The oscillation signal was provided by an audio generator (Rapid Electronics), which fed a power amplifier driving the electro-mechanical oscillator on which the inlet manifold and membrane were mounted. The injection manifold had internal drillings to allow passage of the organic phase by a syringe pump (Harvard Apparatus 11 Plus).

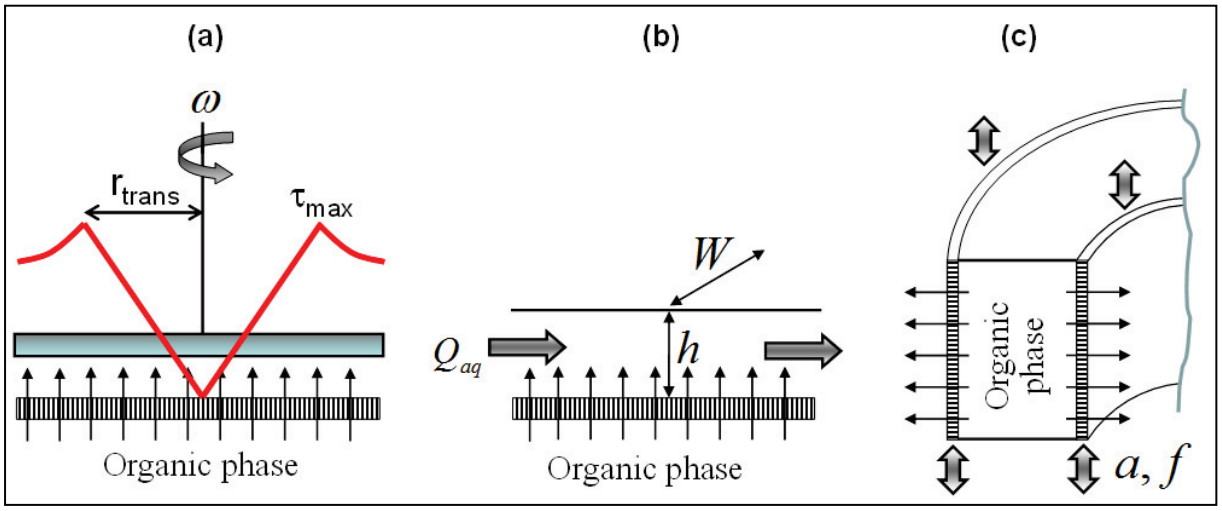

Figure 2. Membrane devices used in this work supplied by Micropore Technologies Ltd. (Hatton, Derbyshire, UK): **(a)** stirred cell (Dispersion Cell); **(b)** cross-flow membrane system; **(c)** vibrating ring membrane. The red line in figure (a) shows the distribution of the shear stress on the membrane surface.

Experimental procedure

In all membrane devices the organic phase was a lipid mixture composed of 20 mg/ml POPC and 5 mg/ml cholesterol dissolved in ethanol. The stirred cell was filled with 60 ml of ultrapure water and agitated at 600 rpm, followed by injection of 13 ml of the organic phase through the membrane at 2 ml/min. In the cross-flow system, overall 107 ml of the organic phase was injected through the membrane at 36 ml/min into 480 ml of the aqueous phase recirculating in the system. The flow rate above the membrane was maintained at 3.7 l/min. In the oscillating membrane system, the ring membrane, oscillating with 40 Hz frequency and 1.2 mm amplitude, was immersed into a beaker containing 480 ml of the aqueous phase and 107 ml of the organic phase was injected through the membrane at 8 ml/min. In all membrane devices, a special precaution was taken to remove all air bubbles from the organic phase before injection. The above mentioned operating conditions were so adjusted to keep a constant transmembrane flux of 140 l/m^2/h, a constant maximum shear stress on the membrane surface of 4.7 Pa, and a constant aqueous to organic phase volume ratio in the preparation before ethanol evaporation of 4.5. After each experiment, the membrane was washed by sonication in ethanol for 1 h, followed by soaking in a hydrophilic wetting agent for 30 min.

The maximum shear stress on the membrane surface was calculated using the equations given in Table 1.

Table 1. Equations for the maximum shear stress at the membrane/aqueous phase interface in different membrane devices as a function of system geometry, process parameters and physical properties of the continuous phase.

Membrane set-up	Maximum shear stress on membrane surface	Shear variations	
		Temporal	Local
Stirred cell	$\tau_{\max} = \frac{0.825\eta_{aq}\omega r_{trans}}{\sqrt{\eta_{aq}/(\rho_{aq}\omega)}}$ *	-	+
Cross flow membrane	$\tau_{\max} = \frac{3Q\eta_{aq}}{2h^2W}$	-	-
Oscillating membrane	$\tau_{\max} = (2\pi af)^{3/2}(\eta_w\rho_w)^{1/2}$	+	-

* $r_{trans} = 1.23\frac{D}{2}\left(0.57 + 0.35\frac{D}{T}\right)\left(\frac{b}{T}\right)^{0.036} n_b^{0.116}\,\mathrm{Re}/(1000 + 1.43\,\mathrm{Re})$

Shear stress on the membrane surface in a stirred cell varies in the radial direction and has a maximum value at the transitional radius, r_{trans}. The transitional radius depends on the stirring rate, physical properties of the continuous phase and cell geometry **[19]** and was 1.1 cm for the conditions used in this work. In oscillating membrane system, a shear stress on the membrane surface is a sinusoidal function of time and the maximum shear is reached twice during each period of oscillation **[20]**. In a cross-flow system, shear stress on the membrane surface is neither time nor location dependent and can be controlled by the rate of recirculation of the aqueous phase and the dimensions of the cross-flow channel.

2.3 Co-microfluidic device

The main body of the microfluidic device was made up of two glass capillaries: a round inner capillary (1 mm outer diameter and 0.58 mm inner diameter), and an outer square capillary (1 mm inner dimension). One end of the inner capillary was shaped into a tapering orifice with an inner diameter ranging from 40 to more than 200 μm. A P-97 Flaming/Brown micropipette puller (Sutter Instrument Co.) was used to produce a sharp tip of about 20 μm in diameter. The orifice diameter was then increased by sanding the tip against sandpaper until the orifice with a required size and smooth rim was obtained. A microforge (MF-830, Intracel Ltd.) microscope was used to inspect the orifice size via a built-in scale. The round capillary was then inserted halfway into the square capillary and aligned. Both capillaries were glued onto a microscope slide and two needles (BD Precisionglide®, Sigma-Aldrich, O.D. 0.9 mm) were glued onto the slide such that the entrances to each capillary were situated inside the hubs (**Fig. 3a**). A PTFE tubing (I.D. 0.80 mm) was used to deliver the organic phase to the inner capillary, while a PE tubing was used to deliver the aqueous phase to the square capillary. Another PTFE tubing (I.D. 1.5 mm) was attached to the outlet of the square capillary to transfer the liposomal solution into a vial.

CFD simulations

Computational Fluid Dynamics (CFD) simulations were performed to study flow dynamics and mixing in the vicinity of the orifice. The problem was solved in dimensional form using Comsol Multiphysics 4.3b. The computational geometry was simplified by considering one fourth of the microfluidic device along the central axis. The length of the square capillary after the orifice was chosen to be sufficiently long (3.5 times the width of the square channel) to avoid end effects affecting the dynamics in the vicinity of the orifice. The model was developed using Laminar Flow model (for fluid flow) and Transport of Concentrated Species (for convection and diffusion). The density and viscosity of water-ethanol solution were determined using the Jouyban-

Acree model **[21]**. The boundary conditions for the system were specified as no-slip and no flux at walls, velocity and mass fractions at the inlets and pressure boundary at the outlet. Computations were carried out using 1,438,532 tetrahedral mesh elements on a Windows workstation following a grid resolution study. The flow ratio between ethanol and water was varied using parametric continuation feature available in the package.

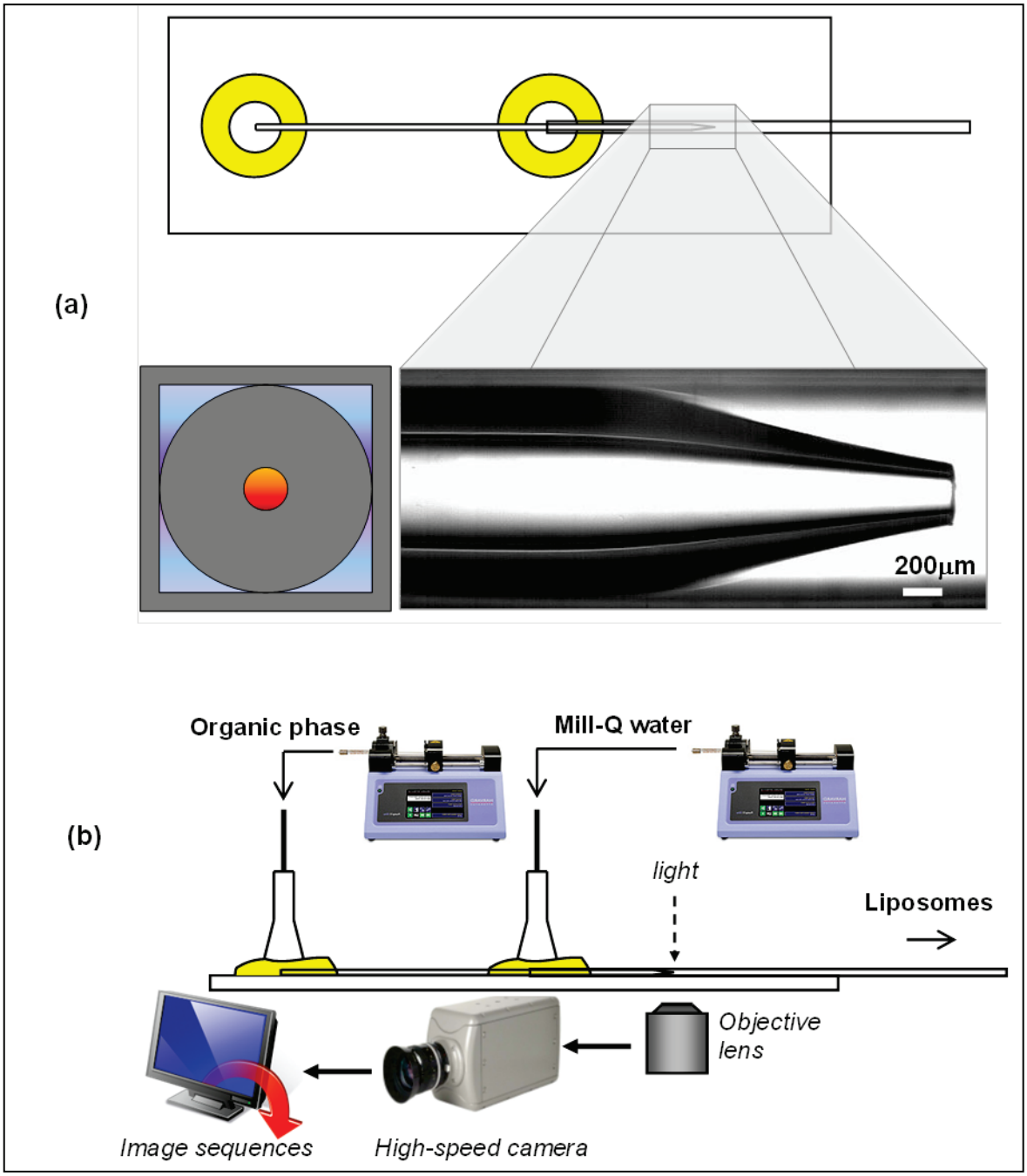

Figure 3. Microfluidic co-flow device consisted of coaxial assembly of glass capillaries glued onto a microscope slide: **(a)** Top view and microscopic image of a tapered section of the inner capillary with 209 µm orifice diameter; **(b)** side view of the device and the experimental set-up.

Experimental investigations

In all microfluidic experiments the organic phase was a lipid mixture composed of 20 mg/ml Lipoid E80 and 5 mg/ml cholesterol dissolved in ethanol. The organic and aqueous phases were delivered from SGE gas tight syringes to their respective capillaries using 11 Elite syringe pumps (Harvard Apparatus). The micro-scale mixing process then took place in the square capillary as the organic stream was diluted by Milli-Q water. This was observed through a Phantom V9.0 high-speed camera (Ametek, USA) mounted on an inverted microscope (XDS-3, GX Microscopes, UK). The process was recorded with 25 frames per second at 576 × 288 resolution and the recordings were analysed using ImageJ software.

2.4 Analysis and characterization of samples

After production, the liposomal suspension was collected and remaining ethanol was removed by evaporation under reduced pressure in a vacuum oven (Buchi, Flawil, Switzerland). The particle size distribution was measured by differential centrifugal sedimentation using a CPS disc centrifuge, model DC 24000 (CPS instruments, Florida, USA). Prior to the analysis, the instrument was calibrated using an aqueous suspension of polybutadiene particles of a known size distribution and a mean size of 402 nm. The mean particle size of liposomes was expressed as the number-average mean diameter, d_{av} and the polydispersity was expressed as the coefficient of variation, $CV = (\sigma/d_{av}) \times 100$, where σ is the standard deviation of particle diameters.

3. Results and discussion

3.1 Membrane dispersion

The particle size distribution of multilamellar liposomes prepared in different devices is shown in **Fig. 4**. The mean vesicle size of 80±3 nm was consistent across all of the devices, indicating that local or temporal variations of the shear stress on the membrane surface had a negligible effect on the mean vesicle size, on the condition that a maximum shear stress was kept constant. The largest mean vesicle size (d_{av} = 86 nm) and the widest size distribution (CV = 36%) were obtained in the cross flow system, due to the long recirculation time of the liposomal suspension of nearly 300 min, which can lead to deposition of newly formed bilayered fragments onto the surface of the vesicles already present in the suspension. The smallest and most uniform vesicles (d_{av} = 80 nm and CV = 26%) were obtained in the oscillating system, which can be attributed to shear stress generated only on the membrane surface, while agitation was negligible in the bulk of the aqueous phase. The fabrication process using oscillating membrane holds greatest potential to be transferred from batch to continuous operation, because hydrodynamic conditions on the membrane surface are independent on the geometry of the cross-flow channel, flow rate above the membrane

surface or membrane size. In cross-flow membrane systems, shear stress on the membrane surface is controlled by fluid flow over the membrane surface, which means that the aqueous phase flow rate must be relatively high to generate sufficiently high stress on the membrane surface to achieve satisfactory mixing efficiency. As a result, recirculation of the aqueous phase is inevitable because the liposomal suspension would be too diluted in a single-pass operation. In oscillating membrane system, the shear stress on the membrane surface is decoupled from the cross flow velocity and controlled only by the frequency and amplitude of the membrane oscillation. Thus, very low cross-flow velocities can be used in continuous operation and recirculation of the aqueous is not needed, which can help to limit secondary interactions between particles in the product stream.

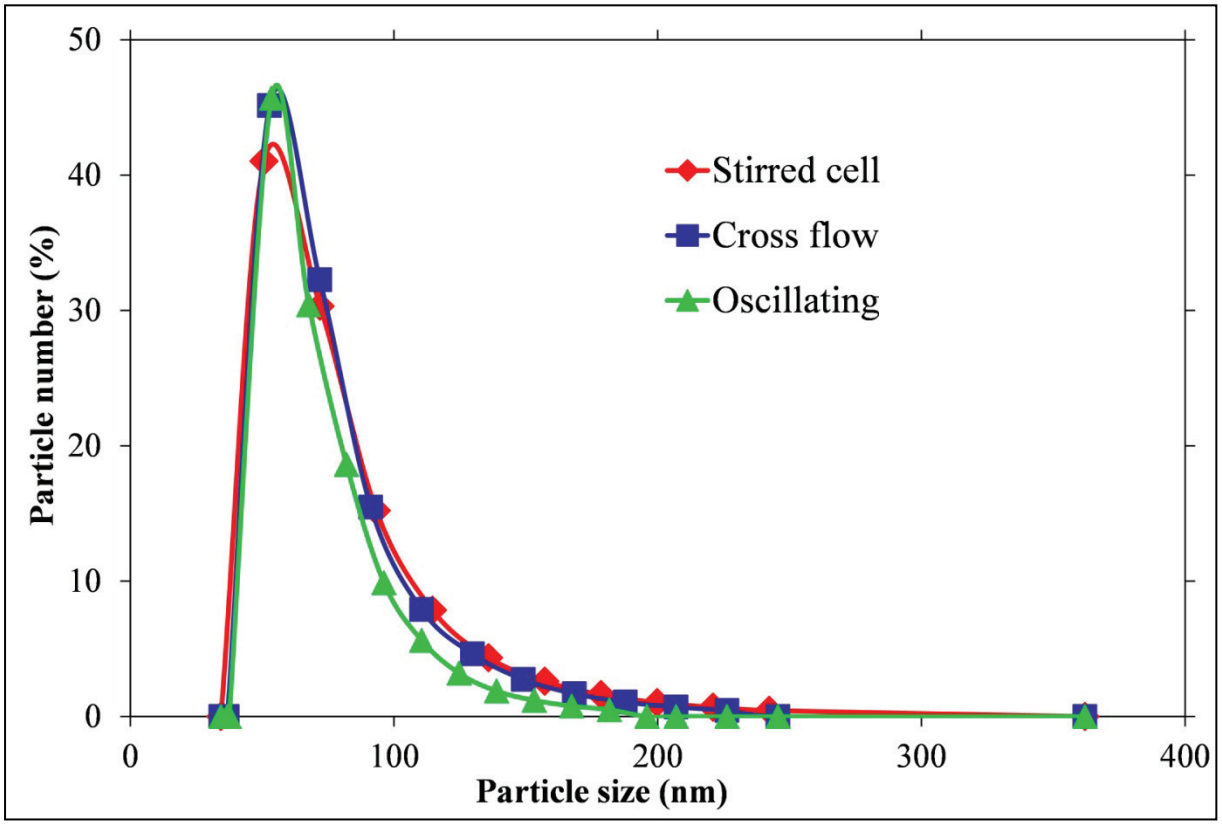

Figure 4. Particle size distribution of liposomal suspensions prepared using three different membrane dispersion devices.

3.2 Microfluidic vesicle formation

We have used CFD to simulate flow patterns in co-flow microfluidic device at constant organic phase flow rate (Q_o = 0.6 ml/h) and a variable water flow rate. **Fig. 5** shows the distribution of local velocities within the device with an orifice diameter of 209 μm. The maximum velocity was reached in the centre of the orifice. The organic phase velocity dropped significantly downstream of the orifice, due to sudden increase in the cross-sectional area and the drag force imposed by the surrounding water phase.

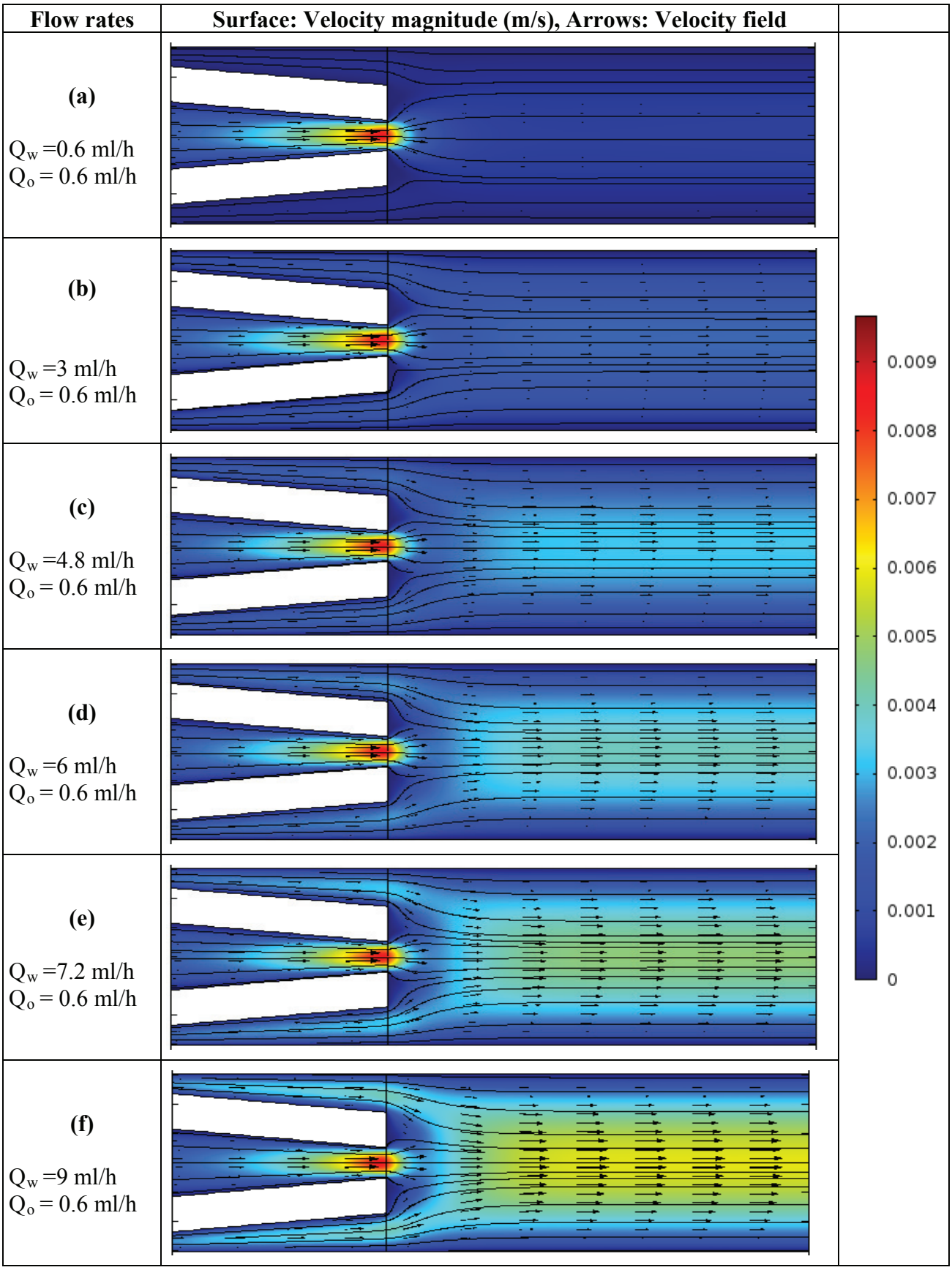

Figure 5. Distribution of fluid velocities in co-flow capillary device at the organic phase flow rate, Q_o, of 0.6 ml/h and increasing water flow rate, Q_w. The orifice diameter is 209 μm.

The velocity profile was flat at a distance of one orifice diameter (D) downstream of the orifice with almost no difference in fluid velocity over the cross section. A parabolic velocity profile was established at a distance of 2-3D downstream of the orifice.

The distribution of fluid densities in the device is shown in **Fig. 6**. The orifice size and fluid flow rates are the same as those in **Fig. 5**. The organic phase forms a jet that extends downstream of the orifice. As the water flow rate increases from 0.6 to 9 ml/h, the jet gets progressively shorter and thinner. The smaller jet diameters at the higher water flow rates were due to the higher jet velocities, as shown in **Fig. 5**. The mixing of the two liquids is more efficient at the higher water flow rates, because of the shorter diffusion distances x for thinner jets. In laminar flow, the average time for molecules to diffuse over a distance x is given by **[22]**:

$$t = x^2/2D \quad (1)$$

where D is the diffusion coefficient. In this study, x is the jet radius and therefore, the mixing time is proportional to the square of the jet radius.

Microscopic images of real flow patterns at different flow rates of the two phases are shown in **Fig. 7**. We have identified three main regimes of fluid flow in the collection capillary: parallel two-phase flow, dripping, and jetting. At low flow rates of both phases, two parallel coexisting streams were formed – organic stream in the central part of the capillary and liposomal suspension in the annular space between the organic stream and the wall (**Fig. 7a**). The flow pattern was similar to that predicted by the CFD simulation shown in **Fig. 6(a)**. The rate of convective transport of ethanol in the downstream direction was large compared to the rate of molecular diffusion of ethanol in the radial direction and consequently, a diameter of the organic stream in the square capillary was almost constant. Vesicles were visible in the aqueous phase, because they formed microscopic unstable aggregates, which disappeared upon dilution. As the water flow rate increased from 0.6 to 5 ml h^{-1}, the organic phase formed a short hemispherical jet near the orifice (**Fig. 7b**). The interface between the organic and water phase was visible due to difference in refractive indices of water (1.33) and ethanol (1.36) and accumulation of phospholipid bilayers at the interface caused by an abrupt change in the ethanol concentration. The position of the interface would be stationary under steady-state conditions, but due to small periodic fluctuations in the flow rates caused by the pumps imperfections, the interface oscillated slightly in the axial direction, which enhanced the interfacial mass transfer. Aggregation of vesicles in the aqueous phase was less pronounced than in the previous case, due to higher dilution of the organic phase.

Flow rates	Surface: Density (kg/m), Contour: Mass fraction	
(a) Q_w =0.6 ml/h Q_o = 0.6 ml/h	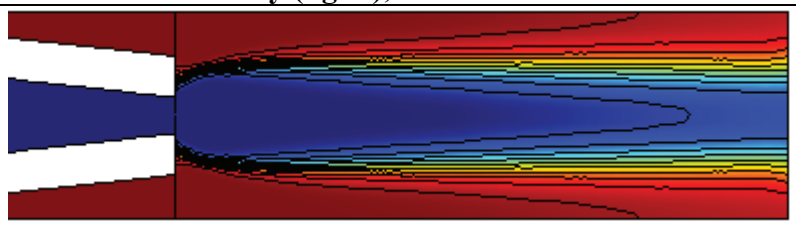	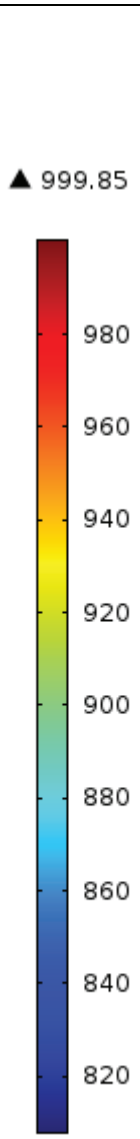
(b) Q_w =3 ml/h Q_o = 0.6 ml/h	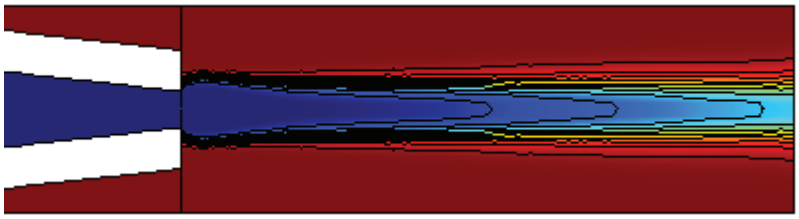	
(c) Q_w =4.8 ml/h Q_o = 0.6 ml/h	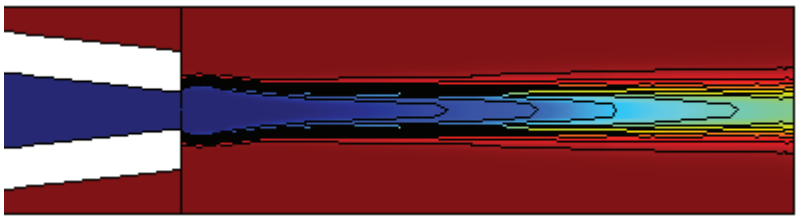	
(d) Q_w =6 ml/h Q_o = 0.6 ml/h	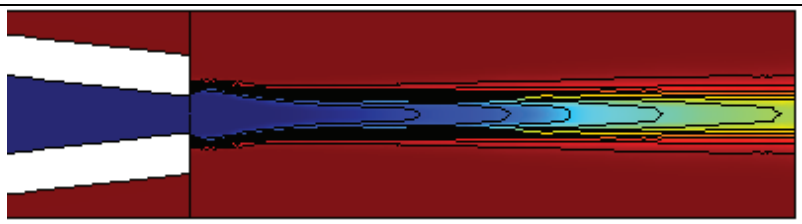	
(e) Q_w =7.2 ml/h Q_o = 0.6 ml/h	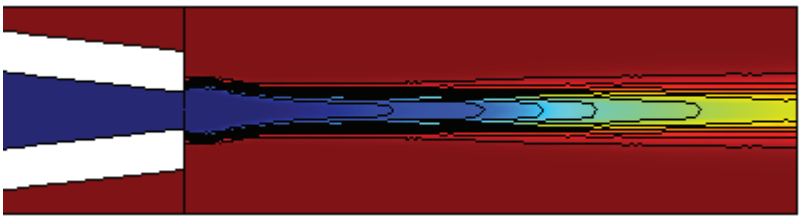	
(f) Q_w =9 ml/h Q_o = 0.6 ml/h	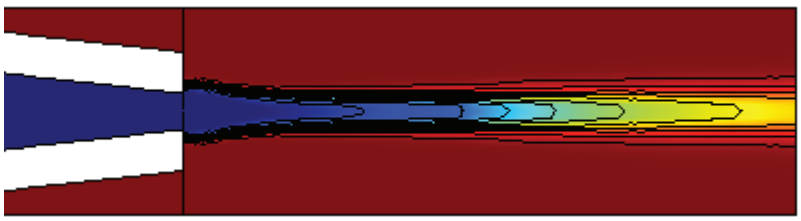	

Figure 6. Distribution of fluid densities in co-flow capillary device at the organic phase flow rate,Q_o,of 0.6 ml/h and increasing water flow rate, Q_w. The orifice diameter is 209 μm.

As the water flow rate increased from 5 to 15 ml h^{-1}, the interface was pulled downstream, forming a cylindrical jet with a diameter approximately equal to the orifice diameter (**Fig. 7c**). We observed two distinct jet morphologies in the jetting regime. A narrowing jet was generated when the average velocity of the water stream at the orifice was higher that the organic phase velocity ($U_w > U_o$), as shown in **Figs. 7(d)** and **(e)**. In **Fig. 7(d)**, U_w = 4.3 mm/s and U_o = 0.8 mm/s. This velocity difference accelerated the jet, causing it to narrow as it moved downstream. The jet was longer at the higher water flow rate, as shown in **Figs. 7(d)** and **(e)**. A good match between CFD simulation and real flow pattern at the experimental conditions is shown in **Figs. 7(e)** and **(f)**.

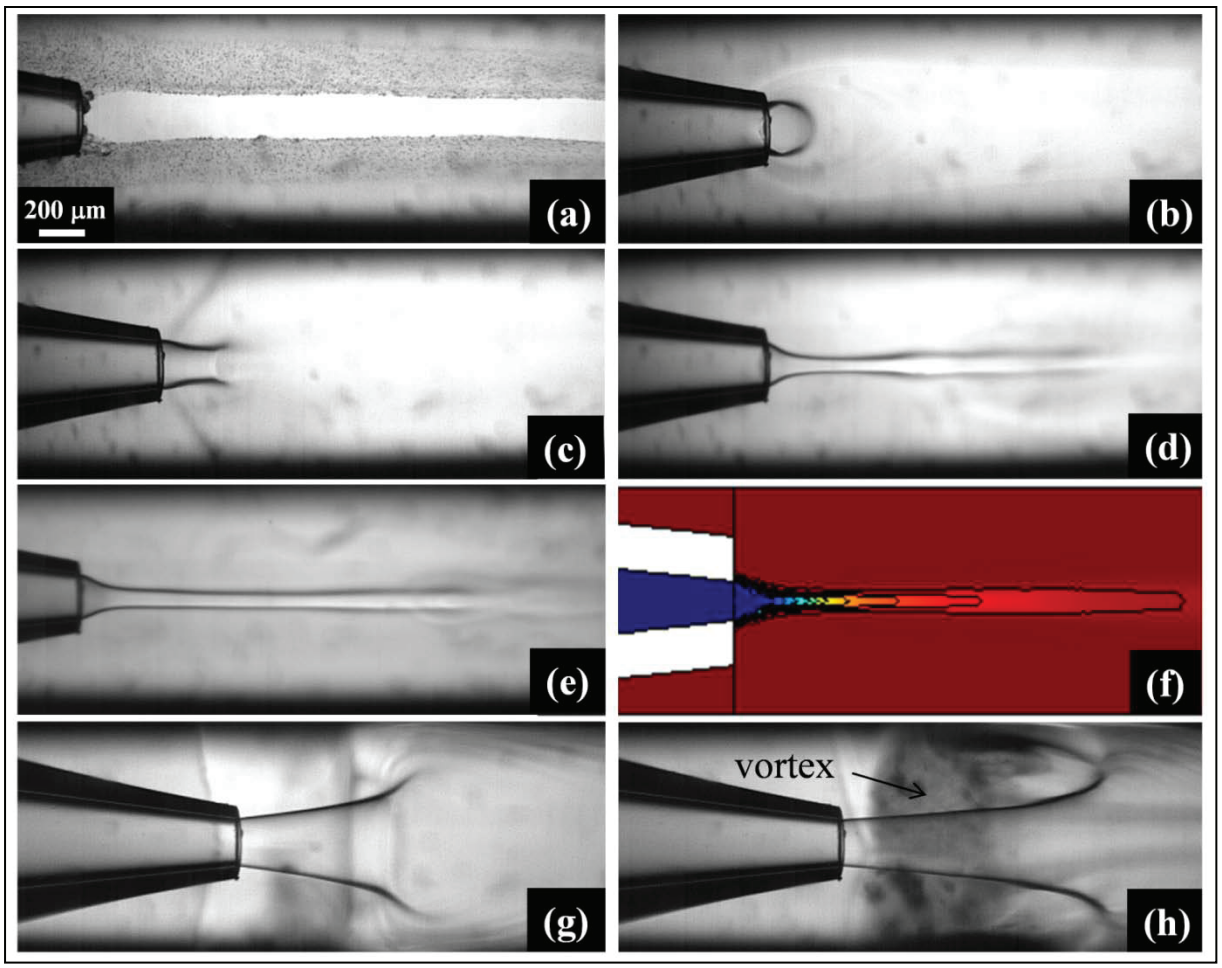

Figure 7. Flow patterns in co-flow capillary device with an orifice size of 209 μm at different phase flow rates: **(a)** Q_w = 0.6 ml/h, Q_o = 0.6 ml/h; **(b)** Q_w = 5 ml/h, Q_o = 0.6 ml/h; **(c)** Q_w = 15 ml/h, Q_o = 0.6 ml/h; **(d)** Q_w = 15 ml/h, Q_o = 0.1 ml/h; **(e)** Q_w = 25 ml/h, Q_o = 0.1 ml/h; **(f)** Q_w = 25 ml/h, Q_o = 0.1 ml/h, CFD simulation; **(g)** Q_w = 25 ml/h, Q_o = 12 ml/h; **(h)** Q_w = 25 ml/h, Q_o = 20 ml/h.

A widening jet was observed when the organic phase was injected at a much higher velocity than the average velocity of the water (**Fig. 7f**). A high shear at the interface due to large difference in fluid velocity at the outlet of the injection tube (U_o = 97 mm/s, U_w = 7 mm/s) decelerated the jet, causing it to widen until it was disintegrated. At very high velocities of both phases in the collection capillary, a vortex was formed in the aqueous phase around a jet, characterised by high concentration of aggregated liposomes (**Fig. 7h**).

The particle size distribution of liposomes prepared using co-flow capillary devices with a variable orifice size is given in **Fig. 8**. At the aqueous and organic phase flow rate of 25 and 5.55 ml/h, respectively, the mean vesicle size decreased from 131 to 73 nm when the orifice diameter decreased from 209 to 42 μm. It can be explained by the fact that the organic phase jet got thinner when the orifice size was reduced, which reduced significantly the mixing time, according to Eq. (1). The smaller vesicles are formed at the higher mixing efficiency **[23]**.

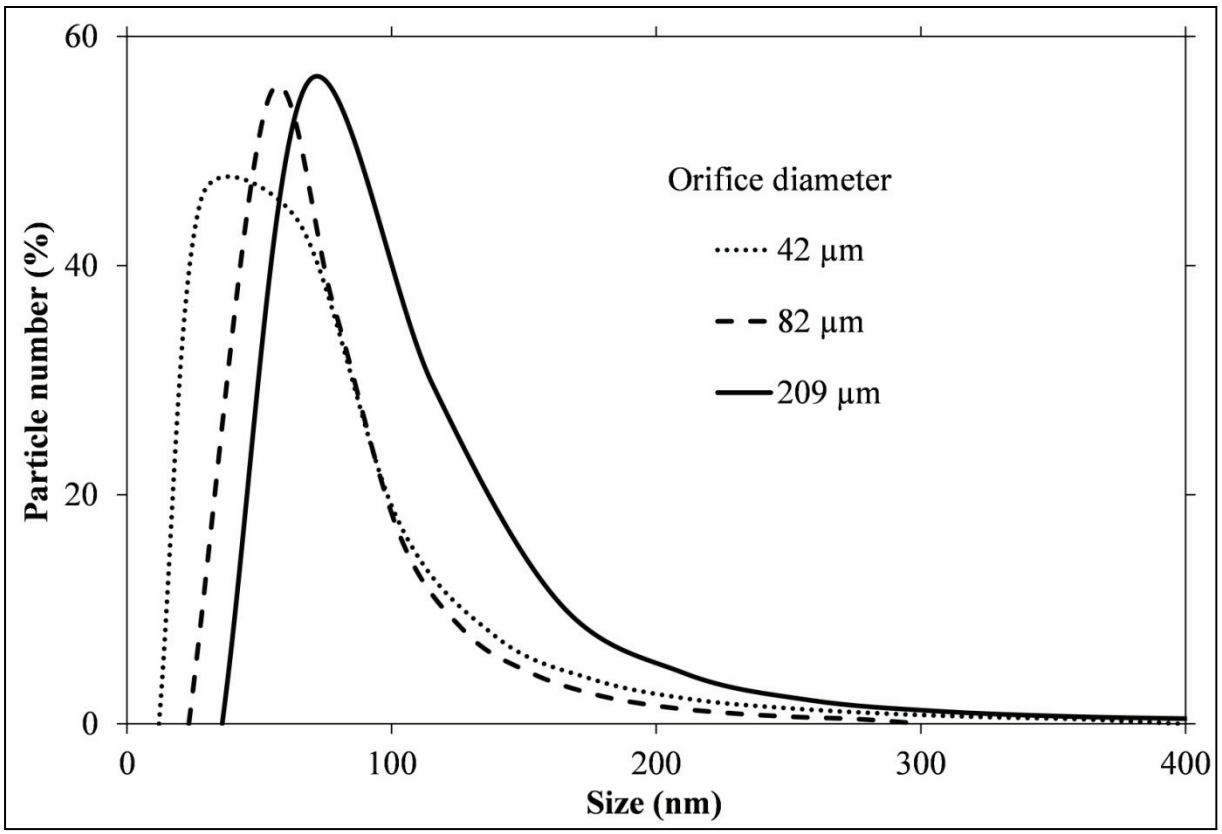

Figure 8. Particle size distribution of liposomal suspensions prepared using co-flow capillary device as a function of orifice diameter. Q_w = 25 ml/h, Q_o = 5.55 ml/h, Q_w/Q_o = 4.5.

4. Conclusion

Size-controlled liposomes were produced by controlled mixing of ethanolic lipid solutions with water via a microengineered membrane or tapered-end glass capillary. The mean size of liposomes produced in different membrane devices was highly consistent when the maximum shear stress on the membrane surface was kept constant, although temporal or spatial distribution of shear stress in these devices was significantly different. The oscillating membrane system was found to be very suitable for scale-up, because shear stress on the membrane surface was independent on the system geometry, fluid flow rate and membrane size.

A mixing rate in co-flowing laminar streams depends on the morphology of an organic phase jet formed downstream of the injection orifice. A high mixing efficiency and low mixing time associated with small vesicle size were achieved at high flow rates of aqueous phase and/or small orifice diameter. The microfluidic strategies developed in this work can be used for production of a wide range of nanopraticles, such as micelles, gold nanoparticles, biodegradable polymeric nanoparticles, etc.

Nomenclature

a	Amplitude of membrane oscillation
b	Height of stirrer blade (=12 mm)
D	Stirrer diameter (=32 mm)
f	Frequency of membrane oscillation
h	Height of cross flow channel (=1 mm)
n_b	Number of stirrer blades
r_{trans}	Radial distance from the axis of rotation at which the shear is maximal
Q	Volume flow rate in cross-flow channel
Re	Rotating Reynolds number of continuous phase (= $\omega\rho_c D^2/(2\pi\eta_c)$)
T	Internal diameter of stirred cell (=40 mm)
W	Width of cross flow channel (=20 mm)
η_w	Viscosity of aqueous phase
ρ_w	Density of aqueous phase
ω	Angular velocity of stirrer
τ_{max}	Maximum shear stress on membrane surface

References

[1] A.D. Bangham, R.W. Horne, Negative staining of phospholipids and their structural modification by surface-active agents as observed in the electron microscope, J. Mol. Biol. 8 (1964) 660–668.

[2] V.P. Torchilin, Recent advances with liposomes as pharmaceutical carriers, Nat. Rev. Drug Discovery 4 (2005) 145–160.

[3] P. Walde, S. Ichikawa, Enzymes inside lipid vesicles: preparation, reactivity and applications, Biomol. Eng. 18 (2001) 143–177.

[4] N.S. Templeton, D.D. Lasic, P.M. Frederik, H.H. Strey, D.D. Roberts, G.N. Pavlakis, Improved DNA: liposome complexes for increased systemic delivery and gene expression, Nat. Biotechnol. 15 (1997) 647–652.

[5] E. Unger, D. Shen, T. Fritz, B. Kulik, P. Lund, G.L. Wu, D. Yellowhair, R. Ramaswami, T. Matsunaga, Gas filled lipid bilayers as imaging contrast agents, J. Liposome Res. 4 (1994) 861–874.

[6] A. Graff, M. Winterhalter, W. Meier, Nanoreactors from polymer-stabilized liposomes, Langmuir 17 (2001) 919–923.

[7] M.J. Campbell, Lipofection reagents prepared by a simple ethanol injection technique, Biotechniques 18 (1995) 1027–1032.

[8] T. Kuroiwa, H. Kiuchi, K. Noda, I. Kobayashi, M. Nakajima, K. Uemura, S. Sato, S. Mukataka, S. Ichikawa, Controlled preparation of giant vesicles from uniform water droplets obtained by microchannel emulsification with bilayer-forming lipids as emulsifiers, Microfluid. Nanofluid. 6 (2009) 811–821.

[9] H.C. Shum, D. Lee, I. Yoon, T. Kodger, D.A. Weitz, Double emulsion templated monodisperse phospholipid vesicles, Langmuir 24 (2008) 7651–7653.

[10] A. Jahn, S.M. Stavis, J.S. Hong, W.N. Vreeland, D.L. DeVoe, M. Gaitan, Microfluidic mixing and the formation of nanoscale lipid vesicles, ACS Nano 4 (2010) 2077–2087.

[11] A.S. Utada, A. Fernandez-Nieves, J.M. Gordillo, D.A. Weitz, Absolute instability of a liquid jet in a coflowing stream, Phys. Rev. Lett. 100 (2008) Art. No. 014502.

[12] G.T. Vladisavljević, W.J. Duncanson, H.C. Shum, D.A. Weitz, Emulsion templating of poly(lactic acid) particles: droplet formation behavior, Langmuir 28, (2012) 12948–12954.

[13] E. Egidi, G. Gasparini, R.G. Holdich, G.T. Vladisavljević, S.R. Kosvintsev, Membrane emulsification using membranes of regular pore spacing: Droplet size and uniformity in the presence of surface shear, J. Membr. Sci. 323 (2008) 414–420.

[14] G.T. Vladisavljević, H. Schubert, Influence of process parameters on droplet size distribution in SPG membrane emulsification and stability of prepared emulsion droplets, J. Membr. Sci. 225 (2003) 15–23.

[15] A. Laouini, C. Jaafar-Maalej, S. Sfar, C. Charcosset, H. Fessi, Liposome preparation using a hollow fiber membrane contactor—Application to spironolactone encapsulation, Int. J. Pharm. 415 (2011) 53–61.

[16] T.T. Pham, C. Jaafar-Maalej, C. Charcosset, H. Fessi, Liposome and niosome preparation using a membrane contactor for scale-up, Colloids Surf., B 94 (2012) 15–21.

[17] G.T. Vladisavljević, M. Shimizu, T. Nakashima, Permeability of hydrophilic and hydrophobic Shirasu-porous-glass (SPG) membranes to pure liquids and its microstructure, J. Membr. Sci. 250 (2005) 69–77.

[18] G.T. Vladisavljević, I. Kobayashi, M. Nakajima, Production of uniform droplets using membrane, microchannel and microfluidic emulsification devices, Microfluid. Nanofluid. 13 (2012) 151–178.

[19] M.M. Dragosavac, M.N. Sovilj, S.R. Kosvintsev, R.G. Holdich, G.T. Vladisavljević, Controlled production of oil-in-water emulsions containing unrefined pumpkin seed oil using stirred cell membrane emulsification, J. Membr. Sci. 322 (2008) 178–188.

[20] R.G. Holdich, M.M. Dragosavac, G.T. Vladisavljević, S.R. Kosvintsev, Membrane emulsification with oscillating and stationary membranes, Ind. Eng. Chem. Res. 49 (2010) 3810–3817.

[21] I.S. Khattab, F. Bandarkar, M.A.A., Fakhree, A. Jouyban, Density, viscosity, and surface tension of water+ethanol mixtures from 293 to 323 K, Korean J. Chem. Eng. 29 (2012) 812–817.

[22] Z. Zhang, P. Zhao, G. Xiao, Focusing-enhanced mixing in microfluidic channels, Biomicrofluidics 2 (2008) 014101.

[23] A. Laouini, C. Charcosset, H. Fessi, R.G. Holdich, G.T. Vladisavljević, Preparation of liposomes: a novel application of microengineered membranes, RSC Adv. 3 (2013) 4985-4994.

Encapsulation de la vitamine E dans une nano-émulsion en utilisant des membranes SPG

Encapsulation de la vitamine E dans une nano-émulsion en utilisant des membranes SPG

Les nano-émulsions sont le plus souvent des émulsions H/E dont la taille des gouttelettes lipidiques est comprise entre 20 et 200 nm. Cette grande finesse de la taille des globules lipidiques confère à ce genre d'émulsion un certain nombre d'avantages : (i) contrairement aux émulsions classiques et aux microémulsions qui nécessitent une teneur élevée de tensioactifs, les nano-émulsions requirent généralement de très faibles quantités de surfactants, (ii) une meilleure efficacité de la délivrance des médicaments due à la très grande surface spécifique du vecteur, (iii) une très bonne stabilité physique. Au vu de tous ces avantages, l'utilisation des nano-émulsions comme vecteurs de molécules actives en pharmacie et en cosmétologie ne cesse de progresser.

Les nano-émulsions peuvent être préparées par diverses méthodes; la plus connue est celle qui utilise des homogénéisateurs du type rotor/stator. Toutefois cette technique présente l'inconvénient d'une consommation très élevée d'énergie et une faible maîtrise de l'uniformité de la taille de l'émulsion obtenue. La préparation des émulsions en utilisant une membrane, appelé encore émulsification membranaire, permet de pallier à ces inconvénients. Ce travail, réalisé au Laboratoire d'Automatique et de Génie des Procédés (LAGEP), compte parmi les premiers à étudier la préparation de nano-émulsions en utilisant des contacteurs à membrane.

Ce travail présente les différentes étapes d'encapsulation de la vitamine E dans une nano-émulsion en commençant par l'optimisation de la formulation galénique (études de solubilités et construction de diagrammes ternaires), puis par l'optimisation du procédé de fabrication en utilisant des membranes SPG. Une attention particulière a été accordée à la reproductibilité du procédé développé ainsi que la stabilité des préparations. Il en sort principalement de cette étude que la vitamine E peut être encapsulée dans des nano-émulsions préparées par émulsification membranaire. Le procédé de préparation peut être parfaitement maitrisé par simple ajustement des paramètres opératoires. La méthode développée s'avère simple rapide et efficace pour une production contrôlée de nano-émulsions.

Ce chapitre sera présenté sous forme d'un article qui a été publié en 2012 dans « Journal of Membrane Science ».

Membrane Emulsification: A Promising Alternative for Vitamin E Encapsulation within Nano-emulsion

Abdallah Laouini, Hatem Fessi, Catherine Charcosset

Université Claude Bernard Lyon 1, Laboratoire d'Automatique et de Génie des Procédés (LAGEP), UMR-CNRS 5007, CPE Lyon, Bât 308G, 43 Boulevard du 11 Novembre 1918, F-69622 Villeurbanne Cedex, France.

Journal of Membrane Science, 423-424, 85-96, 2012

Impact factor: 4.093

Abstract

The purpose of our study was to develop a vitamin E-loaded nano-emulsion which could be a convenient drug carrier to be used for targeting the lungs. The nano-emulsion components (MCT oil and surfactant mixture Tween 80/Brij 35) were selected after solubility studies, and the concentration range was chosen after construction of ternary phase diagrams. For emulsion manufacturing, an SPG membrane emulsification process was developed. Key parameters influence on nano-emulsion characteristics was investigated. It has been established that small droplets and narrow size distribution were favored at low transmembrane pressure, high continuous phase flow rate and high agitation speed. Under optimal conditions, nano-emulsion with a span factor of 0.25 ± 0.01, which meant high monodispersity, and an average size of 78 ± 3 nm, was prepared. The high zeta potential of -22.9 ± 0.9 mV was sufficient to prevent droplet coalescence. Vitamin E was successfully encapsulated within the optimized nano-emulsion with high entrapment efficiency value (99.7 ± 0.4%). Transmission electron microscopy images revealed spherical-shaped and well-distributed nano-droplets. Additionally, special attention was paid on process reproducibility and preparations stability. Results confirmed the robustness of the optimized membrane emulsification technique which seems to be fast, simple and reliable.

Key words: Nano-emulsion – SPG membrane – Membrane emulsification – Vitamin E – Cigarette smoke toxicity.

Contents

1. Introduction

Emulsions with droplet size in the nanometric scale (typically in the range 20–200 nm) are often referred in the literature to as mini-emulsions **[1]**, submicron emulsions **[2]**, nano-emulsions **[3]**, etc. The term nano-emulsion is preferred because in addition to give an idea of the nanoscale size range of the droplets, it avoids misinterpretation with the term micro-emulsion (which are thermodynamically stable systems). Due to their size characteristics, nano-emulsions appear transparent to slightly milky. The very small droplet size causes a large reduction in the gravity force and the Brownian motion may be sufficient for overcoming sedimentation or creaming. Therefore, the long-term physical stability of nano-emulsions (with no apparent flocculation or coalescence) makes them unique and they are sometimes referred to as "approaching thermodynamic stability" **[4]**. These properties make nano-emulsions of interest not only for fundamental studies, but also for practical applications (pharmaceutical, cosmetic, food, chemical fields, etc). In addition to their inherently high colloid stability, the interest for nano-emulsions could be explained by the following advantages: (i) unlike microemulsions (which require a high surfactant concentration usually around 20% and higher), nano-emulsions could be prepared using surfactant concentration less than 10%. (ii) nano-emulsions are suitable for efficient delivery of active ingredients, as the large surface area of the nano-emulsion system allows rapid penetration of actives.

Emulsion manufacturing is a very important process since there is a need to produce emulsions in which the droplets have a defined size and a narrow size distribution. Conventional methods for emulsion production are based on rotor–stator or high pressure homogenizer systems, in which emulsion droplet formation is mainly dependent on the exertion of strong external dissipated energy into fluid mixtures **([5,6]**). However it is well known that a number of problems may be associated with these existing methods of production. Indeed, because the dissipated energy cannot be controlled homogeneously and efficiently, an emulsion with a broad size distribution is often obtained and this, in turns affects the emulsion characteristics and stability **[7]**. Thus, a great amount of work has focused on exploring new devices with milder and more controllable dissipating techniques to produce a uniform emulsion. Among them, the phase inversion temperature method could be an alternative to high-energy emulsification methods. This technique involves transitional inversion induced by changing factors that affect the HLB of the system, such as temperature, electrolyte concentration, etc **[8]**. However, this method has several limitations such as requiring a large amount a surfactant and a careful selection of surfactant–cosurfactant combination, and is not applicable to large scale industrial productions **[9]**.

Membrane emulsification, developed for the first time by *Nakashima et al.* **[10]**, has therefore received increasing attention over the last 2 decades. This relatively new

method is attractive given the low energy consumption, the better control of droplet size and size distribution and especially the mildness of the process. Applications of membrane emulsification were reviewed by several authors (for example *Nakashima et al.* **[11]**, *Jocelyne and Tragardh* **[12]**, *Vladisavljevic and Williams* **[13]**, *Charcosset* **[14]**). This technique allowed the preparation of emulsions, precipitates, polymeric and lipidic nanoparticles and it was also recently reported for liposomes production (**[15]** and **[16]**). In membrane emulsification, the to-be-dispersed phase is pressed through a porous membrane while the continuous phase flows along the membrane surface. Droplets grow at pores and detach at a certain size, which is determined by the balance between the forces acting on the droplets. It follows that the characteristics of the produced emulsions, particularly their size distribution, are influenced by several factors including membranes properties (hydrophobicity, nominal pore size…), experimental conditions (tangential flow, transmembrane pressure, temperature…) and properties of the continuous and dispersed phases (viscosity of the 2 phases, emulsifiers responsible for stabilizing the emulsion…). Considerable amount of work has been carried out in the field of emulsions, whereas there is only one report to our knowledge on the preparation of nano-emulsions using membranes **[17]**.

In this study, we examined the influence of several factors when producing oil-in-water nano-emulsions. Understanding the effect of these factors allowed suitable choice of operating parameters in order to produce nano-emulsions with a narrow droplet size distribution. The optimized process was then applied to vitamin E encapsulation. Vitamin E is an essential nutrient which has several isomers including α-, β-, γ- and δ-tocopherols. The activity and bioavailability of which vary depending on their structures and physico-chemical properties. Among these isomers, α-tocopherol has the highest bioavailability **[18]**. This isomer prevents oxidative damage and lipid peroxidation in central and peripheral nervous systems **[19]**. Because of its promising therapeutic potential and safety, α-tocopherol has been tested to prevent cigarette smoke toxicity since several pulmonary disorders are mainly caused by oxidative stress phenomena **[20]**. Nevertheless, the oral or intravenous administration failed to restore the broncho-alveolar level of vitamin E **[21]**. Recently, attention has been drawn to nanoencapsulated systems, showing high intracellular uptake and improved stability and solubility of active substances; in particular nanoemulsion formulations have been used for the solubilization of poorly water-soluble drugs **[22]**. Therefore, vitamin E-loaded nano-emulsion with adequate size distribution and high loading capacity could be an effective drug carrier to target the lungs after its pulmonary administration.

The aims of our study are to:

– Develop a nano-emulsion formula for vitamin E encapsulation. For this, solubility studies were achieved in order to choose the suitable components (oil and surfactants)

and ternary phase diagram were constructed in order to determine the best concentration range.

– Optimize the preparation method. For this, the influence of process parameters (oil phase pressure, aqueous phase flow rate, agitation speed and working temperature) on nano-emulsion characteristics was investigated.

– Apply the optimized method to vitamin E encapsulation. The prepared nano-emulsions were characterized for their size, size distribution, zeta potential, viscosity, encapsulation efficiency and microscopic morphology.

– Finally, study the reproducibility of the process, as well as the stability of the prepared nano-emulsions.

2. Materials and methods

2.1 Materials

2.1.1 Reagents

α-tocopherol, ascorbic acid, phosphotungstic acid, Tween 20, Tween 60 and Tween 80 were purchased from Sigma-Aldrich Chemicals (Saint Quentin Fallavier, France). Butyl-hydroxy-toluene, Brij 35 and Brij 98 were supplied from MP Biomedicals (Illkrch- Graffenstaden, France). The oils used in this study (diethylhexyladipate, ethylhexyl caprilate/caprate, ethylhexyl ethylhexanoate, ethylhexyl laurate, ethylhexyl stearate, isononyl isononanoate and Medium Chain Triglyceride MCT 55/45) were a kind gift from Stéarinerie Dubois (Boulogne-Billancourt, France). Ethanol 95% and other organic solvents of HPLC grade (acetonitrile, methanol and water) were supplied by Carlo Erba Reagenti (Milano, Italy). They were used such as without further purification. Ultra-pure water (resistivity of 18 MO/cm) was obtained from a Millipore Synergys system (Ultrapure Water System, Millipore).

2.1.2 SPG membranes

Shirasu Porous Glass (SPG) tubular membranes were purchased from SPG Technology (Miyazaki, Japan). SPG membranes are prepared by phase-separated glass leaching in the Na2–O–CaO–MgO–Al2O3–B2O3–SiO2 system, which is synthesized from volcanic ash, called Shirasu, used as the main raw material **[23]**. SPG membranes are widely used for membrane emulsification. These membranes have a narrow pore size distribution and high mechanical strength. In the present study, 3 hydrophilic SPG membranes were used with 0.4 μm, 0.9 μm and 10.2 μm as nominal pore size. The SPG membrane dimensions were as follows: 0.125 m in length, 10^{-2} m in inner diameter, and 10^{-3} m in thickness. Therefore, the active membrane surface was 3.9×10^{-3} m^2.

2.2 Methods

2.2.1 Vitamin E assay

The concentration of vitamin E was determined using an HPLC system (Spactra System SCM 1000, Providence, Rhode Island, USA). The HPLC equipment consisted of a P1000XR pump, an AS3000 autosampler and an UV6000LP UV/VIS detector. The column was a LiChrospher RP C18 column (5 mm, 15 cm×0.46 cm) (Supelco, Bellefonte, USA). The separation was carried out using a mixture of methanol and water (96:4 v/v) as the mobile phase at a flow rate of 1.6ml/min. The eluent was monitored at 292 nm and peaks were recorded using the chromatography data system software Chromo-Quest version 5.0 (Thermo Fisher Scientific, Philadelphia, USA). It should be noted that before chromatographic data were collected, the column was equilibrated for 30 min with a minimum of 30 column volumes. At the end of the assay, a washing of the column was performed using water–acetonitrile (50:50 v/v) for 60min. This HPLC analytical method was validated as usually required (data not shown).

2.2.2 Solubility studies

Solubility of vitamin E in different surfactants

An excess of vitamin E (about 1.5 g) was added to 15 ml of 10% w/v surfactant solutions containing ascorbic acid as antioxidant (15mg/ml). The solutions were shaken in a water bath at 25 1C for 4 day, followed by a centrifugation for 10min at 12,000 rpm (OptimaTM Ultracentrifuge, Beckman Coulter, USA). The supernatant was then filtered through a membrane filter (0.22 mm) (Millipore non-sterile filters, Billerica, USA). The resulting solution was assayed for vitamin E using the previously described HPLC method.

The surfactants tested were: Brij 35 (polyoxyethylene glycol dodecyl ether), Brij 98 (Polyoxyethylene glycol monooleyl ether), Labrafil (Oleoyl macrogol-6 glycerides), Phosphatidylcholine, Span 40 (Sorbitan monopalmitate), Span 60 (Sorbitan monostearate), Tween 20 (polyoxyethylene glycol sorbitan monolaurate), Tween 60 (polyoxyethylene glycol sorbitan monostearate) and Tween 80 (polyoxyethylene glycol sorbitan monooleate). All experiences were conducted in triplicate and the mean values were taken.

Solubility of vitamin E in different oils

To find the suitable oil for preparing the nano-emulsion, the solubility of vitamin E in various oils was measured. An excess amount of vitamin E (about 1.5 g) was added to 3 g oil containing BHT as anti-oxidant (2 mg/g). The obtained solutions were shaken in a water bath at 25 °C for 4 day, followed by a centrifugation for 10 min at 12,000

rpm. To extract vitamin E from the resulting supernatant, 2 ml of methanol containing BHT (1 mg/ml) was added followed by a centrifugation at 12,000 for 10 min. The remaining pellet was re-extracted as previously described with 2 ml methanol-BHT. The second extract was combined to the first one and the final mixture was centrifuged at 10,000 rpm for 8 min. The resulting solution containing extracted vitamin E was passed through a membrane filter (0.22 μm) and then assayed using the HPLC analytical method.

The oils tested were: diethylhexyl adipate, ethylhexyl caprilate/ caprate, ethylhexyl ethylhexanoate, ethylhexyl laurate, ethylhexylstearate, isononyl isononanoate and Medium Chain Triglyceride MCT 55/45.

2.2.3 Ternary phase diagram

Construction of a phase diagram is a useful approach to study the complex series of interactions that can occur when different components are mixed. Nano-emulsions may be formed along with various other structures (including emulsions, micelles, micro-emulsions and various gels and oily dispersions) depending on the chemical composition and concentration of each component. The existence of the nano-emulsion field was identified from the ternary phase diagrams of systems containing oil, surfactant and water. The oil and the surfactant that showed higher solubility for vitamine E were selected for the preparations of the nano-emulsions. All the mixtures were homogenized, and then 3 heating-cooling cycles were carried out (between 45 °C and 5 °C, with storage of 12 h at each temperature). Finally, the mixtures were kept at room temperature for 72 h. Visual observations were made; a slightly milky and easily flowable mixture was considered to be a nano-emulsion. After the 3 day storage, 3 nano-emulsion categories were assigned: (a) stable emulsion: an homogenous solution, (b) partially stable emulsion: a trend to separation between the 2 phases after storage, and (c) unstable emulsion: separation of the 2 phases after the preparation.

2.2.4 Nano-emulsion preparation protocol

A schematic diagram of the experimental set-up used in this study is shown in **Fig. 1**. The system included a positive displacement pump (Filtron, France), a pressurized vessel (equipped with a manometer M3) connected on one side to a nitrogen bottle (Linde Gas, France) and on the other side to the membrane module (with two manometers M1 and M2, respectively, placed at the inlet and outlet of the device). For the nano-emulsion preparation, the MCT oil was placed in the pressurized vessel. The connecting valve to the nitrogen bottle was opened and the nitrogen pressure was set at a fixed level. The aqueous phase, containing the surfactant mixture, was then pumped through the membrane module using the positive displacement pump. When the aqueous phase arrived to the outlet of the membrane device, the valve connecting the

pressurized vessel to the filtrate side of the membrane module was opened so that the oil phase permeated through the pores of the SPG membrane into the aqueous phase. Nano-emulsion formation occurred as soon as the MCT was in contact with the aqueous phase. The experiment was stopped when air bubbles started to appear in the tube connecting the pressurized vessel to the membrane module, indicating that the pressurized vessel was empty. Then, the nano-emulsion was stabilized for 15 min under magnetic stirring (RW 20, Ika-Werk). All experiments were carried out in a close loop configuration. Drug-loaded nanoemulsions were prepared as described above and adding the vitamine E in the oil phase.

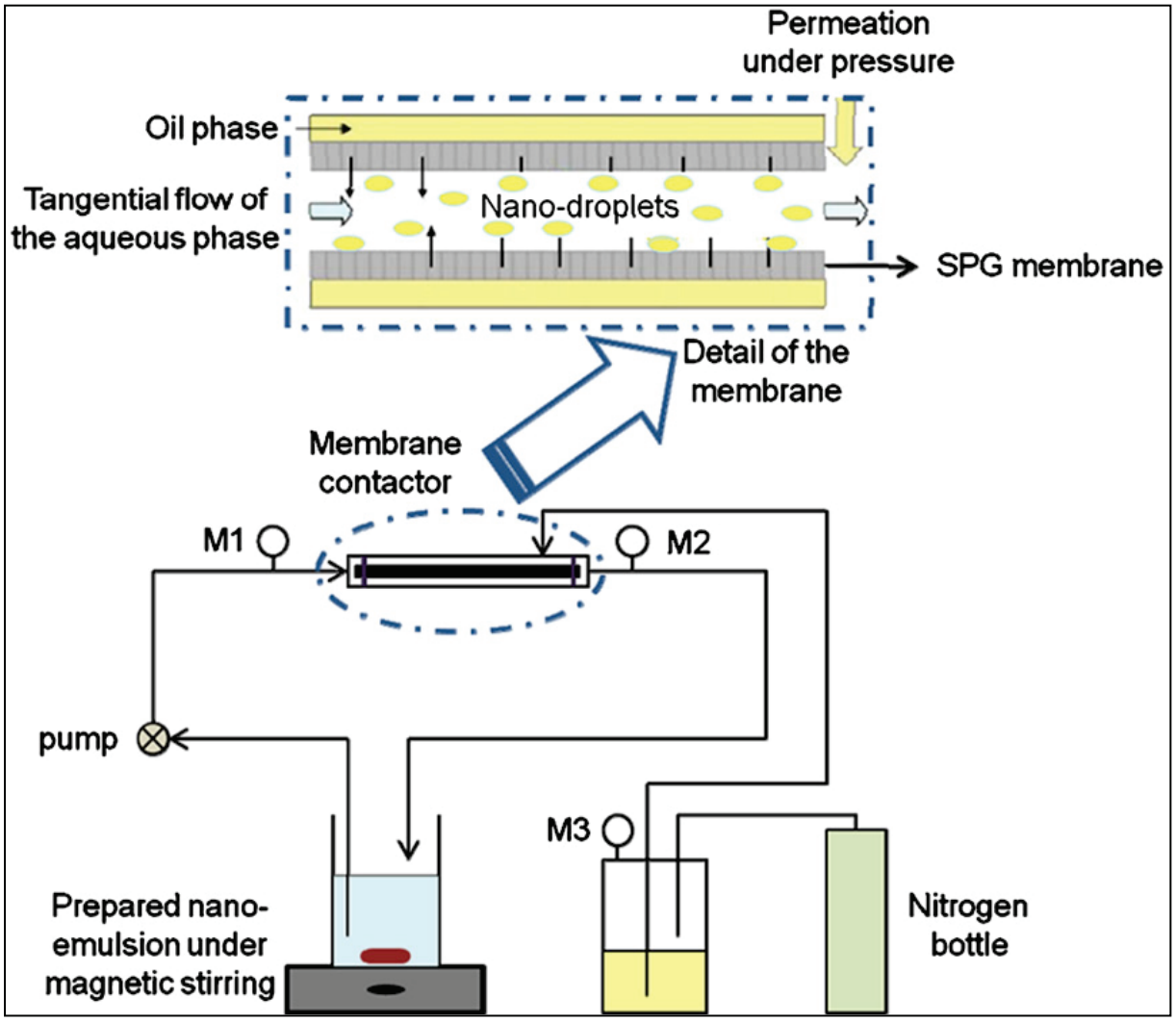

Fig. 1. Schematic diagram of the experimental set-up.

At the end of the experiment, the SPG membrane was regenerated. The washing was performed by flushing the module twice with 400 ml of water and 200 ml of ethanol in the pressurized vessel. The membrane permeability (the slope of the permeate flow rate versus transmembrane pressure) was measured at the beginning of each experiment and was checked to be around 90% of its initial value.

2.2.5 Nano-emulsion characterization

In order to assess the nano-emulsion quality and to obtain quantitative measurements that allow comparison between different batches, various parameters were measured. The methods included average mean size and span factor determination, zeta potential analysis, viscosity measurement, microscopic observation and encapsulation efficiency.

Size analysis

Dynamic light scattering (DLS), otherwise known as photon correlation spectroscopy (PCS), is extensively used in size distribution analysis since it is a simple and fast technique which allowed the detection of droplets in the range of 0.6–6000 nm **[24–26]**. In this study, a Malvern Zetasizer Nano-series (Malvern Instruments Zen 3600, Malvern, UK) was used. Each sample was diluted 100-fold with ultra-pure water immediately before measurement and then was analyzed in triplicate at 25 °C. A previous report has indicated that the dilution of samples did not change the particle size distribution **[27]**. The data on droplet size distribution were collected using the DTS nano software (version 5.0) provided with the instrument. The mentioned Z-average diameter corresponds to the harmonic intensity-weighted average hydrodynamic diameter of these droplets. In addition, the polydispersity was assessed by the mean of span factor defined as $(d_{90}–d_{10})/d_{50}$; where d_{10}, d_{50} and d_{90} are the droplets diameters at 10%, 50% and 90% of the cumulative intensity, respectively. The span factor is a good indicator of the width of droplet size distribution of a sample: the smaller the value of the span factor, the narrower the size distribution. Usually if the span factor < 0.4, the size distribution can be considered to be monodispersed (**[28,29]**). These data (droplet size and span factor) were expressed as the mean ± standard deviation (S.D.).

Zeta potential determination

Measurements of zeta potential are commonly used to predict the colloidal system stability **[30]**. The zeta potential was determined using a Malvern Zetasizer Nano-series (Malvern Instruments Zen 3600, Malvern UK). After dilution of the nano-emulsion in water, all the measurements were performed at least three times and the data were expressed as the mean size ± standard deviation (S.D.). The zeta potential was calculated from the electrophoretic mobility by the Helmholtz–Smoluchowski equation **[31]**.

Viscosity determination

The apparatus used for viscosity determination was a viscometer TVe-05 (Lamy, Caluire, France). First, the spindle to be used was attached to the measurement system.

Then the rotation speed needed for the measurement was selected. The dynamic viscosity was directly displayed on the apparatus screen.

Encapsulation efficiency

In this study, the vitamin E encapsulation efficiency was determined using the ultracentrifugation technique. Briefly, to determine the total amount of the drug (T.A.), a sample of the nano-emulsion was dissolved in methanol and then assayed for vitamin E using the HPLC method previously described. Then, to determine the encapsulated amount of the drug (E.A.), a sample of the nano-emulsion was centrifuged (OptimaTM Ultracentrifuge, Beckman coulter, USA) at 50,000 rpm during 50 min at +4 °C and under reduced pressure. The obtained pellet was dissolved in methanol and assayed for vitamin E.

The vitamin E encapsulation efficiency (E.E.) was calculated as follows:

$$E.E. = (E.A. / T.A.) \times 100$$

For each batch of vitamin E-loaded nano-emulsion, the encapsulation efficiency was determined in triplicate.

Microscopic observation

The sample preparation was performed according to recent studies **[32–34]**. An aliquot of the emulsion was diluted 10-fold using ultrapure water and a drop of the diluted sample was placed onto a carbon-coated copper grid. The sample was allowed to stand for 5 min, after which the excess fluid was absorbed by a filter paper leaving a thin liquid film over the holes. One drop of a 2% phosphotungstic acid solution (w/w) was then applied and allowed to dry for 5 min. Finally, the negatively stained samples were observed and images were taken using a CM 120 microscope (Philips, Eindhoven, Netherlands) operating at an accelerating voltage of 80 kV.

2.2.6 Reproducibilty

Once all the process parameters were assessed, the experiment under optimal conditions was repeated three times. The technique reproducibility was evaluated in terms of z-average size, zeta potential, viscosity, and encapsulation efficiency, using the methods described above.

2.2.7 Stability study

The prepared nano-emulsion samples were stored under conditions required by the 2008 guidelines of the ICH (International Conference on Harmonization of Technical Requirements for Registration of Pharmaceuticals for Human Use): 5 ± 3 °C for normal stability study and 25 ± 2 °C, 60 ± 5 % RH (relative humidity) for accelerated

stability study. The storage period was of 4 months for drug-free nano-emulsions and 2 months for drugloaded nano-emulsions. The stability was assessed by comparing the initial z-average size, zeta potential and microscopic observation with those obtained during the storage period.

3. Results and discussion

3.1 Development of the nano-emulsion formula

3.1.1 Screening components: solubility studies

Screening surfactant

The solubility of vitamin E in 10% w/v surfactant solutions is presented in **Table 1**. The aqueous solution of vitamin E was about 49.41×10^{-6} mg/ml. Our results confirmed that vitamin E is very poorly soluble in water. The drug was more soluble in all the surfactants according to the solubility data.

Table 1. Solubility of vitamin E in 10% w/v surfactant solutions.

Surfactants	Solubility* (mg/ml)
Water	$49.41 \pm 0.21 \times 10^{-6}$
Brij 35	74.32 ± 1.21
Brij 98	51.10 ± 0.16
Labrafil	$89.29 \pm 0.03 \times 10^{-2}$
Phosphatidylcholine	$26.20 \pm 0.50 \times 10^{-3}$
Span 40	2.52 ± 0.05
Span 60	7.04 ± 0.02
Tween 20	49.16 ± 1.02
Tween 60	15.62 ± 0.09
Tween 80	87.25 ± 0.16

* Each value represents the mean ± S.D. (n=3).

The nano-emulsion consisting of oil, surfactant(s) and water should be a stable monodispersed system. Therefore, the choice of surfactants is important for the production of uniformly sized nano-emulsion droplets via SPG membrane emulsification. Among the surfactants tested in this study Tween 80 and Brij 35 were selected since they gave the highest drug solubility, respectively (87.25 mg/ml and 74.32 mg/ml).

Screening oil

The solubility of vitamin E in different oils is presented in **Table 2**. For the 7 tested oils, the solubility of vitamin E was highest in MCT (241.22 mg/ml) followed by ethyhexyl laurate (235.59 mg/ml). MCT was then selected as the oil phase since it

gave the higher solubility of vitamin E which may lead to a better encapsulation of the drug within the nano-emulsion.

Table 2. Solubility of vitamin E in various oils.

Oils				Solubility* (mg/ml)
Name	Molecular weight (g/mol)	Density (g/ml)	Melting point (°C)	
Diethylhexyle adipate	370.64	0.922	67.8	231.65 ± 0.75
Ethylhexyl caprilate / caprate	426.67	0.876	NA	219.26 ± 3.60
Ethylhexyl ethylhexanoate	256.42	0.863	NA	144.99 ± 0.52
Ethylhexyl laurate	312.53	0.858	27	235.59 ± 1.88
Ethylhexyl stearate	369.68	0.859	4	156.38 ± 0.38
Isononyl isononanoate	284.47	0.857	NA	220.96 ± 0.23
MCT	372.54	0.950	10	241.22 ± 4.09

* Each value represents the mean ± S.D. (n=3).

3.1.2 Screening concentration range: ternary phase diagram

The construction of the phase diagram makes it easy to determine the range of concentrations for the nano-emulsion formulation. Phase diagrams were constructed to determine the individual component ratio for the O/W nano-emulsion consisting of water, MCT as oil phase and Tween 80 (**Fig. 2A**) or Brij 35 (**Fig. 2B**) or a mixture Tween 80–Brij 35 50:50 w/w (**Fig. 2C**) as the surfactants. As can be seen in **Fig. 2.**, the area corresponding to a stable O/W nano-emulsion varied with the surfactant.

The system with combined use of two surfactants appeared to have the largest region of nano-emulsion compared to the systems using Tween 80 or Brij 35 alone. A similar result was reported by *Li et al.* **[35]**; the combined use of surfactants showed advantages over the single use of surfactant as the emulsion region was greatly increased in the phase diagram and the produced emulsion had small particle size, increased drug loading capacity and improved physical stability. Based on these finding, the formulation composed of water, MCT and the surfactant mixture Tween 80–Brij 35 (50:50 w/w) at weight ratio of 80:14:6 was selected for further studies.

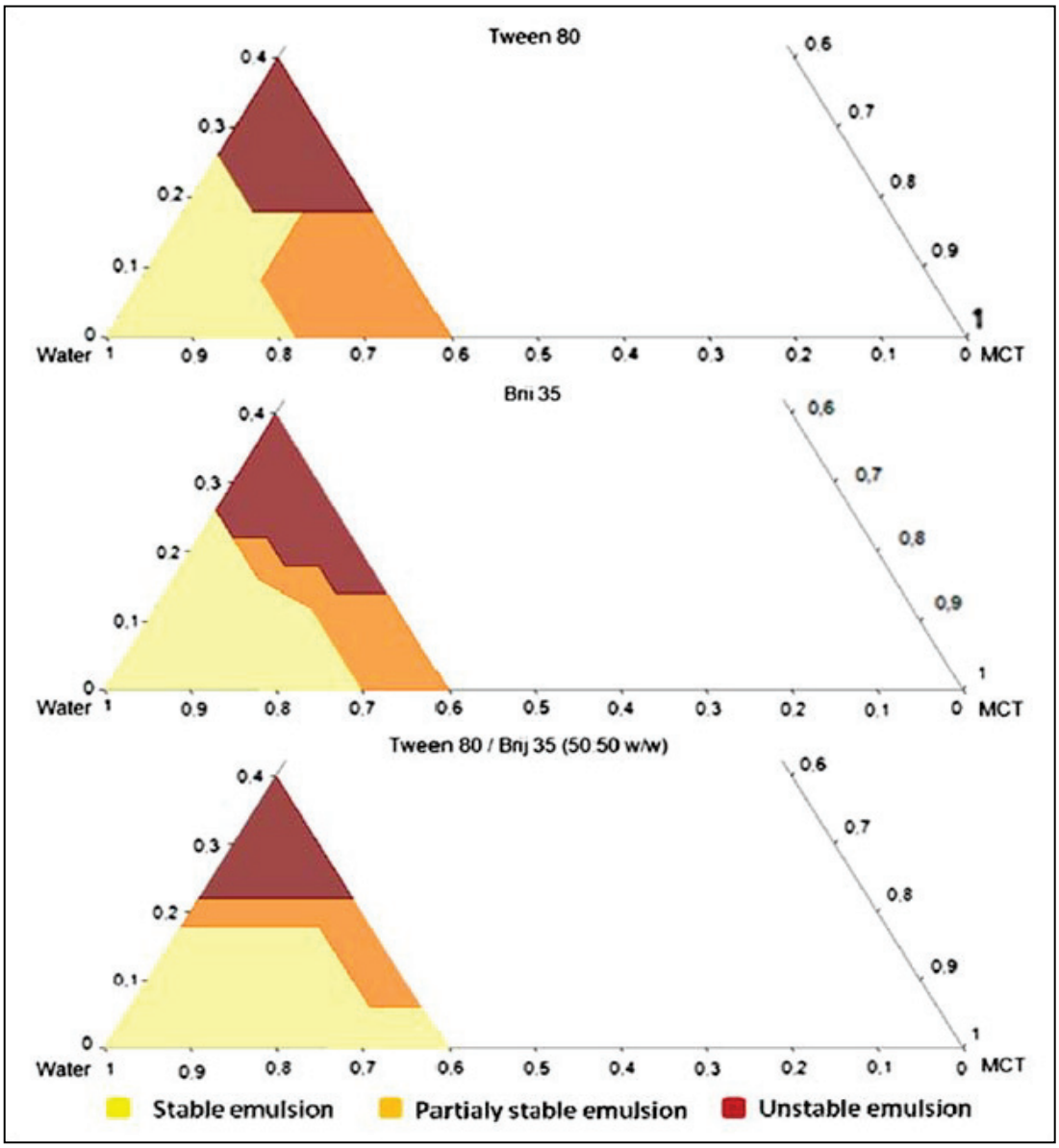

Fig. 2. Ternary phase diagrams: **(A)** water, MCT and Tween 80; **(B)** water, MCT and Brij 35; **(C)** Water MCT and Tween 80–Brij 35 (50:50 w/w).

3.2 Optimization of the process parameters and the surfactant concentration

3.2.1 Influence of the oil phase pressure on the nano-emulsion characteristics

The pressure applied on the dispersed phase control the flow rate through the membrane pores and the detachment of the droplets. During preliminary studies, it has been observed that below 2.4 bar no oil phase flow was obtained. Thus, the effect of the oil phase pressure over the range of 2.4–4 bar on the nanoemulsion characteristics was investigated. **Fig. 3A.** shows the size distribution of samples prepared for 3 different oil phase pressures.

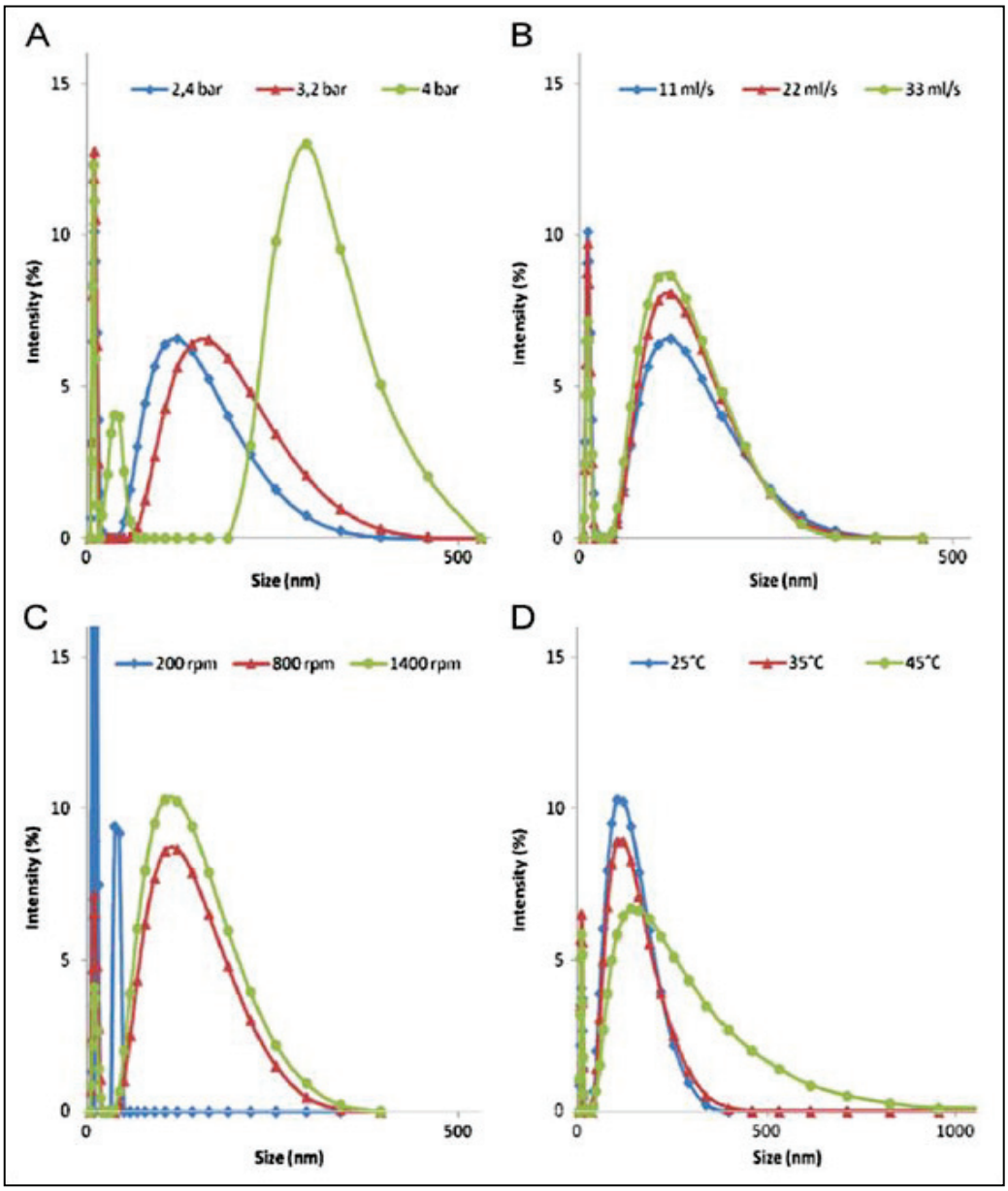

Fig. 3. Influence of process parameters on droplets size distribution: **(A)** effect of the transmembrane pressure, **(B)** effect of the continuous phase flow rate, **(C)** effect of the agitator speed and **(D)** effect of the temperature. Other experimental parameters are specified in **Table 3**.

It can be observed that when the pressure was set at 4 bar, the emulsion size distribution presented 3 peaks: at 9 nm, 50 nm and 382 nm, representing 44%, 14% and 42% of the total intensity, respectively. Besides, when the pressure was fixed at 3.2 bar, the emulsion size distribution presented only 2 peaks: at 10 nm and 170 nm, this last peak represented 45% of the total intensity. When the pressure decreased to 2.4 bar, the emulsion size distribution seems to be better with 2 peaks: the first peak remained at 10 nm and the second one at 132 nm and represented 49% of the total intensity. The peaks situated around 10 nm correspond to micelles formed by the

association of surfactant molecules. As could be seen, when the dispersed phase transmembrane pressure increased, the uniformity of the emulsion decreased. It is suggested that a high dispersed phase flow led to a poly-disperse emulsion.

Liu et al. **[36]** had obtained similar results when they investigated the effect of the pressure on droplets of a w/o emulsion prepared using an acrylic polymer microchannel. The authors reported that when the applied pressure was increased from 0.3 kPa to 0.6 kPa, an increase of the average diameter was observed (from 62 mm to 98 mm).

Table 3 shows that the span factor increased (+ 38%) when the pressure was increased from 2.4 bar to 4 bar.

Vladisavljevic and *Schubert* **[37]** studied the influence of the transmembrane pressure on droplet size distribution of an emulsion prepared using a 4.8 µm SPG membrane. The authors found that at high pressures, the droplet distribution became much wider. Indeed, a 3-fold increase of the feed pressure led to a 2-fold increase of the span factor (from 0.27 to 0.52). *Hao et al.* **[38]** also observed the effect of different emulsification pressure on droplet size distribution. They reported that the increase in transmembrane pressure resulted in the formation of a polydispersed emulsion. Indeed, they found that the span factor value increased from 0.11 to 0.26 when the dispersed phase pressure was increased from 8 kPa to 28 kPa. *Yasuno et al.* **[39]** observed the formation of droplets during SPG membrane emulsification using a microscope video. The microscopic visualization of the droplet formation revealed that increasing the dispersed phase flux induced the formation of polydispersed emulsion.

In addition, *Schroder et al.* **[40]** and *Jocelyne* and *Tragardh* **[41]** explained the effect of transmembrane pressure by the interfacial tension dynamics. The increase of the transmembrane pressure induces increasing of the oil phase flux; if the formation time of droplets is shorter than the time needed by the emulsifier to decrease the interfacial tension, then too high pressure lead to jets of oil and very large droplets. In another word, at higher pressure the organic phase surface expand very rapidly leading to high interfacial tension and because of that a higher shear rate is needed to keep the same droplet size. In conclusion, if the shear stress is kept constant, larger droplets are formed at higher pressure.

In the present study we considered that 2.4 bar was the optimum data for the transmembrane pressure and thus the pressure was fixed at this level for subsequent experiments.

Table 3. Influence of (i) process parameters (oil phase pressure, aqueous phase flow rate, agitator speed and emulsification temperature) and (ii) surfactant concentration on nano-emulsions polydispersity.

Oil phase pressure (bar)	Aqueous phase flow rate (ml/s)	Agitator speed (rpm)	Emulsification temperature (°C)	Surfactant concentration (% w/w)	Span factor*
2.4	**11**	800	25	**6**	0.57±0.015
3.2	11	800	25	6	0.59±0.004
4	11	800	25	6	0.80±0.024
2.4	**22**	800	25	6	0.57±0.014
2.4	**33**	**800**	25	6	0.53±0.008
2.4	33	**200**	25	6	0.70±0.027
2.4	33	**1400**	**25**	6	0.53±0.003
2.4	33	1400	**35**	6	0.66±0014
2.4	33	1400	**45**	6	0.90±0.013
2.4	33	1400	25	**4**	0.52±0.004
2.4	33	1400	25	**3**	0.44±0.005
2.4	33	1400	25	**2.5**	0.36±0.009
2.4	33	1400	25	**2.25**	0.25±0.005
2.4	33	1400	25	**2**	0.41±0.017

* Each value represents the mean ± S.D. (n=3).

3.2.2 Influence of the aqueous phase flow rate on nano-emulsion characteristics

Droplets formed at the membrane surface detach under the influence of the flowing continuous phase. Thus, the continuous phase flow rate is another parameter which may have a strong influence on droplet size distribution. The effect of this parameter was determined by comparing the size distribution and the span factor of three nano-emulsions prepared under different conditions. **Fig. 3B.** shows that the different nano-emulsions presented 2 peaks: the micelles peak was at 10 nm and the second one depended on the crossflow. An increase of the aqueous phase flow rate shows an improvement in the size distribution. Indeed, with a high flow rate (33 ml/s) the main peak was at 122 nm and represented 64% of the total intensity whereas at a low flow rate (11 ml/s) the main peak was at 132 nm and presented 49% of the total intensity.

Joscelyne and *Tragardh* **[41]** reported that the droplet size decreased sharply as the crossflow velocity increased and reached a size where it became more or less independent of the flow velocity. The authors concluded that at low shear stresses the droplets grow and coalesce at the membrane surface before finally being dislodged. The influence of the continuous phase velocity may vary depending on the concentration of dispersed phase in the circulating solution. It has been shown by *Williams et al.* **[42]** that no significant influence could be observed if the oil is more than 30% in an o/w emulsion.

Our results suggest that 33 ml/s was the optimal crossflow. All the following experiments were then realized under this condition.

3.2.3 Influence of the agitation speed on nano-emulsion characteristics

The influence of the agitator speed over a range of 200–1400 rpm on the nano-emulsion characteristics are shown in **Fig. 3C.** and **Table 3**. As the agitator speed increased from 800 rpm to 1400 rpm, the z-average of the main peak did not significantly change, however its percentage increased from 64% to 82%. When the agitator speed was fixed at 200 rpm, the size determination quality report noticed the existence of big droplets with very high mean size, which had not been measured (exceeding the upper limit of the Zetasizer: 6000 nm). Because the emulsion droplets generated by membrane emulsification may coalesce before they sufficiently disperse in the continuous phase, the increase in stirring rate could improve the droplets dispersion and then prevent their coalescence. Moreover, the mixing tank geometry may help the droplets break up when the agitation speed is increased leading to small particle size.

The effect of agitator speed on the properties of an emulsion was studied by *Tsukada et al.* **[43]**. The authors reported that the particle sizes decreased from 220 nm to 170 nm with increasing agitation speed from 100 rpm to 1000 rpm. In another study **[44]**, the stirring rate influence on the properties of nanoparticles produced by the emulsification-diffusion method was investigated. As expected, increasing the stirring rate from 8000 rpm to 24,000 rpm was associated to a reduction of the mean size from 554 nm to 276 nm.

In this study, we considered that an agitator speed of 1400 rpm was the optimal speed. For further experiments, the agitation was set at this level.

3.2.4 Influence of temperature on nano-emulsion characteristics

Temperature can be an important parameter in membrane emulsification, affecting the viscosity of both the dispersed and the continuous phases. In this study, we investigated the effect of the temperature on the droplet size distribution. As shown in **Fig. 3D.** and **Table 3**, the increase in temperature from 25 °C to 45 °C gave a larger average size for the main peak (respectively, 125 nm and 215 nm, at 25 °C and 45 °C) and a much broader size distribution (span factor increased from 0.53 to 0.90).

For w/o emulsions, heating the continuous phase is needed so that there is a substantial decrease in its viscosity which makes it easier to circulate. *Katoh et al.* **[45]** found that heating the continuous phase led to smaller droplet size. For o/w emulsions, there have been few studies of the effect of the temperature on the size uniformity of emulsions during membrane emulsification. In a recent study, *Oh et al.* **[17]** reported that increasing the emulsification temperature from 25 °C to 35 °C induced a decrease in the uniformity of the formed oil droplets. In a literature review, *Jocelyne* and *Tragardh* **[12]** concluded that the emulsification temperature is usually dictated by the requirements of a product. For instance, the authors prepared in a previous work **[41]** an o/w emulsion where the operating temperature was significantly above room temperature (65 °C). Heating was used to dissolve the emulsifier in the continuous phase.

In our study, 25 °C was selected as the optimum temperature since it gave relatively uniform emulsion droplets.

3.2.5 Influence of surfactant concentration on nano-emulsion characteristics

The presence of emulsifiers dissolved in the continuous phase plays a critical role in membrane emulsification. First they lower the interfacial tension between oil and water. This facilitates droplets disruption given that the interfacial tension force is one of the essential forces holding a droplet at a pore during the membrane emulsification

process. Second, emulsifiers stabilize the formed droplets by restricting coalescence and/or aggregation. According to *Tadros et al.* **[3]**, the amount of surfactant required to produce the smallest droplets size depends on its properties. Generally, the mean size decreases with increase in surfactant concentration till it reaches eventually a plateau value.

In our study, the optimization of the process parameters was not sufficient to obtain a narrow size distribution. Indeed the nano-emulsion size distribution presented two peaks: a main peak at 125 nm representing 82% of the total intensity and corresponding to the oil droplets, and a second peak at 11 nm representing 18% corresponding to micelles. The formation of these micelles was believed to be due to the presence of emulsifiers in excess. For that reason, the surfactants concentration was decreased progressively in order to find an optimum value. Results in **Fig. 4.** and **Table 3** confirm the aforementioned assumption. When the surfactants concentration was decreased from 6% to 2.25%: the peak corresponding to micelles decreased progressively and finally disappeared. The size distribution became more uniform and therefore the span factor decreased from 0.52 to 0.25. When the surfactants concentration was set at 2%, the main peak was situated at 290 nm, the size distribution became broader and the span factor increased to 0.41. This could be explained by the fact that the emulsifiers' amount was not enough, so that the surfactant molecules did not adsorb rapidly at newly formed interfaces and thus larger droplets were formed. Another explanation would be the coalescence of the formed droplets.

Vladisavljevic and *Schubert* **[37]** found similar results when studying the dynamic interfacial tension of Tween 80 solution at two different concentrations (0.2 wt % and 2 wt %). The more concentrated Tween 80 solution caused a faster decrease of the interfacial tension. Thus, when the emulsifiers' concentrations increased, the droplet size became smaller and the size distribution narrower, till a plateau value. After this plateau value (which is in our study the concentration of 2.25%), increasing the emulsifiers concentration did not affect the droplets size (the main peak was always about 125 nm) but could lead to a broader size distribution given that the surfactant excess induced micelles formation (a second peak at 11 nm appeared then).

To the authors' knowledge, there have been no systematic studies of the effect of surfactant excess on nano-emulsion characteristics. *Oh et al.* **[17]** investigated the effect of stabilizer excess on the droplets size distribution. The nano-emulsions prepared with 1, 2 and 4% PVA showed span factor values of 0.25, 0.24 and 0.33, respectively. This study confirmed that when the stabilizer (which plays a similar role as the surfactant during membrane emulsification) was used in excess, this may result on a large droplets size distribution. In addition to its effect on the size distribution, the presence of surfactant in excess could also affect the emulsion stability. *Izquiedro et*

al. **[8]** compared the stability of 5 nano-emulsions prepared using different surfactant concentrations (from 4 wt % to 8 wt %). The authors found that as the surfactant concentration increased, the nano-emulsion became less stable. They explained this result by the formation of micelles, which increased with the surfactant concentration. The presence of micelles increases the oil molecules diffusion between emulsion droplets and the oil phase solubilized by surfactant micelles. This exchange of oil molecules between different size droplets enhances Ostwald ripening **[46]**. Indeed, Ostwald ripening process causes growth of the larger droplets of an emulsion in the expense of smaller ones due to molecular diffusion through the continuous phase. Since the mutual miscibility between the continuous and the dispersed phase is often very low, the effect of Ostwald ripening is often neglected. Nevertheless, in the case of nano-emulsion droplets, all liquid pairs are mutually miscible to some finite extent and this may lead to rapid ripening **[47]**. As could be seen, the concentration of surfactants affects the production process as well as the long term stability of nano-emulsions. Our study confirms the importance and the complexity of the optimization of the emulsifier concentration for the production of stable nano-emulsions. Apart from stability and productions issues, it is often desirable to minimize the use of surfactants especially for pharmaceutical applications because they are usually costly and some of them may have potential toxic effects.

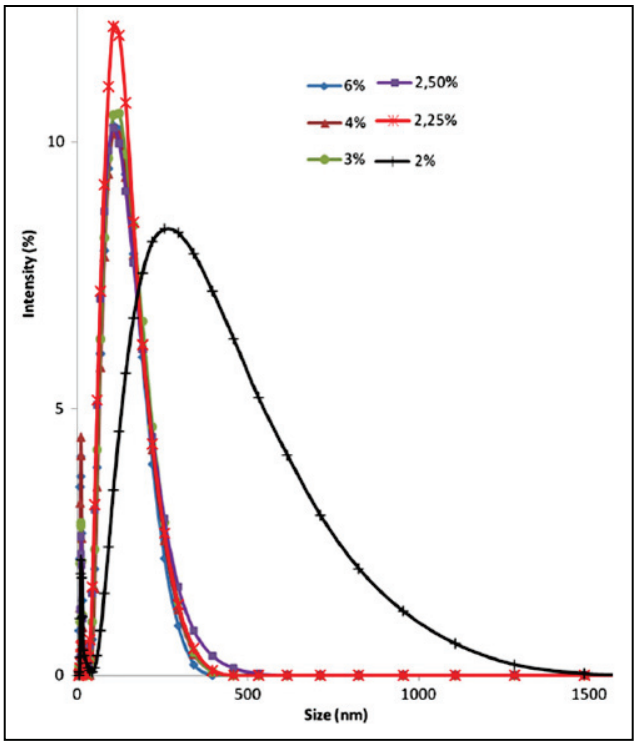

Fig. 4. Influence of surfactant concentration on droplets size distribution. Other experimental parameters are specified in Table 3.

In conclusion, and based on the findings during the preparation optimization, the formulation composed of MCT, water and the surfactant mixture Tween 80–Brij 35 (50:50 w/w), at the weight ratio of 17.75/80/2.25 was selected to produce an optimal uniform nano-emulsion using an SPG membrane at an agitator speed of 1400 rpm, a transmembrane pressure of 2.4 bar, a continuous flow rate of 33 ml/s and a temperature of 25 °C.

3.3 Vitamin E loading in the nano-emulsion

To prepare drug-loaded nano-emulsion, vitamin E was added in the oil phase, since it is poorly soluble in water and very soluble in oil. The preparation process was the same as the one used for the drug-free nano-emulsion.

3.3.1 Influence of loading amount on vitamin E nano-emulsion characteristics

To prepare vitamin E-loaded nano-emulsion, 3 concentrations were tested: 5, 7 and 10% w/w. The effect of the drug amount on the droplets size was investigated. Results reported in **Fig. 5A.** show that increasing the vitamin E proportion in the oil phase led to an increase of the average droplet size (the peak was situated at 151, 235 and 278 for the 3 different ratios 5, 7 and 10% w/w, respectively). In the other hand the size distribution became larger; as could be seen in **Table 4**, the span factor increased from 0.29 to 0.46.

Similar results was reported by *Hatanaka et al.* **[32]**; when the α-tocopherol ratio in the nano-emulsion composition increased from 10% w/w to 50% w/w, the droplets mean diameter increased from 85 nm to 381 nm. The authors explained that the differences in mean size was attributed to the loading amount and suggested that a high amount of a-tocopherol might also affect the morphology of emulsion systems, possibly leading to a decrease in long-term stability. The study of *Cheong et al.* **[48]** confirmed also this trend. Indeed the authors reported that the droplet size of α-tocopherol nanodispersions prepared with 90% of aqueous phase was about 106 nm and increased to about 146 nm when the aqueous phase ratio changed to 70%. There are a number of possible reasons to explain this trend: (i) higher vitamin E content increased the to-be-dispersed phase viscosity and thereby droplet disruption and break-up at the surface of membrane pores would be more difficult leading to high size droplets. (ii) According to *Jafari et al.* **[9]**, the emulsifier concentration may be insufficient to completely cover the new formed interfaces; this could favor droplets aggregation and thus increases the emulsion mean size.

Due to these reasons, a 5% w/w concentration of vitamin E was selected for subsequent study.

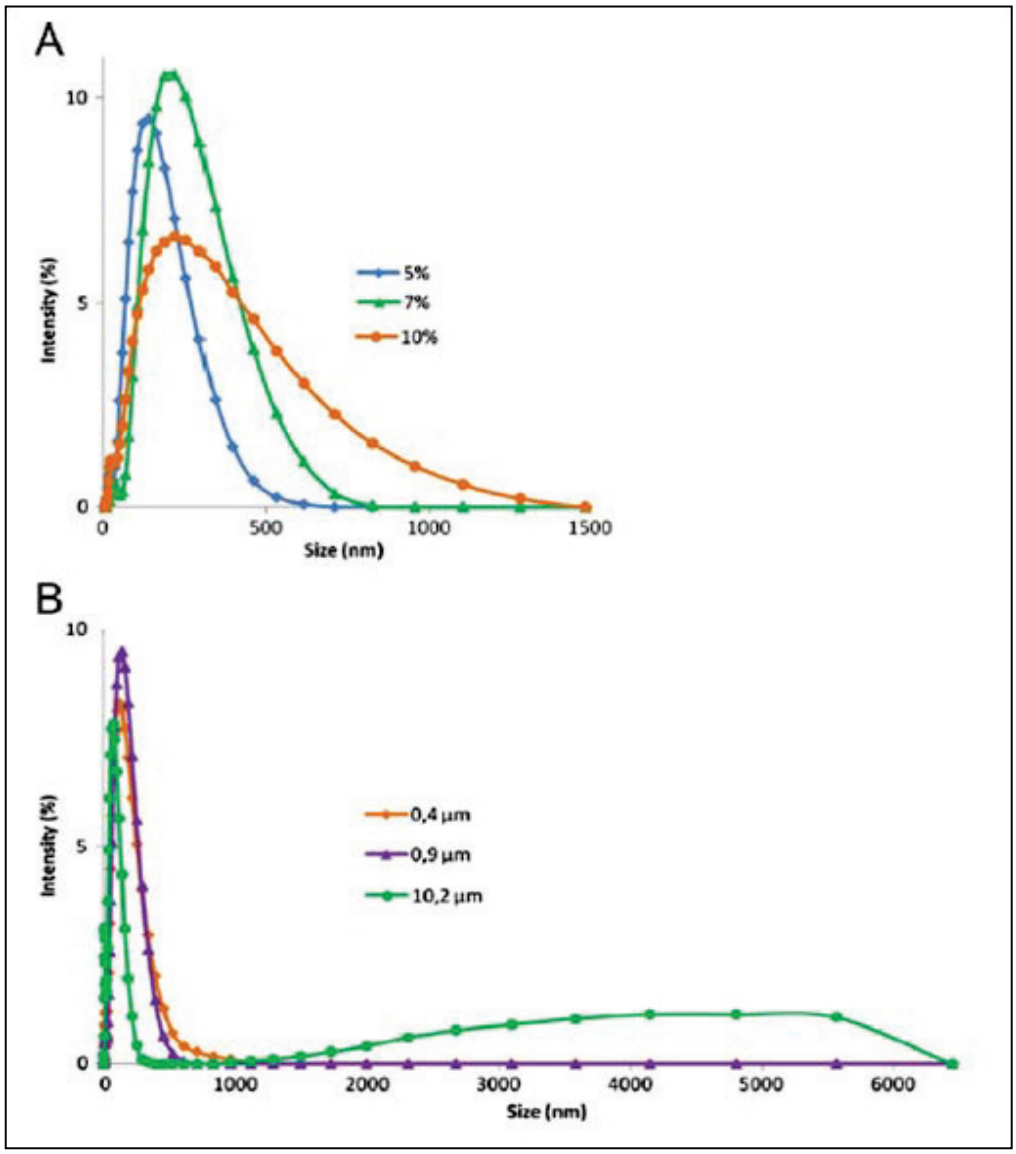

Fig. 5. Influence of (A) vitamin E loading amount (% w/w) and (B) SPG membrane nominal pore size on droplets size distribution. Other experimental parameters are specified in **Table 4**.

Table 4. Influence of (i) vitamine E loading amount and (ii) membrane pores size on drug loaded nano-emulsions polydispersity.

Vitamin E concentration (% w/w)	Membrane nominal pore size (µm)	Span factor*
5	**0.9**	0.29 ± 0.007
7	0.9	0.37 ± 0.005
10	0.9	0.46 ± 0.012
5	**0.4**	0.37 ± 0.016
5	**10.2**	0.49 ± 0.021

* Each value represents the mean ± S.D. (n=3).

3.3.2 Influence of membrane pore size on nano-emulsion characteristics

In order to investigate the effect of membrane pore size on the droplet size during membrane emulsification, experiments were conducted using 3 different SPG membranes (nominal pore size of 0.4 µm, 0.9 µm and 10.2 µm). **Fig. 5B** shows the droplet size distribution as a function of the membrane nominal pore size and **Table 4** summarizes the effect of nominal pore size on the span factor. As could be seen, between 0.4 µm and 0.9 µm there was no great difference on the peak average size (respectively, 160 nm and 151 nm). However the experiment lasted 9 min with the 0.9 µm membrane and more than 1 h when the 0.4 µm membrane was used. This could be explained by the high viscosity of the oil phase which had much more difficulty to pass through the narrow pores of the 0.4 µm membrane. *Cheng et al.* **[28]** prepared w/o emulsions using different SPG membranes with an average pore size of 1.8, 2, 2.5 and 4.8. However the preparation was unsuccessful when an SPG membrane with average pore size of 0.6 mm was used even if the transmembrane pressure was set to its higher level. In the study of *Cheng et al.* **[28]**, results suggest that membranes with pore size less than 0.6 mm may be used only for the preparation of emulsion at low dispersed phase proportion. In general, the pore size of the membrane which would be used for the emulsification is greatly dependent on the properties of both continuous and dispersed phases (viscosity, density, interfacial tension, etc)

On the other hand, when the 10.2 mm membrane was used, the dispersed phase passed very rapidly in a few seconds. The average size increased and the size distribution became broader.

Our results were in a good agreement with those reported in the literature. Indeed many studies using SPG membranes **[37,42,49]** revealed that the droplet size of an emulsion could be related to the pore size of the used membrane by a linear relationship. Our data fitted well to a linear model with $R_2 = 0.996$. Thus, our study confirmed that the droplet size depends on the pore size of the membrane used to prepare the emulsion. This raises the possibility of controlling the emulsion droplet size using various pore size membranes. In our case, the use of the 0.4 µm membrane was not convenient since the process was too slow. In addition, the use of the 10.2 µm membrane was not convenient too since it gave an emulsion with high average size and very large size distribution. Based on these findings, the 0.9 µm membrane was considered to be the optimal and was therefore used for the reproducibility tests.

3.4 Reproducibility tests

3.4.1 Drug free nano-emulsion reproducibility

The nano-emulsion preparation was repeated 3 times in order to study the technique reproducibility (Batches N1, N2 and N3). Resulting data shown in **Table 5** revealed the very good accordance, in terms of Z-average size, span factor, zeta potential, viscosity and processing time between the 3 batches prepared under identical conditions.

3.4.2 Vitamin E loaded nano-emulsion reproducibility

The reproducibility of the preparation technique of the vitamin E-loaded nano-emulsion was investigated. Three batches were produced under the same conditions (Batches E1, E2 and E3). Data shown in **Table 5** revealed the very good reproducibility of the preparation process.

3.5 Characteristics of the optimized vitamin E loaded nano-emulsion

The effect of the drug entrapment on the nano-emulsion characteristics was investigated; data are shown in **Table 6**. The addition of the drug increased the droplets average size (respectively, 78 nm and 106 nm without and with vitamin E) and the span factor (respectively, 0.25 and 0.30 without and with vitamin E). This increase is due to the entrapment of vitamin E within the MCT oil droplets.

Kuo et al. **[50]** reported similar results; when loading α-tocopherol within nano-emulsion the span factor increased from 0.23 to 0.28. The droplet size and size distribution are important parameters affecting emulsion stability. *Saito et al.* **[51]** reported that small droplets tend to be more stable to droplets coalescence than large droplets. Indeed, the small droplets size of nano-emulsions confers stability against creaming and sedimentation because of the high Brownian motion **[4]**. Thus, in our study, the narrow size of the prepared nano-emulsion allows predicting a good stability of the preparation.

Zeta potential has also been identified as an important factor for the stability of colloidal systems **[52]**. In our study, negative zeta-potential values were obtained (-22.9 mV for drug-free nano-emulsion). This value could be explained by the presence of negatively charged carboxyl groups of free fatty acids present in the MCT oil. According to the certificate of analysis, the free fatty acids present in the MCT oil are: the caprylic acid (C8: 62%), the capric acid (C10: 37.9%) and the lauric acid (C12: 0.1%).

Table 5. Reproducibility data of drug free and drug-loaded nano-emulsions.

Batch No	Z-average* (nm)	Span factor*	Zeta potential* (mV)	Viscosity* (mPa s)	Processing time* (min)	E.E.* (%)
N1	76 ± 0.8	0.24 ± 0.001	-22.8 ± 0.4	4.3 ± 0.1	4.3	
N2	78 ± 2.1	0.25 ± 0.005	-23.9 ± 0.5	4.5 ± 0.2	4.2	
N3	80 ± 0.7	0.26 ± 0.030	-22.1 ± 0.5	4.5 ± 0.1	3.9	
E1	104 ± 0.3	0.29 ± 0.007	-16.0 ± 0.1	5.6 ± 0.1	10.1	99.99 ± 0.03
E2	110 ± 3.7	0.31 ± 0.012	-16.1 ± 0.5	6.0 ± 0.3	9.8	99.19 ± 0.02
E3	105 ± 4.2	0.32 ± 0.009	-17.5 ± 0.6	5.5 ± 0.2	9.2	99.81 ± 0.04

* Each value represents the mean ± S.D. (n=3).

Table 6. Effect of vitamin E entrapment on nano-emulsion characteristics.

Preparation	Z-average* (nm)	Span factor*	Zeta potential* (mV)	Viscosity* (mPa s)	Processing time* (min)	E.E.* (%)
Drug free nano-emulsion	78 ± 2.0	0.25±0.010	-22.9 ± 0.9	4.4 ± 0.1	4.1 ± 0.1	
Drug-loaded nano-emulsion	106 ± 3.2	0.30±0.015	-16.5 ± 0.8	5.7 ± 0.2	9.7 ± 0.4	99.7±0.4

* Each value represents the mean of reproducibility batches ± S.D. (n=3).

The zeta potential measurements give information on the surface properties of the colloidal system and could therefore be useful to determine the type of the association between the active substance and the colloidal system (for example whether the drug is encapsulated in the lipidic matrix or simply adsorbed on the surface) **[53]**. As could be seen in **Table 6**, the negative surface charge was further shielded in the presence of the drug; the vitamin E-loaded nano-emulsion had an upper zeta potential (-16.5 mV). This result suggests that a part of vitamin E was adsorbed to the MCT droplets surface and the rest was incorporated within the oil droplets. Many authors (*Mora-Huertas et al.* **[54]**, *Wiacek and Chibowski* **[55]** and *Lyklema* and *Fleer* **[30]**) reported that greater the zeta potential the more likely the suspension to be stable, because the charged particles repel one another and thus overcome the natural tendency to aggregate. It is currently admitted that zeta potential under $\left|15\right|$ mV is required for a good electrostatic stabilization **[56]**. Thus, our zetapotential values were sufficient to prevent droplets coalescence and predict a good stability of the prepared nano-emulsions.

The high encapsulation efficiency of vitamin E within nanoemulsion (99.7 ± 0.4%) was believed to be due to the high lipophilicity of the drug. This result was in agreement with those reported in the literature. Indeed, *Anais et al.* **[44]** reported that the association rate of vitamin E in nanocapsules was equal to 92.8% when the nanoprecipitation method was used and equal to 97.8% when nanocapsules were prepared by the emulsification–diffusion method.

Finally, the vitamine E-loaded nano-emulsion was more viscous than the drug-free nano-emulsion; this is logical since that adding the vitamin E during the drug loading experiments increased the viscosity of the oil phase (viscosity of MCT oil and vitamin E are 30 mPa s and 660 mPa s, respectively).

3.6 Stability study

Stability studies were carried out over 4 months for the drug free nano-emulsion and over 2 months for the vitamin E-loaded nano-emulsion. The three batches of reproducibility were selected in order to follow the droplets size, the zeta potential and morphological observation during storage at 5 °C and 25 °C. Stability data are shown in **Table 7** and **Fig. 6**.

According to *Heurtault et al.* **[56]**, the size determination is a good indicator of stability since in most cases the particle sizes increased before macroscopic changes appeared. Our stability data shows that the Z-average size and the span factor remained nearly unchanged during the storage period. There were also no significant changes in the droplets size distribution during the same period (data not included). In addition, the zeta potential was maintained to its initial value and no coalescence was observed during storage.

Table 7. Stability data of the prepared nano-emulsions for storage temperature of 5 °C and 25 °C.

(a) Drug free nano-emulsion							
Time	Day 0	Day 45		Day 90		Day 120	
Storage temperature (°C)		5	25	5	25	5	25
Average size* (nm)	78 ± 2.0	85 ± 0.9	84 ± 2.1	85 ± 1.2	92 ± 0.6	89 ± 0.7	99 ± 0.8
Span factor*	0.25 ± 0.01	0.31 ± 0.00	0.38 ± 0.01	0.25 ± 0.00	0.22 ± 0.01	0.22 ± 0.01	0.20 ± 0.01
Zeta potential* (mV)	-23 ± 0.9	-21 ± 0.5	-22 ± 0.6	-21 ± 0.7	-23 ± 1.4	-20 ± 0.5	-25 ± 0.7
(b) Vitamin E-loaded nano-emulsion							
Time	Day 0	Day 30		Day 60			
Storage temperature (°C)		5	25	5	25		
Average size* (nm)	106 ± 3.2	108 ± 1.6	109 ± 1.1	105 ± 0.5	102 ± 1.4		
Span factor*	0.30 ± 0.01	0.29 ± 0.01	0.27 ± 0.00	0.23 ± 0.01	0.22 ± 0.01		
Zeta potential* (mV)	-17 ± 0.8	-20 ± 1.0	-15 ± 0.3	-16 ± 0.2	-16 ± 0.3		

* Each value represents the mean of reproducibility batches ± S.D. (n=3).

The microscopic investigation illustrates the droplets appearance and size (**Fig. 6.**). TEM images indicated that the nanoemulsion droplets were spherical and well distributed. The morphological investigation, as well as the size and zeta potential determination, demonstrate the good stability of the nano-emulsions and thus indicate an adequate formulation of the preparation and optimum process conditions.

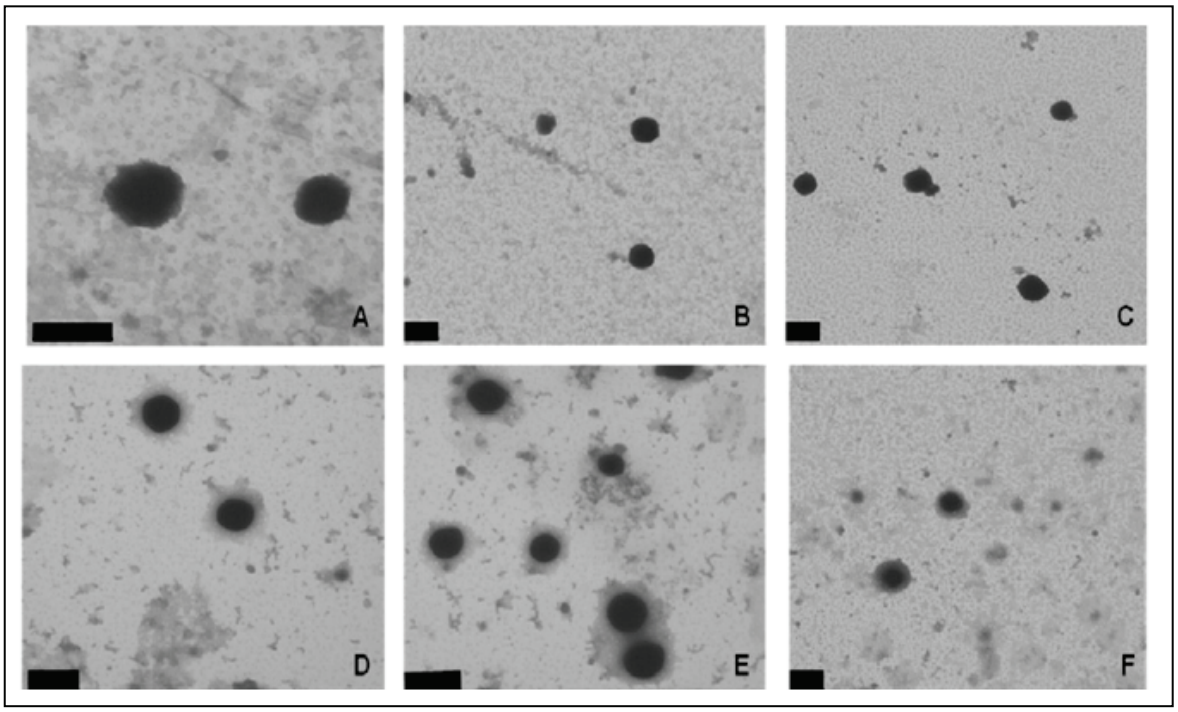

Fig. 6. TEM micrographs of the prepared nano-emulsions stored at 5 °C. **A**, **B** and **C**: TEM pictures of drug-free nano-emulsion at day 0, day 60 and day 120, respectively. **D**, **E** and **F**: TEM pictures of vitamin E-loaded nano-emulsion at day 0, day 30 and day 60, respectively. Scale bar represents 200 nm.

4. Conclusion

In this study, a vitamin E-loaded nano-emulsion composed of water, MCT, surfactant mixture (Tween 80–Brij 35 (50:50 w/w)) and vitamin E at the weight ratio of 80/12.75/2.25/5 was prepared using a 0.9 mm SPG membrane at an agitator speed of 1400 rpm, an oil phase pressure of 2.4 bar and an aqueous phase flow rate of 33 ml/s. The prepared nano-emulsion had an average size of 106 nm, a uniform size distribution (span factor = 0.30) and a relatively high zeta potential (-16.5 mV) sufficient to prevent droplet coalescence and a high encapsulation efficiency (99.7%). Moreover, the obtained nano-emulsions showed a good stability for at least 2 months.

The results presented in this study, confirmed that nanoemulsions can be produced in a controlled way by adjusting the processing parameters. Therefore, membrane emulsification seems to be a simple, effective and reliable technique for the encapsulation of vitamin E within nano-emulsion.

References

[1] M.S. El-Aasser, E.D. Sudol, Mini-emulsions: overview of research and applications, JCT Res. 1 (2004) 21–31.

[2] S. Amselel, D. Friedman, Submicron emulsions as drug carriers for topical administrations, in: S. Benita (Ed.), Submicron Emulsions in Drug Targeting and Delivery, Harwood Academic Publishers, London, 1998, pp. 153–173.

[3] T. Tadros, P. Izquiedro, J. Esquena, C. Solans, Formation and stability of nanoemulsions, Adv. Colloid Interface Sci. 108–109 (2004) 303–318.

[4] C. Solans, P. Izquiedro, J. Nolla, N. Azemar, M.J. Garcia-Celma, Nanoemulsions, Curr. Opin. Colloid Interface 10 (2010) 102–110.

[5] K. Urban, G. Wagner, D. Schaffner, D. Roglin, J. Ulrich, Rotor–stator and disc systems for emulsification processes, Chem. Eng. Technol. 29 (2006) 24–31.

[6] S. Schutz, G. Wagner, K. Urban, J. Ulrich, High-pressure homogenization as a process for emulsion formation, Chem. Eng. Technol. 27 (2004) 361–368.

[7] J. Floury, A. Desrumaux, J. Legrand, Effect of ultra-high-pressure homogenization on structure and on rheological properties of soy protein-stabilized emulsions, J. Food Sci. 67 (2002) 3388–3395.

[8] P. Izquiedro, J. Esquena, T.F. Tadros, C. Dederen, J. Feng, M.J. Garcia, et al., Formation and stability of nano-emulsions prepared using the phase inversion temperature method, Langmuir 18 (2002) 26–30.

[9] S.M. Jafari, E. Assadpoor, Y. He, B. Bhandari, Re-coalescence of emulsion droplets during high-energy emulsification, Food Hydrocolloids 22 (2008) 1191–1202.

[10] T. Nakashima, M. Shimizu, M. Kukizaki, Membrane emulsification by microporous glass, Key Eng. Mater. 61/62 (1991) 513–516.

[11] T. Nakashima, M. Shimizu, M. Kukizaki, Particle control of emulsion by membrane emulsification and its application, Adv. Drug Deliv. Rev. 45 (2000) 47–56.

[12] S.M. Joscelyne, G. Tragardh, Membrane emulsification—a literature review, J. Membr. Sci. 169 (2000) 107–117.

[13] G. Vladisavljevic, R.A. Williams, Recent developments in manufacturing emulsions and particulate products using membranes, Adv. Colloid Interface Sci. 113 (2005) 1–20.

[14] C. Charcosset, Membrane processes in biotechnology: an overview, Biotechnol. Adv. 24 (2006) 482–492.

[15] C. Jaafar-Maalej, C. Charcosset, H. Fessi, A new method for liposome preparation using a membrane contactor, J. Liposome Res. 3 (2011) 213–220.

[16] A. Laouini, C. Jaafar-Maalej, S. Sfar, C. Charcosset, H. Fessi, Liposome preparation using a hollow fiber membrane contactor—application to spironolactone encapsulation, Int. J. Pharm. 415 (2011) 53–61.

[17] D.H. Oh, P. Balakrishnan, Y. Oh, D. Kim, C.S. Yong, H. Choi, Effect of process parameters on nanoemulsion droplet size and distribution in SPG membrane emulsification, Int. J. Pharm. 404 (2011) 191–197.

[18] M. Hidiroglu, K. Karpinski, Pharmacokinetic disposition in sheep of various vitamin E preparations given orally or intravenously, Br. J. Nutr. 59 (1988) 509–518.

[19] A.M. Terrasa, M.H. Guajardo, C.A. Marra, G. Zapata, α-tocopherol protects against oxidative damage to lipids of the rod outer segments of the equine retina, Vet. J. 182 (2009) 463–468.

[20] M. Scherrer-Crosbie, M. Paul, M. Meignan, E. Dahan, G. Lagrue, G. Atlan, et al., Pulmonary clearance and lung function: Influence of acute tobacco intoxication and of vitamin E, J. Appl. Physiol. 81 (1996) 1071–1077.

[21] Y. Kato, K. Watanabe, M. Nakakura, T. Hosokawa, E. Hayakawa, K. Ito, Blood clearance and tissue distribution of various formulations of α-tocopherol injection after intravenous administration, Chem. Pharm. Bull. 41 (1993) 599–604.

[22] F. Shakeel, M.S. Faisal, Nano-emulsion: a promising tool for solubility and dissolution enhancement of celecoxib, Pharm. Dev. Technol. 15 (2010) 53–56.

[23] G. Vladisavljevic, I. Kobayashi, M. Nakajima, R.A. Williams, M. Shimizu, T. Nakashima, Shirasu porous glass membrane emulsification: characterization of membrane structure by high-resolution X-ray microtomography and microscopic observation of droplet formation in real time, J. Membr. Sci. 302 (2007) 243–253.

[24] N. Berger, A. Sachse, J. Bender, Filter extrusion of liposomes using different devices: comparison of liposome size, encapsulation efficiency, and process characteristics, Int. J. Pharm. 223 (2001) 55–68.

[25] S. Kolchens, V. Ramaswamia, J. Birgenheiera, Quasi-elastic light scattering determination of the size distribution of extruded vesicles, Chem. Phys. Lipids 65 (1993) 1–10.

[26] T. Provder, Challenges in particle size distribution measurement past, present and for the 21st century, Prog. Org. Coat. 32 (1997) 143–153.

[27] R.H. Muller, M. Radtke, S.A. Wissing, Solid lipid nanoparticles (SLN) and nanostructured lipid carriers (NLC) in cosmetic and dermatological preparations? Adv. Drug. Delivery Rev. 54 (2002) 131–155.

[28] C. Cheng, L. Chu, R. Xie, Preparation of highly monodisperse w/o emulsions with hydrophobically modified SPG membranes, J. Colloid Interface Sci. 300 (2006) 375–382.

[29] A. Nazir, K. Schroen, M. Boom, Premix emulsification: a review, J. Membr. Sci. 362 (2010) 1–11.

[30] J. Lyklema, G. Fleer, Zeta electrical contributions to the effect of macromolecules on colloid stability, Colloid Surf. 25 (1987) 357–368.

[31] R. Hunter, H.Z. Midmore, Zeta potential of highly charged thin double-layer systems, J. Colloid Interface Sci. 237 (2001) 147–149.

[32] J. Hatanaka, H. Chikamori, H. Sato, S. Uchida, K. Debari, S. Onoue, et al., Physicochemical and pharmacological characterization of α-tocopherol loaded nano-emulsion system, Int. J. Pharm. 396 (2010) 188–193.

[33] A.C. Sintov, H.V. Levy, S. Botner, Systemic delivery of insulin via the nasal route using a new microemulsion system: In vitro and in vivo studies, J. Controlled Release 148 (2010) 168–176.

[34] Y. Gao, Y. Wang, Y. Ma, A. Yu, F. Cai, W. Shao, et al., Formulation optimization and in situ absorption in rat intestinal tract of quercetin-loaded microemulsion, Colloid Surf. B 71 (2009) 306–314.

[35] P. Li, A. Ghosh, R.F. Wagner, S. Krill, Y.M. Joshi, A.T.M. Serajuddin, Effect of combined use of nonionic surfactant on formation of oil-in-water microemulsions, Int. J. Pharm. 288 (2005) 27–34.

[36] H. Liu, M. Nakajima, T. Kimura, Production of monodispersed water-in-oil emulsions using polymer microchannels, J. Am. Oil Chem. Soc. 81 (2004) 705–711.

[37] G. Vladisavljevic, H. Schubert, Influence of process parameters on droplet size distribution in SPG membrane emulsification and stability of prepared emulsion droplets, J. Membr. Sci. 225 (2003) 15–23.

[38] D.X. Hao, F.L. Gong, G.H. Hu, Y.J. Zhao, G.P. Lian, G.H. Ma, et al., Controlling factors on droplets uniformity in membrane emulsification: Experiment and modeling analysis, Ind. Eng. Chem. Res. 47 (2008) 6418–6425.

[39] M. Yasuno, M. Nakajima, S. Iwamoto, T. Maruyama, S. Sugiura, I. Kobayashi, et al., Visualization and characterization of SPG membrane emulsification, J. Membr. Sci. 210 (2002) 29–37.

[40] V. Schr ¨ oder, O. Behrend, H. Schubert, Effect of dynamic interfacial tension on the emulsification process using microporous ceramics membranes, J. Colloid Interface Sci. 202 (1998) 334–340.

[41] S.M. Joscelyne, G. Tragardh, Food emulsions using membrane emulsification: conditions for producing small droplets, J. Food Eng. 39 (1999) 59–64.

[42] R.A.Williams, S.J. Peng, D.A.Wheeler, N.C. Morley, D. Taylor, M. Whalley, et al., Controlled production of emulsions using a crossflow membrane Part II. Insustrial scale manufacture, Chem. Eng. Res. Des. 76 A (8) (1998) 902–910.

[43] Y. Tsukada, K. Hara, Y. Bando, C.C. Huang, Y. Kousaka, Y. Kawashima, et al., Particle size control of poly(dl-lactide-co-glycolide) nanospheres for sterile applications, Int. J. Pharm. 370 (2009) 196–201.

[44] J.P. Anais, N. Razzouq, M. Carvalho, A. Fernandez, A. Astier, M. Paul, et al., Development of a-tocopherol acetate nanoparticles: influence of preparative processes, Drug Dev. Ind. Pharm. 35 (2009) 216–223.

[45] R. Katoh, Y. Asano, A. Furuya, K. Sotoyama, M. Tomita, S. Okongi, Conditions for preparation of w/o food emulsions using a membrane emulsification system, Nippon. Shokuhin. Kagaku. Kaishi 44 (1997) 44–49.

[46] Y. De Semet, L. Deriemaeker, R. Finsy, Ostwald ripening of alkane emulsions in the presence of surfactant micelles, Langmuir 15 (1999) 6745–6754.

[47] Y. De Smet, J. Malfait, C. De Vos, L. Deriemaeker, R. Finsy, Ostwald ripening of concentrated alkane emulsions: a comparison of fiber-optics dynamic light scattering and conventional dynamic light scattering, Prog. Colloid Polym. Sci. 105 (1997) 252–255.

[48] J.N. Cheong, C.P. Tan, Y.B.C. Man, M. Misran, α-tocopherol nanodispersions: preparation, characterization and stability evaluation, J. Food Eng. 89 (2008) 204–209.

[49] Y. Mine, M. Shimizu, T. Nakashima, Preparation and stabilization of simple and multiple emulsions using a microporous glass membrane, Colloid Surf. B 6 (1996) 261–268.

[50] F. Kuo, B. Subramanian, T. Kotyla, T. Wilson, S. Yoganathan, R.J. Nicolosi, Nanoemulsions of an anti-oxidant synergy formulation containing gamma tocopherol have enhanced bioavailability and anti-inflammatory properties, Int. J. Pharm. 363 (2008) 206–213.

[51] M. Saito, L.J. Yin, I. Kobayashi, M. Nakajima, Comparison of stability of bovine serum albumin-stabilized emulsions prepared by microchannel emulsification and homogenization, Food Hydrocolloids 20 (2006) 1020–1028.

[52] C. Washington, Stability of lipid emulsions for drug delivery, Adv. Drug Delivery Rev. 20 (1996) 131–145.

[53] G. Barratt, Colloidal drug carriers: achievements and perspectives, Cell. Mol. Life Sci. 60 (2003) 21–37.

[54] C.E. Mora-Huertas, H. Fessi, A. Elaissari, Polymer-based nanocapsules for drug delivery, Int. J. Pharm. 385 (2010) 113–142.

[55] A. Wiacek, E. Chibowski, Zeta potential, effective diameter and multimodal size distribution in oil/water emulsion, Colloid Surf. A 159 (1999) 253–261.

[56] B. Heurtault, P. Saulnier, B. Pech, J.E. Proust, J.P. Benoit, Physico-chemical stability of colloidal lipid particles, Biomateriels 24 (2003) 4283–4300.

Encapsulation de la vitamine E dans des micelles polymériques en utilisant des membranes microsieves

Encapsulation de la vitamine E dans des micelles polymériques en utilisant des membranes microsieves

Les micelles sont des structures, constituées par l'association de quelques dizaines de molécules, qui se forment dans les solutions aqueuses au-dessus d'une certaine concentration qu'on appelle la concentration micellaire critique « C.M.C. ». Les molécules qui composent les micelles doivent être amphiphiles c.-à-d. comportant dans leurs structures une ou des parties hydrophiles (ayant une forte affinité pour l'eau) et une ou des parties lipophiles (ayant une forte affinité pour les huiles, hydrocarbures et autres liquides non polaires). Les exemples de composés amphiphiles sont multiples. On peut citer les tensioactifs, les phospholipides, et certains copolymères en blocs. Les copolymères sont qualifiés de matériaux intelligents car leurs structures peuvent être modifiées afin d'obtenir une réponse suite à des diverses stimuli (changement de température, de force ionique, de pH, etc).

Dans notre étude réalisée principalement à l'Université de Loughborough puis complétée au Laboratoire d'Automatique et de Génie des Procédés, des copolymères sensibles au pH ont été synthétisés et appliquées à la formation de micelles polymériques. La méthode de préparation des micelles, basée sur l'utilisation des contacteurs à membrane, a été choisie afin de pallier aux inconvénients des méthodes existantes. En effet, les techniques de préparation décrites dans la littérature présentent un certain nombre d'inconvénients tel que l'obtention d'une distribution de taille poly-disperse, un taux d'encapsulation insuffisant, un manque de reproductibilité ou un passage difficile à une échelle de production plus large. Cette étude présente les différentes étapes de préparation et de caractérisation de copolymères sensible au pH. Puis, elle détaille l'influence des paramètres opératoires sur le procédé de formation de micelle en vue de son optimisation. Une fois le procédé optimisé, l'encapsulation de la vitamine E a été étudiée et une attention particulière a été accordée à la reproductibilité du procédé et au profil de libération de la vitamine E en fonction des conditions de pH. La préparation de micelles par la méthode de dispersion membranaire a été reportée pour la première fois au cours de ce travail. Cette méthode présente un très grand potentiel pour la production à large échelle et de manière contrôlée de micelles polymériques.

Ce chapitre sera présenté sous forme d'un article qui a été publié en 2013 dans «ACS Applied Materials and Interfaces» (un journal de l'ACS « American Chemical Society »).

pH-Sensitive Micelles for Targeted Drug Delivery Prepared Using a Novel Membrane Contactor Method

Abdallah Laouini[1, 2], Konstantinos P. Koutroumanis[2], Catherine Charcosset[1], Stella Georgiadou[2], Hatem Fessi[1], Richard G. Holdich[2], Goran T. Vladisavljević[2]

[1]: Université Claude Bernard Lyon 1, Laboratoire d'Automatique et de Génie des Procédés (LAGEP), UMR-CNRS 5007, CPE Lyon, Bât 308G, 43 Boulevard du 11 Novembre 1918, F-69622 Villeurbanne Cedex, France.

[2]: Department of Chemical Engineering, Loughborough University, Loughborough, LE11 3TU, United Kingdom

American Chemical Society (ACS) Applied Materials and Interfaces, 5 (18), 8939-8947, 2013

Impact factor: 5.008

Abstract

A novel membrane contactor method was used to produce size-controlled poly(ethylene glycol)-b-polycaprolactone (PEG-PCL) copolymer micelles composed of diblock copolymers with different average molecular weights, M_n (9200 or 10400 Da) and hydrophilic fractions, f (0.67 or 0.59). By injecting 570 $l/m^2/h$ of the organic phase (a 1 mg/ml solution of PEG-PCL in tetrahydrofuran) through a microengineered nickel membrane with a hexagonal pore array and 200 μm pore spacing into deionized water agitated at 700 rpm, the micelle size linearly increased from 92 nm for a 5-μm pore size to 165 nm for a 40-μm pore size. The micelle size was finely tuned by the agitation rate, transmembrane flux and aqueous to organic phase ratio. An encapsulation efficiency of 89 % and a drug loading of ~75 % (w/w) were achieved when a hydrophobic drug (vitamin E) was entrapped within the micelles, as determined by ultracentrifugation method. The drug-loaded micelles had a mean size of 146 ± 7 nm, a polydispersity index of 0.09 ± 0.01, and a zeta potential of -19.5 ± 0.2 mV. When drug-loaded micelles where stored for 50 h, a pH sensitive drug release was achieved and a maximum amount of vitamin E (23 %) was released at the pH of 1.9. When a pH-sensitive hydrazone bond was incorporated between PEG and PCL blocks, no significant change in micelle size was observed at the same micellization conditions.

Key words: Polymeric micelles - pH-sensitivity - Membrane contactor - Stirred cell - Vitamin E encapsulation - Hydrazone bond.

Contents

1. Introduction

In recent years, there has been growing interest in drug delivery using nano-carriers such as liposomes, core-shell nanocapsules, solid lipid nanoparticles, and micelles. Polymeric micelles are self-assembled aggregates of amphiphilic polymers consisting of a hydrophobic inner core and hydrophilic outer shell **[1]**. The core can be used to solubilize drugs with poor water solubility, while the hydrophilic shell can prolong circulation time in blood by inhibiting opsonins from adsorption on the micelle surface. Long circulation time in vivo is ensured by the micelle size of less than 200 nm **[2]**. Particles with such a small size remain undetected by reticuloendothelial systems (RES) **[3]**, which can be exploited to achieve prolonged therapeutic action **[4]**.

Micelles can be modified by incorporation of various functional groups and bonds to achieve targeted or triggered release. Of the many stimuli that can be exploited, changes in pH are particularly interesting because significant pH gradients can be found physiologically, for instance between normal tissues and some pathological sites, between the extracellular environment and some cellular compartments, and along the gastrointestinal tract. Some pathological states are associated with pH profiles different from that of normal tissues. Examples include ischemia, infection, inflammation and tumor acquisition, which are often associated with acidosis **[5]**. Compared to normal blood pH of 7.4, extracellular pH values in cancerous tissues can be as low as 5.7 due to rapid expansion of tumor cells, leading to production of lactic acid and hydrolysis of ATP in an energy-deficient manner **[6]**. To achieve pH sensitivity, the hydrophobic block of the copolymer can be modified to introduce acid-liable bonds which degrade at mildly acidic pH, causing the micelle to collapse, thus releasing the encapsulated drug. The examples of pH sensitive groups are acetal bonds **[7, 8]** and poly(ortho ester) side chains **[9]** that allow chemical conjugation of drugs to the side chain.

There is a plethora of methods available for the preparation of polymeric micelles. If a copolymer is soluble in water, micellization is usually performed by direct dissolution in water or film casting. If a copolymer is insoluble in water, the most common methods are dialysis, oil-in-water (O/W) emulsion and co-solvent evaporation or displacement. The direct dissolution consists of dissolving polymer and drug in water. The method is not widely applicable, since both blocks of the copolymer and the drug should be readily soluble in water. The method has been applied successfully for the encapsulation of hydrophobic drugs, but produced micelles are large and polydisperse **[10]**. In film casting, polymer and drug are dissolved in a volatile organic solvent, which after evaporation leaves a thin drug-impregnated film. Micelles are formed upon addition of warm water and stirring. The method is often used when other methods give poor drug loading efficiencies, as is the case with paclitaxel **[11]**. Micelles produced by film casting typically have large sizes and bimodal size distributions **[12]**.

In order to avoid detection by the RES and premature elimination, the micelle solution must be filtered, which results in drug losses and poor yields. In the dialysis method, drug and polymer are dissolved in a water-miscible organic solvent followed by dialysis to replace the organic solvent with water. The technique generally yields large micelles with low drug contents **[13]** and lacks reproducibility **[14]**. These problems can be partially addressed by adding water to the polymer/drug solution prior to the dialysis, which kinetically freezes the micelles **[15]**. Dialysis often requires days to complete and is difficult to scale up. In the O/W emulsion technique, polymer and drug are dissolved in a water-immiscible organic solvent and this mixture is then emulsified followed by evaporation of the organic solvent. The co-solvent evaporation method is similar, except that the organic solvent is miscible with water **[16]**. This method is often more suitable than the emulsion method, since it leads to the formation of smaller micelles with higher drug loading **[17]** and ICH (International Conference on Harmonization) class 2 solvents, such as chloroform and dichloromethane, can be avoided **[18]**. Therefore, most of the established techniques for micelle formation are not suitable for scaling-up from laboratory level to industrial production and suffer from low reproducibility and poor control over the micelle size **[19]**. Thus, there is a strong need for improvements in micelle preparation techniques.

The main objective of this work was to develop and investigate a novel membrane dispersion method for micelle preparation, suitable for large scale production. Membranes are increasingly used for fabrication of emulsions and particles **[20]** including nanoparticles such as solid lipid nanoparticles **[21]**, liposomes **[22]**, and nanoemulsions **[23]**. However, to the best of our knowledge, fabrication of micelles by dispersion through a microporous membrane has never been reported.

2. Experimental section

2.1 Reagents

Poly(ethylene glycol) methyl ether (Mn ~5000 Da) (PEG), ε-caprolactone monomer 99% (ε-CL), tin(II) 2-ethylhexanoate 95%, Sn(Oct)2, and sodium silicotungstate were supplied by Sigma-Aldrich. Toluene, extra dry grade, was purchased from Acros Organics. PEG was dried by azeotropic distillation with toluene prior to the polymerization reaction. ε-CL was dried prior use by distillation under reduced pressure onto 3A molecular sieves. O-[2-(6-Oxocaproylamino)ethyl]-O′-methylpolyethylene glycol (Mn = 5000 g/mol), PEG-CHO, and 2-hydroxyethylhydrazine 98%, 2-HEH, were purchased from Sigma-Aldrich Co Ltd, Gillingham, Dorset, UK. Tetrahydrofuran (THF) and acetone of analytical grade were purchased from Fischer Scientific and used without further purification. Ultra-pure water was obtained from a Millipore Synergy® system (Ultrapure Water System, Millipore).

2.2 Equipments

The micelles suspension was prepared using a stirred cell with a flat disc membrane fitted under the paddle blade stirrer, as shown in **Figure 1 (a)**.

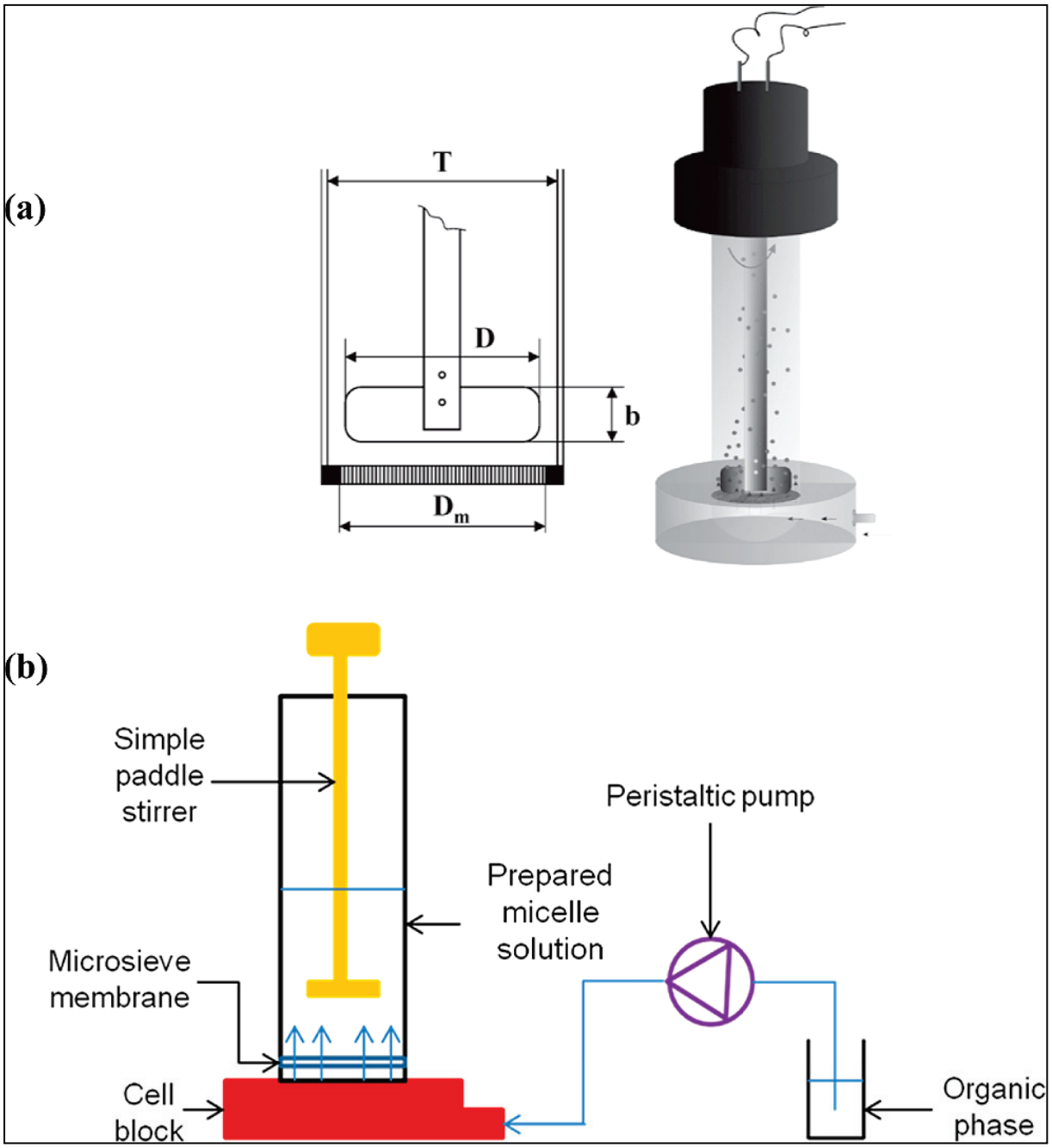

Figure 1. (a) Schematic illustration of the stirred cell with simple paddle stirrer above a flat disc membrane (b = 12 mm, D = 32 mm, D_m = 33 mm, and T = 40 mm). **(b)** Schematic diagram of the experimental set-up.

Both stirred cell and membranes were supplied by Micropore Technologies Ltd. (Hatton, Derbyshire, UK). The agitator was driven by a 24 V DC motor (INSTEK model PR 3060) and the paddle rotation speed was controlled by the applied voltage.

The membranes used were nickel membranes with regular hexagonal pore array containing uniform cylindrical pores with a diameter of 5, 10, 20 or 40 μm, arranged at uniform spacing of 80 or 200 μm (**Figure S1** in the supplementary material). The membranes were fabricated by the UV-LIGA (ultraviolet lithography, electroplating, and molding) process, which involves galvanic deposition of nickel onto the template formed by photolithography **[24]**.

The porosity of a membrane with the hexagonal pore array is given by:

$$\varepsilon = \frac{\pi}{2\sqrt{3}}\left(\frac{d_p}{S}\right)^2 \quad (1)$$

where d_p is the pore diameter and S is the interpore distance. The porosities of the membranes calculated from Eq. (1) are given in the supplementary material (**Table S1**).

2.3 Preparation procedures

2.3.1 PEG-PCL synthesis

1 g of PEG and 40% (v/v) ε-CL solution in toluene were dissolved in 20 ml of refluxing toluene under nitrogen atmosphere. The mole ratio of PEG to ε-CL in the reaction mixture varied from 1:22 to 1:88. The polymerization was initiated by the addition of a 20% (v/v) solution of $Sn(Oct)_2$ in toluene (0.75 w/w) and carried out at 110 °C under nitrogen atmosphere and constant stirring for 18 h. The PEG-PCL copolymer was isolated by precipitation in diethyl ether and dried under vacuum.

2.3.2 PEG-Hyd-PCL synthesis

1 g of PEG-CHO was dissolved in 12 ml of ethanol at 35 ^oC under nitrogen atmosphere and 2-HEH 10% (v/v) solution in ethanol was added in excess ($CHO/NHNH_2$ = 1:5). After 48 h, PEG-Hyd-OH was isolated from diethyl ether, washed with cold (-18 ^oC) ethanol and dried under vacuum at 40 ^oC for 24 h. Polymerization of ε-CL from PEG-Hyd-OH was carried out under the same conditions used in synthesis of PEG-PCL copolymers.

2.3.3 Micellization and drug loading

A schematic diagram of the experimental set-up is shown in **Figure 1 (b)**. The cell was filled with 15-35 ml of ultrapure water and the stirring speed was adjusted between 400 and 1000 rpm. A 1 mg/ml of the copolymer (PEG-PCL-3 or PEG-PCL-4) was prepared by dissolving the copolymer in THF or acetone. The organic phase was injected through the membrane using a peristaltic pump (Watson Marlow 101U, Cornwall, UK) at a constant flow rate of 2-8 ml/min corresponding to the dispersed

phase flux of 142-568 l/m^2/h. The experiment was run until a predetermined organic to aqueous phase ratio was achieved. Spontaneous formation of micelles started as soon as the organic phase was brought in contact with the aqueous phase, but the micelle suspension was kept under stirring for 15 min. The suspension was then collected and the organic solvent was removed by stirring under vacuum for 24 h. After each experiment, the membrane was sonicated in THF for 1 h, followed by soaking in a siloxane-based wetting agent for 30 min. Drug-loaded micelles were prepared as described above with the only difference being that 2.5 mg/ml vitamin E was dissolved in the organic phase containing the polymer.

2.4 Polymers characterization

2.4.1 Gel Permeation Chromatography (GPC)

GPC analysis was performed on an Agilent 1100 HPLC System equipped with a refractive index detector (G1362A) and an Agilent PLgel MIXED-C column, 5 μm, 300 × 7.5 mm, in series with an Agilent PLgel guard column, 5 μm, 50 × 7.5 mm. The flow rate of the mobile phase (THF) was 1 ml/min and the column temperature was 30 °C. The calibration was performed using polystyrene standards with a narrow molecular weight distribution (EasiVials PS-M).

2.4.2 Fourier Transform-Infrared Spectroscopy (FTIR)

FTIR spectra were obtained using a Shimadzu FTIR-8400S spectrometer. A small amount of each material was mixed with KBr and compressed to tablets. The IR spectra of these tablets were obtained in absorbance mode and in the spectral region of 600 to 4000 cm^{-1} using a resolution of 4 cm^{-1} and 64 co-added scans.

2.4.3 Nuclear Magnetic Resonance Spectroscopy (NMR)

Polymers were solubilised in deuterated chloroform ($CDCl_3$) and ^{1}H-NMR spectra were obtained on a Bruker Ultrashield Av-400 spectrometer, operating at 400.13 MHz, employing a 5 mm high-resolution broad-band ATMA gradients probe. Spectra were recorded using the zg30 pulse program with P_{90} = 14.5 μs covering a sweep width of 20.7 ppm (8278 Hz) with 64 k time domain data points giving an acquisition time of 3.95 s, Fourier transformed using 128 k data points and referenced to an internal TMS standard at 0.0 ppm.

2.5 Micelle characterization

2.5.1 Size analysis

Particle size distribution was determined by dynamic light scattering (DLS), otherwise known as photon correlation spectroscopy (PCS) **[25, 26]**, using a Malvern Zetasizer Nano-series (Malvern Instruments Zen 3600, Malvern, UK). Each sample was diluted

10-fold with ultra-pure water before measurement and analyzed in triplicate at 25 °C. The particle size distribution data were generated using the DTS nano software (version 5.2). The micelle size polydispersity was expressed by the polydispersity index, PDI.

2.5.2 Zeta potential

The zeta potential was determined using a Malvern Zetasizer Nano-series (Malvern Instruments Zen 3,600, Malvern UK) and measurements were performed at least three times after dilution in water. The zeta potential was calculated from the electrophoretic mobility applying the Helmholtz-Smoluchowski equation **[27]**.

2.5.3 Encapsulation efficiency

The encapsulation efficiency of vitamin E in micelles was determined using the ultracentrifugation technique. The total amount of vitamin E (TA) was determined after disrupting drug-loaded micelles in ethanol using an ultrasound bath for 10 min. The amount of vitamin E encapsulated in micelles (EA) was determined by centrifuging solutions of vitamin E-loaded micelles using an OptimaTM Ultracentrifuge (Beckman Coulter, USA) at 50,000 rpm for 50 min at +4 °C to separate micelles from non-encapsulated drug. The resulting micelle sediment was dissolved in ethanol and assayed for encapsulated vitamin E content (EA). The vitamin E encapsulation efficiency (E.E.) was calculated as follows:

$$E.E. = EA / TA \times 100 \quad (2)$$

E.E. was determined in triplicate. The concentration of vitamin E was measured using an HPLC system (Agilent System series 1100, Agilent Technologies, California, USA) consisted of a pump, an auto-sampler and a UV/VIS detector. The column used was a LiChrospher RP C18 column (5 μm, 15 cm × 0.46 cm) (Supelco, Bellefonte, USA). The separation was carried out using a mixture of methanol and water (96:4 v/v) as the mobile phase at a flow rate of 1.6 ml/min. The eluent was monitored at 292 nm and peaks were recorded using the chromatography data system software provided by Agilent. The column was equilibrated for 30 min with a minimum of 30 column volumes. The column was washed after use using water - acetonitrile mixture (50:50 v/v) for 60 min. This HPLC analytical method was validated (data not shown).

2.5.4 Transmission Electron Microscopy (TEM)

TEM observation was carried out according to a previously reported protocol **[28]**. Briefly, an aliquot of the micelle solution was diluted 10-fold using ultrapure water and a drop of the diluted sample was placed onto a carbon-coated copper grid. The sample was allowed to stand for 3 min, after which the excess fluid was absorbed by a

filter paper leaving a thin liquid film over the holes. One drop of a 1% (w/w) sodium silicotungstate solution was then applied and allowed to dry for 2 min. Finally, the stained samples were observed and images were taken using a CM 120 microscope (Philips, Eindhoven, Netherlands) operating at an accelerating voltage of 80 kV.

2.6 Process reproducibility

The experiments conducted under the optimum conditions were repeated three times in order to estimate reproducibility of the fabrication process.

2.7 pH-responsive drug release

A drug-loaded micelle solution was divided into 4 aliquots and the pH of each aliquot was adjusted to 1.9, 4.5, 6.3 and 9.8. pH 1.9 was adjusted by potassium phosphate buffer consisting of potassium dihydrogen phosphate and phosphoric acid solution. pH 4.5 or 6.3 was adjusted by a buffer solution of potassium dihydrogen phosphate and sodium hydrogen phosphate. At pH 9.8, the drug release medium was a buffer solution of boric acid and potassium borate. At chosen time intervals, samples were taken and encapsulation efficiency was determined using the method previously described.

3. Results and discussion

3.1 Polymers characterization

3.1.1 Gel Permeation Chromatography (GPC)

The molecular weight of the synthesized polymers, as calculated by GPC, is shown in **Table 1**. The hydrophilic fraction, f, is the mass fraction of the hydrophilic block to the total polymer mass and it dictates the structure of the micelles. For diblock amphiphilic copolymers, *Discher* and *Eisenberg* **[29]** suggest that micelles are formed if $f > 0.5$; a condition that is satisfied for all four synthesized polymers.

Table 1. Number average molecular weight, M_n, polydispersity index, M_w/M_n, and hydrophilic fraction, *f*, of the synthesized copolymers, as determined by GPC.

Polymer	PEG/ε-CL mole ratio in the feed mixture	M_n (Da)	M_w/M_n	*f*
PEG-PCL-1	1:22	7400	1.10	0.82
PEG-PCL-2	1:44	8200	1.14	0.74
PEG-PCL-3	1:66	9200	1.17	0.67
PEG-PCL-4	1:88	10400	1.25	0.59

3.1.2 Fourier Transform-Infrared Spectroscopy (FTIR)

FT-IR spectra are presented in **Figure 2**. All materials show characteristic absorbancies for PEG, the C-O-C etheric bond bending vibration at 1109 cm^{-1} and the absorbancies at 842 and 1333 cm^{-1}, attributed to PEG crystalline regions. On the PEG-PCL spectra, new absorbances emerge; one at 1724 cm^{-1} is attributed to stretching of the esteric carbonyl, while the two at 2935 and 729 cm^{-1} are due to C-H bond stretching in the PCL block. All absorbancies attributed to the PCL block increase in intensity from PEG-PCL-1 to PEG-PCL-4, as the molecular weight of the hydrophobic block increases respectively.

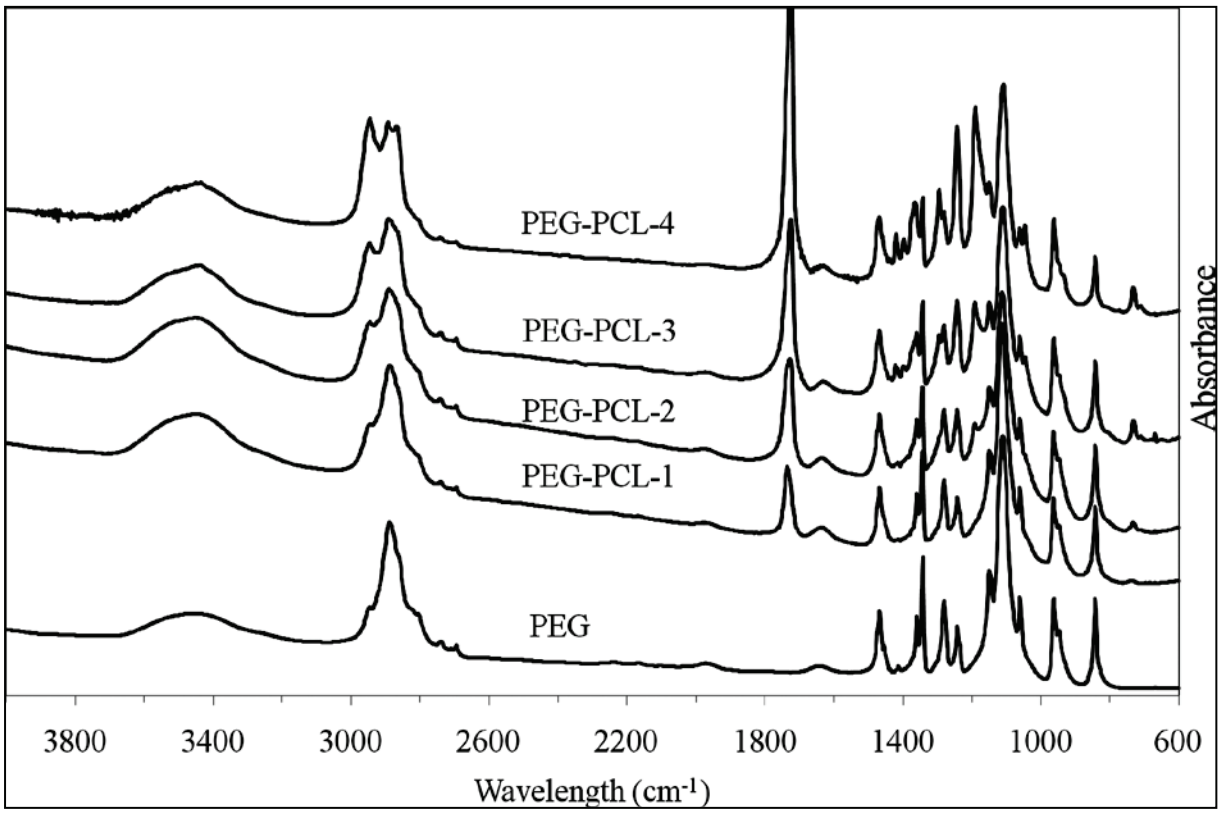

Figure 2. FT-IR spectra for PEG and the synthesized copolymers.

3.1.3 Nuclear Magnetic Resonance Spectroscopy (NMR)

Chemical structure, proton numbering and 1H-NMR spectra for polymers is shown in **Figure 3**.

The degree of polymerization, DP, of PCL was calculated using the equation:

$$DP_{PCL} = (A_{4.0}/2)/(A_{3.3}/3) = (A_{2.3}/2)/(A_{3.3}/3) \quad (3)$$

Absorbancies at 4.0 and 2.3 δ are due to protons in the PCL block, while the absorbance at 3.3 δ is due to the three protons in the methoxy terminal-group of PEG.

This allowed the calculation of the molecular weight for each polymer using NMR spectroscopy.

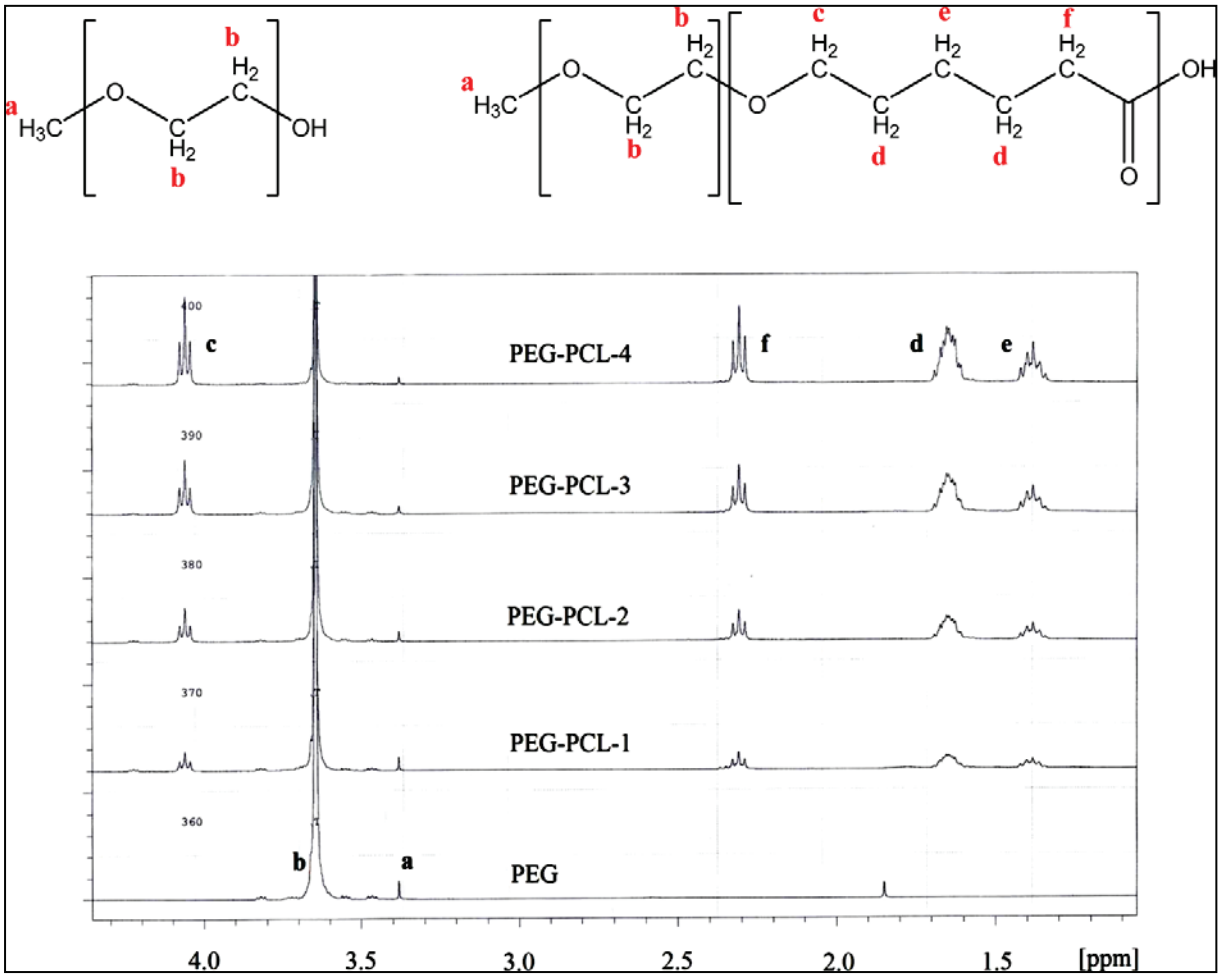

Figure 3. Proton numbering and ^{1}H-NMR spectra for PEG and synthesized di-block PEG-PCL copolymers.

The M_n results presented in **Table 2** are in relatively good agreement with those obtained using GPC.

Table 2. Degree of polymerization, DP, and number average molecular weight, M_n, of the synthesized copolymers, as determined by ^{1}H-NMR.

Polymer	DP	M_n (Da)
PEG-PCL-1	10	7300
PEG-PCL-2	13	7600
PEG-PCL-3	31	9600
PEG-PCL-4	54	12300

3.2 Parameters affecting the micellization process

3.2.1 Membrane used

In order to investigate the role of membrane during micellization process, two micelle suspensions were prepared under the same operating conditions (agitation speed = 700 rpm and organic phase flow rate = 4 ml/min) and using the same formulation (polymer PEG-PCL-4 concentration = 1 mg/ml, organic solvent = THF, and aqueous to organic phase volume ratio = 5). In one experiment, the organic phase was injected directly in the aqueous phase, whereas in another experiment the organic phase was passed through the membrane with a pore size of 20 μm and pore spacing 80 μm. As shown in **Figure 4**, the mean particle size of micelle suspension was 552 nm for direct injection and 132 nm for injection through the membrane. In direct injection micromixing occurs after macromixing (breaking macrovolumes of the organic phase into microvolumes by agitation), whereas in membrane injection micromixing is a sole means of mixing. Therefore, membrane injection is associated with better uniformity of polymer and organic solvent distribution through the aqueous phase resulting in a more uniform distribution of micelle sizes and significantly smaller particle size.

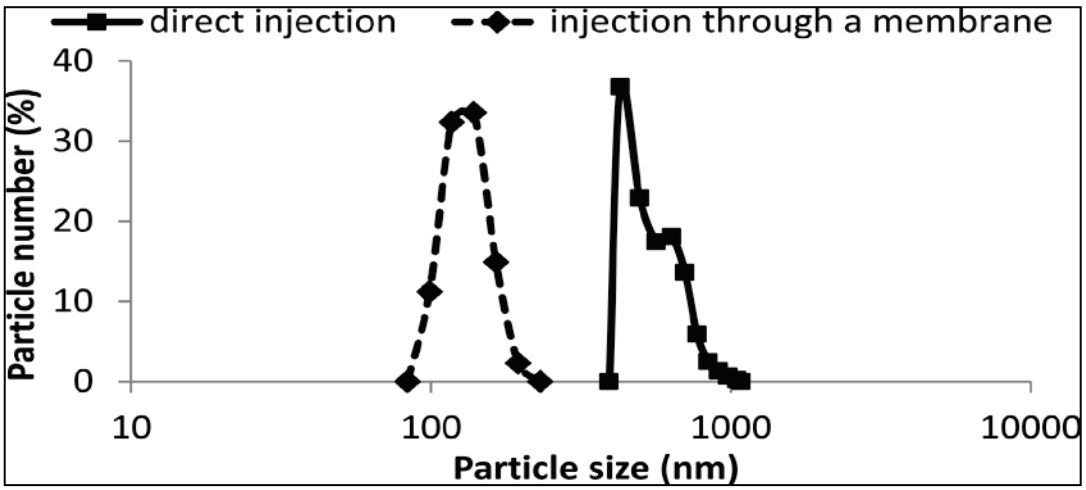

Figure 4. Size distribution of micelles prepared by direct or membrane injection of the organic phase. Experimental conditions: organic phase flow rate = 4 ml/min, membrane pore size = 20 μm, pore spacing = 80 μm, polymer PEG-PCL-4 concentration = 1 mg/ml, organic solvent = THF, agitation speed = 700 rpm, aqueous to organic phase volume ratio = 5.

3.2.2 Aqueous to organic phase volume ratio

The particle size distribution of micelles was compared by injecting 5 ml of the organic phase through the membrane into respectively 15, 25 and 35 ml of water (corresponding to an AOR of 3, 5 and 7). As shown in **Table 3** and **Figure 5(a)**, when the AOR increased from 3 to 7, the mean micelle size decreased from 127 to 90 nm and the PDI increased from 0.24 to 0.29. A similar behavior was observed during

fabrication of liposomes in a hollow fiber module, with the particle size reduction from 189 to 114 nm as a result of increase in AOR from 0.4 to 2 **[30]**. By increasing AOR, the polymer is more rapidly dispersed in the aqueous phase due to a higher concentration gradient during mixing and the critical micellar concentration (CMC) is reached faster, which means that less time is allowed for the polymer molecules to redistribute into larger micelles. In addition, at the higher AOR value, micelles are more diluted after mixing with the aqueous phase, which may reduce their tendency to aggregation. Based on the obtained results and taking into consideration the final micelle concentration and their size and uniformity, the AOR was fixed at 5 in the following experiments.

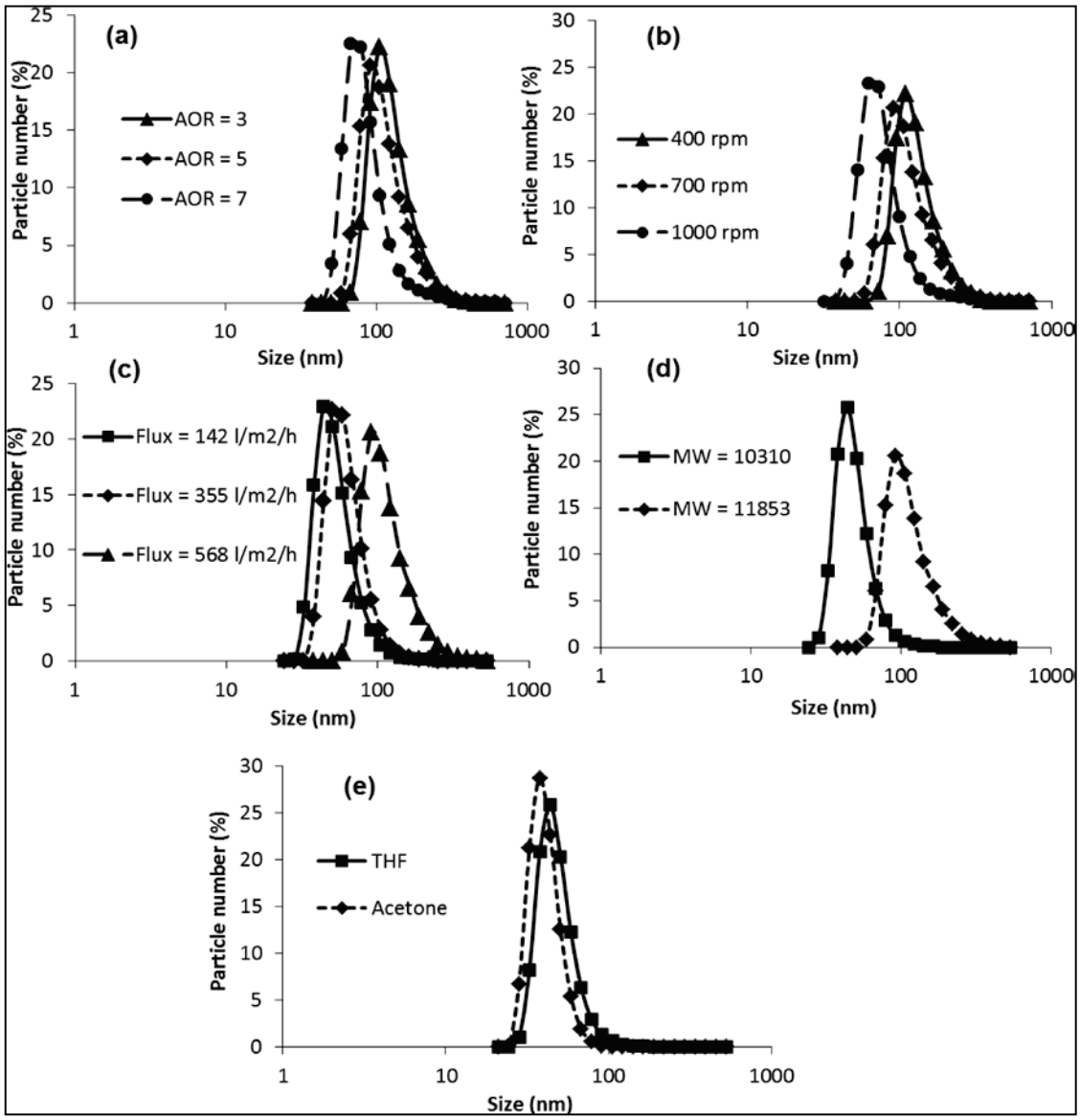

Figure 5. The effect of different process parameters on the micelle size distribution: **(a)** Aqueous to organic phase volume ratio, AOR, **(b)** Agitation speed, **(c)** Transmembrane flux, **(d)** Polymer molecular weight, and **(e)** Type of the organic solvent. Other conditions are specified in **Table 3**.

Table 3. Influence of formulation factors and process parameters on micelle size characteristics. The membrane pore size was 20 μm and the interpore distance was 200 μm.

AOR	Agitation speed (rpm)	Flux ($l/m^2/h$)	Polymer used (PEG-PCL)	Organic solvent	Mean size (nm)	PDI	Zeta potential (mV)
3	700	568	4	THF	127	0.24	-20.1
5	**700**	**568**	**4**	THF	117	0.28	-27.6
7	700	568	4	THF	90	0.29	-24.2
5	**400**	568	4	THF	131	0.24	-24.8
5	**1000**	568	4	THF	82	0.41	-24.0
5	700	**142**	4	THF	54	0.23	-26.1
5	700	**355**	4	THF	62	0.26	-24.2
5	700	568	**3**	**THF**	49	0.36	-26.8
5	700	568	3	**Acetone**	41	0.47	-25.0

3.2.3 Agitation speed

The influence of agitation speed over a range of 400-1000 rpm on the micelle size is shown in **Table 3** and **Figure 5(b)**. The micelle size decreased from 131 to 82 nm when the agitation speed increased from 400 to 1000 rpm and the most uniform micelles (PDI = 0.24) were obtained at the stirring rate of 400 rpm. The shear stress at the membrane/continuous phase interface increases with increasing the stirring rate. It was previously found that the particle size in membrane-based particle fabrication processes was smaller at the higher wall shear stress **[24, 31]**, which was associated with higher mixing efficiency **[32, 33]**. Thus, high homogenous supersaturation may occur in a short time, leading to rapid self-arrangement of polymers and formation of small micelles. Our results suggest that for a given set of conditions, an agitator speed of 700 rpm was the optimal speed, since the produced micelles were both relatively uniform and of suitable size.

3.2.4 Transmembrane flux

As shown in **Table 3** and **Figure 5(c)**, by increasing the dispersed phase flux from 142 to 568 $l/m^2/h$, the mean micelle size increased from 54 to 117 nm and PDI increased from 0.23 to 0.28. The higher dispersed phase flux resulted in the higher amount of the polymer injected through the membrane per unit time **[34]**, which has an effect to prolong mixing time and reduce the mixing efficiency. The maximum micelle size in **Table 3** corresponds to the maximum polymer concentration at the

membrane/continuous phase interface. Thus, the largest micelles were formed at the maximum transmembrane flux and the minimum agitation speed.

3.2.5 Copolymer molecular weight

The results in **Table 3** and Figure **5(d)** show that larger micelles were prepared using a copolymer with the higher MW. Both polymers are suitable for preparation of micelles with a convenient mean size (between 49 and 117 nm) and acceptable size distribution (PDI between 0.26 and 0.36) for drug release applications.

3.2.6 Organic solvent

Numerous organic solvents have been used for micelle preparation, such as methanol **[35]**, THF **[36]**, dimethylsulfoxide **[37]**, N,N-dimethylformamide, and acetone **[38]**. Although removed by evaporation, solvents may remain as traces in the final formulation, representing a possible risk for human health. In this work, THF and acetone were selected as organic solvents due to their low toxicity and good vitamin E and PEG-PCL solubility. **Table 3** and **Figure 5(e)** show that the particle size distribution is virtually unaffected by the organic solvent used.

3.2.7 Membrane structure

Micelle suspensions were prepared using 6 different membranes with pore diameters of 5, 10, 20 and 40 μm and pore spacing of 80 or 200 μm. At the constant pore spacing of 200 μm, a strong linear correlation between the mean micelle size and the membrane pore size was found, with a gradient of 2 nm /μm and $R^2 > 0.99$, as shown in **Figure 6**. A similar linear relation between the particle size and pore size of microengineered membrane was obtained in fabrication of liposomes **[39]** and membrane emulsification **[40, 41]**. The results clearly show that the micelle size can be controlled by the membrane pore size. The size uniformity increased with decreasing the pore size **(Figure 6b)**. As shown in **Table 4**, the micelle size decreased by 4-10 % as a result of increase in the pore spacing from 80 to 200 μm. There are two consequences of increasing pore spacing at constant transmembrane flux: (i) organic phase stream is fragmented into smaller number of sub-streams, and (ii) the flow velocity of each sub-stream is higher. The micromixing is more efficient when at the higher velocity of organic phase, probably because the organic phase micro-jets can penetrate deeper into the aqueous phase before being disintegrating due to mixing with a surrounding aqueous phase.

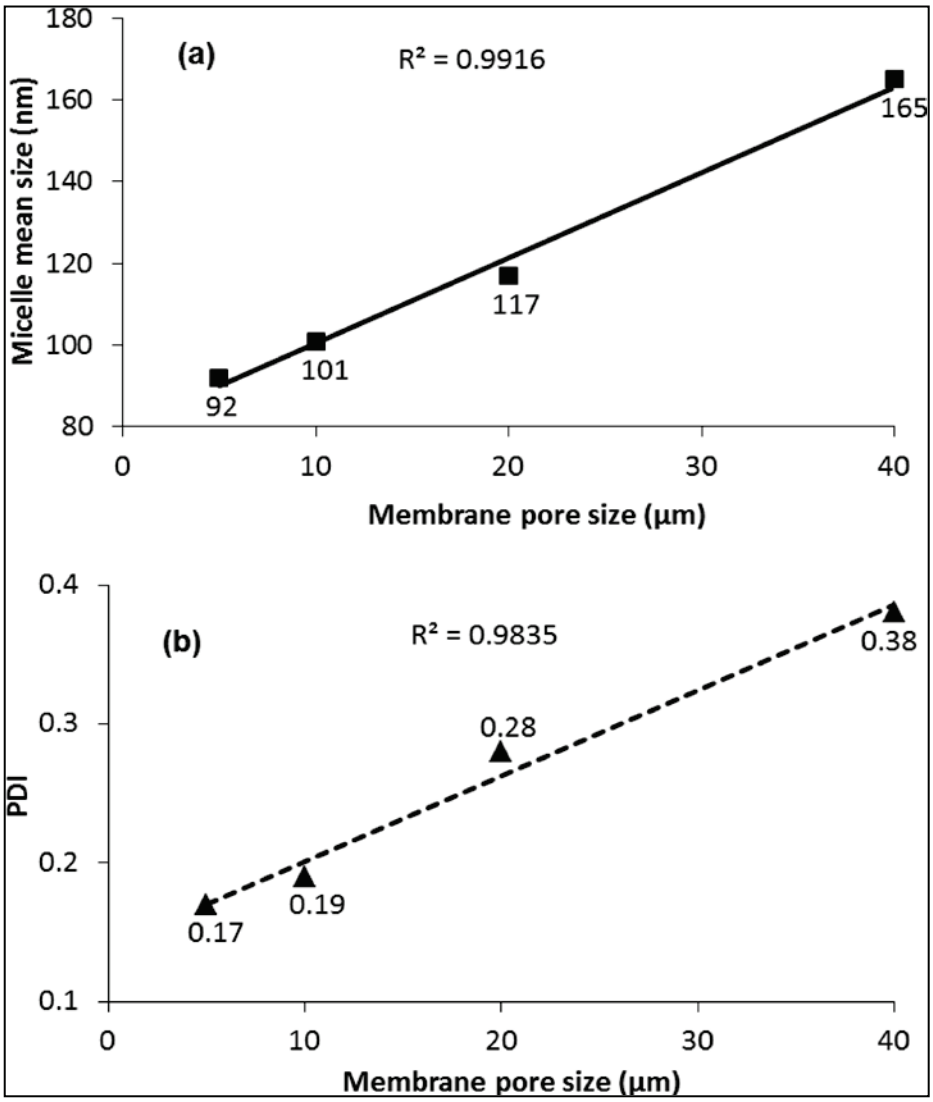

Figure 6. Effect of the membrane pore size on the micelle size characteristics: **(a)** mean micelle size, and **(b)** PDI of the micelles. The membrane pore spacing is 200 µm and other conditions are specified in **Table 4**.

Table 4. Influence of membrane on the micelle size characteristics. The experimental conditions: aqueous to organic phase volume ratio AOR = 5, organic solvent = THF, polymer PEG-PCL-4 concentration: 1 mg/ml, agitation speed = 700 rpm, transmembrane flux = 568 l/m^2/h.

Membrane characteristics		Micelles size characteristics	
Spacing (µm)	Pore size (µm)	Mean size (nm)	PDI
200	5	92	0.17
	10	101	0.19
	20	117	0.28
	40	165	0.38
80	10	105	0.21
	20	130	0.23

3.3 Vitamin E loading

Vitamin E was chosen as a hydrophobic drug for the preparation of drug-loaded micelles. This active agent was widely used as an antioxidant in many medical and cosmetic preparations and was encapsulated in the micelles by hydrophobic forces, due to its affinity to the hydrophobic block of the copolymers, without chemical conjugation. The effect of drug entrapment on the vesicle size and zeta potential is presented in **Table 5** and **Figure 7**.

Table 5. The effect of vitamin E loading on the micellization process. Organic solvent: THF, polymer PEG-PCL-4 concentration = 1 mg/ml, vitamin E concentration in the organic phase = 2.5 mg/ml, agitation speed = 700 rpm, AOR = 5, transmembrane flux = 568 l/m^2/h.

	Size (nm)	PDI	Zeta potential (mV)	Encapsulation efficiency (%)
Drug-free micelles	92	0.17	-27.0	
Drug-loaded micelles	154	0.09	-19.3	87.4

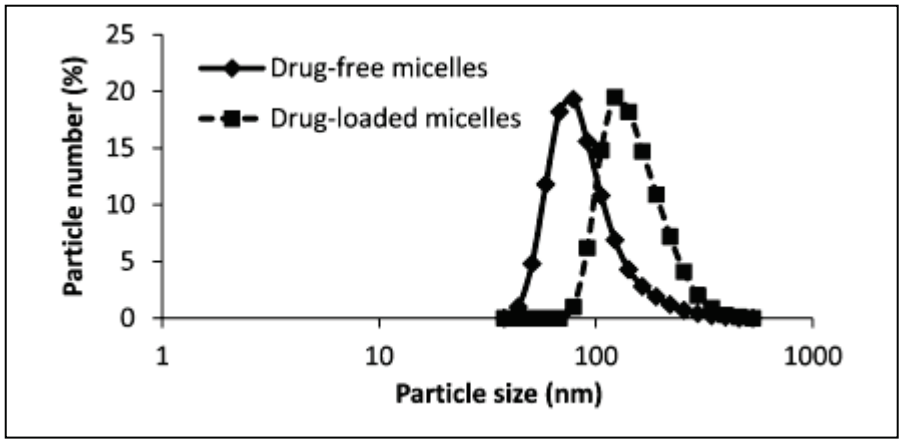

Figure 7. The effect of loading vitamin E into micelles on their size distribution. The experimental conditions are specified in **Table 5**.

The mean micelle size increased from d_0 = 92 to d_1 = 154 nm when vitamin E was encapsulated under otherwise constant experimental conditions. Thermodynamically stable drug-loaded micelles can be referred to as “microemulsion droplets” or “swollen micelles” and these two terms can be used interchangeably **[42]**. Although there is no single particle size that can be used as a definitive cut-off point to distinguish a swollen micelle from a conventional emulsion, most authors assume that the mean particle diameter in a stable O/W microemulsion should be less than 200 nm **[43]**.

Assuming that the micelles are spherical and volumes of vitamin E and copolymer are additive, the drug loading percentage is as follows:

$$Loading(\%) = \frac{\text{Mass of drug in a micelle}}{\text{Mass of } \textit{drug-loaded} \text{ micelle}} \times 100 = \frac{(d_1^3 - d_0^3)\rho_E}{(d_1^3 - d_0^3)\rho_E + d_0^3 \rho_{PEG-PCL}} \times 100 \qquad (3)$$

where ρ_E = 0.95 g ml^{-1} is the density of vitamin E and $\rho_{PEG\text{-}PCL}$ = 1.135 g ml^{-1} is the density of PEG-PCL diblock copolymer, based on melt densities of PEG and PCL homopolymers of 1.13 and 1.4 g ml^{-1}, respectively. The drug loading calculated using Eq. (3) is 75%, which means that vitamin E constitutes 75% of the total mass of a drug-loaded micelle and the copolymer 25%. The drug loading can be also estimated from the mass balance of vitamin E. It is reasonable to suggest that neither vitamin E nor copolymer was adsorbed onto the membrane surface due to low internal pore volume of the membrane. The volume of organic phase injected through the membrane was 5 ml, the concentration of vitamin E in the organic phase was 2.5 mg/ml and the efficiency of vitamin E encapsulation was 87.4 % (**Table 5**), which means that the total amount of vitamin E entrapped within the micelles was 10.9 mg. The critical micelle concentration (CMC) of PEG-PCL diblock copolymer with a molecular weight of 12600 Da, as determined by GPC, was found to be 0.018 mg/ml **[44]**. The total amount of non-aggregated PEG-PCL-4 molecules in the final preparation was 0.45 mg, based on the volume of aqueous phase in the final preparation of 25 ml and the above value of CMC. The concentration of PEG-PCL-4 in the organic phase was 1.0 mg/ml and thus, the total amount of PEG-PCL-4 incorporated in the micelles was 4.55 mg. The drug loading estimated from the process mass balance is now: 10.9/(4.55+10.9)×100=71%, which is close to 75%, calculated from Eq. 3. A small difference can be attributed to the fact that Eq. (3) does not take into account the effect of molecular interactions on the volumes of vitamin E and copolymers in the micelles.

The zeta-potential of vitamin E-loaded micelles and drug-free micelles was -19.3 and -27.0 mV, respectively (**Table 5**), which can be attributed to the presence of terminal carboxyl groups on PCL chains. Zeta potential measurements can give information about the type of association between the active substance and the carrier **[45]**, for example whether the drug is encapsulated in the core material or adsorbed onto the shell **[46]**. Here, the negative surface charge was partially shielded in the presence of the drug suggesting that at a small part of the drug might have been adsorbed onto the surface, while the rest was incorporated within the micelle cores. The zeta potential data suggest that the micelles should exhibit a good colloidal stability, since a negative zeta potential near or lower than -20 mV was found to prevent vesicle coalescence **[47]**. A high encapsulation efficiency of 87.4% was probably due to the high hydrophobicity of the vitamin E as many studies reported that the encapsulation

efficiency was proportional to the drug solubility in the organic phase **[48]**. Drug-loaded micelles were more uniform in size than unloaded micelles as evidenced by the lower PDI value in **Table 5**. It was found that core-entrapping drug, in this case α-tocopherol, may act as a filler molecule and enhance the stability of the micelle **[49]**.

3.4 Process reproducibility

The reproducibility of the preparation technique was investigated by repeating 3 times a typical micellization experiment with and without drug loading. The results in **Figure 8** and **Table S2** (supplementary material) suggest a very good reproducibility in terms of size characteristics, zeta potential and encapsulation efficiency between the samples produced under the same conditions.

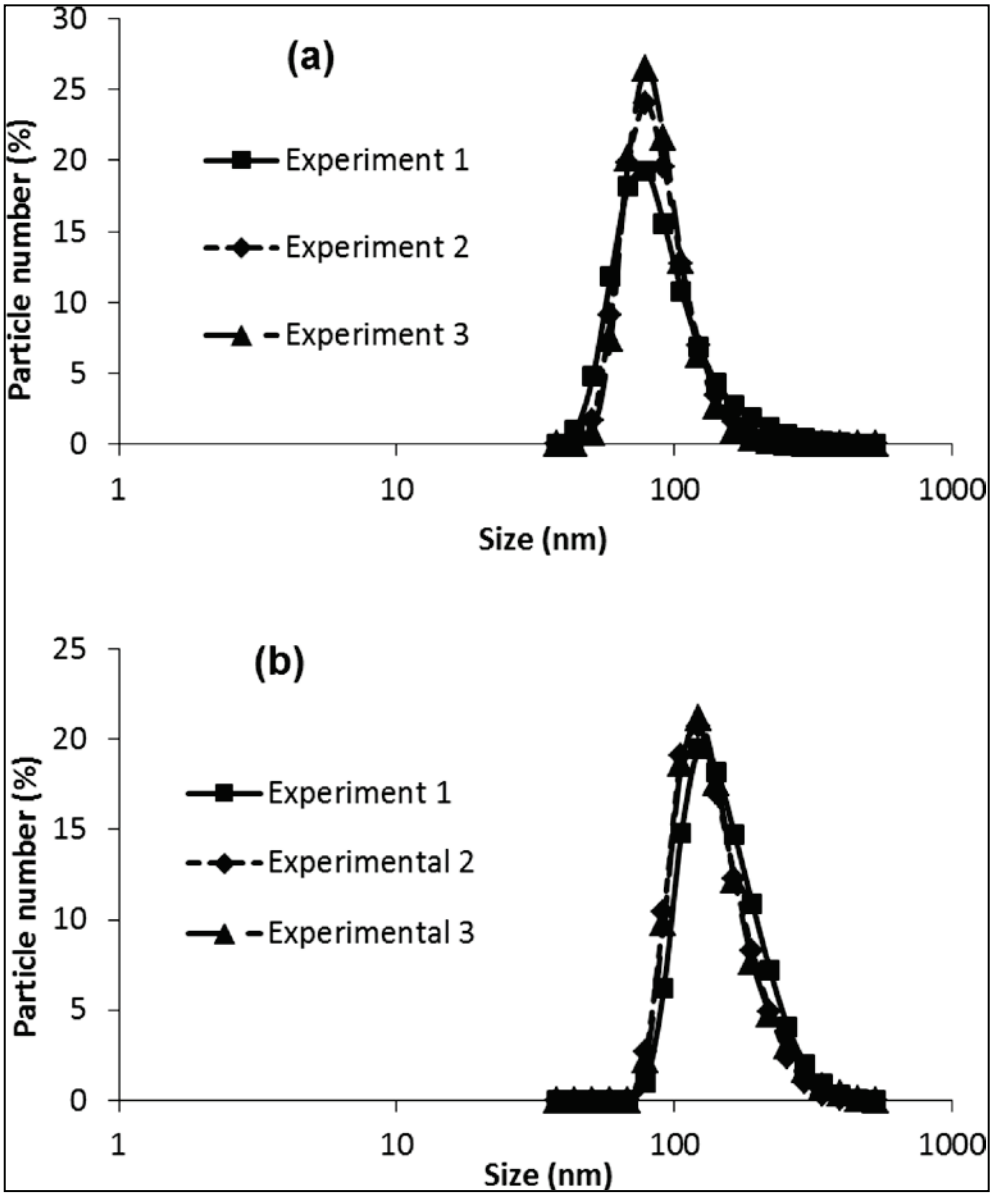

Figure 8. Reproducibility of the micelle preparations: **(a)** Drug-free micelles and **(b)** Drug-loaded micelles. Experimental conditions are specified in **Table 5**.

3.5 TEM observation

Figure 9 revealed nanometric, quasi-spherical shape of vitamin E-loaded micelles. According to this morphological investigation, micelles ranged in size from 100 to 200 nm, which is in good correlation with the dynamic light scattering measurements.

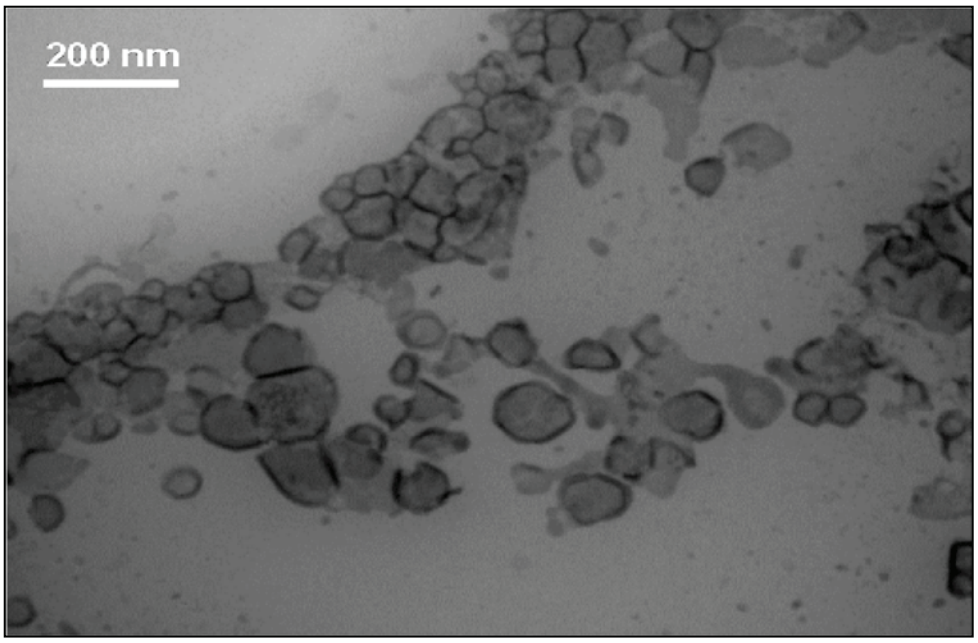

Figure 9. TEM micrograph of vitamin E-loaded micelles.

3.6 pH-responsive drug release

The release of vitamin E from micelle preparations stored under different pH conditions was monitored as a function of time. The results in **Figure 10** show that the micelles kept under acidic pH were unstable due to hydrolysis of the ester bonds in the PCL block and formation of 6-hydroxycaproic acid.

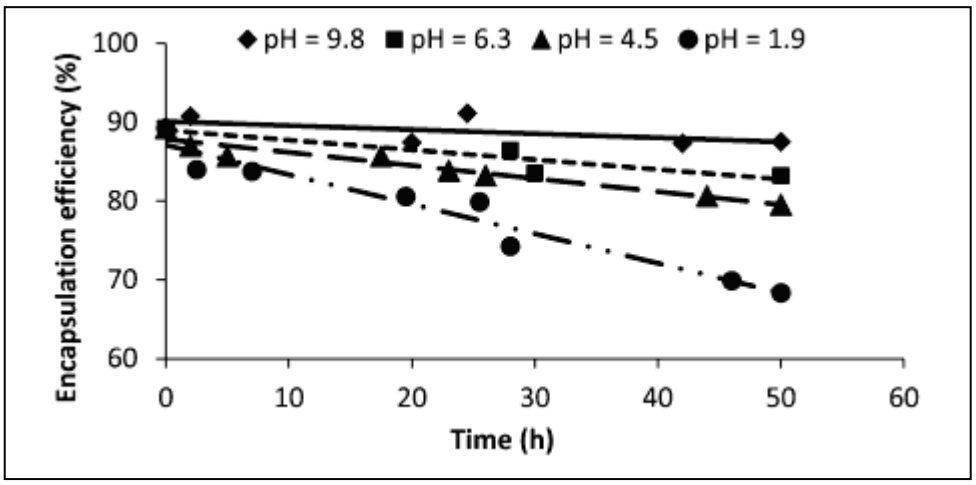

Figure 10. Time evolution of the encapsulation efficiency of vitamin E-loaded micelles stored under different pH conditions.

Since vitamin E is predominantly encapsulated within a hydrophobic core, hydrolytic degradation of hydrophobic PCL segments led to the release of vitamin E. A decrease in the drug encapsulation efficiency was proportional to the medium acidity, because PCL hydrolysis was catalyzed by hydrogen ions. Indeed, within 50 hours, the encapsulation efficiency decreased from an initial value of 89.2% to 83.2, 79.5 and 68.3% at the pH of 6.3, 4.5 and 1.9, respectively. When the micelles were stored at the pH of 9.8, no release of vitamin E occurred and the encapsulation efficiency remained nearly unchanged.

3.7 Preparation of PEG-Hyd-PCL micelles

The maximum percent of vitamin E released from PEG-PCL micelles after 50 h was 23 % at pH = 1.9. In order to increase the release rate and pH sensitivity at mildly acidic pH, we have synthesized highly pH sensitive PEG-Hyd-PCL micelles by incorporating a pH-sensitive hydrazone bond between the PEG and PCL blocks. When the micelles are exposed to mildly acidic pH, the bond hydrolyzes and the micelle collapses releasing the drug. We have prepared PEG-PCL and PEG-Hyd-PCL micelles under the same conditions by transferring 5 ml of the organic phase containing 5 mg/ml of each polymer dissolved in THF to 25 ml of deionized water at the flow rate of 0.5 ml/min and pH = 7.4 to obtain the final micelle concentration of 1 mg/ml and AOR = 5. The micelle suspension was gently stirred for 6 hours and any residual THF was removed with vacuum distillation. As can be seen in **Figure 11**, both micelle types were found to show identical micellization behaviour forming micelles of identical particle size distribution. It shows that the micellization behavior is determined only by the type of the hydrophobic and hydrophilic block and molecular weight of the polymer and not by the presence of hydrazone bond.

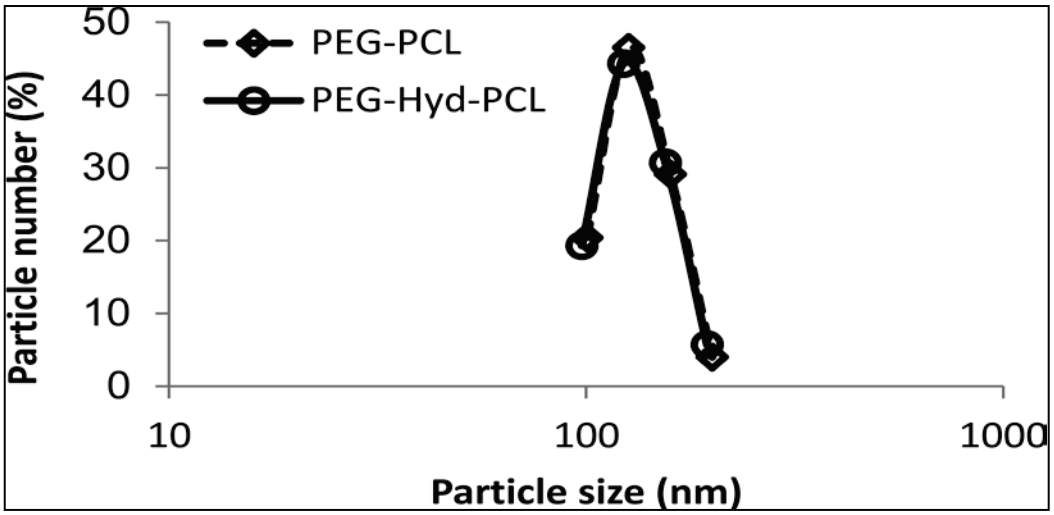

Figure 11. Particle size distributions of micelles composed of PEG-PCL and PEG-Hyd-PCL copolymers. The molecular weight of PEG and PCL block was the same in both copolymers.

The main difference between the two micelle types was in a higher pH sensitivity of PEG-Hyd-PCL micelles. We have confirmed the hydrolysis of hydrazone bond by GPC, showing bimodal MW distributions in PEG-Hyd-PCL dispersions exposed to pH< 6. The hydrolysis leads to the dissolution of the PEG blocks and the release of the PCL blocks and the entrapped drug. This was confirmed by optical transmittance and DLS measurements in PEG-Hyd-PCL dispersions at pH<6. By decreasing pH, the transmittance of PEG-Hyd-PCL dispersions at 500 nm decreased significantly, while the average particle size increased, which can be both explained by the agglomeration of released PCL blocks.

4. Conclusion

Di-block copolymers composed of hydrophilic poly(ethylene) glycol (PEG) and hydrophobic polycaprolactone (PCL) segments were successfully synthesized, characterized, and used for the preparation of pH sensitive PEG-PCL micelles using a new membrane dispersion method. The organic phase composed of a mixture of the copolymer and a volatile organic solvent was split into numerous microscopic sub-streams by injection through a microsieve membrane and mixed with an agitated aqueous phase. A precise control over the micelle size and size distribution was achieved by controlling the pore size and interpore distance of the membrane, molecular weight of the copolymer, solvent type, and micromixing conditions in the stirred cell device, such as transmembrane flux, aqueous to organic phase ratio, and agitation speed. The micelles were obtained with a sufficiently small mean size, satisfying zeta potential, and high encapsulation efficiency of a hydrophobic drug (vitamin E), and can be used as a pH-sensitive delivery system. The preparation technique is simple, fast, reproducible, and has a potential for an industrial scale-up.

Supplementary material

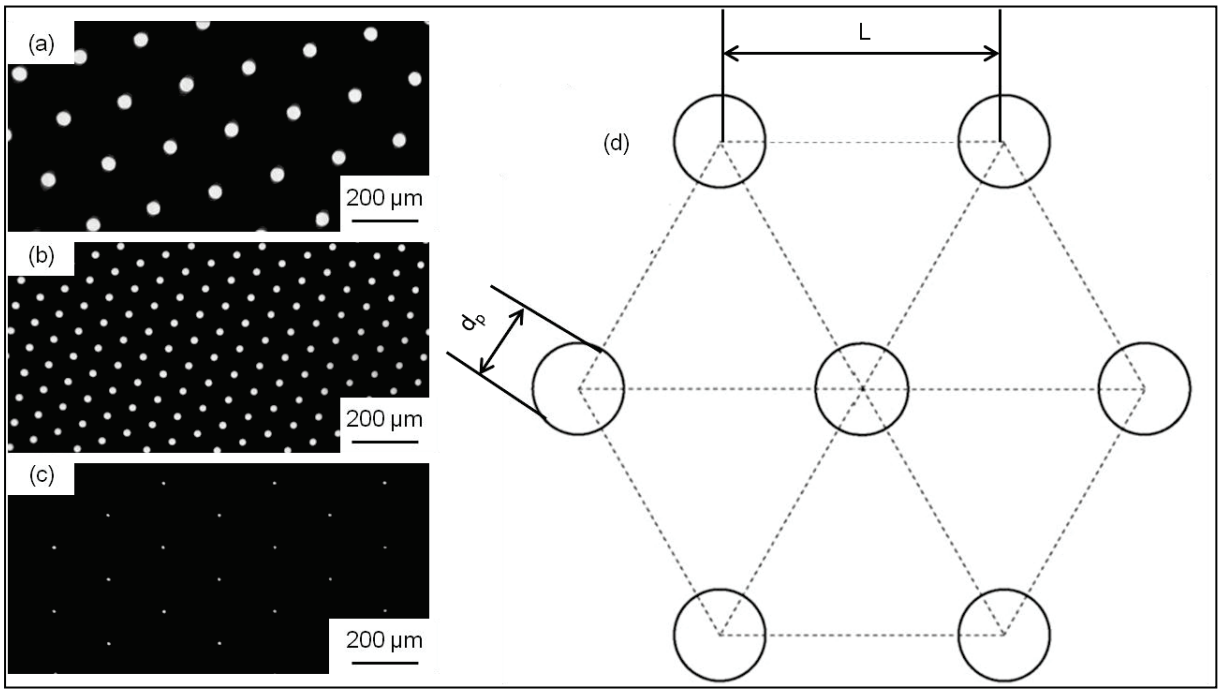

Fig. S1 Microscopic images of some membranes used in this study: **(a)** dp = 40 µm, L = 200 µm, **(b)** dp = 20 µm, L = 80 µm, and **(c)** dp = 10 µm, L = 200 µm. **(d)** Schematic view of the pore arrangement showing a regular hexagonal array of cylindrical pores with uniform pore spacing.

Table S1. Pore diameters, pore spacing and porosities of the membranes used in this study

Pore diameter (µm)	Pore spacing (µm)	Membrane porosity (%)
5	200	0.06
10	200	0.2
20	200	0.9
40	200	3.6
10	80	1.4
20	80	5.7

Table S2. Reproducibility of the fabrication method. The experimental conditions are specified in **Table 4**.

		Size (nm)	PDI	Zeta potential (mV)	E.E. (%)
Drug free micelles	Experiment 1	92	0.17	-27.0	
	Experiment 2	88	0.18	-27.3	
	Experiment 3	87	0.18	-27.8	
	Average±S.D.	89±3	0.18±0.00	-27.4±0.4	
Vitamin E-loaded micelles	Experiment 1	154	0.09	-19.3	87.4
	Experiment 2	140	0.08	-19.8	89.2
	Experiment 3	144	0.10	-19.5	86.7
	Average±S.D.	146±7	0.09±0.01	-19.5±0.2	87.8±1.3

References

[1] Wein, H.; Zhang, X.; Zhou, Y.; Cheng, S.; Zhuo, R. *Biomaterials*. **2006**, *27*, 2028−2034.

[2] Du, J.; O'Reilly, R. K. *Soft Matter*. **2009**, *5*, 3544−3561.

[3] Grislain, L.; Couvreur, P.; Lenaerts, V.; Roland, M.; Deprez-Decampeneere, D.; Speiser, P. *Int. J. Pharm*. **1983**, *15*, 335−345.

[4] Maeda, H. *Adv. Enzyme Regul*. **2001**, *41*, 189−207.

[5] Ganta, S.; Devalapally, V. P.; Shahiwala, A.; Amiji, M. *J. Controlled Release*. **2008**, *126*, 187−204.

[6] Engin, K.; Leeper, D. B.; Cater, J. R.; Thistlethwaite, A. J.; Tupchong, L.; MacFarlane, J. D. *Int. J. Hyperthermia*. **1995**, *11*, 211−216.

[7] Gillies, E. R.; Fréchet, J. M. *J. Chem. Commun.* **2003**, *14*, 1640−1641.

[8] Chen, W.; Meng, F. H.; Li, F.; Ji, S. J.; Zhong, Z. Y. *Biomacromolecules*. **2009**, *10*, 1727−1735.

[9] Tang, R.; Ji, W.; Panus, D.; Palumbo, R.N.; Wang, C. *J. Controlled Release*. **2011**, *151*, 18−27.

[10] Yang, L.; Wu, X.; Liu, F.; Duan, Y.; Li, S. *Pharm. Res*. **2009**, *26*, 2332−2342.

[11] Liggins, R. T.; Burt, H. M. *Adv. Drug Delivery Rev*. **2002**, *54*, 191-202.

[12] Zeng, F.; Liu, J.; Allen, C. *Biomacromolecules*. **2004**, *5*, 1810−1817.

[13] Yokoyama, M.; Opanasopit, P.; Okano, T.; Kawano, K.; Maitani, Y. *J. Drug Targeting*. **2004**, *12*, 373−384.

[14] Vangeyte, P.; Gautier, S.; Jérôme, R. *Colloids Surf., A*. **2004**, *242*, 203−211.

[15] Kohori, F.; Yokoyama, M.; Sakai, K.; Okano, T. *J. Controlled Release*. **2002**, *78*, 155−163.

[16] Aliabadi, H. M.; Elhasi, S.; Mahmud, A.; Gulamhusein, R.; Mahdipoor, P.; Lavasanifar, A. *Int. J. Pharm.* **2007**, *329*, 158−165.

[17] Elhasi, S.; Astaneh, R.; Lavasanifar, A. *Eur. J. Pharm. Biopharm*. **2007**, *65*, 406−413.

[18] Tyrrell, Z. L.; Shen, Y.; Rados, M. *Prog. Polym. Sci.* **2010**, *35*, 1128−1143.

[19] Aliabadi, H. M.; Lavasanifar, A. *Expert Opin Drug Deliv*. **2006**, *3*, 139−162.

[20] Vladisavljević, G. T.; Williams, R. A. *Adv. Colloid Interface Sci*. **2005**, *113*, 1−20.

[21] Charcosset, C.; El Harati, A.; Fessi, H. *J. Controlled Release*. **2005**, *108*, 112−120.

[22] Laouini, A.; Jaafar-Maalej, C.; Sfar-Gandoura, S.; Charcosset, C.; Fessi, H. *Prog. Colloid Polym. Sci*. **2012**, *139*, 23−28.

[23] Laouini, A.; Fessi, H.; Charcosset, C. *J Membr. Sci*. **2012**, *423−424*, 85−96.

[24] Vladisavljević, G. T.; Kobayashi, I.; Nakajima, M. *Microfluid. Nanofluid*. **2012**, *13*, 151−178.

[25] Kölchens, S.; Ramaswamia, V.; Birgenheiera, J. *Chem. Phys. Lipids*. **1993**, *65*, 1−10.

[26] Provder, T. *Prog. Org. Coat*. **1997**, *32*, 143−153.

[27] Hunter, R.; Midmore, H. Z. *J. Colloid Interface Sci*. **2001**, *237*, 147−149.

[28] Laouini, A.; Jaafar-Maalej, C.; Limayem-Blouza, I.; Sfar-Gandoura, S.; Charcosset, C.; Fessi, H. *J. Colloid Sci. Biotechnol*. **2012**, *1*, 147−168.

[29] Discher, D. E.; Eisenberg, A. *Science*. **2002**, *297*, 967−973.

[30] Laouini, A.; Jaafar-Maalej, C.; Sfar-Gandoura, S.; Charcosset, C.; Fessi, H. *Int. J. Pharm*. **2011**, *415*, 53−61.

[31] Kobayashi, I.; Yasuno, M.; Iwamoto, S.; Shono, A.; Satoh, K.; Nakajima, M. *Colloids Surf., A*. **2002**, *207*, 185−196.

[32] Jaafar-Malej, C.; Diab, R.; Andrieu, V.; Elaissari, A.; Fessi, H. *J. Liposome Res*. **2010**, *20*, 228−23.

[33] Zhang, Y. L.; Frangos, J. A.; Chachisvilis, M. *Biochem. Biophys. Res. Commun*. **2006**, *347*, 838−841.

[34] Xu, J. H.; Luo, G. S.; Chen, G. G.; Wang, J. D. *J. Membr. Sci*. **2005**, *266*, 121−131.

[35] Li, X.; Zhang, Y.; Fan, Y.; Zhou, Y.; Wang, X.; Fan, C.; et al. *Nanoscale Res. Lett*. **2011**, *6*, 275−283.

[36] Huang, X.; Xiao, Y.; Lang, M. *J. Colloid Interface Sci*. **2011**, *364*, 92−99.

[37] Yin, H.; Bae, Y. H. *Eur J. Pharm. Biopharm*. **2009**, *71*, 223−230.

[38] Qiu, L.; Zheng, C.; Jin, Y.; Zhu, K. *Expert Opin. Ther. Pat*. **2007**, *17*, 819−830.

[39] Laouini, A.; Charcosset, C.; Fessi, H.; Holdich, R. G.; Vladisavljević, G. T. *RSC Adv.* **2013**, *3*, 4985−4994.

[40] Dragosavac, M. M.; Holdich, R. G.; Vladisavljević, G. T.; Sovilj, M. N. *J. Membr. Sci*. **2012**, *392−393*, 122−129.

[41] Vladisavljević, G. T.; Schubert, H. *J. Membr. Sci*. **2003**, *225*, 15−23.

[42] Mitchell, J.; Ninham, B. W. *J. Chem. Soc., Faraday Trans*. **1981**, *77*, 601−629.

[43] McClements, D. J. *Soft Matter*. **2012**, *8*, 1719−1729.

[44] Sun, H.; Guo, B.; Cheng, R.; Meng, F.; Liu, H.; Zhong, Z. *Biomaterials*. **2009**, *30*, 6358−6366.

[45] McClements, D. J. *Food Emulsions*, 2nd Edition, CRC Press; Boca Raton, 2005, pp. 191.

[46] Brratt, G. *Cell. Mol. Life Sci*. **2003**, *60*, 21−37.

[47] Wiacek, A.; Chibowski, E. *Colloids Surf., A*. **1999**, *159*, 253−261.

[48] Xu, Q.; Tanaka, Y.; Czernuszka, J. T. *Biomaterials*. **2007**, *28*, 2687−2694.

[49] Kataoka, K.; Harada, A.; Nagasaki, Y. *Adv. Drug Delivery Rev*. **2001**, *47*, 113−131.

Acknowledgments

Abdallah LAOUINI held a CMIRA Explora fellowship from “Région Rhône-Alpes”. The additional funding came from The Engineering and Physical Sciences Research Council of the United Kingdom (reference number: EP/HO29923/1).

Encapsulation de la vitamine E dans des particules lipidiques solides en utilisant des membranes classiques et des membranes dynamiques

Encapsulation de la vitamine E dans des particules lipidiques solides en utilisant des membranes classiques et des membranes dynamiques

Les particules lipidiques solides ont été développées au cours des années 1990. Le cœur de ces particules est constitué d'une matrice de lipides qui est solide à température ambiante; cette matrice plus ou moins cristallisée est stabilisée par une couche de surfactants. Ces particules présentent l'avantage d'avoir une capacité d'encapsulation des molécules lipophiles supérieure à celle des liposomes ou des micelles. Par ailleurs, ces particules peuvent être synthétisées en l'absence de solvant organique. De point de vue stabilité, ces préparations sont plus stables que les émulsions.

Plusieurs techniques de préparation ont été reportées, parmi lesquelles figure la méthode de contacteur à membrane. Toutefois cette méthode présente un inconvénient majeur à savoir le colmatage des membranes en cas d'utilisation d'une huile très visqueuse associé à d'énormes difficultés du lavage des membranes utilisées. Une alternative envisageable consiste à utiliser des membranes dynamiques à la place des membranes classiques. Ces membranes dynamiques sont constituées par un lit de billes en verre et présentent l'avantage de se nettoyer facilement par simple désintégration du lit de billes. Ce travail a été réalisé à l'Université de Wageningen (Pays-Bas) pour la partie membranes dynamiques et au Laboratoire d'Automatique et de Génie des Procédés pour la partie membranes classiques.

Ce travail étudie l'influence des différents paramètres opératoires sur les caractéristiques de la préparation finale et sur le colmatage des membranes utilisées. Il présente aussi une comparaison entre la méthode d'émulsification directe utilisant des membranes en céramique et la « premix emulsification » utilisant un lit de billes en verre. Il en sort de cette étude que les particules lipidiques solides peuvent être préparées en utilisant un lit de billes en verre. Le procédé de préparation peut être contrôlé via l'ajustement des différents paramètres expérimentaux. En évitant les cas extrêmes dans le choix des conditions opératoires, aucun colmatage de la membrane n'a été observé.

Ce chapitre sera présenté sous forme d'un article qui a été accepté pour publication au « Chemical Engineering Journal».

Use of Dynamic Membranes for the Preparation of Vitamin E-Loaded Lipid Particles: An Alternative to Prevent Fouling Observed in Classical Cross-Flow Emulsification

A. Laouini[1, 2], C. Charcosset[2], H. Fessi[2], K. Schroen[1]

[1]: Food Process Engineering Laboratory, Wageningen University, Bomenweg 2, 6703 HD Wageningen, The Netherlands.

[2]: Université Claude Bernard Lyon 1, Laboratoire d'Automatique et de Génie des Procédés (LAGEP), UMR-CNRS 5007, CPE Lyon, Bât 308G, 43 Boulevard du 11 Novembre 1918, F-69622 Villeurbanne Cedex, France.

Submitted to the "Chemical Engineering Journal"

Abstract

Solid lipid particles (SLP) were introduced at the beginning of the 1990s as an alternative to encapsulation systems such as emulsions and liposomes used in cosmetic and pharmaceutical preparations. The present paper investigated for the first time the preparation of SLP based on premix emulsification with packed beds of micron-sized glass beads. A coarse pre-emulsion was prepared by mixing the aqueous phase (water and Tween 80) and the lipid phase (Precirol and vitamin E) under magnetic stirring at 1200 rpm during 15 min, followed by passing the premix through the glass beads layer. SLP were formed by cooling to room temperature of the final emulsion. SLP were successfully produced under various conditions, but was most optimally carried out by extruding a coarse O/W emulsion 6 times under a pressure of 2 bar through a dynamic membrane. For example, when a 2 mm layer of glass beads sized 63 μm was used, the premix size of 5 μm was reduced to 1.5 μm. It was found that particle size tended to decrease with increasing feed pressure, increasing number of passes, decreasing glass bead size and decreasing bed height. Even more importantly, the dynamic membrane was hardly prone to fouling compared to the membranes used in traditional cross-flow emulsification which typically need small pore size for the production of particles of similar size. In addition, the small beads could be easily cleaned by disintegrating the bed. The preparation process developed was easy to use, easy to scale-up, and the particle size could be controlled by appropriate choice of process parameters.

Key words: Packed glass beads – Premix emulsification – Vitamin E-loaded lipid particles – Membrane fouling – Scaling-up

Contents

1. Introduction

A large number of products is targeted to be beneficial for human health and used in the prevention of many diseases; however, not all of the active components in these products arrive at the targeted organs. Thus, in recent years the development of suitable drug carrier systems has attracted increasing attention. One of the beneficial natural products is vitamin E, which prevents oxidative damage and lipid peroxidation in central and peripheral nervous systems **[1]**. Owing to its promising therapeutic potential and safety, vitamin E has for example been tested to prevent cigarette smoke toxicity since several pulmonary disorders are mainly caused by oxidative stress phenomena **[2]**. Nevertheless, the oral or intravenous administration failed to restore the broncho-alveolar level of vitamin E since that the use of conventional pharmaceutical forms doesn't allow precise transport of drugs to their specific action sites **[3]**. Recently, attention has been drawn to nanoencapsulated systems, showing high intracellular uptake and improved stability and solubility of active substances. The solid lipid particles consisted of a solid lipid core matrix, stabilized by surfactants, in which lipophilic compounds are solubilized **[4]**. Since the production of lipid microparticles by spray congealing was described by Speiser in 1990 **[5]**, these new carriers have been extensively studied as drug delivery systems. Since they are solid, lipid particles offer a better stability compared to emulsions. Moreover, unlike liposomes, their preparation doesn't require any organic solvents, which is a major advantage. In addition, large scale production can be performed in a cost-effective and relatively simple way **[6]**. For all these reasons, attention from various research groups has been focused on lipid particles as an alternative to traditional lipid based carriers (emulsions, liposomes, nanodispersions, etc).

Different techniques have been proposed for lipid particle preparation such as high pressure homogenization, microemulsification, emulsification-solvent evaporation, emulsification-solvent diffusion, solvent displacement, phase inversion, multiple emulsion technique and ultrasonication **[7]**. Besides cross flow membranes, that are also applied for the preparation of liposomes **[8-10]**, nano-emulsions **[11]**, gel micro beads **[12]** and microcapsules **[13]** also used for lipid particle preparation **[14, 15]**.

The use of membrane contactor for the preparation of solid lipid particles presents several advantages compared to classic methods: (i) less energy consumption, (ii) better mixing efficiency due to an increased contact surface between both phases, (iii) better control of the final particles size characteristics via a careful tuning of the process parameters, (iv) easy extrapolation of the results obtained at laboratory scale and thus an improved scaling up ability from conventional batch process to continuous large scale industrial production, (v) low cost, and (vi) facility of use.

In cross-flow membranes set-up, the lipid phase was pressed, at a temperature above the melting point of the lipid, through the membrane pores allowing the formation of small droplets. The aqueous phase circulated inside the membrane device and swept away the droplets formed at the pores outlets. Solid lipid particles (SLP) were obtained by cooling of the emulsion to room temperature. The major drawback of this technique was the fouling of the membrane which was reported to lead to difficult and long cleaning procedures.

As an alternative a novel preparation strategy is presented in this study; the technique is based on premix emulsification using a dynamic membrane consisting of small glass beads. Premix emulsification is a two-step process: first a coarse pre-emulsion is prepared, which is subsequently passed through a porous structure to obtain small droplets. This process was chosen since it was reported to produce stable emulsions at high fraction of dispersed phase in which the droplets were of small mean size **[16]**. A packed bed of small glass beads was used; it is quite similar in morphology to the conventional membranes, but presents a great advantage that the beads could be easily cleaned by disintegrating the bed. The bed could easily be formed again before a new experiment.

The packed bed of glass beads, otherwise known as "dynamic membrane", has already been used to prepare hexadecane in water emulsions, stabilized by Tween 20 by Van Der Zwan et al **[17]**, while Nazir et al **[18]** used the same system and focused on the droplet break-up mechanism during premix emulsification. In the current study, glass beads will be applied for the first time to prepare solid particles that are known to foul regular membranes.

The main objectives of this work were: (i) to investigate the process parameters influencing the size of SLP, (ii) to study scale-up of the developed process, and (iii) to compare the dynamic premix technique with regular membrane emulsification.

2. Materials and methods

2.1 Materials

2.1.1 Reagents

Precirol® ATO 5 (glyceryl palmitostearate) was a kind gift from Gattefossé (Saint Priest, France). Its melting point, according to the supplier analysis certificate, is 56°C. Tween® 80 (polyoxyethylene sorbitan monooleate) and α-tocopherol were purchased from Sigma-Aldrich (Saint Quentin Fallavier, France). Ultra-pure water was obtained from a Synergy® Ultrapure Water System Millipore (Massachusetts, USA). Ethanol, acetone and acetonitrile, of analytical grade, were supplied by Fischer Scientific (Illkirch, France). The cleaning agent Derquim® was purchased from Derquim company (Ileida, Spain).

2.1.2 Membranes

Packed bed of glass beads

Four different fractions of hydrophilic glass beads (10HFL, Pneumix SMG-AF) having mean diameters between 30 and 90 µm were used in this study. The particle density (ρ_p) and the bulk density (ρ_b) of each fraction were measured in water and in air, respectively. Subsequently, the porosity (ε) was calculated according to the following equation:

$$\varepsilon = 1 - \rho_b / \rho_p \quad (1)$$

The capillary model for fixed bed **[19]** was used to determine the structural properties of the porous medium like the interstitial void diameter and tortuosity. This model assumes the packed beds to consist of a bundle of identical cylindrical tortuous pores.

The interstitial void diameter, d_v, was defined as:

$$d_v = 4\,\varepsilon / [A_v\,(1 - \varepsilon)] \quad (2)$$

where A_v is the dynamic specific surface area, a ratio of wetted surface area to volume of solid, and is related to bead diameter d_b by:

$$A_v = 6 / d_b \quad (3)$$

The bed tortuosity, τ, was calculated as follows:

$$\tau = 1 + q\,ln\,(1 / \varepsilon) \quad (4)$$

where $q = 0.41$ for tightly packed spheres.

The characteristics of the packed beds used in the present study are presented in **Table1**.

Table 1. Characteristics of the packed beds used in this study.

Beads fraction	d_b (µm)	ρ_p (kg.m^{-3})	ρ_b (kg.m^{-3})	ε	d_v(µm)	τ
1	90	1519	2500	0.392	38.7	1.38
2	75	1528	2500	0.388	31.7	1.39
3	63	1516	2500	0.393	27.2	1.38
4	30	1510	2500	0.396	13.1	1.38

Kerasep® membrane

The membrane used was a ceramic membrane with an active zirconium oxide, ZrO_2, layer on an aluminum titanium oxide, Al_2O_3-TiO_2, support. The membrane length was

0.4 m, the inner diameter 6 10^{-3} m and the outer diameter 10^{-2} m. Thus, the active membrane surface was 7.5 10^{-3} m^2. The mean pore size was 10.2 µm. The membrane was supplied by Orelis (Salindres, France).

2.1.3 Emulsification set-up

Dynamic membrane set-up

A schematic representation of the emulsification set-up is shown in **Figure 1.A**. The pressurized vessel (containing the coarse emulsion) was connected to a Plexiglas column having a packed bed of glass beads pre-deposited on top of a sieve support with an effective surface area of 9.4 10^{-4} m^2. The sieve support was held in place by two o-ring rubbers (above and below) at the bottom junction of the column. Both the pressurized vessel and the membrane module were placed in an oven at 65°C in order to keep the temperature of the overall system above the lipid melting point. The fine emulsion was collected in a flask placed on a balance for digital recording of the mass every second using the custom written Mem-Fil Lite Software (lab of FPE, WU).

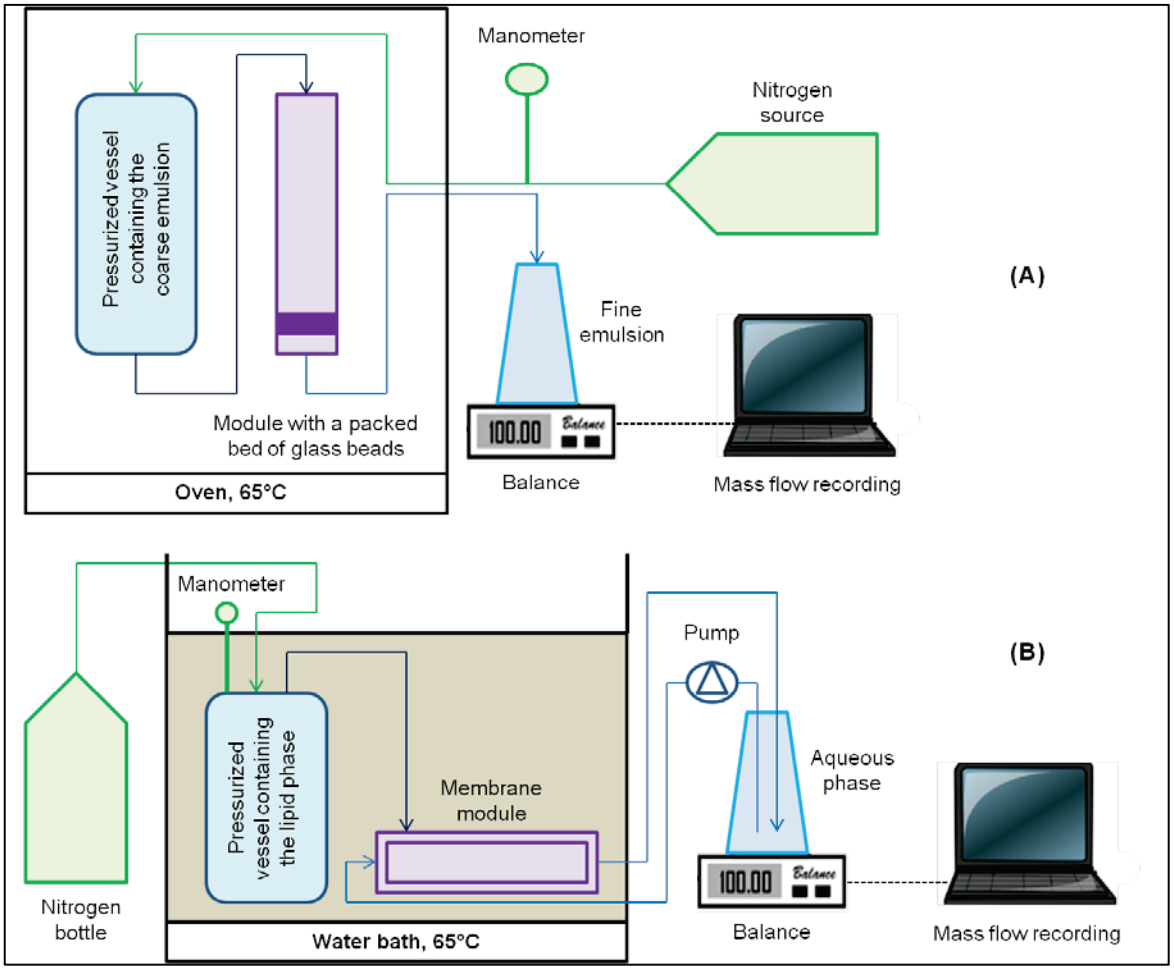

Figure 1. Schematic representation of the experimental set-ups: **(A)** Dynamic membrane set-up and **(B)** Conventional membrane set-up.

The volume flux, J, across the packed bed was calculated from the mass flow rate, Φ_m, using the following equation:

$$J = \Phi_m / (\rho_e A) \quad (5)$$

where ρ_e is the emulsion density = 980 kg/m^3 and A is the packed bed effective cross-sectional area.

The flow inside the packed bed was characterized using the pore Reynolds number, Re_p, which is the ratio of the inertial to the viscous forces defined as:

$$Re_p = \rho_e v_v d_v / \eta_e \quad (6)$$

where η_e is the emulsion viscosity = 0.434 g/m/s and v_v is the average interstitial void velocity, defined as:

$$v_v = v_0 \tau / \varepsilon \quad (7)$$

where τ is the tortuosity (see table 1) and, v_0 is the superficial velocity defined as:

$$v_0 = J / \varepsilon \quad (8)$$

Before starting an experiment, a small amount of continuous phase was introduced inside the Plexiglas column in order to properly wet the packed bed with the continuous phase. The column was then turned upside down for a few times and placed vertically to let the glass beads settle down under the influence of gravity.

Conventional membrane set-up

The experimental set-up used for the cross-flow emulsification is shown in **Figure 1.B**. It includes a Quatro-Flow 1000S pump (Pall, France) used to circulate the aqueous phase through the membrane device and a pressurized vessel (equipped with a manometer) connected on one side to a nitrogen bottle (Linde Gas, France) and on the other side to the membrane module. Both the pressurized vessel and the membrane module were placed in a water bath at 65°C. The emulsion was collected in a beaker placed on a balance. The balance was interfaced to a computer in order to collect the mass versus time data.

2.2 Methods

2.2.1 Preparation procedures

The following formulation was used for all experiments. The aqueous phase contains water (91.2%) and Tween 80 (1.8%) and the lipid phase contains Precirol (6.5%) with vitamin E (0.5%). Before emulsification, both aqueous and lipid phase were heated to 65°C.

Premix emulsification protocol

O/W emulsions were prepared in a two-step emulsification system. The first step was the preparation of a coarse emulsion by mixing the aqueous and the lipid phases using a magnetic stirrer (Ika RTC basic, Boutersum, Belgium.) at 1200 rpm for 15 minutes at 65°C. This led to reproducible starting emulsions for our experiments; the droplets mean size of the coarse emulsion was around 4.8 µm. Next, the coarse emulsion was put in the pressure vessel of which the connecting valve to the nitrogen source was opened and set at a fixed level (between 0.5 to 5 bar). Then the valve connecting the pressure vessel to the dynamic membrane module was opened so that the coarse emulsion permeated through the glass beads after opening the outlet valve of the packed bed module. The fine emulsion resulting from this process was collected in a flask placed on a balance while the increase in mass was digitally recorded. The premix procedure was repeated up to 8 times. SLP were formed by immediate cooling to a temperature below 35°C. Glass beads were cleaned by injection of ethanol through the Plexiglas column.

Direct emulsification protocol

The SLP preparation process using cross-flow emulsification was previously investigated by Charcosset et al **[14, 15]**. In the present study, the lipid phase was introduced in the pressure vessel and the pressure was set at 5.5 bar. The aqueous phase was pumped through the membrane device at a flow rate of 4 10^{-2} L/s corresponding to a velocity of 1.4 m/s. The valve connecting the pressure vessel to the filtrate side of the membrane module was then opened so that the lipid phase permeated through the pores of the membrane into the aqueous phase which circulated tangentially. The membrane used was made of ceramic and presented a pore size of 10.2 µm. The experiment was stopped when air bubbles started to appear, indicating that the pressure vessel was empty. SLP were formed by immediate cooling to a temperature below 35°C. At the end of the experiment, the membrane was regenerated. The washing was performed by flushing the module several times with a detergent (Derquim®) followed by a circulation of acetone and acetonitrile. The membrane permeability (the slope of the permeate flow rate versus transmembrane pressure) was then measured and the cleaning procedure was stopped when the permeability was found to be more than 90% of its initial value.

2.2.2 Size characterization

A Malvern Zetasizer Nano-series (Malvern Instruments Zen 3600, Malvern, UK) was used for size distribution analysis. Each sample was diluted 100-fold with ultra-pure water and analyzed in triplicate at 25°C. The data on particle size distribution was collected using the DTS nano software (version 5.1) provided with the instrument. The

sizes mentioned correspond to the average particle diameter (d_{32}). In addition the polydispersity was assessed through the polydispersity index PDI.

3. Results and discussion

3.1 Premix emulsification using a packed bed of glass beads

3.1.1 Number of homogenization cycles

Emulsification was repeatedly carried out using 75 μm beads with a bed height of 2 mm at an applied pressure of 1.5 bar. **Figure 2.A** shows the coarse emulsion size distribution with a main peak around 5.6 μm. After the 2nd pass, the intensity of this peak decreased and a new peak appeared around 1.4 μm. As shown in **Figure 2.B**, the intensity of this new peak increased with the number of cycles while the peak around 5.6 μm disappeared, and the particle z-average was reduced as can be seen in **Figure 2.C**. Significant reduction occurred till the 6th pass, after which no decrease in size was observed. Therefore it was decided to carry the other experiments out at 6 passes.

3.1.2 Bead diameter

The size of the interstitial voids between the beads is directly related to the bead size and packing arrangement. These voids could be seen as interconnected asymmetric capillaries that follow an irregular path through the packed bed, somewhat comparable to pores in ceramic membranes which are prepared by sintering a packed bed of individual ceramic particles **[18]**. Thus, the bead size is an important factor to consider for the emulsification process.

Experiments were carried out using 4 different beads (30, 63, 75 and 90 μm) at a constant bed height of 2 mm with an applied pressure of 2 bar. **Figure 3.A** shows the particle size distribution as a function of bead size and **Table 2** summarizes the effect of bead size on particle size reduction during the premix emulsification process. For the bead sizes 90, 75 and 63 μm, the particles size reduction ratio increased when the beads size decreased, which is related to smaller interstitial void diameters, which are 38.7, 31.7 and 27.2 μm for bead size 90, 70 and 63 μm, respectively.

The final particle to interstitial void size ratio was calculated; and values between 0.05 and 0.06 where found, which indicated that the produced particles are considerably smaller than the interstitial voids. Compared with other premix membrane emulsification studies, it is clear that the current reduction in size is much larger as found in any of the other works which are in the range from 0.2 to 4.1 **[18, 20-27]** (more details could be found in **Table S1** in supplementary material); which is indicative of the effectiveness of the current process.

The 30 µm glass beads didn't follow the general trend. The mass flow through the packed bed decreased from 9.4 to 7.7 g s^{-1} during the 1st and 6th pass, and this may indicate fouling occurred, which will be discussed in detail in section **3.1.7**.

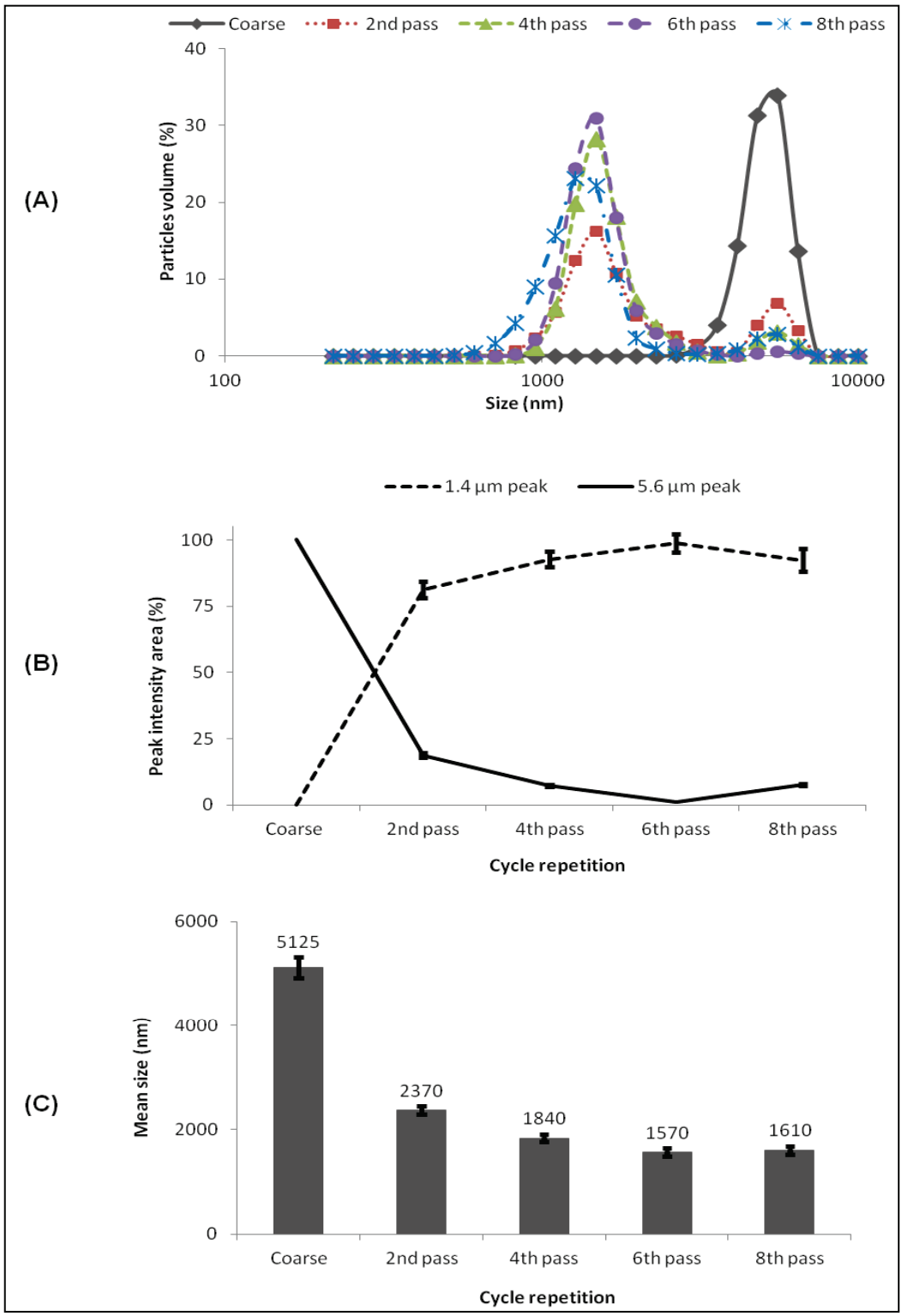

Figure 2. Evolution of the size during the premix emulsification process: (A) size distribution, (B) main peak intensity, and (C) z-average. Experimental parameters: feed pressure = 1.5 bar, glass bead size = 75 µm, and packed bed height = 2 mm.

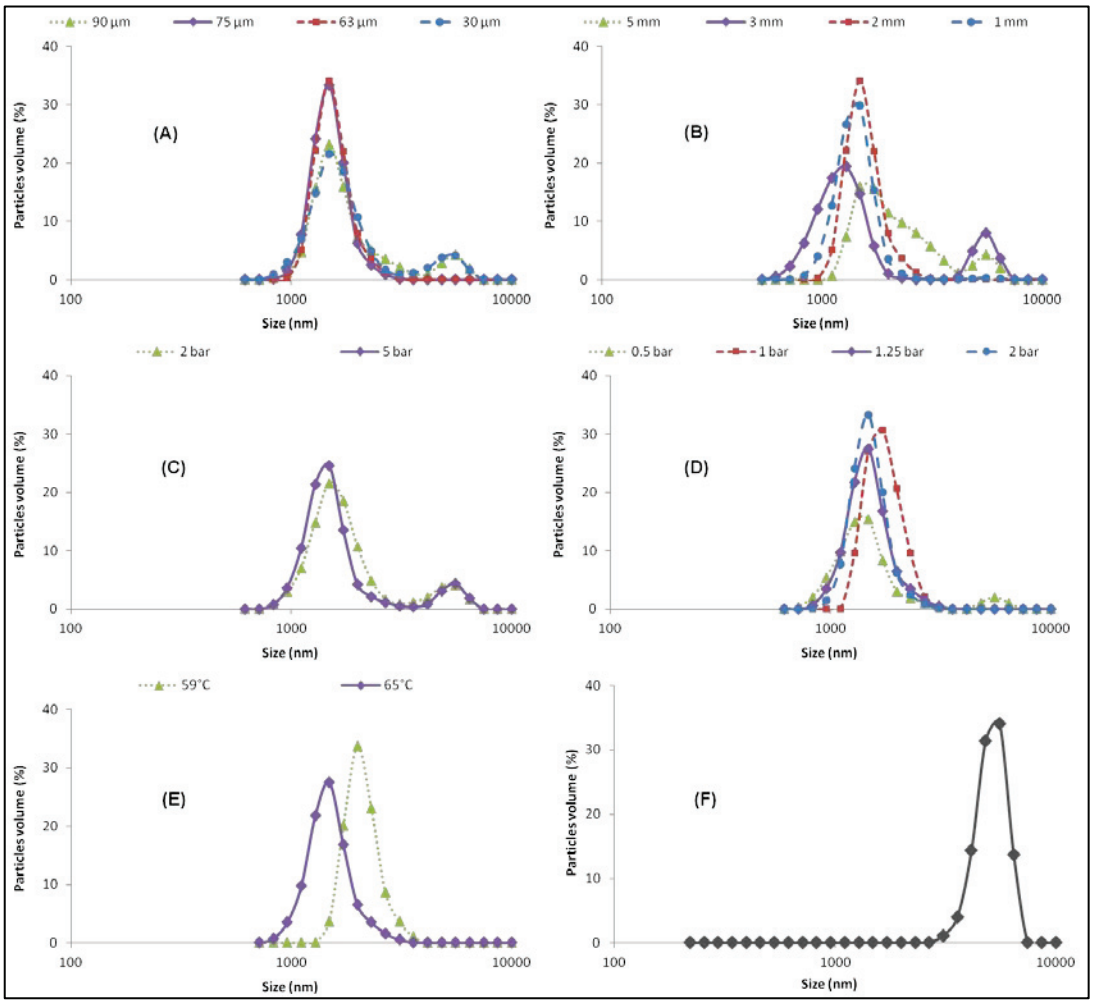

Figure 3. Effect of the process parameters on the particle size distribution: **(A)** effect of the bead diameter, **(B)** effect of the bed height, **(C)** and **(D)** effect of the feed pressure, **(C)**: 30 µm beads, **(D)**: 75 µm beads, and **(E)** effect of the temperature. Experimental parameters are described in Tables 2, 4, 5 and 6. **(F)** size distribution of the starting emulsion.

3.1.3 Packed bed height

The effect of the bed height was investigated with 63 µm glass beads using heights ranging from 1 to 5 mm at an applied pressure of 2 bar. Results presented in **Figure 3B** and **Table 2** show higher size reductions for lower bed heights. The relationship was found to be linear (see **Figure S1** in supplementary material); although the overall effect is not that large in the range investigated here. This result could be attributed to a decrease in void velocity with increasing bed height, resulting in less shear force acting on the droplets **[17]**. On the other hand, at high bed height, the emulsion would spend more time in the packed bed, which may increase the chances that newly formed droplets meet inside the packed bed, possibly leading to coalescence.

Table 2. Effect of the process parameters on particle size.

Experimental conditions					Particle size characteristics				
d_b (µm)	Bed height (mm)	Pressure (bar)	Temperature (°C)	Calculated Re_p	Starting preparation mean size* (µm)	Final preparation mean size* (µm)	Size reduction ratio	5.6 µm peak intensity* (%)	1.4 µm peak intensity* (%)
90	2	2	65	22.9	4.99 ± 0.20	2.09 ± 0.02	2.39	11.8 ± 0.3	88.2 ± 1.3
75	2	**2**	65	20.9	4.72 ± 0.19	1.51 ± 0.02	3.12	0 ± 0	100 ± 0
63	**2**	2	65	17.8	4.99 ± 0.20	1.56 ± 0.02	3.20	0 ± 0	100 ± 0
30	2	2	65	2.7	4.86 ± 0.16	2.05 ± 0.03	2.37	14.1 ± 0.4	85.9 ± 3.5
63	**1**	2	65	19.4	4.71 ± 0.17	1.45 ± 0.06	3.25	0.6 ± 0	99.4 ± 4
63	**3**	2	65	15.9	4.87 ± 0.17	1.74 ± 0.07	2.79	17.8 ± 0.3	82.2 ± 3.3
63	**5**	2	65	8.8	4.87 ± 0.23	2.00 ± 0.08	2.44	11.3 ± 0.1	88.7 ± 2.8
30	2	5	65	6.6	5.04 ± 0.24	1.91 ± 0.06	2.64	11.2 ± 0.1	88.2 ± 3.1
75	2	**0.5**	65	6.8	4.43 ± 0.11	1.68 ± 0.06	2.64	6 ± 0.1	94 ± 4.6
75	2	**1**	**65**	14.1	4.94 ± 0.14	1.75 ± 0.06	2.82	0 ± 0	100 ± 0
75	2	**1.25**	65	16.7	4.78 ± 0.14	1.63 ± 0.08	2.93	0 ± 0	100 ± 0
75	2	0.5	**59**	6.55	5.21 ± 0.08	2.11 ± 0.10	2.46	0 ± 0	100 ± 0

* Each value represents the mean ± S.D. (n=3).

When the bed height is very low (1 mm), a small fraction of the 5.6 μm peak was detected (0.6%), indicating that the height of the packed bed has to be carefully optimized. Indeed the packed bed should be high enough to allow break up of all droplets of the coarse emulsion but not too high to negatively affect droplet size. Therefore it was decided to keep the bed height constant at 2 mm which seems to be the optimum bed height value since it gave a high size reduction ratio and allowed production of particles with a mono-modal size distribution.

3.1.4 Transmembrane pressure

As shown in **Table 2**, for both sizes of glass beads, the particle size decreased with increasing applied pressure, which is expected to be caused by the resulting increase in the flow velocities and shear rate. A linear relationship was found when size reduction ratios were plotted versus the applied pressure (See **Figure S2** in supplementary material); although the effect on size is not that large. More importantly, **Figure 3C** and **3D** also show that at lower pressure, the size distribution is much wider and becomes narrower at higher pressure; this effect will be further discussed in section **3.1.6** On Re_p numbers.

3.1.5 Temperature

Temperature should be kept over the melting point of the solid lipid during the entire premix emulsification process. In this work, the melting point of the used lipid is stated to be 56°C, and during experimental work two temperature values were used: 59 and 65°C. Results presented in **Table 2** and **Figure 3E** show that the lower temperature led to greater average size and smaller size reduction ratio. This could be explained by the fact that at low temperature, the actual volume fluxes are lower, resulting in lower void velocities and less droplet break-up.

3.1.6 Size reduction versus Reynolds pore number

To summarize all investigated effects, the pore Reynolds number is used to compare the obtained size reductions (**Figure 4**). At higher Reynolds number, the droplets became smaller leading to a virtually linear increase in size reduction ratio, which indicates that the break-up mechanism became similar and was characterized by a dominance of constriction and shear forces, irrespective of the bed height, bead size and pressure. These results are comparable to those recently reported by Nazir et al **[18]** for emulsions.

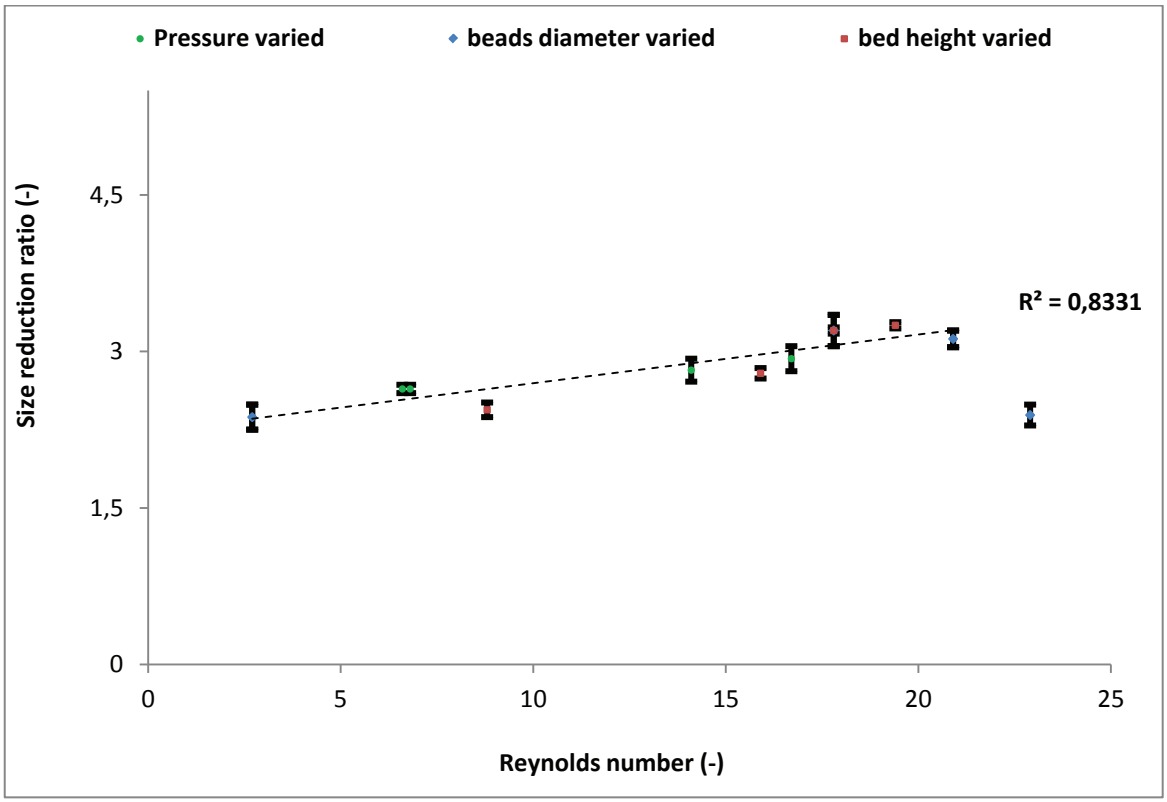

Figure 4. Size reduction ratio as a function of the Reynolds pore number for all experiments.

3.1.7 Fouling

Table 3 shows the mass flux evolution during premix emulsification under different process parameters. It can be noticed that mostly no flux reduction took place, but at four conditions the flux became lower, which we consider to be an indication for fouling. For instance when the 30 µm glass beads were used, the flux during the 6th passage was 20% lower than the initial value, while for the other bead sizes similar fluxes were found. Fouling observed with 30 µm beads could explain the bi-modal size distribution of SLP described in section **3.1.4.** Flux loss was also observed during the experiments carried out at different feed pressure. When the 75 µm beads were used, it was observed that at low pressure (0.5 bar) the flux was reduced. Illustrative is also the experiment carried out at 59°C in which the viscosity was large with possibly solidification happening inside the bed. All parameters affect the flow inside the packed bed and from the Reynolds numbers could be concluded that fouling of the membrane was only observed for Reynolds number values under 8. Obtained results underline the possibility of avoiding membrane fouling during the preparation of SLP by a suitable choice of the working conditions.

Tableau 3. Mass flux evolution during the premix emulsification process

Experimental conditions					Mass flux evolution		
d_b (µm)	Bed Height (mm)	Feed Pressure (bar)	Temperature (°C)	Calculated Re_p	Mass flux during the 1st pass* (g/s)	Mass flux during the 6th pass* (g/s)	Membrane behavior
90	2	2	65	22.9	26.8 ± 0.8	26.8 ± 0.9	No fouling
75	2	**2**	65	20.9	29.0 ± 1.4	29.7 ± 0.7	No fouling
63	**2**	2	65	17.8	28.6 ± 1.3	29.9 ± 0.8	No fouling
30	2	2	65	2.7	9.4 ± 0.3	7.7 ± 0.1	Fouling
63	**1**	2	65	19.4	32.2 ± 0.3	32.6 ± 0.3	No fouling
63	**3**	2	65	15.9	26.7 ± 0.4	25.7 ± 0.4	No fouling
63	**5**	2	65	8.8	15.1 ± 0.6	15.0 ± 0.6	No fouling
30	2	5	65	6.6	23.4 ± 0.6	19.3 ± 0.9	Fouling
75	2	**0.5**	65	6.8	9.5 ± 0.2	7.7 ± 0.3	Fouling
75	2	**1**	**65**	14.1	18.8 ± 0.6	19.5 ± 0.6	No fouling
75	2	**1.25**	65	16.7	23.3 ± 1.1	23.3 ± 0.5	No fouling
75	2	1	**59**	8.0	12.1 ± 0.5	3.1 ± 0.1	Fouling

* Each value represents the mean ± S.D. (n=3).

3.1.8 Scale-up of the optimized process

To test scalability, a 4-fold volume increase was realized (from 200 to 800 g; which is the maximum capacity of the pressure vessel). As shown in **Table 4**, under similar conditions (bead diameter = 63 µm, bed height = 2 mm, and feed pressure = 2 bar), the flow inside the packed bed (calculated Re_p) and size reduction ratio was the same. Furthermore, **Figure 5** shows a very good agreement in size distributions; this shows the proof of principle that the premix emulsification process, using a packed bed of glass beads, can be operated successfully at larger scale, with all of the larger particles in the premix effectively reduced in size.

Table 4. Scale-up of SLN prepared by premix emulsification

Preparation final weight (g)	Calculated Re_p	Starting preparation size* (µm)	Final preparation size* (µm)	Size reduction ratio	5.6 µm peak intensity (%)	1.4 µm peak intensity (%)
200	17.8	4.99 ± 0.16	1.56 ± 0.02	3.20	0	100
800	17.2	5.02 ± 0.05	1.59 ± 0.01	3.16	0	100

* Each value represents the mean ± S.D. (n=3).

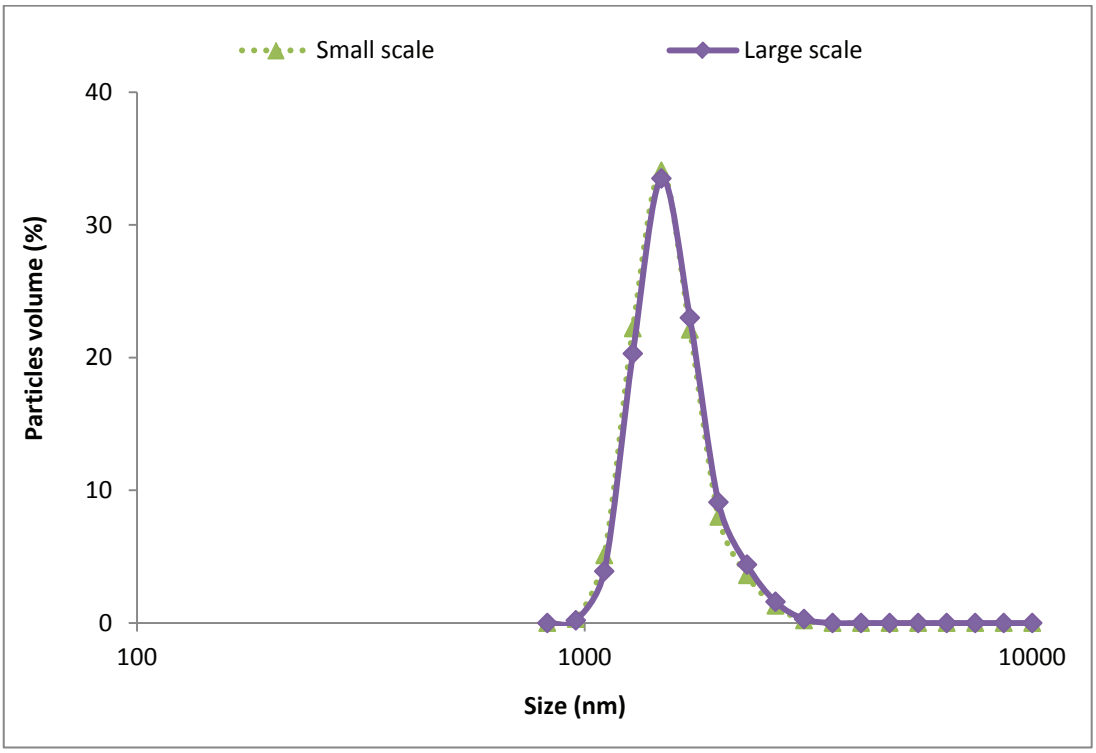

Figure 5. SLP size distribution during process scale-up

3.2 Comparison

SLP preparation using a ceramic membrane was previously investigated by Charcosset et al **[14, 15]**. Under optimum conditions and using the same formulation as in the premix emulsification process, SLP prepared by cross flow emulsification had a mean size of 2.51 µm. Thus, compared to SLP obtained by premix emulsification the mean size was larger (as previously discussed). The major drawback of the direct emulsification process was membrane fouling as could be seen in **Figure 6**. Indeed the maximum amount of dispersed phase which could be injected through the membrane was around 45 g before blockage occurred. However, when the premix emulsification process was applied using a packed bed of glass beads, an amount of 52 g of lipid could be used without any fouling of the dynamic membrane. In addition, the packed bed allowed the production of 851 kg of SLP preparation per m^2 of active area in less than 5 minutes, versus a preparation of 93 kg per m^2 of active area within more than 15 minutes when the classic cross-flow emulsification technique was used; the glass bead system clearly outperforms cross-flow emulsification. **Table 5** summarizes the main differences between both preparation processes used in this study.

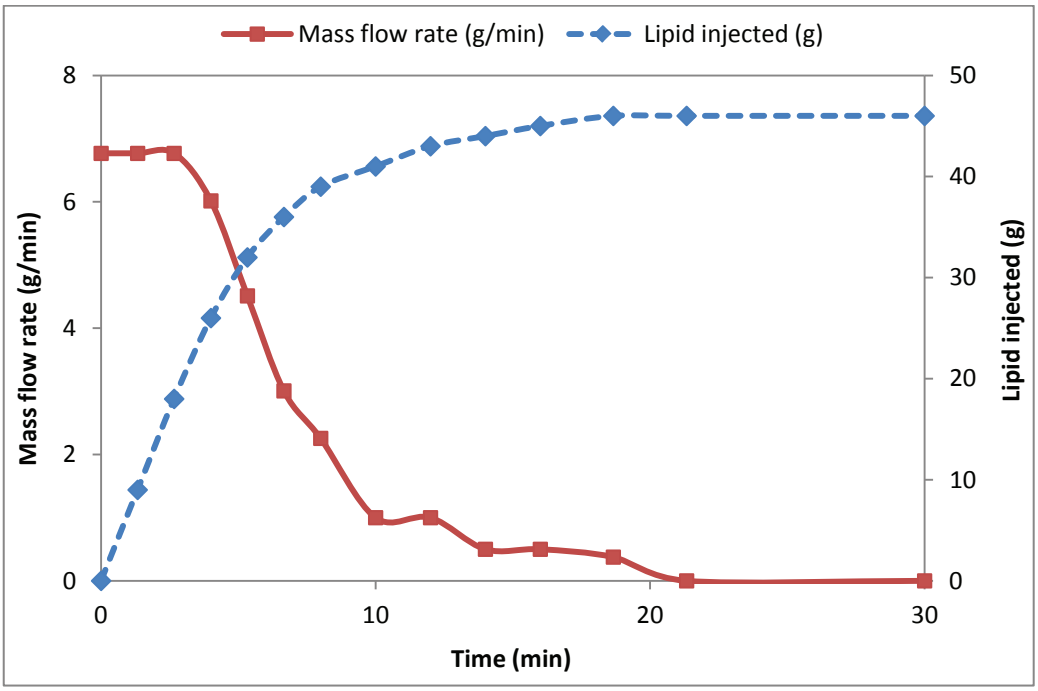

Figure 6. Membrane fouling during SLP preparation using a ceramic tubular membrane: Time evolution of the weight of the lipid phase injected through the membrane and time evolution of the mass flow rate during the preparation. Experimental conditions are described in section 2.2.1.

Table 5. Comparison between membrane emulsification and premix emulsification for the preparation of SLP.

Classical membrane emulsification process (using a ceramic tubular membrane)	**Dynamic membrane premix emulsification process** (using a packed bed of glass beads)
- Continuous phase recirculation resulting in interactions between newly formed droplets and droplets of the emulsion and leading to coalescence and an increase of the final size.	- High fluxes could be achieved (around 30 g s^{-1}) / No recirculation needed and no risk to damage the produced particles.
- SLP mean size = 2.51 µm (particles to pore size ratio of 0.25).	- Production of smaller particles: SLP mean size = 1.59 µm (particles to void size ratio of 0.06)
- PDI = 0.222.	- Wider size distribution: PDI = 0.581.
- High membrane fouling: no more than 45 g of lipid phase could pass through the membrane / Process allowing only preparations with low disperse phase fraction.	- No membrane fouling observed for 52 g lipid phase / Process suitable for preparations with high dispersed phase fraction
- Costly and time-consuming membrane cleaning: several cleaning cycles using detergents and organic solvents at high pressure.	- Easy cleaning of the glass beads: one pass of organic solvent through the packed bed system.
- Membrane active area = 7.5 10^{-3} m^2 and maximum batch size = 700 g (93 kg m^{-2}) / For large scale preparation, membrane area should be important: expensive technology.	- Packed bed active area = 9.4 10^{-4} m^2 and batch size = 800 g (851 kg m^{-2}) / No fouling of membrane system: easy process scale-up.
- High energy costs, including: continuous phase cross flow = 4 10^{-2} L s^{-1}, feed pressure for lipid phase injection = 5.5 bar, and several cleaning cycles.	- Low energy costs: no cross flow required, applied pressure for premix injection = 2 bar, and easy membrane cleaning.

4. Conclusion

The purpose of this research was to determine whether SLP preparation could be achieved by premix emulsification using a packed bed of glass beads. The experiments reported in this work showed that this was feasible and particle size could be adjusted by tuning the operational parameters. It was found that size reduction ratio tended to increase with increasing feed pressure, increasing number of homogenization cycles, decreasing glass bead size and decreasing bed height. When process conditions were chosen appropriately, there was no indication of fouling. Besides it was shown that the process could easily be scaled-up with a factor of 4. Therefore, premix emulsification process appears asa promising alternative for classical membrane emulsification especially for preparations with high fouling risk.

Supplementary material

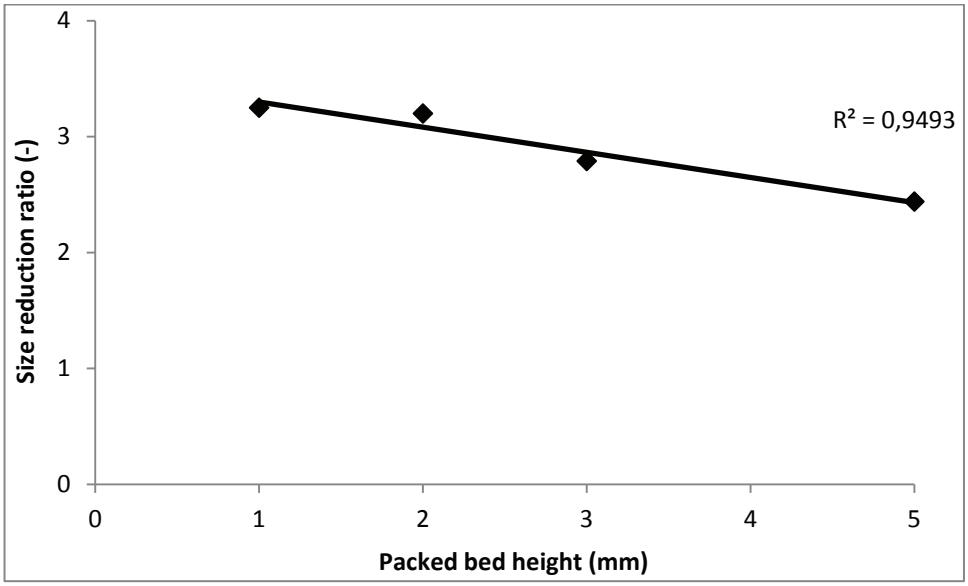

Figure S1. Effect of the packed bed height on the particle size reduction ratio

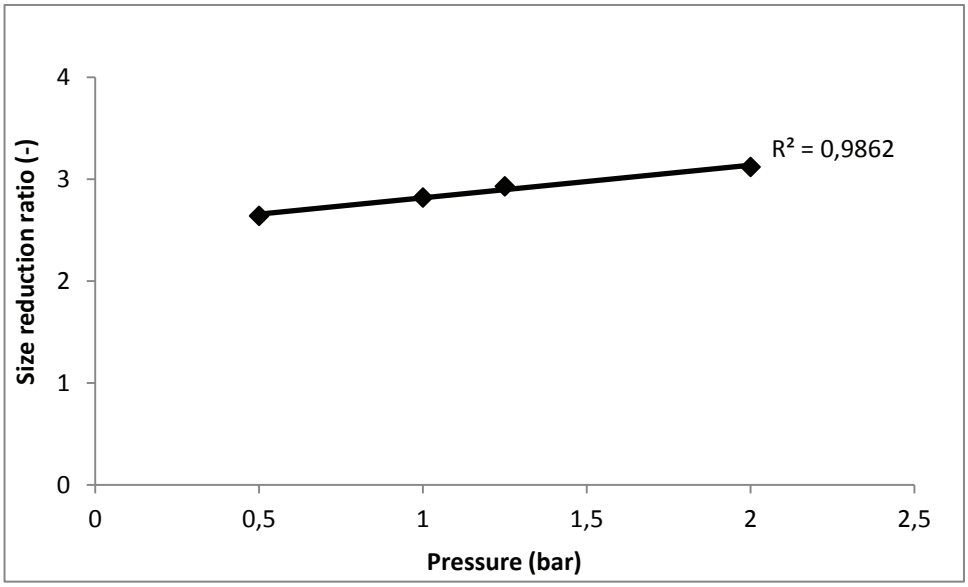

Figure S2. Effect of the pressure on the particle size reduction ratio for the 75 µm glass beads.

Table S1. Comparison of particle size to pore size ratios obtained in the present study with ratios reported in other premix emulsification studies.

Membrane system used		Membrane pore size (μm)	Particles to pore size ratio	Reference
Dynamic membranes	Packed bed of glass beads	13 - 39	0.05 – 0.06	**Present study**
		23 - 39	0.20 – 0.28	**[18]**
Conventional membranes	Tubular SPG	1.1 – 20.3	0.20 – 2.1	**[20-22]**
	Tubular ceramic	1.5	1.5 – 1.8	**[23]**
	Flat cellulose	0.2 - 3	1 – 3.5	**[24]**
	Flat PTFE	1	1.2 – 4.1	**[25-26]**
	Flat Polycarbonate	0.33 - 1	< 1.6	**[27]**

Nomenclature

A: Packed bed effective cross-sectional area (m^2)

A_v: Dynamic specific surface area (m^{-2} m^{-3})

d_b: Bead diameter (m)

d_v: Interstitial void diameter (m)

J: Flux ($m.s^{-1}$)

q: Equation 4 constant (dimensionless)

Re_p: Pore Reynolds number (dimensionless)

v_0: Superficial velocity ($m.s^{-1}$)

v_v: Average interstitial void velocity ($m.s^{-1}$)

ε: Porosity (dimensionless)

η_e: Emulsion viscosity (Pa.s)

ρ_b: Bulk density ($kg.m^{-3}$)

ρ_e: Emulsion density ($kg.m^{-3}$)

ρ_p: Particle density ($kg.m^{-3}$)

τ: Bed tortuosity (dimensionless)

Φ_m: Mass flow rate ($g.s^{-1}$)

References

[1] A.M. Terrasa, M. H. Guajardo, C.A. Marra, G. Zapata, Vet. J., 182 (2009) 463-468.

[2] M. Scherrer-Crosbie, M. Paul, M. Meignan, E. Dahan, G. Lagrue, G. Atlan, et al., J. Appl. Physiol. 81 (1996) 1071–1077.

[3] Y. Kato, K. Watanabe, M. Nakakura, T. Hosokawa, E. Hayakawa, K. Ito, Chem. Pharm. Bull. 41 (1993) 599–604.

[4] R. H. Muller, K. Mader, S. Gohla, Eur J Pharm Biopharm, 50 (2000) 161-177.

[5] P. Speiser, European patent EP 0167825, (1990).

[6] M. Gonnet, L. Lethuaut, F. Boury, J Control Rel, 146 (2010) 276-290.

[7] Y. Li, H. Fessi, C. Charcosset, Adv Sci Lett, 4 (2011) 591-595.

[8] C. Jaafar-Maalej, C. Charcosset, H. Fessi, J. Liposome Res. 3 (2011) 213-220.

[9] A. Laouini, C. Jaafar-Maalej, S. Sfar-Gandoura, C. Charcosset, H. Fessi. Int J Pharm., 415 (2011) 53-61.

[10] A. Laouini, C. Charcosset, H. Fessi, R. G. Holdich, G. T. Vladisavljevic. RSC Adv, 3 (2013) 4985-4994.

[11] A. Laouini, H. Fessi, C. Charcosset, J. Membr. Sci., 423-424 (2012) 85-96.

[12] Q. Z. Zhou, L. Y. Wang, G. H. Ma, Z. G. Su. J. Colloid Interface Sci., 311 (2007) 118-127.

[13] N. A. Wagdare, A. T. M. Marcelis, R. M. Boom, C. J. M. Van Rijn. J. Colloid Interface Sci., 355 (2011) 453-457.

[14] C. Charcosset, A. Al-Harati, H. Fessi. J. Control. Release., 108 (2005) 112-120.

[15] C. D'oria, C. Charcosset, A. A. Barresi, H. Fessi, Colloid. Surf. A., 338 (2009) 114-118.

[16] A. Trentin, M. Ferrando, F. Lopez, C. Guell. Desalination, 245 (2009) 388-395.

[17] E. A. van der Zwan, K. Schroen, K. van Dijke, R. Boom. Colloids Surf. A, 277 (2006) 223-229.

[18] A. Nazir, R. M. Boom, K. Schroen. Chem. Eng. Sci., 92 (2013) 190-197.

[19] J. Comiti, M. Renaud, Chem. Eng. Sci., 44 (1989) 1539-1545.

[20] G. T. Vladisavljevic, M. Shimizu, T. Nakashima. J. Membr. Sci., 244 (2004) 97-106.

[21] G. T. Vladisavljevic, M. Shimizu, T. Nakashima. J. Membr. Sci., 284 (2006) 373-383.

[22] G. T. Vladisavljevic, J. Surh, J. D. McClements. Langmuir, 22 (2006) 4526-4533.

[23] W. H. Jing, J. Wu, W. H. Xing, W. Q. Jin, N. P. Xu. AlChE J, 51 (2005) 1339-1345.

[24] M. Shima, Y. Kobayashi, T. Fujii, M. Tanaka, Y. Kimura, S. Adachi, et al. Food Hydrocolloids, 18 (2004) 61-70.

[25] K. Suzuki, I. Fujiki, Y. Hagura. Food Sci. Technol. Int., 4 (1998) 164-167.

[26] K. Suzuki, K. Hayakawa, Y. Hagura. Food Sci. Technol. Res., 5 (1999) 234-238.

[27] S. H. Park, T. Yamaguchi, S. Nakao. Chem. Eng. Sci., 56 (2001) 3539-3548.

Acknowledgments

The authors are grateful to the "*Frans Nederlandse Academie*" for their financial support.

The authors wish also to thank Sami Sahin for fruitful discussions and useful advices.

Caractérisation des aérosols générés et prédiction du niveau de dépôt pulmonaire

Caractérisation des aérosols générés et prédiction du niveau de dépôt pulmonaire

L'efficacité thérapeutique des aérosols dépend de la répartition en masse et du site de dépôt du principe actif inhalé. Malgré la complexité des paramètres physiques et physiologiques influençant le devenir des particules inhalées, la taille des particules exprimée en diamètre aérodynamique massique médian semble être le paramètre qui a le plus d'effet sur la déposition pulmonaire et par conséquent sur l'activité pharmacologique d'un aérosol.

Diverses techniques d'évaluation des préparations inhalables ont été décrites dans la littérature. Les techniques d'évaluation des aérosols *in vitro* permettent principalement une caractérisation dimensionnelle des particules. La diffraction laser et l'impaction inertielle sont deux méthodes largement utilisées pour mesurer le diamètre géométrique et aérodynamique des gouttelettes d'aérosol, respectivement.

La modélisation mathématique de la déposition pulmonaire a été développée pour une meilleure quantification et localisation des zones de dépôts des aérosols en fonction de la taille des particules. La modélisation consiste à décrire le système respiratoire par des relations mathématiques. L'interprétation des résultats permet de réaliser des simulations numériques afin de prévoir le trajet et le devenir des aérosols *in vivo*.

Le travail réalisé sur l'évaluation des aérosols constitue le fruit d'une collaboration entre le Laboratoire d'Automatique et de Génie des Procédés (LAGEP), le Laboratoire de Pharmacie Galénique de la Faculté de Pharmacie de Marseille et le Laboratoire Aerodrug de la Faculté de Médecine de Tours. Ce dernier chapitre de la thèse est présenté sous forme d'un article qui sera soumis pour publication. Il décrit les résultats de caractérisation de la taille des aérosols générés suite à la nébulisation des différents systèmes d'encapsulation de vitamine E précédemment développés (liposomes, micelles, nano-émulsion, particules lipidiques solides). Il présente aussi les résultats de prédiction mathématique du niveau de dépôt pulmonaire des aérosols générés et la fraction de la dose inhalée qui peut atteindre son site d'action.

Characterization of different vitamin E carriers intended for pulmonary drug delivery

A. Laouini[1], V. Andrieu[2], L. Vecellio[3], H. Fessi[1], C. Charcosset[1]

[1]: Université Claude Bernard Lyon 1, Laboratoire d'Automatique et de Génie des Procédés (LAGEP), UMR-CNRS 5007, CPE Lyon, Bât 308 G, 43 Boulevard du 11 Novembre 1918, F-69622 Villeurbanne Cedex, France.

[2]: Université Aix Marseille, Faculté de Pharmacie, Laboratoire de Pharmacie Galénique Industrielle, 27 Boulevard Jean Moulin 13385 Marseille Cedex 5, France.

[3]: Université François Rabelais de Tours, Faculté de Médecine, Laboratoire Aerodrug, Bâtiment M, 10 ter Boulevard Tonnellé 37032 Tours Cedex, France.

To be submitted

Abstract

The controlled release of drugs for pulmonary delivery is a research field which has been so far rather unexploited but is currently becoming increasingly attractive. Colloidal suspensions encapsulating vitamin E (liposomes, micelles, nano-emulsion, and solid lipid particles) were prepared using various methods based on membrane contactor. The suspensions were nebulised and aerodynamic characteristics of the generated aerosols were assessed using two different methods: laser light scattering and cascade impaction. When the laser diffraction technique was used, results showed that fine particle fractions (< 5 μm) were 19, 29, 38 and 71% for solid lipid particles, micelles, nano-emulsion and liposomes, respectively. When the impaction method was applied, using a next generation pharmaceutical impactor operated at 30 l/min, results showed that fine particle fractions were 39, 78, 82 and 87% for solid lipid particles, micelles, nano-emulsion and liposomes, respectively. The differences observed between the results obtained from both methods confirm that the laser diffraction method is not always suitable for aerodynamic characterization of aerosols and should be validated against an impaction method. Nebulisation of the drug-carrier suspensions led to an increase of their size. The size was increased by a factor of 2 to 26 depending on the encapsulation system. The most important aggregation was obtained with nano-emulsion; the less one with solid lipid particles. The mass median aerodynamic diameter (MMAD) of the generated aerosols ranged from 1.76 to 6.10 μm. The application of a mathematical model, the Multiple-Path Particle Dosimetry (MPPD), for the prediction of the pulmonary deposit gave encouraging results. The rate of vitamin E able to reach the lung ranged from 37.6 (for the liposomes) to 51.6% (for the micelles). The obtained results showed that the different systems developed for vitamin E encapsulation were suitable to target the lung after pulmonary administration by nebulisation.

Key words: drug-carrier, vitamin E encapsulation, aerosols, pulmonary administration, lung deposit

Contents

1. Introduction

Vitamin E, a natural antioxidant, has been tested to prevent cigarette smoke toxicity since several pulmonary disorders are mainly caused by oxidative stress phenomena **[1]**. Nevertheless, the use of conventional pharmaceutical forms (oral or intravenous administration) doesn't allow precise transport of vitamin E to its specific action site, the lung alveoli **[2]**. According to *Zaru et al.* **[3]**, pulmonary disorders can be efficiently treated only if high and prolonged drug concentrations are maintained in the lungs. Thus, pulmonary drug delivery has become an increasingly attractive route for administration of a wide spectrum of drug substances.

Pulmonary administration for the treatment of local lung disorders offers many advantages over other routes of administration. The direct deposition of the drug at the specific site could increase local drug concentration. This increase in local drug concentration may improve the pulmonary receptor occupancy and potentially reduces the overall dose required, thereby avoiding the side effects that result from high doses of drug and enhancing patient compliance **[4, 5]**.

A number of micrometer and nanometer sized drug carrier systems such as liposomes, micelles, nano-emulsion, microparticles, etc have been investigated as potential pulmonary delivery systems because of the many advantages they can offer: (i) a decrease in particle size leading to an increase in surface area and therefore an enhanced dissolution rate as well as a relatively uniform distribution of drug dose among the alveoli, (ii) an enhanced solubility of the drug than its own aqueous solubility, (iii) a sustained release of the drug in the lung tissue, and (iv) the potential of cell targeting due to the possibility of surface properties modifications **[6, 7]**.

As opposed to the intravenous or oral application of such drug delivery systems, the pulmonary application via inhalation is accompanied by several unique challenges. The major challenge is the atomization of the drug formulation in a suitable form for inhalation. It is generally accepted that aerosol particles of 1 – 5 μm are required for deposition in the alveolar region of the lung, which shows the highest drug absorption.

The aims of this study were to:
- assess the aerodynamic characteristics of aerosols generated by nebulisation of different drug-carrier systems encapsulating vitamin E.
- predict the pulmonary deposit of the aerosols particles and the rate of vitamin E that can reach its action site, the broncho-alveolar level.

2. Materials and methods

2.1 Materials

1.1.1. Tested suspensions

Four different drug-carriers encapsulating the vitamin E were prepared using membrane contactors (liposomes, micelles, nano-emulsion and solid lipid particles). The characteristics of these suspensions are summarized in **Table 1**.

1.1.2 Reagents

HPLC grade methanol and acetonitrile were supplied by Carlo Erba Reagenti (Milano, Italy) and used as such, without further purification. Ultra-pure water was obtained from a Millipore Synergy® system (Ultrapure Water System, Millipore, France).

1.1.3. Vitamin E delivery rate

The breathing simulator, used for the drug delivery rate determination, is a dual phase control respirator pump Model 613, also called large animal volume controlled ventilator (Havard Appartus, USA). The specifications of the apparatus used for this test are presented in **Table S1** in supplementary material.

Filter Pads were supplied by Pari Gmbh (Starnberg, Germany); these low-resistance filters are capable of collecting the aerosol and enable recovery of the active substance with an appropriate solvent. The electronic nebulizer “eflow rapid” was also purchased from Pari Gmbh.

1.1.4 Aerodynamic assessment of nebulised aerosols

Nebulised products were characterized for their size using 2 methods. The first technique was based on laser light scattering and used the Mastersizer 2000 particle size analyzer (Malvern, United Kingdom). The second technique was based on cascade impaction and used a next generation pharmaceutical impactor supplied by Copley scientific (Nottingham, United Kingdom). The impactor configuration is shown in **Figure S1** in supplementary material. There are 3 main sections in the impactor: (i) the bottom frame that holds the removable impaction cups, (ii) the seal body that holds the jets, and (iii) the lid that contains the interstage passageways. In routine operation, the seal body and lid are held together as a single assembly. The impaction cups are accessible when this assembly is opened at the end of an inhaler test. The impaction cups are held in a support tray so that all cups could be removed from the impactor simultaneously by lifting out the tray. The flow passes through the impactor in a saw-tooth pattern.

Table 1. Characteristics of the preparations tested

Drug carrier	Formulation	Type of membrane used for the preparation process	Preparation characteristics			Reference
			Size (nm)	Zeta potential (mV)	Encapsulation efficiency (%)	
Nano-emulsion	- Water 80% - MCT oil 12.75% - Surfactants (Tween 80 + Brij 35) 2.25% - Vitamine E 5%	SPG membrane (pore size: 0.9 µm)	106	-16.5	99.7	**[8]**
Liposomes	- Water 99.4% - Lipoid E80 0.4% - Cholesterol 0.1% - Vitamine E 0.1%	Microsieve membrane (pore size: 10 µm – interpore distance: 200 µm)	96	-28.5	99.9	**[9, 10]**
Micelles	- Water 99.93% - PEG-PCL polymer 0.02% - Vitamine E 0.05%		154	-19.3	87.4	**[11]**
Solid lipid particles	- Water 91.2% - Precirol 6.5% - Tween 80 1.8% - Vitamine E 0.5%	Ceramic membrane KERASEP (pore size: 10.2 µm)	2510			Submitted work

1.1.5 Mathematical model for pulmonary deposit prediction

The Multiple-Path Particle Dosimetry (MPPD) model, version 2.9, was used for the prediction of the pulmonary deposit. The model was originally developed jointly by the Chemical Industry Institute of Toxicology (CIIT, currently The Hamner Institutes for Health Sciences, USA) and the National Institute for Public Health and the Environment (RIVM, Netherlands). The MPPD model calculates the deposition and clearance of monodisperse and polydisperse aerosols in the respiratory tracts of rats and human for particles ranging in size from ultrafine (0.01 μm) to coarse (20 μm). The multiple-path method calculates particle deposition in all airways of the lung and provides lobar-specific and airway-specific information. Within each airway, deposition is calculated using theoretically derived efficiencies for deposition by diffusion, sedimentation, and impaction within the airway or airway bifurcation. Filtration of aerosols by the nose and mouth is determined using empirical efficiency functions **[12]**.

2.2 Methods

Products used for nebulisation and intended for pulmonary delivery are characterized using the following tests: (i) active substance delivery rate, and (ii) aerodynamic assessment of the nebulised aerosols. These tests standardize the approach given to the assessment of the dose that would be delivered to a patient.

2.2.1 Vitamin E delivery rate

This test was performed to assess the delivery rate of the active substance to the patient using standardized conditions of volumetric flow rate. The method used a standard breathing pattern defined for adults. It is essential to use breathing patterns rather than continuous flow rates to provide a more appropriate measure of the mass of active substance that would be delivered to patients. In this test, the filter (contained in the filter holder) was attached to the breath simulator as shown in **Figure 1**. The mouthpiece of the nebuliser was attached to the inhalation filter using an adapter in order to ensure airtight connections. The breathing simulator was set to generate the breathing pattern specified in **Table S1**. At the beginning of an inhalation cycle, the nebulizer was started and kept in operation for 60 s. The mass of vitamin E collected on the filters was determined using an HPLC method (see section **2.2.3**). The active substance delivery rate was then calculated by dividing the mass of vitamin E collected on the inhalation filter by the collection time.

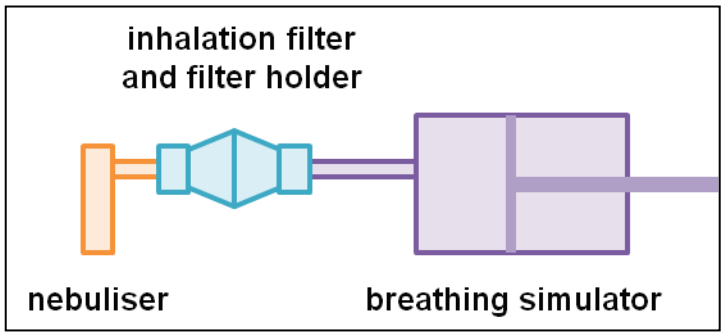

Figure 1. Experimental set-up used for vitamin E delivery rate determination.

2.2.2 Aerodynamic assessment of nebulised aerosols

Laser light scattering

Each pharmaceutical suspension (3 ml) was nebulised. The nebulizer mouthpiece was held approximately 1 cm from the center of the laser beam so that the air, containing the generated aerosol, is directed in a well defined steam through the laser beam of the particle size analyzer. The redirected laser light was detected by a photo detector; the amplitude of light scattered was then measured and size distribution results were displayed. All experiments were performed at room temperature (25 - 30 °C) and relative humidity of 80 – 85 %; three replicates of each measurement were performed.

Cascade impaction

The impaction cups were placed in the cup tray which was inserted then into the bottom frame of the impactor. The impactor lid was hermetically closed using the handle so that the system is airtight. The induction port was connected to the impactor inlet and a suitable mouthpiece adapter was placed at the end of the induction port to allow its connection to the nebulizer. A pump was connected to the outlet of the impactor and air flow was adjusted to 30 l/min. For each test, 5 ml of each pharmaceutical suspension was introduced in the nebulizer. The pump was switched on followed after 15 s by the suspension nebulisation. A schematic presentation of the experimental set-up is shown in **Figure 2**.

At the end of the test, the induction port was removed and the impactor was opened by releasing the handle. The cup tray holding the impaction cups was then removed and the vitamin E collected in each cup was dissolved in methanol. The mass of vitamin E collected on the filters was determined using an HPLC method (see section **2.2.3**). This test was repeated 3 times for each pharmaceutical suspension.

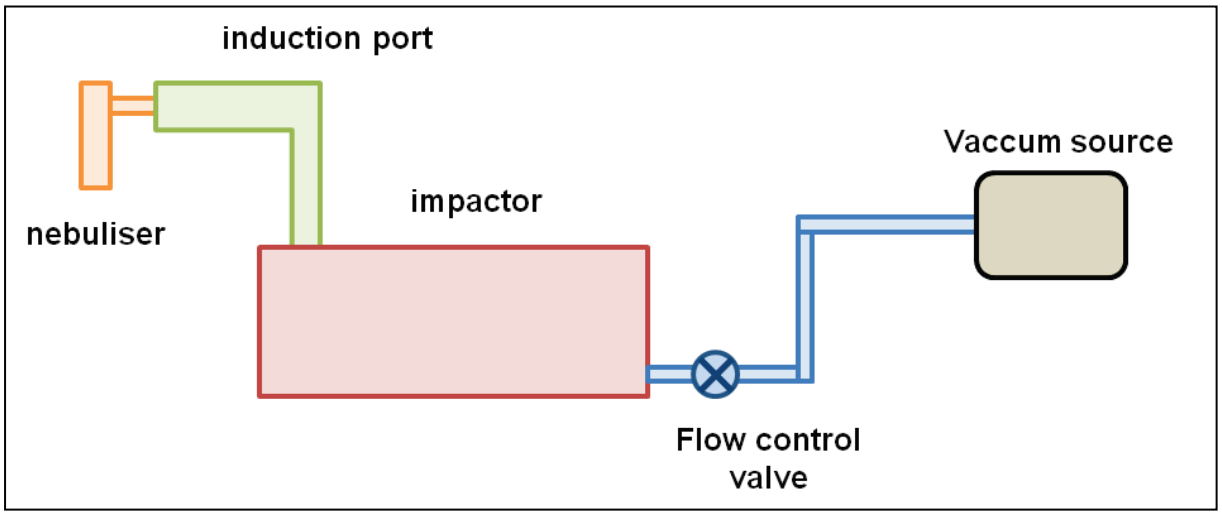

Figure 2. Experimental set-up for measuring the size distribution of aerosols

Calculation of the aerodynamic parameters

The cumulative mass fraction of vitamin E was plotted versus the cut-off diameters; the plot was then used to determine the values of the mass median aerodynamic diameter (MMAD) and the fine particles (less than 5 µm) dose (FPD). The geometric standard deviation (GSD) was calculated according to the following equation:

$$GSD = \sqrt{\frac{d84.1\%}{d15.9\%}} \quad (1)$$

where $d_{84.1\%}$ and $d_{15.9\%}$ are the particles diameters at 15.9 and 84.1 % of the cumulative particles number, respectively.

2.2.3 Vitamin E assay

The concentration of vitamin E was determined using an HPLC system (Spactra System SCM 1000, Rhode Island, USA). The HPLC equipment consisted of a P1000XR pump, an AS3000 autosampler and an UV6000LP UV/VIS detector. The column was a LiChrospher RP C18 column (5 mm, 15 cm × 0.46 cm) (Supelco, Bellefonte, USA). The separation was carried out using a mixture of methanol and water (96:4 v/v) as the mobile phase at a flow rate of 1.6 ml/min. The eluent was monitored at 292 nm and peaks were recorded using the chromatography data system software Chromo-Quest version 5.0 (Thermo Fisher Scientific, Philadelphia, USA). It should be noted that before chromatographic data were collected, the column was equilibrated for 30 min with a minimum of 30 column volumes. At the end of the assay, a washing of the column was performed using water–acetonitrile (50:50 v/v) for 60 min. This HPLC analytical method was validated as usually required (data not shown).

2.2.4 Pulmonary deposit prediction

In order to predict the aerosol pulmonary deposit using the MMPD model, the following parameters were fixed as follow:
- The functional residual capacity “FRC” (volume of air present in the lungs at the end of a passive expiration) = 2800 ml.
- Upper respiratory tract “URT” volume (volume of the nasal cavity, larynx and trachea) = 50 ml.
- Breathing frequency, also called pulmonary ventilation rate (number of breaths taken within a set amount of time) = 15/min.
- Tidal volume (the lung volume representing the normal volume of air displaced between normal inspiration and expiration) = 500 ml.
- Inspiratory fraction (inspiratory-to-total lung capacity ratio) = 0.5.

In addition to these parameters, aerodynamic characteristics of the aerosol particles (MMAD and ETG) have been entered. The model predicts the percentage of the aerosol deposited in each region of the respiratory tract: (i) ear, nose and throat “ENT” sphere, (ii) peripheral lung and (iii) central lung.

3. Results and discussion

3.1 Vitamin E delivery rate

The delivery rate of vitamin E was assessed for the different drug-carriers (**Table 2**).

Table2. Vitamin E delivery rate from various nebulised suspensions

Preparation	Delivery rate* (mg/min)
Nano-emulsion	13.43 ± 0.50
Liposomes	0.42 ± 0.01
Micelles	0.23 ± 0.01
Solid lipid particles	1.00 ± 0.01

*: Values represent the mean ± S.D. (n=3)

Active substance delivery rate is an important characteristic of aerosols since it allows the delivered mass of active substance to be characterized in a standard way regardless of the nebulizer used. In our study, the highest delivery rate was obtained with nano-emulsion preparation; the lowest one was obtained with micelles. This result could be explained by the vitamin E concentration in each suspension which was the highest for the nano-emulsion and the lowest for micelles (**Table 1**).

3.2 Aerodynamic assessment of nebulised aerosols

Light scattering counters are used for the determination of the size distribution of aerosols particles. The intensity of light scattered into a certain solid angle is measured

and used to determine particle size by electronically classifying response pulses according to their magnitude. A comparison of the MMAD, GSD and FPD of the four colloidal suspensions is presented in **Table 3**. A difference of size could be noticed between the particles in the to-be-nebulised suspensions and those present in the nebulised aerosols. Indeed, after nebulisation, the particle size increased by a factor of 3, 37, 39 and 52 for solid lipid particles, micelles, liposomes and nano-emulsion, repectively. This increase in size could be explained by particles aggregation that occurred during aerosols formation.

Table 3. The aerosols aerodynamic parameters assessed by laser diffraction analyzer.

Preparation	DAMM* (µm)	Size increase ratio	GSD*	FPD* (%)
Nano-emulsion	5.58 ± 0.09	52	1.58 ± 0.03	38.3 ± 1.4
Liposomes	3.79 ± 0.06	39	1.55 ± 0.01	71.3 ± 1.1
Micelles	5.84 ± 0.03	37	1.42 ± 0.04	29.3 ± 1.4
Solid lipid particles	7.73 ± 0.06	3	1.68 ± 0.04	19.3 ± 0.7

*: Values represent the mean ± S.D. (n=3)

Size distribution of generated aerosols was also determined using a cascade impaction method; results are shown in **Table 4**. As previously noticed, the particle size increased when the suspension were nebulised. The size was multiplied by a fold-factor of 2, 20, 18 and 26 for solid lipid particles, micelles, liposomes and nano-emulsion, repectively. Several previous studies have shown that the aerosolization of colloidal systems would enhance their aggregation which is dependent on the nebulizer design. No specific correlation was found between the initial size and the size of the nebulized droplets **[13, 14]**. For instance, the mass median diameters of aerosols generated upon nebulization were 2 to 20 folds larger than primary geometric particle diameters **[15]**

Table 4. The aerosols aerodynamic parameters assessed by cascade impaction.

Preparation	DAMM* (µm)	Size increase ratio	GSD*	FPD* (%)
Nano-emulsion	2.83 ± 0.09	26	1.98 ± 0.08	82.4 ± 2.5
Liposomes	1.73 ± 0.05	18	1.56 ± 0.05	87.1 ± 2.3
Micelles	3.16 ± 0.05	20	1.65 ± 0.06	78.0 ± 1.7
Solid lipid particles	6.10 ± 0.08	2	2.15 ± 0.04	39.6 ± 1.1

*: Values represent the mean ± S.D. (n=3)

It can be seen that the results obtained from both methods are quite different. Larger aerosols particle sizes are obtained when the light scattering method was used. Indeed, this technique works on the assumption that within a certain volume illuminated there is only one particle present; thus determination of the particle size from the light response may not be very reliable. Moreover, this technique presents other limits: not

all the aerosol is uniformly illuminated and not all particles spend the same time in the illuminated volume **[16, 17]**.

Unlike the cascade impaction technique, the light scattering method doesn't detect the active substance; rather it measures the size distribution of the aerosols droplets irrespective of their content. This may not be a problem with homogenous solutions, but it may result in significant error if the product to be nebulised is a suspension, as in our study. Cascade impactor technique enables the aerosol to be characterized unambiguously in terms of the mass of active substance as a function of aerodynamic diameter.

Although the laser light scattering instrument can provide rapid size distribution measurements of nebulizer-generated aerosols, this technique may be used only if it has been validated against a cascade impaction method. In our study, the preparations to be nebulised are colloidal suspensions; the impaction method seems to be the only suitable one for aerodynamic assessment.

On another hand, both size characterization methods showed that during the nebulisation, the highest aggregation was obtained with nano-emulsion and the lowest one with solid lipid particles. This observation shows that during suspension aerosolisation, solid lipid particles system, in which the dispersed phase is solid, is more stable than the nano-emulsion system, in which the dispersed phase is liquid. Liposomes and micelles showed similar aggregation behavior, this could be explained by the fact that both vesicles have similar composition (composed by amphiphiles molecules).

3.3 Pulmonary deposit prediction

In order to reach the lower respiratory tract, aerosols need to present aerodynamic diameters between 1 and 5 µm. Large particles impact in the oro-pharynx while submicron particles remains suspended in the air and are exhaled **[18]**. *Sung et al.* **[19]** reported that particles with aerodynamic diameter of 1 to 3 µm deposit optimally in the alveolar region of the lungs.

In this study, the MMAD of the different drug-carriers ranged from 1.76 to 6.10 µm which seems to be suitable to reach the broncho-alveolar region. In order to confirm the drug deposition, a mathematical model (MPPD) was applied and obtained results are reported in **Figure 3**.

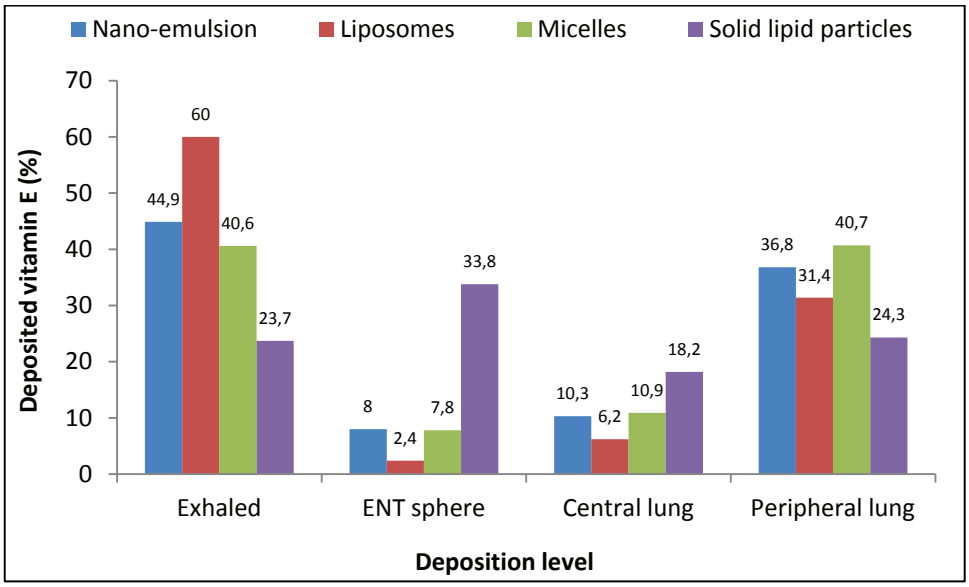

Figure 3. Vitamin E deposition level as predicted by the MMPD model for different drug-carriers. Modeling parameters: human 21 years old, body orientation: upright, breathing scenario: mouth only. Other parameters are specified in section **2.2.4**.

The highest exhalation rate (60%) was observed with liposomes (MMAD of 1.76 μm) and the lowest one (23.7%) was observed with solid lipid particles (MMAD of 6.1 μm). Due to its size, the latter system was mostly retained in the ENT sphere and only ¼ of the inhaled dose could reach the alveoli. It is evident that the suitable drug-carrier systems for vitamin E delivery are: micelles and nano-emulsion. When loaded within micelles, only 40.6% of vitamin E is exhaled and 51.6% could reach the lung (peripheral and central). When encapsulated within nano-emulsion, 47.1% of the inhaled dose could reach the lung versus an exhalation of 44.9% of the dose.

Liposomes are one of the most extensively investigated systems for controlled delivery of drug to the lung. This colloidal form is particularly appropriate for therapeutic agent delivery to the lung, since vesicles are prepared from compounds endogenous to the lungs, such as the components of lung surfactant, and these properties make liposomes attractive candidates as drug delivery vehicles **[20]**. However, concerns arise from drug stability in the liquid state and leakage when nebulizers are used to deliver a liposomal encapsulated agent **[21]**. Solid lipid particles (SLP) are made from solid lipids (at room temperature), surfactants and water. Since the beginning of the 1990s, the SLP have been investigated as an alternative to other drug delivery systems. The main advantage of SLP is the high tolerability in the lungs especially when prepared using physiological lipids with little or no cytotoxicity **[22]**. Although they seem to be suitable drug carriers for lung delivery, especially due to their biocompatibility, liposomes and solid lipid particles could not be convenient systems in our study because of their size. The MMAD values of these carriers allow prediction of either high exhalation rate or high retention by the upper respiratory tract.

Therapeutically used micelles are composed of biodegradable or biocompatible polymers such as polycaprolactone (PCL) or polyethylene glycol (PEG). Micelles are attractive drug delivery systems due to their biocompatibility, surface modification capability and sustained release properties. In addition, compared to liposomal formulations, the presence of polymers confers to micelles a greater stability during the nebulisation process, thus eliminating the possibility of drug leakage **[23]**. In our study, micelles with a mean size of 154 nm generated aerosols with a MMAD of 3.06 µm. In addition, more than the half of the inhaled dose could reach its action site.

Concerning nano-emulsions, until now they have not yet been fully exploited for pulmonary drug delivery and very little has been published in this area. Extensive studies are required for a successful formulation of inhalable nano-emulsions due to possible adverse effects of surfactants and oils on lung alveoli function (adverse interactions with lung surfactant) **[24]**. In our study, the nano-emulsion system seems to be a promising way for vitamin E delivery to the lung since that half of the administrated dose could reach the broncho-alveolar level.

4. Conclusion

In this study, different systems for vitamin E encapsulation were characterized in terms of aerodynamic parameters using laser diffraction and cascade impaction techniques. The standard inertial impaction method, which describes the phenomenon of the deposition of aerosol particles on the walls of an airway conduct, remains the most reliable one to measure particle aerodynamic size of pharmaceutical aerosol delivery systems. Obtained results showed that during nebulisation, aggregation was the highest for the nano-emulsion (size increased by a 26 fold-factor).

A balance between exhaled and lung deposited drug rates exists and it depends on the aerosols particle size. For small sizes, the nebulised suspension is mostly exhaled; for example after their nebulisation, liposomes generated particles with a size of 1.76 µm and 60% of the administrated dose was predicted to be exhaled. Larger sizes of the nebulised suspension led to its retention in the upper respiratory tract; for instance when nebulised, solid lipid particles aggregate to form particles with a size of 6.10 µm and a third of the dose was retained in the ENT sphere. In this study, micelles and nano-emulsions present the highest deposition rate in the broncho-alveolar level; around 50% of the inhaled dose was predicted to reach the lung. Among these two systems, nano-emulsion presents the highest vitamin E delivery rate (13.43 mg/min).

Few studies have investigated the use of nano-emulsions in pulmonary drug delivery. Thus the nebulization of nano-emulsions would be a new and upcoming research area since that these sytems offer the potential to improve targeting, release and therapeutic

effects of drugs. Coming work includes an *in-vivo* administration of vitamin E loaded nano-emulsion to rats in order to confirm its safety and therapeutic efficiency.

Supplementary material

Table S1. Breathing simulator specifications

Tidal volume (ml)	Frequency (cycles / min)	Waveform	Inhalation / exhalation ratio
500	15	Sinusoidal	1:1

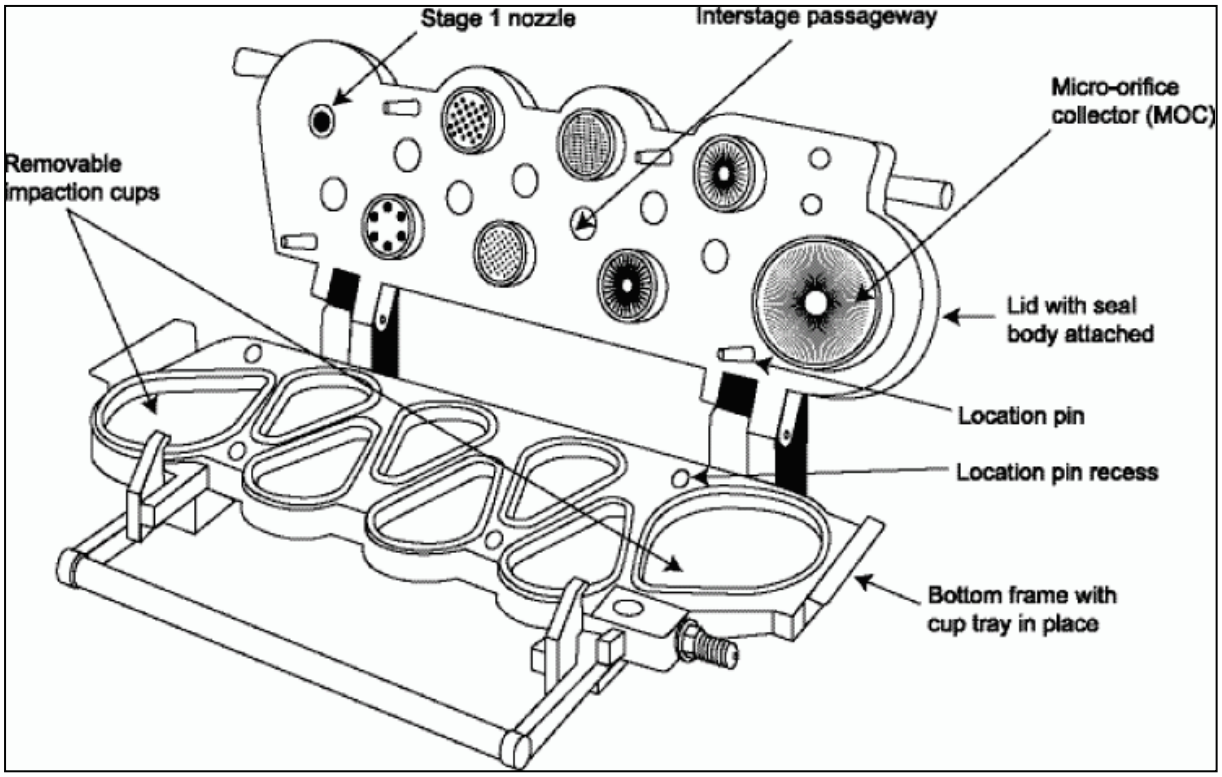

Figure S1. Next generation pharmaceutical impactor configuration.

References

[1] M. Scherrer-Crosbie, M. Paul, M. Meignan, E. Dahan, G. Lagrue, G. Atlan, et al. Pulmonary clearance and lung function: influence of acute tobacco intoxication and of vitamin E. Journal of Applied Physiology 81 (1996) 1071–1077.

[2] Y. Kato, K. Watanabe, M. Nakakura, T. Hosokawa, E. Hayakawa, K. Ito. Blood clearance and tissue distribution of various formulations of alpha-tocopherol injection after intravenous administration. Chemical and Pharmaceutical Bulletin 41 (1993) 599–604.

[3] M. Zaru, S. Mourtas, P. Klepetsanis, A. M. Fadda, S. G. Antimisiaris. Liposomes for drug delivery to the lungs by nebulization. European Journal of Pharmaceutics and Biopharmaceutics 67 (2007) 655-666.

[4] M. M. Bailey and C. J. Berkland. Nanoparticle formulations in pulmonary drug delivery. Medicinal Research Reviews 29 (2009) 196-212.

[5] R. O. Cook, R. K. Pannu, I. W. Kellaway. Novel sustained release microspheres for pulmonary drug delivery. Journal of Controlled Release 104 (2005) 79-90.

[6] W. Yang, J. I. Peters, R. O. Williams. Inhaled nanoparticles – A current review. International Journal of Pharmaceutics 356 (2008) 239-247.

[7] J. S. Patton and P. R. Byron. Inhaling medicines: delivering drugs to the body through the lungs. Nature Review Drug Discovery 6 (2007) 67-74

[8] A. Laouini, H. Fessi, C. Charcosset. Membrane emulsification: A promising alternative for vitamin E encapsulation within nano-emulsion. Journal of Membrane Science 423-424 (2012) 85-96.

[9] A. Laouini, C. Charcosset, H. Fessi, R. G. Holdich, G. T. Vladisavljevic. Preparation of liposomes: a novel application of microengineered membranes - investigation of the process parameters and application to the encapsulation of vitamin E. RSC Advances 3 (2013) 4985-4994.

[10] A. Laouini, C. Charcosset, H. Fessi, R. G. Holdich, G. T. Vladisavljevic. Preparation of liposomes: a novel application of microengineered membranes – From laboratory scale to large scale. Colloids and Surface B 112 (2013) 272-278.

[11] A. Laouini, K. P. Koutroumanis, C. Charcosset, S. Georgiadou, H. Fessi, R. G. Holdich, G. T. Vladisavljevic. pH-sensitive micelles for targeted drug delivery prepared using a novel membrane contactor method. ACS Applied Materials and Interfaces 5 (2013) 8939-8947.

[12] S. Anjilvel and B. Asgharia. A multiple-path model of particle deposition in the rat lung. Fundamental and Applied Toxicology 28 (1995) 41-50.

[13] L. A. Dailey, T. Schmel, T. Gessler, M. Wittmar, F. Grimminger, W. Seeger, et al. Nebulization of biodegradable nanoparticles: Impact of nebulizer technology and nanoparticle characteristics on aerosol features. Journal of Controlled Release 86 (2003) 131–144.

[14] O. N. M. Mc Callion, K. M. G. Taylor, M. Thomas, A. J. Taylor. Nebulisation of monodisperse latex sphere suspensions in air jet and ultrasonic nebulisers. International Journal of Pharmaceutics 133 (1996) 203–214.

[15] C. Bosquillon, P. G. Rouxhet, F. Ahimou, D. Simon, C. Culot, V. Preat, et al. Aerosolization properties, surface composition and physical state of spray-dried protein powders. Journal of Controlled Release 99 (2004) 357–367.

[16] R. G. Pinnick and D. J. Hofmann. Efficiency of light-scattering aerosol particle counters. Applied Optics 12 (1973) 2593-2597.

[17] F. Oeseburg. The inftuence of the aperture of the optical system of aerosol particle counters on the response curve. Aerosol Science 3 (1972) 307-311.

[18] J. Heyder, J. Gebhart, G.Rudolf, C. F. Schiller and W. Stahlhofen. Deposition of particles in the human respiratory tract in the size range 0.005 – 15 μm. Journal of Aerosols Science 17 (1986) 811-825.

[19] J. C. Sung, B. L. Pulliam and D. A. Edwards. Nanoparticles for drug delivery to lungs. Trends in Biotechnology 25 (2007) 563-570

[20] H. Schreir, R. J. Gonzalez-Rothi, A. A. Stecenko. Pulmonary delivery of liposomes. Journal of Controlled Release 24 (1993) 209-223.

[21] K. M. G. Taylor, G. Taylor, I. W. Kellaway, J. Stevens. The stability of liposomes to nebulization. International Journal of Pharmaceutics 58 (1990) 57-61.

[22] R. H. Muller, D. Ruhl, S. Runge, K. Schulz-Forster, W. Mehnert. Cytotoxicity of solid lipid nanoparticles as a function of the lipid matrix and the surfactant. Pharmaceutical Research 14 (1997) 458-462.

[23] P. A. Bridges and K. M. G. Taylor. Nebulisers for the generation of liposomal aerosols. International Journal of Pharmaceutics 173 (1998) 117-125.

[24] M. Bivas-Benita, M. Oudshoorn and S. Romeijn. Cationic submicronic emulsions for pulmonary DNA immunization. Journal of Controlled Release 100 (2004) 145-155.

Conclusion

Conclusion

L'objectif de ce travail de recherche consiste à mettre au point différents systèmes de vecteurs encapsulant la vitamine E destinés à une administration pulmonaire par nébulisation. La vitamine E est un antioxydant physiologique qui peut être utilisé pour lutter contre les effets du stress oxydatif en particulier ceux observés au niveau pulmonaire. Malheureusement, l'administration de la vitamine E par voie orale ou intraveineuse ne permet pas d'atteindre une concentration efficace au niveau pulmonaire. L'encapsulation de la vitamine E dans des vecteurs inhalables devrait donc permettre d'améliorer son efficacité thérapeutique. Différents vecteurs de vitamine E ont été développés au cours de ce travail par des procédés de préparation basé sur l'utilisation de contacteurs à membrane. Il s'agit d'un procédé dont le principal avantage est la possibilité de transposition à l'échelle industrielle. De plus, les procédés de fabrication à base de contacteurs à membrane permettent de préparer des particules de distribution de taille convenable et ce sans apport conséquent d'énergie comparé aux méthodes conventionnelles appliquées à la préparation des systèmes colloïdaux.

Les liposomes représentent le système vectoriel le plus largement étudié pour la voie pulmonaire principalement en raison de la présence de phospholipides, composant majeure du surfactant pulmonaire, dans leur formulation. La première partie expérimentale de cette thèse aborde la préparation des liposomes en utilisant des membranes microsieves. La particularité de ces membranes réside dans l'uniformité de la taille des pores et des distances inter-pores. La taille des liposomes obtenus était influencée par la concentration des phospholipides, le débit d'injection de la phase organique dans la phase aqueuse, le rapport des volumes des deux phases, la vitesse d'agitation et la microstructure de la membrane. Ce qui signifie que la taille des liposomes peut être contrôlée par un choix judicieux des paramètres opératoires. Le procédé optimisé a permis de préparer des liposomes encapsulant la vitamine E ayant une taille de 96 ± 3 nm, un potentiel zêta de -28.5 ± 0.8 mV et un taux d'encapsulation de 98.8 ± 1.1 %. Ce procédé présentait une très bonne reproductibilité et les suspensions liposomales étaient stables pendant une période de 3 mois. L'étude du procédé à l'échelle du laboratoire qui a été faite en utilisant une cellule d'agitation, a permis de préparer 73 ml par cycle de préparation. Pour une production continue et à échelle plus large, d'autres dispositifs ont été testés. Le premier est un système membranaire à circulation tangentielle et le deuxième un système membranaire doté de mouvements d'oscillations à l'intérieur de la phase continue. Un scale-up d'un facteur 8 a été réalisé tout en gardant les mêmes conditions expérimentales pour tous les systèmes étudiés. Les résultats ont montré qu'avec le système de circulation tangentielle la

taille obtenue était plus élevée et la distribution de taille plus large. Ceci est certainement dû à la recirculation de la suspension de liposomes lors du procédé de fabrication. Seul le système oscillant a permis de reproduire à large échelle les résultats obtenus à plus petite échelle (en termes de taille et de distribution de la taille). Ceci confirme le potentiel des contacteurs à membrane dans l'intensification des procédés industriels de production des liposomes.

La deuxième partie expérimentale de cette thèse porte sur l'élaboration et la caractérisation d'une nano-émulsion chargée en vitamine E en utilisant des membranes SPG. Les nano-émulsions présentent de nombreux avantages comparés aux microémulsions dont principalement une meilleure stabilité, une capacité d'encapsulation plus élevée et une utilisation moindre de tensioactifs. Préalablement à l'étude du procédé de fabrication, une optimisation de la formulation a été réalisée. Le choix de l'huile et des tensioactifs a été déterminé à partir d'une étude de solubilité de la vitamine E et de la construction de diagrammes de phases ternaires qui ont permis de détecter les zones de formation de nano-émulsion stable. Le dispositif membranaire utilisé est constitué d'une membrane tubulaire SPG à l'intérieur de laquelle circule la phase aqueuse de façon tangentielle. L'influence des paramètres opératoires sur les caractéristiques de la nano-émulsion a été étudiée et a montré que les meilleurs résultats sont obtenus avec la plus faible pression transmembranaire, le débit de la phase continue le plus élevé et la vitesse d'agitation la plus élevée. Pour ces conditions optimales, le procédé de fabrication appliqué à l'encapsulation de la vitamine E a conduit à la préparation de nano-émulsions de taille égale à 106 ± 3 nm, de potentiel zeta égal à -16.5 ± 0.8 mV et avec un taux d'encapsulation de 99.7 ± 0.4%. Les préparations étaient stables pendant 2 mois. Le procédé de fabrication ainsi optimisé était simple, rapide, reproductible et permettait la production contrôlée de nano-émulsion de taille convenable.

La troisième partie de notre étude expérimentale consistait à l'encapsulation de la vitamine E dans des micelles polymériques. Les copolymères ayant servi à la préparation des micelles ont été synthétisé dans le but d'avoir une réponse sensible au changement de pH. La méthode de préparation des micelles impliquait l'utilisation des membranes microsieves et le procédé était optimisé comme précédemment détaillé. Les résultats ont de nouveau confirmé la possibilité d'ajuster la taille des micelles par le choix des paramètres opératoires. Au terme de l'optimisation du procédé de fabrication, des micelles de taille égale à 146 ± 7 nm et de potentiel zêta égal à -19.5 ± 0.2 mV ont été préparés avec un taux d'encapsulation de 89%.

Le dernier système de vectorisation de la vitamine E, auquel a été consacrée la quatrième partie de l'étude expérimentale, porte sur les particules lipidiques

solides. Ces systèmes d'encapsulation de principes actifs associent les avantages des systèmes conventionnels (liposomes, micelles, etc) tout en évitant leurs inconvénients en particulier l'utilisation des solvants organiques lors de la préparation. L'émulsification directe par utilisation des membranes en céramique, a conduit à la formation de particules ayant une taille moyenne de 2.5 µm. L'inconvénient majeure était le colmatage de la membrane qui conduisait à une taille maximale du lot, pouvant être préparé par cette méthode, inférieure à 93 kg/m^2 de surface membranaire. L'alternative qui a été envisagée consistait à l'utilisation d'un lit de billes en verre pour réaliser une « premix emulsification ». Ces systèmes qualifiés de « membranes dynamiques », par opposition aux membranes conventionnelles, permettent de limiter le problème du colmatage puisque le nettoyage du lit de billes est plus aisé comparé à celui des membranes classiques. La méthode de « premix emulsification » consistait à préparer une émulsion grossière de taille moyenne voisine de 5 µm, puis réduire la taille des gouttelettes par passages successifs à travers le lit de billes en verre. Ainsi, sous une pression de 2 bar, après 6 passages à travers un lit de 2 mm de hauteur et constitué par des billes de 63 µm de diamètre, la taille moyenne des gouttelettes de l'émulsion de départ s'est trouvée réduite à 1.5 µm. Ce procédé a permis non seulement la préparation de particules de taille plus petite, mais également de réduire considérablement le colmatage des membranes. En effet, grâce à cette méthode, la taille du lot a atteint 851 kg/m^2 de surface membranaire avec la possibilité de réaliser un système de production en mode continu.

La dernière partie de cette thèse consistait à caractériser les suspensions nébulisées en utilisant deux méthodes différentes : la granulométrie laser et l'impaction à cascade. Les résultats ont confirmé que la méthode de référence pour l'évaluation de la taille des aérosols est l'impaction à cascade. Lors de la nébulisation, une augmentation de la taille a été observée et les diamètres aérodynamiques des aérosols pour les différentes formes de vecteurs ont été compris entre 1.73 et 6.10 µm. Les paramètres aérodynamiques ainsi déterminés ont constitués des données d'entrée pour un modèle mathématique, Le MPPD (Multiple-Path Particle Dosimetry), qui a permis de prévoir le devenir des particules après leur nébulisation. Les résultats ont montré que les micelles, ayant une taille initiale de 154 nm, permettent de générer des aérosols d'une taille de 3.16 µm (soit une augmentation de taille des particules d'un facteur 20 suite à nébulisation). Avec ces caractéristiques, le modèle permet de prévoir que plus de la moitié de la dose inhalée pourrait atteindre son site d'action alvéolo-pulmonaire.

En conclusion, nous avons réussi à préparer et caractériser quatre types de vecteurs pour l'encapsulation de la vitamine E (liposomes, nano-émulsion, micelles et particules lipidiques solides). La préparation est basée sur divers type de

contacteurs à membrane. Pour chaque forme colloïdale, une étude a été conduite systématiquement afin de déterminer l'influence des conditions opératoires sur le procédé de fabrication. Ceci a permis d'obtenir des vecteurs de taille convenable, stable dans le temps et avec un taux d'encapsulation satisfaisant. La déposition pulmonaire simulée *in vitro* en appliquant un modèle mathématique a permis de prévoir une déposition optimale de la vitamine E au niveau du tractus pulmonaire.

Les perspectives de ce travail comportent une étude *in vivo* ayant pour objectif la visualisation du dépôt pulmonaire des vecteurs de vitamine E chez des rats et éventuellement une étude clinique afin de vérifier l'efficacité thérapeutique de nos préparations dans le traitement des symptômes liés au stress oxydatif au niveau pulmonaire.

Valorisation de la thèse

Communications orales

1- 15th Asian Chemical Congress, Singapour – Du 19 au 23 Août 2013:

Preparation of liposomes using microengineered membranes: Investigation of the process parameters with a stirred cell device and study of the scale-up from laboratory scale to large scale. A. Laouini, C. Charcosset, H. Fessi, R. G. Holdich, G. T. Vladisavljevic.

2- 4th International Conference on Colloid Chemistry and Physicochemical Mechanics, Moscou – Du 30 Juin au 5 Juillet 2013:

pH-sensitive micelles for targeted drug delivery prepared with a novel method using a membrane contactor. A. Laouini, K. P. Koutroumanis, C. Charcosset, S. Georgiadou, H Fessi, R. G. Holdich, G. T. Vladisavljevic.

3- Formula VII Conference, Mulhouse – Du 1er au 4 Juillet 2013:

Production of liposomes using microengineered membrane and co-flow microfluidic device. G. T. Vladisavljevic, A. Laouini, C. Charcosset, H. Fessi, R. G. Holdich.

4- 14th European PhD Student Colloid Conference, Berlin – Du 10 au 13 Juin 2013:

Investigation of liposomes preparation using microengineered membranes. A. Laouini, C. Charcosset, H. Fessi, R. G. Holdich, G. T. Vladisavljevic.

5- International Colloid and Surface Symposium, Londres – Du 4 au 6 Juillet 2011:

Influence of process parameters on liposome preparation using a membrane contactor. A. Laouini, C. Jaafar-Maalej, S. Sfar-Gandoura, C. Charcosset, H. Fessi.

Communications par affiche

1- Euromembrane Conference, Londres – Du 23 au 27 Septembre 2012:

Preparation of nano-emulsions using SPG membrane emulsification – Application to vitamin E encapsulation. A. Laouini, H. Fessi, C. Charcosset.

2- Colloids and Nanomedecine Conference, Amsterdam – Du 15 au 17 Juillet 2012:

SPG membrane emulsification as a promising alternative for the encapsulation of the vitamin E: Optimisation of process parameters and stability evaluation of the prepared nanoemulsions. A. Laouini, H. Fessi, C. Charcosset.

3- UK Particle Technology Forum. Loughborough – Du 4 au 5 Avril 2012:

Investigation of the preparation of mono-dispersed liposomes suspension using microsieve membranes. A. Laouini, C. Charcosset, R. G. Holdich, G. T. Vladisavljevic.

4- International Congress on Membranes and Membrane Processes. Amsterdam – Du 23 au 29 Juillet 201:

Liposomes produced in a membrane contactor: an improvement of the ethanol injection technique. C. Jaafar-Maalej, A. Laouini, H. Fessi, C. Charcosset.

Articles de revues

1- Chemical Engineering Journal, 2014, 236, 498-505

Use of dynamic membranes for the preparation of vitamin E loaded lipid particles: An alternative to prevent fouling observed in classical cross-flow emulsification. A. Laouini, C. Charcosset, H. Fessi, K. Shroen.

2- ACS Applied Materials and Interfaces,2013, 5, 8939-8947:

pH-sensitive micelles for targeted drug delivery prepared using a novel membrane contactor method. A. Laouini, K. P. Koutroumanis, C. Charcosset, S. Georgiadou, H Fessi, R. G. Holdich, G. T. Vladisavljevic.

3- Colloids and Surface B, 2013, 112, 272-278:

Preparation of liposomes: A novel application of microengineered membranes – Scale-up from laboratory scale to large scale. A. Laouini, C. Charcosset, H. Fessi, R. G. Holdich, G. T. Vladisavljevic.

4- RSC Advances, 2013, 3, 4985-4994:

Preparation of liposomes: A novel application of microengineered membranes - investigation of process parameters and application to the encapsulation of the vitamin E. A. Laouini, C. Charcosset, H. Fessi, R. G. Holdich, G. T. Vladisavljevic.

5- Journal of Membrane Science, 2012, 423-424, 85-96:

Membrane Emulsification: A promising alternative for vitamin E encapsulation within nano-emulsion. A. Laouini, H. Fessi, C. Charcosset.

6- Journal of Colloid Science and Biotechnology, 2012, 1, 147-168:

Preparation, characterization, and application of liposomes: State of the art. A. Laouini, C. Jaafar-Maalej, I. Limayem-Blouza, S. Sfar-Gandoura, C. Charcosset, H. Fessi.

Enfin … merci à

1- Laboratoire d'Automatique et de Génie des Procédés

2- Université Claude Bernard Lyon 1

3- Ministère Tunisien de l'Enseignement Supérieur et de la Recherche

4- Région Rhône-Alpes

5- Frans Nederlandse Academie

6- Loughborough University – Department of Chemical Engineering

7- Wageningen University – Food Process Engineering Laboratory

8- Université d'Aix Marseille – Faculté de Pharmacie

9- Université de Monastir – Faculté de Pharmacie

10- Laboratoire Aerodrug, Tours

11- Ecole Doctorale de Chimie, Lyon

Encapsulation de la Vitamine E dans des Vecteurs Pharmaceutiques Inhalables Préparés par des Contacteurs à Membrane

Auteur

Abdallah Laouini, né en 1983 à Tunis, est titulaire d'un diplôme de pharmacien délivré en 2007 par la faculté de pharmacie de Monastir. Il a obtenu en 2010 un Master de recherche en développement galénique des médicaments. Actuellement, il occupe un poste d'attaché d'enseignement et de recherche en pharmacie galénique à la Faculté de Pharmacie de Lyon. Ses travaux de recherche concernent l'application des contacteurs à membrane dans l'encapsulation des principes actifs dans des vecteurs pharmaceutiques (liposomes, micelles, nano-émulsion, particules lipidiques solides, etc).

Résumé

L'objectif de ce travail est de développer des vecteurs pharmaceutiques, encapsulant la vitamine E, adaptés à l'administration pulmonaire par aérosolisation. La vitamine E, antioxydant physiologique, peut être utilisée pour lutter contre les phénomènes du stress oxydatif en particulier ceux observés au niveau pulmonaire. L'encapsulation de la vitamine E dans des vecteurs inhalables a été envisagée afin d'optimiser son efficacité thérapeutique en améliorant la concentration du principe actif pouvant atteindre son site d'action, les alvéoles pulmonaires.

Les différents systèmes d'encapsulation de la vitamine E ont été préparés par des méthodes utilisant des contacteurs à membrane. Le principe de préparation se résume au passage de la phase dispersée, à travers les pores d'une membrane microporeuse, au sein de la phase continue. Les avantages de cette technique sont en particulier une bonne reproductibilité et un faible apport d'énergie et par conséquent un coût d'exploitation modéré. De plus, les procédés à base de contacteurs à membrane se prêtent aisément au passage à l'échelle de production industrielle. Au cours de ce travail, les paramètres influençant le procédé de fabrication par contacteur à membrane ont été étudiés; principalement la pression transmembranaire de passage de la phase discontinue, la force de cisaillement de la phase continue et la microstructure de la membrane utilisée. Différentes configurations membranaires ont été testées telles que (i) les modules membranaires tubulaires avec écoulement tangentiel de la phase continue, (ii) les membranes planes montées dans des cellules d'agitation et (iii) les membranes dotées d'un mouvement d'oscillation à l'intérieur de la phase continue. En cas d'émulsification directe, diverses membranes ont été utilisées: des membranes SPG, des membranes microsieves et des membranes en céramique. Pour la « premix emulsification » des membranes dites dynamiques, constituées par un lit de billes en verre, ont été étudiées.

Quatre types de vecteurs ont été développés au cours de ce travail : les liposomes, les micelles, les nano-émulsions et les particules lipidiques solides. La formulation galénique de ces vecteurs a été étudiée en vue de son optimisation. Les préparations ont été caractérisées en termes de distribution de taille, potentiel zêta et efficacité d'encapsulation; la stabilité a été étudiée pour des périodes allant de deux à quatre mois. Les résultats obtenus ont révélé que les vecteurs développés présentent des propriétés très satisfaisantes. La caractérisation des aérosols générés suite à la nébulisation de ces systèmes vectoriels, ainsi que la modélisation mathématique de la déposition pulmonaire *in vitro* ont aboutit à des résultats très prometteurs.

Université Claude Bernard Lyon 1, Laboratoire d'Automatique et de Génie des Procédés (LAGEP), UMR-CNRS 5007, CPE Lyon, Bâtiment 308G, 43 Boulevard du 11 Novembre 1918, F-69622 Villeurbanne Cedex, France